Ministry of Higher Education and Scientific Research

University of Kerbala
College of Education for Pure Sciences

Pure Sciences International Journal of Kerbala

ISSN
2789-6188

Deposit Number
2515

Year: First Folder: First Number:1

Republic of Iraq

Pure Sciences International Journal of Kerbala

(PSIJK) is published in four issues annually- starting from January 2021- emphasize on the main science aspects whose elaboration can yield knowledge and expertise that can equally serve all branches of science discipline.

Editor-in-Chief: Prof. Hamida Edan Salman Al-Ftlawi, Ph.D.

Publisher: College of Education for Pure Sciences

Since: 2021

Pure Sciences International Journal of Kerbala

College of Education for Pure Sciences

University of Kerbala
Kerbala Governorate
Iraq

https://journals.uokerbala.edu.iq

00964 7740811765

ISSN: 2789-6188

e-ISSN: Under processing

Consignment Number in the Housebook and Iraqi

Documents: 2515, 2021

Postal Code: 56001

Mailbox: 232

Karbala University Press

Workflow by OJS/PKP

Pure Sciences International Journal of Kerbala

Editorial board

	Name	Specialized	Work place
1	Prof.Dr. Ayman Nafady	Chemistry , Nanomaterials, Electrochemistry, Energy Storage, Coordination Polymers, Metal-Organic Frameworks	King Saud University
2	Prof.Dr. Nabil Mohie Abdel–Hamid	Biology , Hepatocellular Carcinoma Research (Early Detection, Looking for New Sensitive, Specific Markers and Therapeutic Modalities, Including Chemo and Radio Sensitization, Targeting to Cancer Hepatocyte)	Faculty of Pharmacy, Kafrelsheikh University, Egypt
3	Assit.prof.Dr. Abdul Adheem Mohamad Al-Soodinay	Mathematics , Geometry and Topology of Manifolds	University of Nizwa, Oman.
4	Assit.prof.Dr.Muhammad Akram	Biology , Eastern Medicine, Ethnomedicine, Unani Medicine,	Government College University Faisalabad, Pakistan
5	Assit.prof.Dr.Abdelaziz Radwan	Mathematics , Geometry and Toplology, Algebra	Faculty of Science Ain Shams University, Cairo, Egypt
6	Prof.Dr. Ali Hussein Al-Marzoogee	Biology , Molecular genetics, biotechnology, oncology, medical microbiology	University of Babylon, Babylon, Iraq
7	Prof.Dr. Noori Farhan Al-Mayahi	Magmatic , Mathematical Analysis, Pure Mathematics, Functional Analysis	University of Al-Qadisiyah, Al-Qadisiyah, Iraq
8	Prof.Dr. Ahmed Mehmood Abdul-Lettif	Physics , Material Characterization, Materials, Thin Films and Nanotechnology,	University of Babylon, Babylon, Iraq
9	Assist.prof.Dr. Ali Khorsand Zak	Physics , Nanomaterials, Graphene Composites, and their Applications	University of Technology, Tehran, Iran

10	Prof.Dr. Mohammad Nadhum Bahjat	Chemistry, Material Characterization, Materials, Mechanical Properties	University of Karbala, College of Education for Pure Sciences, Karbala, Iraq
11	Assist.prof.Dr. Reyadh D. Ali	Mathematics , Mathematical Analysis, Pure Mathematics, Topology, Real Analysis, Real and Complex Analysis	University of Karbala, College of Education for Pure Sciences, Karbala, Iraq
12	Assist.prof. Amjad Hamead Al-Husiny	Mathematics , Number Theory, Algebra	University of Karbala, College of Education for Pure Sciences, Karbala, Iraq
13	Prof.Dr. Najem Abdulhussain Najem	Geology , Remote Sensing, Geophysics and Exploration of Natural Resources	University of Kerbala, college of science
14	Prof.Dr. Kawther abd al-hussain	Biology ,parasite	University of Karbala, College of Education for Pure Sciences, Karbala, Iraq

Dear PSIJK's Respectful authors, board of reviewers and all editorial board members

All submitted papers to PSIJK is required for Plagiarism Checker Turnitin

Since January 2021, Pure Sciences International Journal of Kerbala (PSIJK) has effectively utilized plagiarism checker for the detection of the quality of all submitted articles in review process. Once a paper is reviewed before any decision the editorial board meet monthly; we shall provide full report from board of reviewers and Turnitin to assist board members to judge and make correct decision. Based on recommendations the results would be shared with authors for revision and improving the quality of publication in PSIJK. All submitted manuscripts to PSIJK should be original and any part of the article should not be plagiarized. Even reviewed article before any decision, the content is checked for plagiarism through Turnitin data base. For any submitted manuscript, the plagiarism level greater than 20% including author name, affiliation and references is automatically rejected. We are pleased with the services provided by Turnitin data base; in fact PSIJK›s board members welcome any international publishers to provide PSIJK special services for improving internationalization and also help us to get recognition, prefect global impact and publicity to approach Thomson Reuters standard criteria.

About the Journal

The “Pure Sciences International Journal of Kerbala”, published quarterly and distributed internationally by the College of Education for Pure Sciences provides a forum for publication of significant science advancements and developments in chemistry, biology, computer, physics, mathematics and interdisciplinary areas of science. All prospective authors are invited to submit their original contributions on new theoretical and applied aspects of growing research. All manuscripts submitted, including symposium papers, will be peer reviewed by qualified scholars assigned by the editorial board.

You are cordially encouraged to use this journal as a means of dissemination of information on the various facets of science and technical problems; and to impart specialized knowledge, quality and excellence to strengthen the perception of technological resources and needs of the world. The PSIJK is looking forward to receiving your assistance to working together to develop a worthwhile, high quality journal.

Aims and Scope

The objective of the Pure Sciences International Journal of Kerbala is to provide a forum for communication of information among the world›s scientific and technological community and Iraqi scientists. This journal intends to be of interest and utility to researchers and practitioners in the academic, industrial and governmental sectors. All original research contributions of significant value in all areas of science discipline are welcome.

This journal will publish authoritative papers on theoretical and experimental research and advanced applications embodying the results of extensive field, plant, laboratory or theoretical investigation or new interpretations of existing problems. It may also feature - when appropriate - research notes, technical notes, state-of-the-art survey type papers, short communications, letters to the editor, meeting schedules and conference announcements. The language of publication is English. Each paper should contain an abstract both in English and Arabic. However, for the authors who are not familiar with Arabic language, the publisher will prepare the translations. The abstracts should not exceed 250 words.

All manuscripts will be initially checked for plagiarism and then peer-reviewed by qualified reviewers. The material should be presented clearly and concisely:

-Full papers Authors are urged to be succinct; long papers with many tables and figures may require reductions prior to being processed or accepted for publication. Although there is not an absolute length restriction for original papers, authors are encouraged to limit the text to =5,000 words (including references) and references up to 40.

-Review papers are only considered from highly qualified well-known authors generally assigned by the editorial board or editor-in-chief. Author of review papers should have high qualifications with distinct developed research area, an outstanding scholar with an extensive publications.

-Short communications and letters to the editor should contain a text of about 3000 words and whatever figures and tables that may be required to support the text. They include discussion of full papers and short items and should contribute to the original article by providing confirmation or additional interpretation. Discussion of papers will be referred to author(s) for reply and will concurrently be published with reply of author(s).

Instructions for Authors

Submission of a manuscript represents that it has neither been published nor submitted for publication elsewhere and is result of research carried out by author(s). Presentation in a conference and appearance in a symposium proceeding is not considered prior publication.

Authors are required to include a list describing all the symbols and abbreviations in the paper. Use of the international system of measurement units is mandatory.

-On-line submission of manuscripts results in faster publication process and is recommended. Instructions are given in the PSIJK web sites https://journals.uokerbala.edu.iq/

-Hardcopy submissions must include MS Word and jpg files.

-Manuscripts should be typewritten on one side of A4 paper, double-spaced, with adequate margins.

-References should be numbered in brackets and appear in sequence through the text. List of references should be given at the end of the paper.

-Figure captions are to be indicated under the illustrations. They should sufficiently explain the figures.

-Illustrations should appear in their appropriate places in the text.

-Tables and diagrams should be submitted in a form suitable for reproduction.

-Photographs should be of high quality saved as jpg files.

-Tables, Illustrations, Figures and Diagrams will be normally printed in single column width (8cm). Exceptionally large ones may be printed across two columns (17cm).

After Acceptance

Availability of accepted article

This journal makes articles available online as soon as possible after acceptance. This concerns the accepted article (both in HTML and PDF format), which has not yet been copyedited, typeset or proofread. A Digital Object Identifier (DOI) is allocated, thereby making it fully citable and searchable by title, author name(s) and the full text. The article›s PDF also carries a disclaimer stating that it is an unedited article. Subsequent production stages will simply replace this version.

Open access

The Pure Sciences International Journal of Kerbala is an open access journal: all articles will be immediately and permanently free for everyone to read and download. To provide open access, this journal has an open access fee of USD 100 excluding taxes (also known as an article publishing charge APC) which needs to be paid by the authors or on their behalf e.g. by their research funder or institution. If accepted for publication in the Journal following peer review, authors will be notified of this decision and at the same time requested to pay the article processing charge. A CC user license manages the reuse of the article.

Author Checklist

-Author(s)' bio-data including affiliation(s) and mail and e-mail address(es).

-Manuscript including abstracts, key words, illustrations, tables, figures with figure captions and list of references.
-MS Word file of the paper.

Submission Checklist

The following list will be useful during the final checking of an article prior to sending it to the journal for review. Please consult this Guide for Authors for further details of any item.

Ensure that the following items are present:

One author has been designated as the corresponding author with contact details:

E-mail address Phone number(s) Fax number All necessary files have been uploaded, and include: Keywords All figure captions All tables (including title, description, footnotes) Further considerations Manuscript has been ‹spell-checked› and ‹grammar-checked› References are in the correct format for this journal All references mentioned in the Reference list are cited in the text, and vice versa Permission has been obtained for use of copyrighted material from other sources (including the Web) Color figures are clearly marked as being intended for color reproduction on the Web (free of charge) and in print, or to be reproduced in color on the Web (free of charge) and in black-and-white in print If only color on the Web is required, black- and-white versions of the figures are also supplied for printing purposes For any further information please visit our site at https://journals.uokerbala.edu.iq/

Publication Ethics

1. Author responsibility

The authors are exclusively responsible for the contents of their submissions, the validity of the experimental results and must make sure that they have permission from all involved parties to make the data public.

It is the responsibility of each author to ensure that papers submitted to PSIJK are written with ethical standards in mind, concerning plagiarism.

Please note that all submissions are thoroughly checked for plagiarism. If an attempt at plagiarism is found in a published paper, the authors will be asked to issue a written apology to the authors of the original material. Any paper which shows obvious signs of plagiarism will be automatically rejected and its authors will be banned for duration of three years from publishing in PSIJK. The authors will receive proper notification if such a situation arises.

Information on what constitutes plagiarism is provided below.

2.Plagiarism: Definition and Context

Plagiarism, where someone assumes another›s ideas, words, or other creative expression as one›s own, is a clear violation of scientific ethics. Plagiarism may also involve a violation of copyright law, punishable by legal action.

Plagiarism may constitute the following:

Word for word, or almost word for word copying, or purposely paraphrasing portions of another author›s work without clearly indicating the source or marking the copied fragment (for example, using quotation marks);

Copying equations, figures or tables from someone else›s paper without properly citing the source and/or without permission from the original author or the copyright holder.

Self-plagiarism, as a related issue, is the word for word or almost word for word reproduction of portions of one›s own copyrighted work without proper citation of the original material. Self-plagiarism does not apply to publications based on the author›s own previously copyrighted work (for example from conference proceedings) where proper reference was given for the original text.

International Journal of Engineering editorial board will place any plagiarism-related investigation at high priority and will take appropriate action as needed.

CONFLICT OF INTEREST

All authors are requested to disclose any actual or potential conflict of interest such as any financial, personal or other relationships with other people or organizations concerning the submitted work that could inappropriately influence, or be perceived to influence, their work.

COPYRIGHT AND PERMISSIONS

By submitting a manuscript to the editor or publisher you are deemed to have granted permission to publish the manuscript.

PROOFS

Proofs will be sent via e-mail as an Acrobat PDF (Portable Document Format) file. Acrobat Reader will be required in order to
read the PDF. This software can be downloaded from the following website:
http://www.adobe.com/products/acrobat/readstep2. html

This will enable the file to be opened, read on screen and printed out in order for any corrections to be added. To avoid delay
in publication, corrected proofs should be faxed to the publisher within 48 hours of receipt.

content list

Pure Sciences International Journal of Kerbala

Journal Homepage:https://journals.uokerbala.edu.iq/index.php/psijk

Studying the Swelling and Thermodynamic Functions of a Graft Co - polymer Using Different Molar Ratios of Acrylic Acid Monomer

Mazin F. Anad, Hamieda E. Salman and Mohammad N. AL-Baiati

Mazin F. Anad, Department of Chemistry, College of Education for Pure Sciences, University of Kerbala, Holly Kerbala, Iraq.
Hamieda E. Salman, Department of Chemistry, College of Education for Pure Sciences, University of Kerbala, Holly Kerbala, Iraq.
Mohammad N. AL-Baiati*, Department of Chemistry, College of Education for Pure Sciences, University of Kerbala, Holly Kerbala, Iraq.
E-mail: Mohammad.nadhum@uokerbala.edu.iq

PAPER INFO

Paper history:

Keywords:
Polyester Resin, Modified Polymer, Modified Polyester Resin, Condensation Polymerization, Interpenetrating Polymer Network, Swelling, Swelling of Polymer, Swelling of Modified Resin, Swelling of Co-polymer, Rate of Polymerization, Activation Energy, Thermodynamic. Functions.

ABSTRACT

In this work, the of graft co-polymer was prepared, by using glycerol as material containing the three alcoholic groups, and that reacted with terphthalic acid which have two carboxylic group as a first step, and then added 0.5 mole of fumaric acid to prepared graft co-polymer, as a second step. The acrylic acid monomer was added to the graft co-polymer in different number of moles (1.5, 2.0 & 2.5 mole). The swelling ratio measurements of the graft co-polymer, in three different buffer solution (2.2, 7.0 and 8.0), in the constant temperature at 310 K. The results showed that the increases of number of the moles of the acrylic acid monomer, Leads to increased of swelling ratio. Thermodynamic functions were calculated of the linear polymer.

doi: 10.37200/I JPR/V24I5/PR201814

1. INTRODUCTION

Copolymerization is the joint polymerization of two or more monomer species. High–molecular mass compounds obtained by copolymerization are called copolymers [1]. The molecular chain of a copolymer is composed of different units, in accordance with the number of initial monomers [2]. If the reactants of a polycondensation have several different monomers, the result will be a copolymer [3]. The reaction of copolycondensation has acquired great technical importance in recent years and is now widely used for the synthesis of various mixed polyesters and polyamides (e.g. containing ester and amide bonds simultaneously) and other copolymers. For instance co-polycondensation of hexamethylenediamine, adipic acid and terephthalic acid [4]; Polymers may be classified as hydrophobic or hydrophilic, according to whether or not they dissolve or swell in water. The polymers which contain hydrophobic groups (e.g. C_2H_5) are water insoluble. The polymers which contain a hydrophilic group (e.g. OH), are water soluble, in the case of linear polymers or swellable in the case of cross linked polymers. In other words, the hydrogel can be defined as a polymeric material which will swell in solvent and it contains a significant fraction of water (usually more than 20%) within its structure. The term xerogel is given to the polymer network alone (dry state) [5] ,thus:

Xerogel + Water → Hydrogel

Hydrogels, are a coherent system rich in water; they are made up of two principal components; a constant solid component consisting of a polymer network, and a variable liquid component, either water or an aqueous solution. The aqueous component can undergo exchange with the environment by diffusion or evaporation [6, 7]. For getting materials combining biocompatibility with a good mechanical strength, two methods are used [8,9]: Copolymerization of hydrophilic monomers with hydrophobic monomers or with cross-linking agent or grafting of hydrophilic monomers on stronger polymer supports [10, 11, 12].

II. EXPERIMENTAL

1. Chemicals

All chemicals were used in this work analytical grade, imported from different companies.

2. Preparation of graft co-polymer [13, 14]

The first step; In a 500 ml three-necked round bottom flask, (2.0 mole, 332gm) of terphthalic acid, and (1.0 mole, 92gm) of glycerol, were mixed together, this flask was equipped with a thermometer and a mechanical

*Corresponding Author Institutional Email: cauth.@uokerbala.edu.iq
(The name of corresponding author)

Pure Sciences International Journal of Kerbala

Journal Homepage:https://journals.uokerbala.edu.iq/index.php/psijk

stirrer. The mixture warmed carefully with an electric heating mantle to 270C0 until a clear liquor is formed and then about 25 ml of xylene was added carefully to the reaction flask, in the form of batch (two drops in each batch), Withdrawal of water formed in the esterfication process, and the flask was gently heated. Heating was stopped after 150 min. at 325 Co, until no more water came off. **The second step**; The flask was allowed to cool to 110 Co, and (0.5mole, 58gm), of fumaric acid, was added carefully to the reaction flask, and the flask was gently rise heated, after melting material, added the drops of xylene in the form of batch (two drops in each batch), until no more water came off at 275 Co, and 125 min., to prepared of a new graft co-polymer. The flask was allowed to cool to 50Co, and (1.36×10- 3mole, 0.147gm) of hydroquinone was added to the reaction flask, with stirred by mechanical stirrer, and (1.5, 2.0 and 2.5 mole) about (108, 144 and 180 gm), respectively of acrylic acid monomer, was added to the graft copolymer and stirred by mechanical stirrer, until a pourable syrup was formed. The viscosity and density of the prepared co-polymer were calculated using, Brookfild digital viscometer instrument and Hydrometer instrument respectively, and the average number of molecular weight (*Mn*) was determined using end group analysis method.. Table (1), represents the physical properties of modified polyester resin.

TABLE 1. Physical properties of the graft co-polymer

Physical properties	**Value**
Molecular Weight (*Mn*)	Around 2800 gm/mole
Solid content	61 %
Viscosity	23 poise
Gel time	15-20 min at 25C0
Acid Value	26
Density	1.5 (gm/cm3)

3. Preparation of polymeric specimens

The specimens of polymeric material containing different number of moles of the acrylic acid monomer were prepared by using Methylethylketone peroxide (MEKP) as a hardener and cutting as a disc in dimensions (thickness=3mm & diameter=10mm) and the weighted of the xerogel discs was exactly 0.4 gm of all specimens were used in the swelling study.

4. Swelling

The known weight and diameter of dried discs (Xerogel) were put in sample vials. The swelling time was counted when the solvent was added into the sample vials [10, 11]. The buffer solution contents of the hydrogels, were calculated according to the following equations [15]:

Buffer solution % = (Wt. of hydrogel - Wt. of xerogel / Wt. of hydrogel) × 100

5- Thermodynamic Functions

The Arrhenius equation gives the quantitative basis of the relationship between the activation energy and the rate
of polymerization, at which a reaction proceeds. From the equation, the activation energy can be found through the
relation [16]:

$$K = Ae^{-Ea/(RT)}$$

By using Van Huff complementary equation, the thermodynamic functions were determination of the linear copolymer.

The relationships below were used to calculate these functions [17]:

$$\ln K = -\left(\Delta H / RT\right) + \text{constant}$$

$$\Delta G = -RT.\ln K$$

$$\Delta S = (\Delta H - \Delta G)/T$$

III. Results And Discussion

1. Preparation of graft co-polymer

The first step; Figure (1), represent the FT–IR spectrum of the linear co-polymer, showed the appearance of a strong broad band at about 3423 cm^{-1} for stretching alcoholic -OH with stretching (H–bond), and also showed a weak band at about 2902cm^{-1} due to the -OH for Carboxylic acid, the C-H $sp^3$and sp^2hybridization absorption at about 2544 cm^{-1}, 2654 cm^{-1}respectively, and the spectrum also showed a strong band at about1726 cm^{-1} assigned to a stretching band C=O for ester group.

The spectrum appearance a weak sharp bands at about 1597cm^{-1},1581cm^{-1}due to C=C for conjugated system of benzene ring and also showed a bands at about 1284 – 1259cm^{-1} assigned to C-O absorption band [18]. Figure (2), The spectrum of ^{1}HNMR showed, which explain the singlet signal at 13.24 ppm characteristic of proton in carboxylic acid group, furthermore the multiples in the region 7.53- 8.10 ppm back to all protons in aromatic ring, the signals at 6.27-6. 46 ppm for four protons of methylene in the structure of co-polymer, the multiples at 4.24-4.50 ppm of methyl protons, but the triplet signal in 3.44- 3.62 ppm dueto the proton of aliphatic alcohol so this spectrum was confirmed the structure of our target polymer [19].

Pure Sciences International Journal of Kerbala

Journal Homepage:https://journals.uokerbala.edu.iq/index.php/psijk

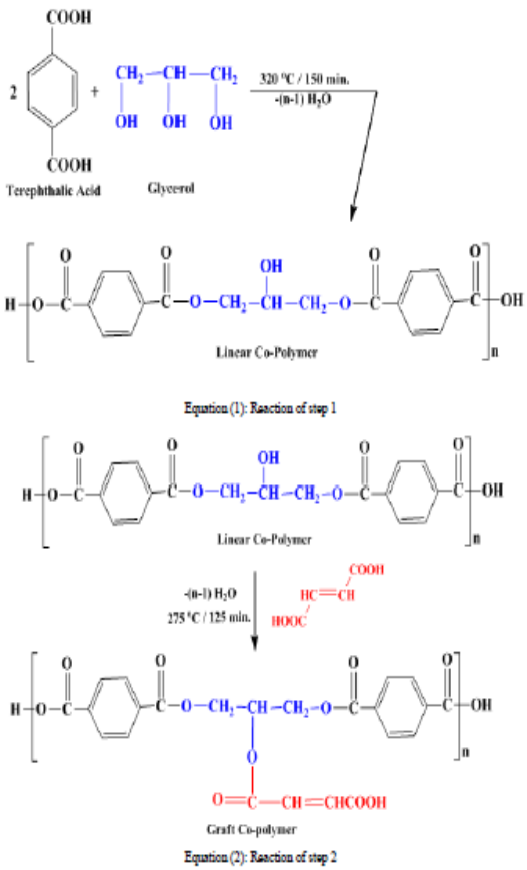

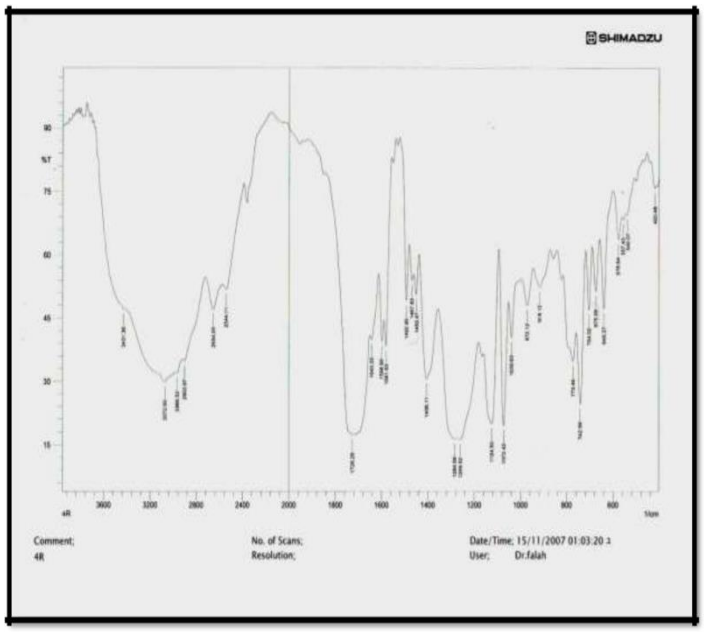

Figure 1: The FT-IR spectrum of linear co-polymer

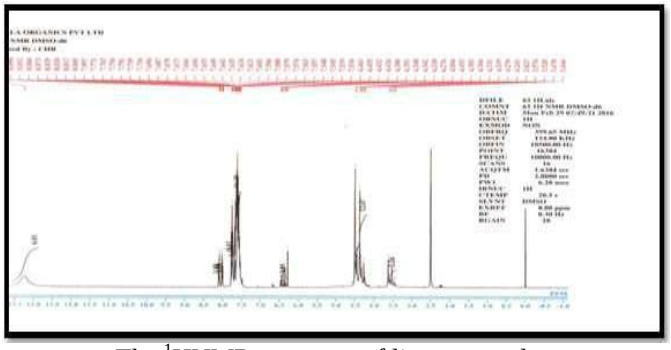

Figure 2: The ^{1}HNMR spectrum of linear co-polymer

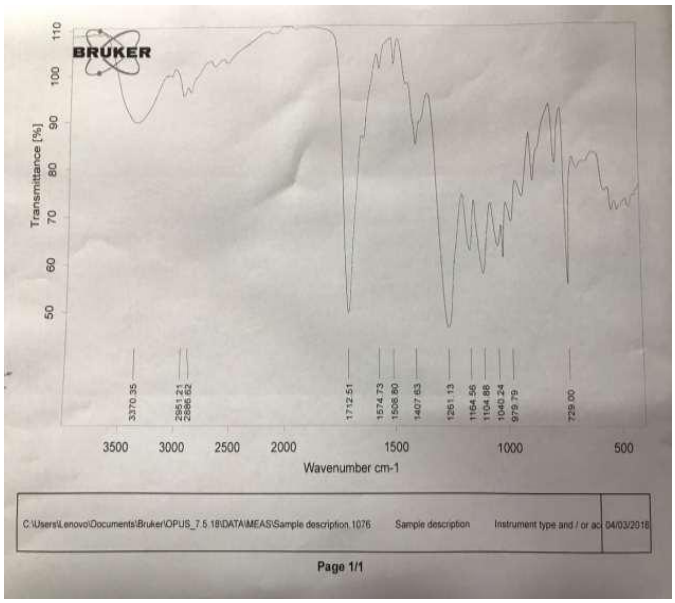

Figure 3: The FT-IR spectrum of graft co-polymer

The second step; Figure(3), showed the FT – IR spectrum of the graft co-polymer, its showed the appearance of a strong broad band at 3500 cm^{-1} for stretching alcoholic -OH with stretching (H–bond), and the spectrum also showed the aliphatic C-H, aromatic =C-H and alkenes =C–H at approximately at 2880 cm^{-1}, 3140 cm^{-1} and 3050 cm^{-1} respectively, and the spectrum also showed a strong sharp band at 1740 cm^{-1} and 1250 cm^{-1} for a stretching band C=O ester and C-O ester respectively.

2-Thermodynamic Functions

The rate of polymerization in different times (Sec.) at a constant temperature was calculated by measuring the acid value. The slope of a plot of acid value (A.V.) versus time (Sec.) represents the rate of polymerization Figure (4). Table (2), showed the acid value in different times at different temperatures. The rate of polymerization of the modified unsaturated polyester resin, was (120 $Sec.^{-1}$) at a constant temperature in 583 K. The activation energy (Ea) of polymerization of the

First Year-First Folder-Number: 0
PSIJK 184-191

Pure Sciences International Journal of Kerbala

Journal Homepage:https://journals.uokerbala.edu.iq/index.php/psijk

modified unsaturated polyester resin was calculated from Arrhenius equation and it was found (2.9×10^6 J/mole) at a constant temperature in 583K.

Table 2: Represent the acid value of linear co-polymer in different times at different temperatures.

Time (Sec.)	Acid Value	Slope	Temp. (K)
120	240.0		
240	220.0	3.254472	563
360	198.8		
480	182.0		
120	176.4		
240	162.4	3.254472	568
360	147.0		
480	135.0		
120	126.0		
240	114.6	3.254472	573
360	103.6		
480	92.4		
120	81.2		
240	73.0	3.254472	578
360	64.4		
480	57.4		
120	47.9		
240	42.8	3.254472	583
360	37.0		
480	30.0		

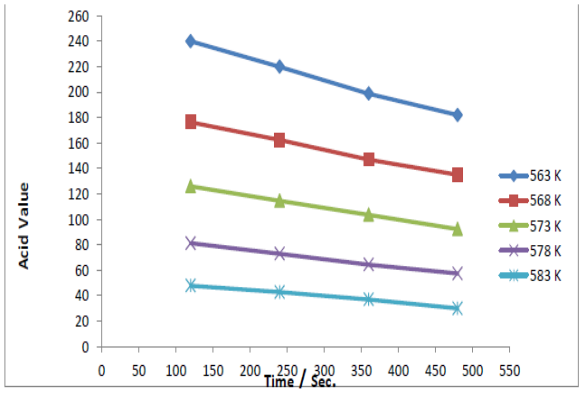

Figure 4: Acid value Vs. Time (Sec.) in different temperatures

By using Van Huff complementary equation, thermodynamic functions were determination of the linea polymer.

Table (3), showed the thermodynamic functions.

T (K^o)	1/T	lnK	ΔH (J/mol)	ΔG (J/mol)	ΔS (KJ/mol.K)
563	1.776×10^{-3}	-0.1003	2.9×10^6	469.482	5.150
568	1.7605×10^{-3}	-9.2992		43914.095	5.097
573	1.7452×10^{-3}	-10.733		51131.174	4.971
878	1.7301×10^{-3}	-15.232		73197.254	4.890
583	1.7152×10^{-3}	-24.063		116634.852	4.774

The swelling curves of graft co-polymer showed a plot of buffer solution content for different compositions against swelling time (hour and day). The initial swelling rate was medium, the maximum being reached within the first few hours of the swelling. The shape of the swelling curves indicated that buffer solution–soluble molecules were being released from the xerogel upon swelling. [14].

A plot of buffer solution content versus time showed hydration curves of graft co-polymer for three different numbers of moles from acrylic acid compositions ranging from 1.5, 2.0 and 2.5 mole, against swelling time at constant temperatures, as shown in Tables (4) to (6) and Figures (5) to (10) respectively.

Table 4: Swelling ratio (%) in different time, of graft co-polymer with different moles of acrylic acid monomers in pH=2.2 at 310 K

Time	Swelling ratio (%)		
	Number of moles acrylic acid monomers		
(hour)	1.5 moles	2 moles	2.5 moles
1	5.0111	5.1241	5.2356
2	5.0433	5.1468	5.2582
3	5.0660	5.1695	5.2708
4	5.0887	5.1822	5.2930
5	5.1114	5.2149	5.3156
(day)			
1	6.0165	6.1600	6.2875
2	6.0580	6.1855	6.3130
3	6.0835	6.2110	6.3385
4	6.1090	6.2365	6.3640
5	6.1345	6.2620	6.3895

Pure Sciences International Journal of Kerbala

Journal Homepage:https://journals.uokerbala.edu.iq/index.php/psijk

Table 5: Swelling ratio (%) in different time, of graft co-polymer with different moles of acrylic acid monomers in pH=7.0 at 310 K

Time	Swelling ratio (%)		
	Number of moles of acrylic acid monomers		
(hour)	1.5 mole	2.0 mole	2.5 mole
1	7.0160	7.2455	7.4555
2	7.0590	7.2890	7.5084
3	7.1035	7.3230	7.5421
4	7.1374	7.3640	7.5859
5	7.1692	7.4192	7.6299
6	7.2023	7.4325	7.6690
(day)			
1	8.0180	8.2526	8.4931
2	8.0571	8.2917	8.5381
3	8.0963	8.3308	8.5831
4	8.1323	8.3699	8.6281
5	8.1744	8.4090	8.6731
6	8.2135	8.4481	8.7181

Table 6: Swelling ratio (%) in different time, of graft co-polymer with different moles of acrylic acid monomers in pH=8.0 at 310 K

Time	Swelling ratio (%)		
	Number of moles acrylic acid monomers		
(hour)	1.5 moles	2.0 moles	2.5 moles
1	9.1011	9.2439	9.3854
2	9.1218	9.2642	9.4056
3	9.1423	9.2844	9.4258
4	9.1627	9.3046	9.4460
5	9.1831	9.3248	9.4662
6	9.2033	9.3450	9.4864
7	9.2236	9.3652	9.5066
(day)			
1	10.0190	10.6150	11.2185
2	10.1040	10.7010	11.3060
3	10.1890	10.7870	11.3935
4	10.2740	10.8730	11.4810
5	10.3590	10.9590	11.5685
6	10.4440	11.0450	11.6560
7	10.5290	11.1310	11.7435

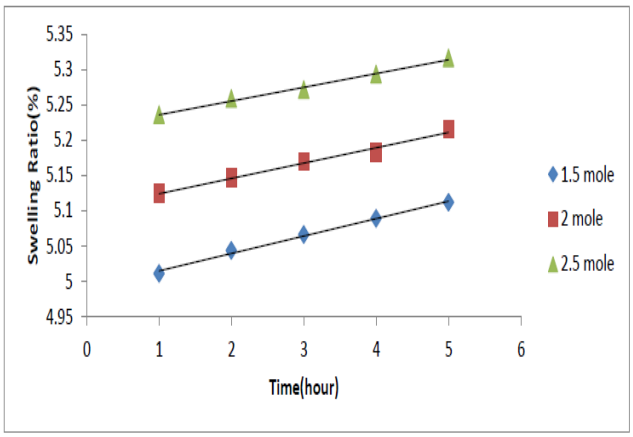

Figure 5: Swelling ratio (%) in hour, of graft co-polymer with different moles of acrylic acid monomers in pH=2.2 at 310 K

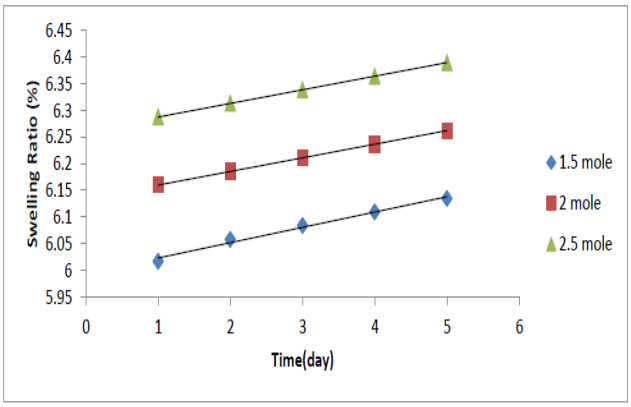

Figure 6: Swelling ratio (%) in day, of graft co-polymer with different moles of acrylic acid monomers in pH=2.2 at 310 K

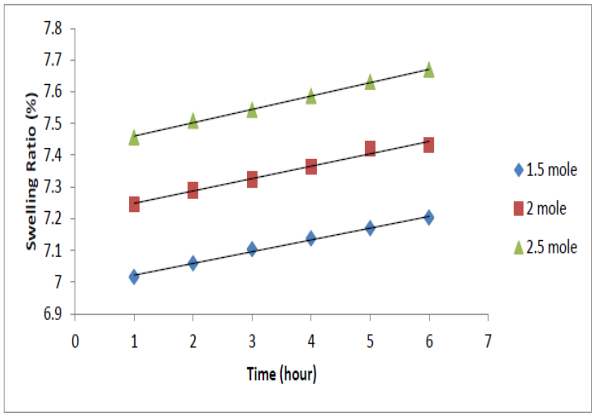

Pure Sciences International Journal of Kerbala

Journal Homepage:https://journals.uokerbala.edu.iq/index.php/psijk

Figure 7: Swelling ratio (%) in hour, of graft co-polyr with different moles of acrylic acid monomers in pH=7 310 K

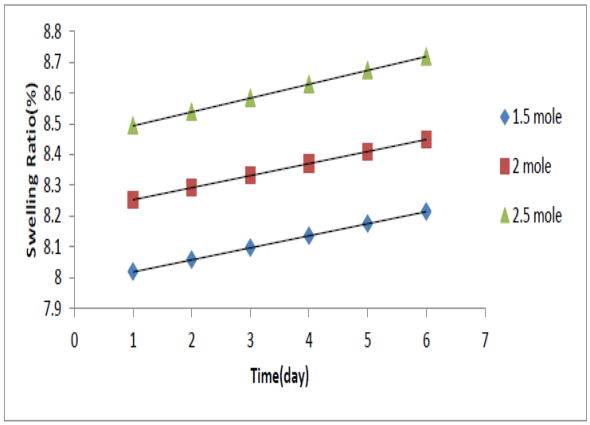

Figure 8: Swelling ratio (%) in day, of graft co-polymer with different moles of acrylic acid monomers in pH=7.0 at 310 K

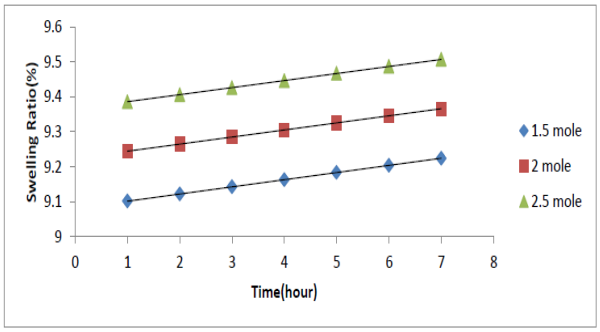

Figure 9: Swelling ratio (%) in hour, of graft co-polymer with different moles of acrylic acid monomers in pH=8.0 at 310 K

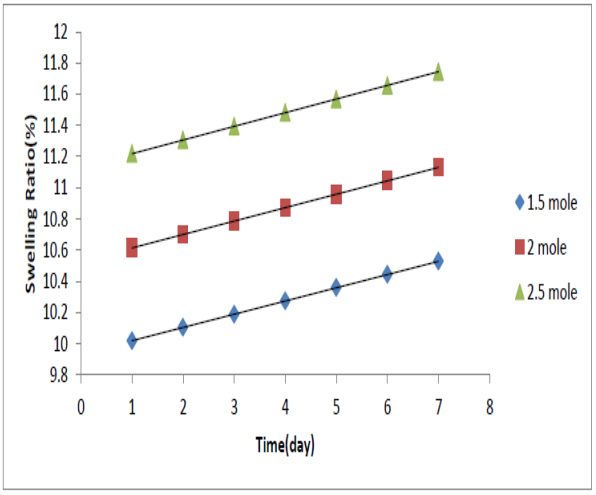

Figure 10: Swelling ratio (%) in day, of graft co-polymer with different moles of acrylic acid monomers in pH=8.0 at 310 K

As clearly shown in these figures increasing the time with increases of the buffer solution content (%), this behavior can be explained due to, the pH of buffer solution and the structure of polymer, i.e., present of the hydrophilic groups in the xerogel, concentration and nature of the pH of buffer solution. All these factors will increase the buffer solution content (%) with the increased of time [14]. The low values of swelling process were affected by High chain flexibility and the degree of cross linking, i.e., in the graft co-polymer with 1.5 mole of acrylic acid, the values will be low comparing with the values in the graft co-polymer with 2.5 mole of acrylic acids.

IV. CONCLUSIONS

Increasing of the number of moles of the acrylic acid monomer due to, increases the hydroxyl content ratio of the product co-polymer, and thus leads to increases the swelling graft co-polymer, and the results also showed that the effect of the pH of buffer solution on swelling.

REFERENCES

[1] Jin G. & Dijkstra J.; Hydrogels for Tissue Engineering Applications; *Springer*, p.59, (2010)

[2] Ebewele R.; Polymer Science and Technology; CRC Press., *New York*, P.71&35. (2000).

[3] Robert A.M.; Handbook of Petrochemicals Production Process; McGraw-Hill Publisher; *New York*, P.110&84, (2006).

[4] Reddy C. & Swamy B.; *Inter. J. Phar. and Pharma. Sci.;* 3 (1), p. 215, (2011).

Pure Sciences International Journal of Kerbala

Journal Homepage:https://journals.uokerbala.edu.iq/index.php/psijk

[5] Boydston A., Xia Y., Kornfield J., Gorodetskaya I. & Grubbs R.; *J. Am. Chem. Soc.;* 130 (38), p.12775, (2008).

[6] You N., Higashihara T., Yasuo S., Ando S. & Ueda M.; *J. Polym. Chem.*; 1, p.480, (2010)

[7] Bastiurea M., Rodeanu M., Dima D., Murarescu M. & Andrei G.; *Digest J. Nanomaterials and Biostructures;* 10, p.521, (2015).

[8] Jin T., Zhu J., Wu F., Yuan W. & Geng, L.; *J. Cont. Rele.;* 128,p.50, (2008).

[9] Mohammad AL-Baiati, Nadhir J. and Rawaa H; *Res. J. Pharma., Bio. and Chem. Sci.;* 7(5); P. 1452; (2016)

[10] Dinarvand R.; *Int. J. Pharm.;* 349, p.249, (2008)

[11] Puapermpoonsiri U., Spencer J. & Van der Walle C. ; *Eur. J. Biopharm. ;* 72, p.26 &33, (2009)

[12] You N., Higashihara T., Yasuo S., Ando S. & Ueda M.; *J. Polym. Chem.;* 1, p.480, (2010)

[13] Mohamed F. & Van der Walle C. ; *J. Pharm. Sci.;* 97, p.71, (2009)

[14] ZahraaM. & Mohammad AL-Baiati; J. Global Pharma Techno.; 2017; 12 (9): 50-56

[15] Chaupart N., Serpe G. & Vedn J.; Polymer; 39, p.1375,(1998).

[16] Mohammad AL-Baiati; pH.D. Thesis; University of Baghdad; (2008); p. 45.

[17] Liu J., Zheng X.& Tang K.; Rev. Adv. Mater. Sci.; Vol. 33, p. 428, (2013)

[18] Pretsch E., Buhlmann P.& Baderscher M.; Structure determine of Organic compound; Springer, 4thEd, p.244, (2009).

[19] Pavia L., Lampman L., Kris S. & Vyvyan R.; Introduction to Spectrophotometer; 4th Ed, (2009)

Pure Sciences International Journal of Kerbala

Journal Homepage:https://journals.uokerbala.edu.iq/index.php/psijk

Synthesis, Characterization and Study of Schiff Base Ligand Type N_2 and Metal Complexes with Di Valence Nickel, Copper and Zinc

Taha H. Alnasrawi[1] , Shatha Abd_Alameer Jawad[2], Hamida Edan Salman[3], Mohammed Ridha Al-Haideri[4]

[1]College of Nursing, University of Warith AL-Anbiyaa, Karbala, Iraq
[2]Department of chemistry, College of education and pure science, University of Karbala, Karbala, Iraq
[4]Ministry of Education, Karbala, Iraq
*Corresponding Author Email ID: taha.hassan@uowa.edu.iq

PAPER INFO

Paper history:

Keywords:
thylene di amine, Schiff base, Metal complex, benzaldehyde, Sodiumborontetrahydride

ABSTRACT

The di dentate ligand type N_2 have been prepared through two steps. The first included the reaction between one equivalent of ethylenediamine with tow equivalent of benzaldehyde the second included the reaction of first step precursor with one equivalent of sodiumborontetrahydride ($NaBH_4$) to obtained the target ligand. Ni^{+2}, Cu^{+2}, Zn^{+2} from there action of the ligand Complexes were prepared with metal ions 1:1 ratio, the proposed compounds were characterized by FT -IR, UV-Vis, NMR for ligand, C.H.N spectroscopies, the biological activity as well as the molar conductivity and magnetic the success stability. Suggested geometry around the Zinc and Copper ions is tetrahedral and square planer around nickel ion.

INTRODUCTION

Schiff base, relative to the German chemist Hugo Schiff, is amines in which the nitrogen atom is bond to aryl or alkyl but not a hydrogen atom. It has the general formula $R_1R_2C = N\text{-}R_3$. The organic bonding with the nitrogen atom has a stabilizing effect of amine [1] .Schiff rules are considered organic compounds containing the group of azomethine -CH = N [2] and are of two types aliphatic are mostly liquid, aromatics are solid materials with high thermal stability and prepared with condensation of aldehydes or aliphatic or aromatic ketones with primary amines (aliphatic or aromatic)[3] Hence its name and several rules were given to these rules including (Anil) and called (Ketimine) when they are derived from ketone or (Aldimine) when they are derived from aldehyde[4] through condensation between the group of carbonyl and primary amines, as the amine Mono alkyl (R- (NH_2)[5] or mono-aryl amine (Ar-NH_2) is added to a group carbon The Carbonell of the aldehyde or ketone compound consists medial Carbinolamine, followed by the loss of water molecule consists of N-substituted imine, which represents a Schiff base as a by-final[6] . Intensification of carbonyl and amine compound in biochemistry, the rules for chef moderation are intermediate compounds that are enzymatic amine accompaniments. They also have other uses as catalysts, in medicine and pharmacy as anticancer agents and as antimicrobial[7] , and fluorescence compounds with high quantum yields[8] and are included in various pharmaceutical industries [9]

MATERIAL AND EQUIPMENT

All chemical that used are obtained from Fluka, Merck and Aldrich, further purification was not need. Melting point was measured by using an (electro thermal) melting point apparatus and they are uncorrected. FT-IR spectra were measured with Shimadzu FT-IR-8 infrared spectrophotometer by using KBr disk, ^1H -NMR spectra were recorded by used Broker - 0MHz Germany and DMSO -d6was the solvent. UV-Visible spectra were recorded by used UV-Visible Spectrophotometer- 0 Shimadzu. Electrical conductivity was measured by Digital Conductivity meter – WT – 2 – inolab (Germany).

Synthesis of legend (T)

To solution of benzaldehyde (2g) was added (1.8 g) ethalendiamen in 0ml bekar in ice bath (0 -5C) and stirrer for (5hr). white -yellow precipitate was formed, filtered off, and washed with 2ml cooled ether.MP: 8 -6C °,yelled: 8% (1 ; mol.formula: $C_6H_6N_2$; M.wt: 8

Synthesis of legend (T1

Pure Sciences International Journal of Kerbala

Journal Homepage:https://journals.uokerbala.edu.iq/index.php/psijk

To (0.2g) of prepared ligand (T) added (0.15g) of NaBH4 and stirring for (6hr) white precipitate was formed, filtered off, then the cooler solution was to cool at room temperature. MP:138-141 C_o ; Yelled: 55% ; mol.formula:$C_{16}H_{20}N_2$; M.wt: 240.43 ; C, 79.95 ;H, 8.40 ; N, 11.65 ;Found, C, 79.77 ; H, 8.44 ; N, 11.60.

Synthesis of complex E1

A Mixture of 0.2g of ligand T1 dissolve in 25 ml of abs.ethanol by stirring and reflex with 0.19g of $NiCl_2$.6H2O for 3hr at 40-50ºC and the brown precipitate was formed, filtrate off. and air dried. MP:289-293 C_o ; yelled: 83.3% ; mol.formula: $C_{16}H_{20}$ N_2Cl_2 Ni ; M.wt: 369.94 ;C, 51.94 ; H, 5.46 ; N, 7.57 ;Found, C, 51,88 ; H, 5.45 ; N, 7.61

Synthesis of complex E2

A Mixture of (0.2g) of ligand (T1) dissolve in (25 ml) of abs.ethanol by stirring and reflex with (0.14g) of $CuCl_2.6H_2O$ for 3hr at 40-50ºC and the blue precipitate was formed, filtrate off. and air dried. MP:243-245 C_o ; yelled: 78.8%; mol. formula: $C_{16}H_{20}$ N_2Cl_2Cu ; M.wt: 374.80 ;C, 51.02; H, 5.39; N, 7.48 ; Found, C, 51.27 ; H, 5.38 ; N, 7.47

Synthesis of complex E3

A Mixture of (0.2g) of ligand (T1) dissolve in (25 ml) of abs.ethanol by stirring and reflex with (0.11g) of $ZnCl_2$.6H $_2$O for 3hr at 40-50ºC and the white precipitate was formed, filtrate off. and air dried. MP:210-213 C_o ; yelled: 70.0%; mol. formula: $C_{16}H_{20}N_2Cl_2Zn$; M.wt: 376.63; C, 51.02; H, 5.36; N, 7.44; Found; C, 51.10; H, 5.29; N, 7.93

The spectral method is an important method for finding possible synthetic formulas for complexes, especially colored ones. The UV - visible spectra are widely used in this field. The molar ratios method is an important method used to determine the ratio of (metal: ligand), and this method includes drawing the relationship between absorption on the y-axis and the concentration of (metal: ligand) on the x-axis, then we draw straight lines until they intersect and the point of intersection is the ratio (Metal: ligand) in complex [10]

It has been shown that the ratio of the ligand to the metal (M:L) is (1:1) and for all the complexes under consideration show Figure(1, 2 and 3)

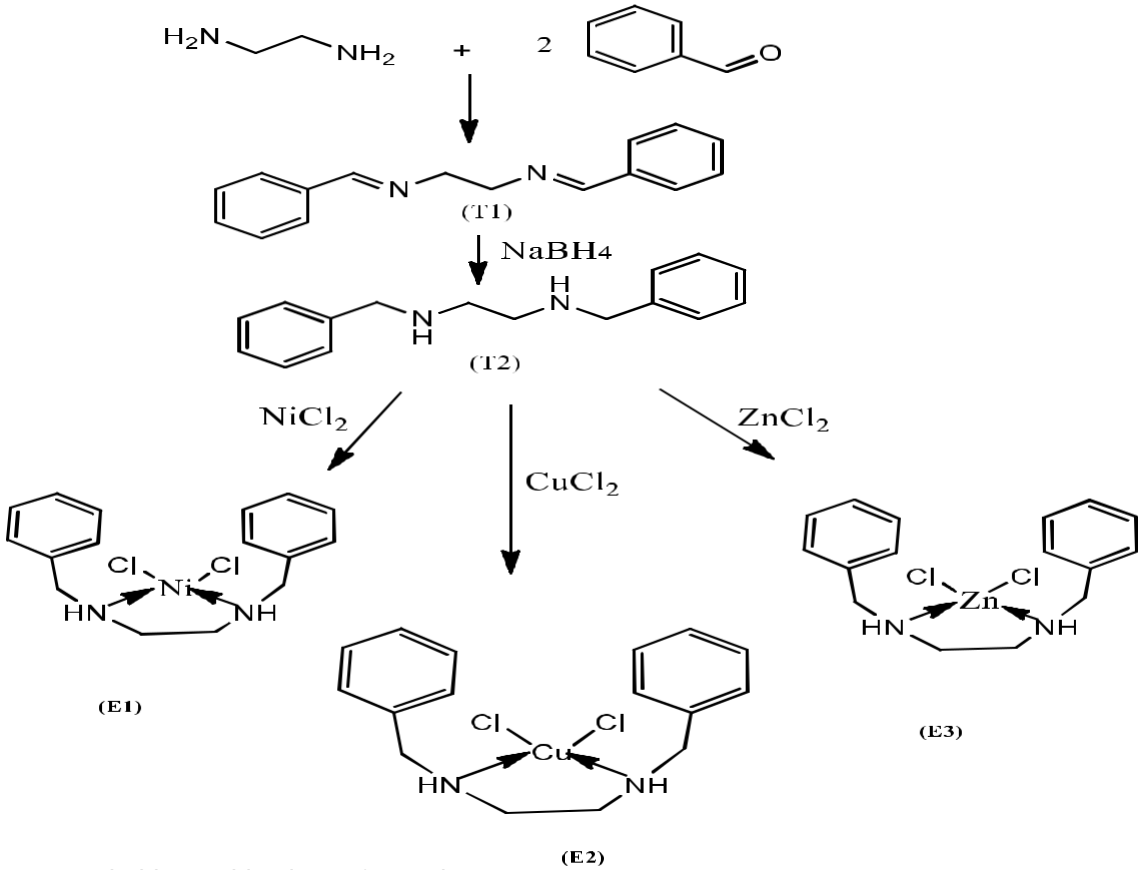

Diagnose probably combinations of complexes

Pure Sciences International Journal of Kerbala

Journal Homepage:https://journals.uokerbala.edu.iq/index.php/psijk

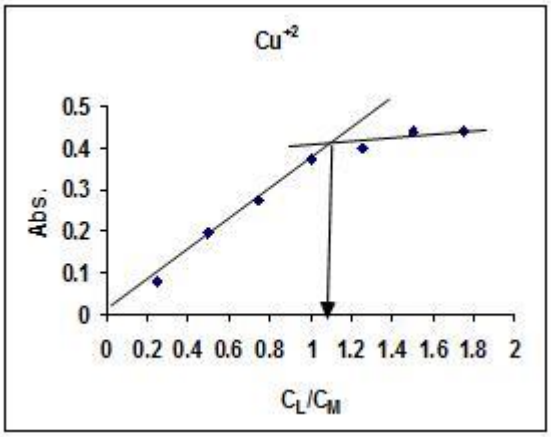

Fig.1: Between the molecular ratio for (Cu+2) with (T)

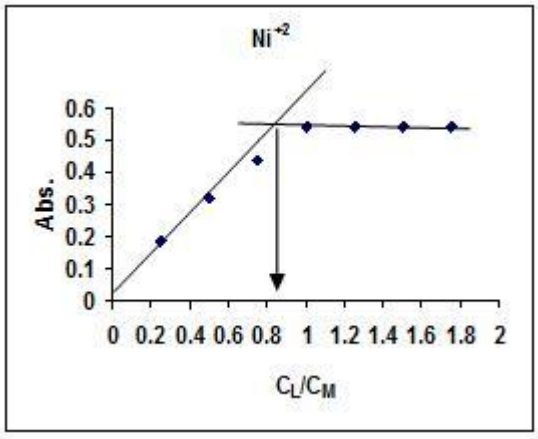

Fig.2: Between the molecular ratio for (Ni+2) with (T)

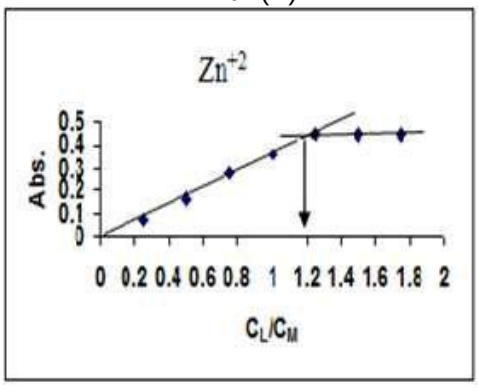

Fig.3: Between the molecular ratio for (Zn+2) with (T)

FT-IR spectra

The FT-IR spectra (KBr disk) for Schiff base (T) show disappearance of the stretching vibration bands that belong to the primary amino group and aromatic carbonyl group of benzaldehyde. A strong bands was appeared in 9 cm -1 which belong to the azomethine group, that conform the formation of the Schiff base[1]. ligand characterized by disappearance of ν(C=N) at 9 cm -1 and ν(CH=N) in compound T and appeared new band at 8for (NH). Different complex characterized by appeared new band in the rang (8 - 9 cm -1 which belong to the metal ligand. the main characteristic FT-IR bands are listed in Table (1).

Ultraviolet-Visible Spectra of the ligands (T) (T1)

The electronic spectra of the Ligand figure (4) show wide band in (λ=9nm belong to π → π* and N → π*, while The electronic spectra of reduced Ligand figure (5) show only two bands in (λ=0) nm belong to π → π* and (λ=8nm belong to N → π*, when we compared it with uv-spectrum of complexes have noticed the differences

Ultraviolet-Visible Spectra of complex (E1) (E2) (E3)

The electronic spectra of the complexes figure (6),(7) and (8) sho ws the peaks in UV region distributed to ligand field and transfer charge, while the visible region show a weak peaks at (λ=5nm and (λ=7nm due to the d -d transition type $^{1}A_{1g}$ $^{1}B_{1g}$, $^{1}A_{1g}$ $^{1}B_{2g}$ as agreement with the square planer geometry around Ni+2ion [2], and (λ=6nm due to the d-d transition type $^{2}T_{2g}$ $^{2}E_{g}$ as agreement with the tetrahedral geometry around Cu+2ion [3], while Zn+2complex show peak in ultraviolet area and not in the colored region, because it is colorless (white),which not have d-d transition and proves that is tetrahedral due to the fullness of the orbital d in it.

Magnetic susceptibility

Magnetic measurements were used extensively in the study of the transition metal complexes, as most of these metals possess single electrons and show Barra magnetic properties. Moreover, the greater the number of individual electrons, the greater the magnetic moment of the ion[4] [1HNMR

1H -NMR data for compound T1was recorded by using DMSO-d6as a solvent and the chemical shift in ppm. the signal of proton of Methylene (Ar-C^{H}2-N) was appeared in (3.6ppm,4H) and the aromatic protons in range of (7.2 -7.4ppm,10H), the signal of proton Methylene group of ethaline di amine (N-C^{H}2-C^{H}2-N) in (2.8ppm,4H) while N ^{H} was appeared in (2.0ppm,2H). [5]

Pure Sciences International Journal of Kerbala

Journal Homepage:https://journals.uokerbala.edu.iq/index.php/psijk

Table 1: The main characteristic FT-IR bands for (T, T1, E1, E2 and E3) compounds

Comp.	(N-H) υ	(CH_2) υ aliphatic	)aromatic CH_2)υ	(CH=N)υ	(C=C) υ	(C=N)υ	(C-N)υ	(C-C)υ	(M-N)υ
T	……	(8	(9	(0	(6	(5	(1	(3	……..
T1	(3	(2	(0	…….	(0	…….	(3	(0	……..
E1	(6	(2	(6	…….	(6	……	(2	(2	(3
E2	(6	(0	(6	……	(6	……	(1	(5	(3
E3	(3	(2	(2	…..	(8	……	(0	(8	(0

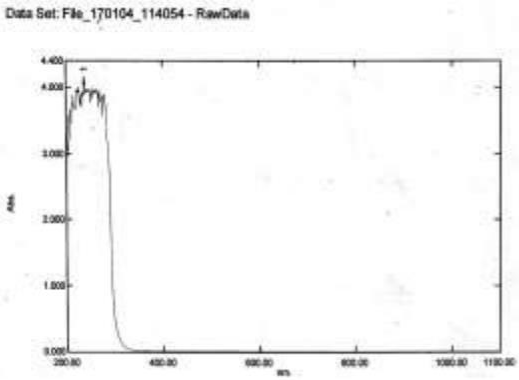

Fig.4: UV-visible spectrum of unreduced ligand

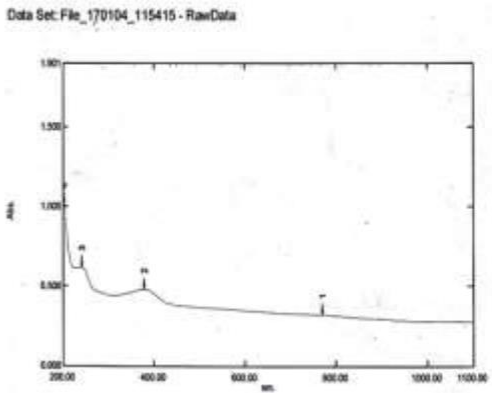

Fig.6: UV-visible spectrum of Ni complex

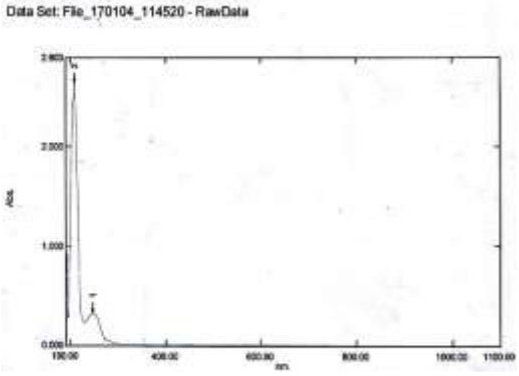

Fig.5: UV-visible spectrum of reduced ligand

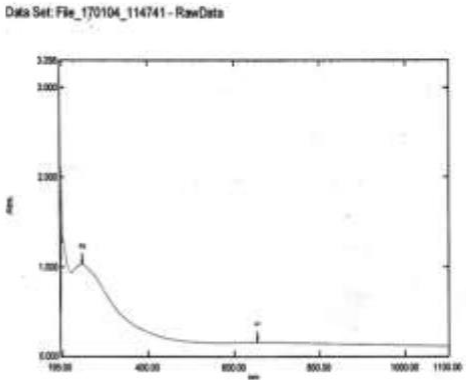

Fig.7: UV-visible spectrum of Cu complex

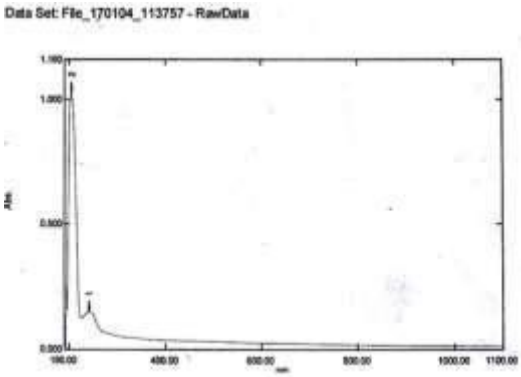

Fig.8: UV-visible spectrum of Zn complex

Table 2: The values of magnetic sensitivity and electronic spectra of complexes

Complexes	μ_{eff}(B.M)	λ^{max}	Assignment	Propsed structure
[Ni (L)Cl_2]	(2	(7 (9	^1B_2g ^1A_1g ^1A_1g ^{1}[redacted]	Sp
[Cu (L)Cl_2]	(7	(5	^2T_2g ^2Eg	Td
[Zn (L)Cl_2]	(0	(2		Td

Pure Sciences International Journal of Kerbala

Journal Homepage:https://journals.uokerbala.edu.iq/index.php/psijk

Fig.9: 1H-NMR of T1

Electrical conductivity

In our research, the molar electrical conductivity of solid alkali complexes of the study ions concerned with prepared ligands was measured at a concentration of (10 -3M x 1) in ethanol solvent and at laboratory temperature. It was found from the results of electrical conductivity that all prepared complexes are non-electrolytic (non-) [6]As shown in Table (3).

The antibacterial activity

The bacterial strain *Escherichia coli* and *Staphylococcus aureus* were used in this work and then cultured on muller-hinton medium and incubated at 37 for 24h the standardized antimicrobial disc were prepared from (L, E1, E2and E3) by using sternal filter paper disc saturated with solution for each compounds

For *Staphylococcus aureus* the highest inhibitory effect was observed in compound E3which showed low effect from bacteria and followed the inhibitory effect is low from E2 to E1and the lowest effect can sow it in compound T show Figure (10). For *E. coli* the highest inhibitory effect was observed in compound E3 followed by E2 and the lowest antibacterial activity was observed with compound E1 and then was no activity with T compound show Figure (11).

Table 3: Electrical conductivity values of prepared ligand and complexes

Complex	Λ_m (S.mol^{-1}.cm^2) In(EtOH)
[T]	38
[T1]	55
[Ni (E1)]	92
[Cu (E2)]	103
[Zn (E3)]	111

Fig.10: Esheriechia coli zone.

Fig.11: Staphylococcus aureas zone.

Table 4: Zone inhibition (Key of symbols: zone inhibition =mm)

Compound	*Staphylococcus aureas*	*Esheriechia coli*
T (1)	1	-
E1(2)	3	1
E2(3)	2	1
E3(4)	3	3

The biological activity as well as the molar conductivity and magnetic the success stability. Suggested geometry around the Zinc and Copper ions is tetrahedral and square planer around nickel ion.

REFERENCES

1. Kadhim KJ, Munahi MG. Synthesis, characterization and biological evaluation of some novel Schiff's bases derived from vanillin. *J Glob Pharma Tech*. 8(8).
2 Hameed A, al-Rashida M, Uroos M, Abid Ali S, Khan KM. Schiff bases in medicinal chemistry: a patent review (0 - 4 *Expert Opin Ther Pat*. 2(2):3 -7
3 Pesek JJ, Frost JH. Synthesis of Imines from Aromatic Aldehydes and Aliphatic Amines in Aqueous Solution. *Synth Commun*. 6(3 -2

Pure Sciences International Journal of Kerbala

Journal Homepage:https://journals.uokerbala.edu.iq/index.php/psijk

4. March J. *Advanced Organic Chemistry: Reactions, Mechanisms, and Structure*. John Wiley & Sons,; 1992.
5. Bhattacharyya S, Pathak U, Mathur S, Vishnoi S, Jain R. Selective N-alkylation of primary amines with R–NH2· HBr and alkyl bromides using a competitive deprotonation/protonation strategy. *RSC Adv*. 2014;4(35):18229-18233.
6. Linden A, Basu Baul TS, Singh KS. 2-{(E) -3-[(E)-4-Bromophenyliminomethyl]-4-hydroxyphenyldiazenyl} benzoic acid toluene hemisolvate. *Acta Crystallogr Sect E Struct Reports Online*. 2006;62(6):o2566-o2568.
7. Alnasrawi TH, Althabet ZA, Salih GS, Al-Jassani MJ. Antibacterial Activity of Some Nanoparticles Against Some Pathogenic Bacteria That Isolated From Urinary Tract Infections Patient. *Int J Drug Deliv Technol*. 2019;9(04):682-685.
8. Al-Haideri MR, Rasool SR. New Imidazolidine-dione Derivatives: Synthesis, Characterization and Spectroscopic study.
9. Sumrra SH, Atif AH, Zafar MN, et al. Synthesis, crystal structure, spectral and DFT studies of potent isatin derived metal complexes. *J Mol Struct*. 2018;1166:110-120.
10. GALEN W. *INSTRUMENTAL METHODS OF CHEMICAL ANALYSIS*.; 1985.
11. Herzfeld R, Nagy P. Studies of the solvent effect observed in the absorption spectra of certain types of Schiff bases. *Curr Org Chem*. 2001;5(3):373-394.
12. Jawad SA. Synthesis and characterization of azo amidazole ligand type N2 and metal complexes with di valence cobalt, nickel and copper. *Al-Qadisiyah J Pure Sci*. 2017;22(3):20-34.
13. Silverstein RM, Bassler GC. Spectrometric identification of organic compounds. *J Chem Educ*. 1962;39(11):546.
14. Skoog DA, West DM, Holler FJ, Crouch SR. *Fundamentals of Analytical Chemistry*. Nelson Education; 2013.

First Year-First Folder-Number: 0
PSIJK 184-191

Pure Sciences International Journal of Kerbala

Journal Homepage:https://journals.uokerbala.edu.iq/index.php/psijk

Assessment of red dragon fruit (Hylocereus Polyrhizus) extract effect on the adverse effects of Sodium Nitrate - induced kidney injury

Rawaa Hamid Abdulshahed [1*], Ashwaq Kadhem Obeid [2], Hussein Ali Abd AL-Latif [3]

[1] Department of Biology, College of Education for pure Sciences, Kerbala University, Kerbala, IRAQ
[2] Assistant Professor, Department of Biology, College of Education for pure Sciences, Kerbala University, Kerbala, IRAQ
3 Professor, Department of Biology, College of Education for pure Sciences, University Kerbala, Kerbala, IRAQ *Corresponding author: Rawaa Hamid abdulshahed

PAPER INFO

Paper history:

Keywords:
Hylocereus polyrhizus Nitrate, histopathology, oxidative stress, kidney, Sodium Nitrate

ABSTRACT

Objective: The study aimed to detect the biological vitality of Hylocereus polyrhizus fruits extract in protecting kidney tissue against oxidative stress induced by Sodium Nitrate toxicity.
Methods: 36 Male albino rats were randomly divided into six groups each group contain 6 rats treated for 30 days: Group 1 a control group, Group 2 treated group with NaNO3 in 150 mg /kg concentration orally by gavage, Group 3: normal rats dosed aqueous extracts of red dragon fruits 250mg /kg, Group 4: normal rats dosed aqueous extracts of red dragon fruits 500 mg /kg, Group 5: normal rats received aqueous extracts of red dragon fruits 250 mg /kg and before 4 h receive Sodium Nitrate with 150 mg/kg and Group 6 received aqueous extracts of red dragon fruits 500 mg /kg before 4 h receive Sodium Nitrate with 150 mg/kg. MDA levels were measured using the Thiobarbituric acid test,) Glutathione was measured using the Ellman's Reagent method, Estimating the level of catalase enzyme using the method Basic principle: $2H2O2 \rightarrow 2H2O + O2$ and kidney histopathology features were stained with Hematoxylin-Eosin.
Results: The aqueous extract polyrhizus of Hylocereus at doses of 250 and 500 mg/kg body weight orally significantly protected the Sodium nitrate induced kidney toxicity in albino rat by increment of Glutathione and Catalyase enzymes and decreases MDA. Histologically the activity of extract was also protect the kidney damage induced by sodium nitrate repsented by degeneration of some tubules and atrophy of glomerular, congestion of glomerular tuft and expanded Bowman Space.
Conclusion: The study suggested that the aqeuous extract of Hylocereus polyrhizus fruit enhances the oxidative stress defense status against renal toxicity.

INTRODUCTION

The Red dragon fruit, also known as the *Hylocereus polyrhizus*, has recently attracted attention stemming from farmers and consumers, and it is now found in exotic fruit markets around the world (Heryani,2016) not only for its famously attractive purple-red color or its economic value as produce, but also for its highly active biological compounds that include antioxidant, anti-inflammatory, anti-microbial (particularly for Salmonella Typhi), and anti-bacterial against Gram (-), Gram (+) (Ortiz *et al*.,2012; Claudya & Febrianti, 2019).

It also has the ability to inhibit the growth of cancer cells and has an anti-diabetic (Kim etal., 2010) as well as an anti-atherosclerotic effect. Moreover, it has the ability to protect the liver and kidneys (reno and hepato-protection according to (Hernawti *et al*.2018). Dragon fruit is a plant that belongs to the cactaceae cactus family. It grows widely in tropical areas such as Southeast Asia, Mexico, Cambodia,

Indonesia, Australia and the United States. It has wide uses in the fields of food, therapy and medicine (Febrianti *et al*., 2018) (Mihi, 2019) The importance of effective phytochemical bioactive compounds in the pulp of the

red dragon fruit like polyphenols, flavonoids, and vitamins A,C & E. As they are anti-oxidants, they are able to assist with the balancing of oxidative stress, which the body is constantly exposed to the environmental and food system, especially foods with food additives, including preservatives (Anand & sati, 2013; Armutcu et al., 2018).

Pure Sciences International Journal of Kerbala

Journal Homepage:https://journals.uokerbala.edu.iq/index.php/psijk

Preservatives are used to inhibit or stop the decomposition of foods by microorganisms, and consequently to prolong the storage period for food. However, these substances have side effects or metabolites that produce toxins that affect human health (Carocho,2014) including sodium nitrate -a salt of nitric acid consisting of one nitrogen atom and three oxygen atoms with sodium ion- which is a colorless crystalline salt that can be naturally obtained either by the body from food containing nitrates (such as lettuce and spinach vegetables), by water containing nitrate ion, or formed in the body by the action of the enzyme Arginie - No synthase (Song et al.,2015) (Nujic & Habuda, 2017).

Sodium Nitrate NaNO3 is also present in some industrial materials such as fertilizers, pesticides, Weapons, fireworks, and medicines used in cardiovascular diseases. Sodium nitrate (e251) is added to processed meat such as sausage and bacon (reddy,2018) for the purpose of preserving it from decomposition by clostridium bacteria (metensen, 2017). When sodium nitrate is present in daily dietary intakes with high concentrations, it causes harmful effects in the body due to the metabolism of nitrates to no2, which has the ability to form carcinogenic nitrous compounds and cause damage to tissues and organs (katan, 2009; rangabhashiyam et al., 2014

MATERIALS AND METHOD

Experimental Animals In this study

36 Adult white Wistar rats (Rattus norvegicus) whose weights ranged between 280-350 grams and whose ages ranged between 12-14 weeks and bred in the animal housing facilities of the College of Pharmacy at the University of Karbala from December 2019 to January 2020. The animals were placed in special plastic cages covered with metal covers, their floors were covered with soft sawdust, and the cleanliness of the cages was meticulously maintained, which included regularly replacing the sawdust and sterilising the floor with disinfectants, as well as continuous care with the cleanliness of the irrigation bottles as well as the dissection room. Moreover, the animals were supplied with the standard amount of water and feed ad libitum (freely) for the duration of the research, and the animals were allowed for two weeks to adapt correctly to the conditions of the environment before the experiment and to make sure they were disease-free.

The plant used

The Red dragon fruit was purchased from Alwa Al-Rasheed Market in Baghdad, which and was transferred to the laboratories of the College of Education for Pure Sciences for the department of biology of the University of Karbala Preparation of aqueous extract of dragon fruit

Aqueous Extract: The fruit was washed under running water and cleaned thoroughly to remove all traces of insects, dust and other types of pollutants. It was then dried and weighed and crushed with fruit juices. Once it had itself turned into juice it was filtered by several layers of gauze paper and then the juice was diluted by 20% with distilled water. The mixture was then left in a container wrapped in aluminum foil & was starred regularly for 12 hours. It was then filtered and poured, with the help of sterile utensils, to be allowed to dry at a temperature of (40 -45) ° C in an oven. The crude extract was then collected using a skimmer and placed in sterile, dark and clean glassware in the refrigerator whose temperature ranged from 2-4° C for later use in the experiment. This method of preparation was like that of Harborne, (1984), and by modifications according to Sato et al. (1990). The mixture was then prepared in doses of the concentration 250mg/kg and 500 mg/kg, according to the body weight of the animals.

Calculation of Sodium Nitrate dose

The dose for the rat was 150mg/kg calculated according to the lethal dose (1921.15mg/kg) calculated by (Speijers et al., 1989; FAO/WHO, 1996; Albabily, 2006)

Experimental design: 36 male rats randomly were divide d into six groups, each consisting of -6 rats each groups treated for 30 days. **Group 1**: Served as control group dosed normal sline; **Group 2:** rats dosed Sodium Nitrate with 150 mg/kg concentrations orally; **Group 3:** normal rats received aqueous extracts of red dragon fruits 250mg /kg; **Group 4**: normal rats received aqueous extracts of red dragon fruits 500 mg /kg. **Group 5**: normal rats received aqueous extracts of red dragon fruits 250 mg /kg and before 4 h receive Sodium Nitrate with 150 mg/kg **Group 6** received aqueous extracts of red dragon fruits 500 mg /kg before 4 h receive Sodium Nitrate with 150 mg/kg

Tissue sampling and processing: Rats from all groups in each were anaesthetized with,. The kidneys were then removed and divided into segments. These segments were fixed in 10% formalin for 48 hours. The samples then dehydrated in ascending grades of alcohol, cleared in xylene and embedded in paraffin wax at 56 C in oven and made as blocks. The blocks were carefully oriented to have the cross in microtome. Five µm thickness serial sections were cut. The sections were deparaffinied and hydrated for hematoxylin and eosin (for general histological picture). (Suvarna et al, 2013).

Pure Sciences International Journal of Kerbala

Journal Homepage:https://journals.uokerbala.edu.iq/index.php/psijk

Blood sampling and processing: after 24 hours of administering, blood samples were collected for biochemical parameters. Samples collection: Blood samples were collected from heart puncture into clean dry centrifuge tubes allowed to clot, serum was separated after centrifugation at 3000rpm for 15 minutes (Fox,1984).

Determination of Catalase Level Estimating the level of catalase enzyme using the method (Hadwan and Abed, 2016) Basic principle: $2H_2O_2 \rightarrow 2H_2O + O_2$ The

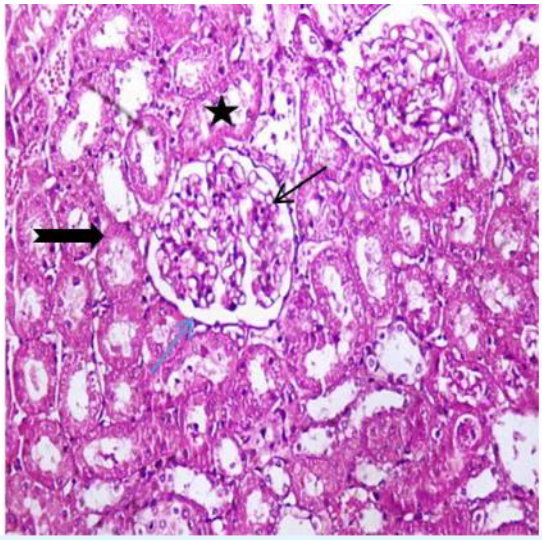

Fig. 1. Kidney section of rat (control) Showing normal appearance of Bowman Capsule (blue arrow), glomerulus (thin arrow), distal tubules (thick arrow) and proximal convoluted tubules(star). (H&E 200X)

catalase activity was evaluated by preparing enzymes in 1.0 ml of the reactant (65 mmol / ml of hydrogen peroxide at 60 mmol / 1 sodium phosphate-potassium PH7.4) at 37 ° C for three minutes, work was stopped with ammonium molybdate, measured Absorption in the yellow compound in molybdates and hydrogen peroxide at 374nm for the blank(Hadwan,2018)

Determination of Reduced Glutathione (GSH) Glutathione was measured using the Ellman's Reagent (DTNB) method described by Moron et al (1979). The absorbance was estimated at 412 nm using the spectrophotometer device

Determination of Malondialdehyde (MDA) The Malondialdehyde was determined by using the method of thiobarbituric acid (TBA). Based on the reaction of TBA with MDA, absorption was read at a 532 nm wavelength using spectrophotometer (Lefevre,1998).

Statistical analysis: Data was estimated via one-way analysis of variance (ANOVA) and were analyzed with SPSS version 22 software and presented in form of means and standard deviation, Statistical significance was set at $p \leq 0.05$. The differences of injury between six groups were analyzed using LSD test.

RESULTS & DISCUSSION

The Histological study

The histological study showed that the histological sections of the kidney of the laboratory rats in the control group, **Fig. 1** showing normal appearance of Bowman Capsule, glomerulus, distal tubules and proximal convoluted tubules. **Fig. 3** and **Fig. 4** groups, sections of kidneys of rats dosed aqueous extract of red dragon fruit at concentrations of 250 and 500 mg/kg, respectively, showing normal appearance Bowman Capsule,and glomerulus,distal tubules and proximal convoluted

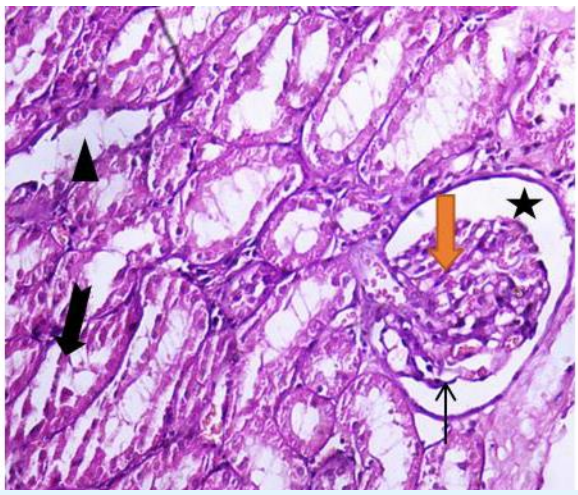

Fig. 2. Kidney section of rat, treated with sodium nitrate showing atrophy of glomerular (thin arrow), congestion of glomerular tuft(red arrow), expanded Bowman Space (star), degeneration renal tubular (thick arrow), dissolution in the cortex)), (H &E 200X)

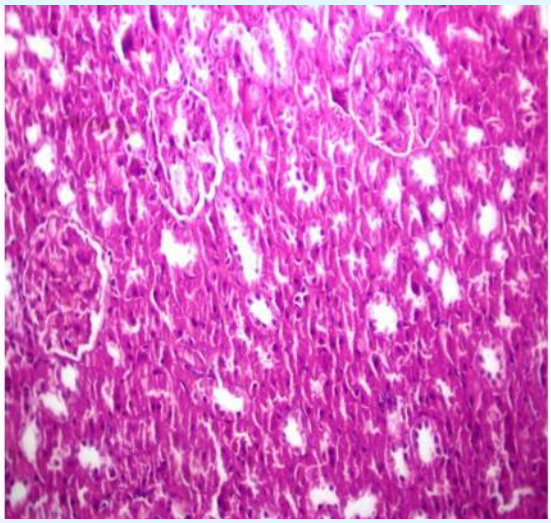

Fig. 3. Kidney section of rat dosed 250 mg/kg of HC extract showing normal appearance Bowman Capsule (blue arrow), and glomerulus (thin arrow), distal tubules (thick arrow) and proximal convoluted tubules (▲). (H&E 200X) HC: **Hylocereus polyrhizus**

Pure Sciences International Journal of Kerbala

Journal Homepage:https://journals.uokerbala.edu.iq/index.php/psijk

tubules under a microscopic enlargement of stain Hematoxylin -Eosin. And these have not differences with control group This is consistent with (Prasetyo *et al*, 2018).

The second group (**Fig. 2**), in which NaNO3 was orally administered, recorded significant tissue changes represented Kidney section of rat, treated with sodium nitrate showing atrophy of glomerular, congestion of
glomerular tuft, expanded Bowman Space, degeneration renal tubular and dissolution in the cortex. This is consistent with (Galaly & Mahmoud,2012.)

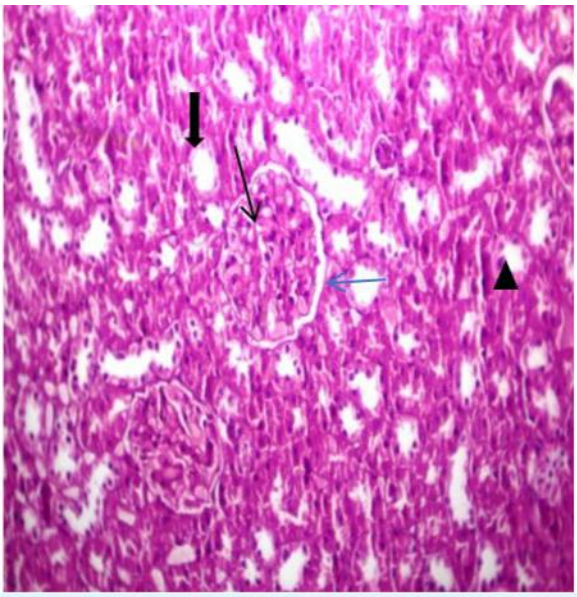

Fig. 4. Kidney section of rat dosed 500 mg/kg of HC extract show intact Bowman Capsule (blue arrow),and glomerulus (thin arrow), distal tubules (thick arrow) and proximal convoluted tubules(▲). (H&E 200X).HC: **Hylocereus polyrhizus**

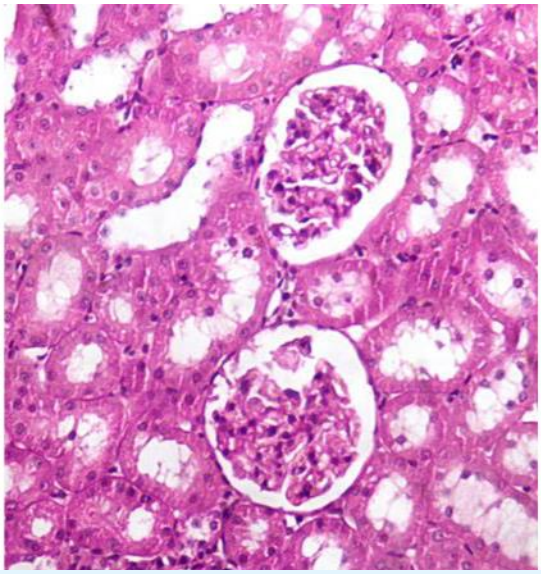

Fig. 5. Kidney section of rat received 250 mg/kg of HC extract and sodium nitrate 150 mg/kg showing nearly normal renal corpuscles (thin arrow), and renal tubules apart from few dilated lumina (thick arrow), expanded Bowman Space (star), and some degeneration of epithelial
lining cell of renal tubule) ▲((H&E 200X).HC: **Hylocereus polyrhizus**

(Anwar & Mohamed, 2018) and the reason is caused by oxidative stress resulting from exposure to nitrogen oxides stem from the metabolism of Sodium Nitrate, which leads to a high level of Nitrite in the urine and serum, and high Nitrite has toxic effects due to the free radical ratios based on nitrogen-based RNS such as NO, Peroxide Nitrite, and the oxygen-based free radicals

Pure Sciences International Journal of Kerbala

Journal Homepage:https://journals.uokerbala.edu.iq/index.php/psijk

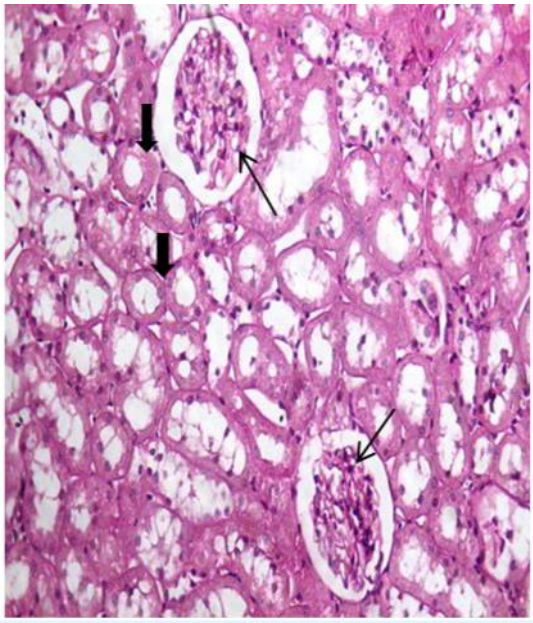

Fig. 6. Kidney section of rat received 500 mg/kg of HC extract and sodium nitrate 150 mg/kg showing nearly normal glomerulus (thin arrow), and renal tubules (thick arrow). (H&E 200X) HC: **Hylocereus polyrhizus**

ROS, that ultimately cause lipid peroxidation and break down the cellular membranes of the renal tubules (Li, *et al*.,2015) (Gheibi *et al*., 2018).

The results of histological examination showed that Kidney section of rat treated with 250 mg/kg of HC extract decrease the damage in the tissue caused by sodium nitrate 150 mg/kg showing kidney tissue was not affected when animals were protective in this extract and with the two above concentrations (**Fig. 5**). As **Fig. 5** (G5) nearly normal renal corpuscles, and renal tubules apart from few dilated lumina, expanded Bowman Space and some degeneration of epithelial lining cell of renal tubule (**Fig. 5**). In **Fig. 6** (HC500+ Sod. Nitrate), Kidney section of rat treated with 500 mg/kg of HC extract and sodium nitrate 150 mg/kg showing nearly normal glomerulus and renal arrow. (**Fig. 6**), according to the, extract's bioactive contents such as poly phenols, flavonoids, Cartenoids, beta-cyanine, betalanine, fatty acids and amino acids give them an antioxidant property, (Liaotrakoon, 2013) (Febrianti, 2018) as they are able to give a hydrogen atom to free radicals and stop their harmful action on the tissue as a result of reducing the lipid peroxidation process and protecting cell membranes from oxidative damage and strengthening the system of repairing cellular damage. this agreed with (Parasetyo *et al*.,2018).

Biochemistery study

The results of the current study showed a significant decrease ($p \leq 0.05$)in the level of (GSH) Glutathione and the effectiveness of the catalase enzyme (CAT) in G2 treated with sodium nitrate for 30 days and a significant increase in the level of Glutathione and catalase enzyme in the groups(G3,G4) treated with the aqueous extract of

Pure Sciences International Journal of Kerbala

Journal Homepage:https://journals.uokerbala.edu.iq/index.php/psijk

Table 1. Effect Of Red Dragon Fruit Auqeous Extract On antioxidants and MDA concentration in Rats Treated With Sod. Nitrate

Mean±S.D Treatment	Catalase CAT KU/L	Glutathione GSH µmol/L	Malondialdehyde MDA µmol/L
G1 control Normal Saline	A 3.56±0.03	A 11.80±0.47	A 12.64±0.47
G2 Sod.Nitrate 150 mg	B 3.07±0.02	B 6.02±0.26	B 16.63±0.97
G3 HC250mg/kg	A 3.43±0.02	C 14.20±0.29	C 11.45±0.34
G4 HC500mg/kg	C 3.62±0.02	D 16.80±0.23	C 10.23±0.24
G5 HC250mg/kg + Sod.Nitrate	D 3.23±0.02	E 7.89±0.73	D 14.60±0.87
G6 HC500mg/kg + Sod.Nitrate	E 3.33±0.02	F 8.40±0.33	E 13.97±0.25

dragon fruit with a concentration of (250 and 500) mg/kg compared to the control group (G1) and a significant increase in the GSH and CAT concentrations in the two groups G5 and G6 compared to the group of sodium nitrate G2 (**Table 1**).

The reason for this decrease in G2 and the reason for the decrease in these antioxidant enzymes comes in agreement with (Ansari *et al*., 2017) if the radicals exist Free and the occurrence of induced oxidative stress state by the MDA height of the same group.

As for the height of the antioxidants enzymes mentioned in groups G3 and G4 and in groups G5 and G6 dosed with aqueous extract of dragon fruit in concentrations of (250 and 500) mg/kg, this is consistent with (Mihir *et al.*, 2019).

The protective role that recorded these groups is attributed to the possession of fruits for a number of phenolic, flavonoids compunds and vitamins, including ascorbic acid and tocopherol, which act as free radical scavengers and reactive oxygen species (ROS), thus working to inhibit oxidative damage and prevent fat peroxidation (Mahdi, 2016)

The study also showed in **Table 1** an increase ($p \leq 0.05$) in the concentration of MDA in the blood serum of the group dosed sodium nitrate for 30 days (G2) from the control group (G1). Also noted was a significant decrease in the concentration of MDA in the two groups dosed the aqueous extract of the red dragon fruit with a concentration of 250 & 500 MG/KG for the same duration symbolized (G3), (G4) respectively in comparison with (G1). That is consistent with (BouAziz, 2014) (Novita *et al*., 2020). It was also observed that there was a significant decrease in the MDA concentration in the two groups (G5) & (G6), the two protective doses extracted at a concentrationy of 250 and 500 mg/kg before being dosed with sodium nitrate compared with (G2) (**Table 1**), and this is consistent with (Mihir *et al*., 2019). The reason for the high concentration of MDA in our study in G2 is due to the generation of free radicals As a result of the NaNO3 transformation after ingestion for NO2 ione due to the commensal of bacteria on the surface of the tongue that continues to metabolize into NO which leads to the formation of free radicals, including ONOO- which leads to oxidative stress (Nujić *, & Habuda-Stanić. 2017) and this leads to damage to important biological molecules such as proteins, fats and nucleic acids. These results are consistent with (Helal, 2001) As for the reason for the low concentration of MDA in the groups of G3, G4, G5, G6, this can be due to the presence of the active compounds present in the extract that improve liver functions and provide an important biological function, which is to give the hydrogen atom to free radicals and prevent peroxidation of fats in the cell membranes, which prevents or reduces the release of MDA, and this is consistent with (Mihir *et al*., 2019).

REFERENCES

Al-bably,E.,(2006) Sodium Nitrate and Sperm Formation in Adult Rats, The First Scientific Conference on Life Sciences. Department of Life Sciences, College of Science, University of Mosul.

Anand, S. P., & Sati, N. (2013). Artificial preservatives and their harmful effects: looking toward nature for safer alternatives. International Journal of Pharmaceutical Sciences and Research, 4(7), 2496

Ansari FA, Ali SN, Arif H, Khan AA, Mahmood R (2017) Acute oral dose of sodium nitrite induces redox imbalance, DNA damage, metabolic and histological changes in ratintestine. PLoS ONE 12(4): e0175196.

Anwar, M.M. & Mohamed, N.E.. (2014). Amelioration of liver and kidney functions disorders induced by sodium nitrate in rats using wheat germ oil. Journal of Radiation Research and Applied Sciences. 1.10.1016/j.jrras.2014.11.004.

Armutcu, F., Akyol, S., & Akyol, O. (2018). The interaction of glutathione and thymoquinone and their antioxidant properties. Electronic Journal of General Medicine, 15(4), em59.

Pure Sciences International Journal of Kerbala

Journal Homepage:https://journals.uokerbala.edu.iq/index.php/psijk

Bouaziz-Ketata, H., Salah, G. B., Salah, H. B., Marrekchi, R., Jamoussi, K., Boudawara, T.,... & Zeghal, N. (2014). Nitrate-induced Biochemical and Histopathological Changes in the Liver of Rats: Ameliorative Effect of Hyparrhenia hirta. Biomed Environ Sci, 27(9), 695-706.

Carocho, M., Barreiro, M. F., Morales, P., & Ferreira, I. C. (2014). Adding molecules to food, pros and cons: A review on synthetic and natural food additives. Comprehensive Reviews in Food Science and Food Safety, 13(4), 377-399

FAO/WHO (1996) Toxicological evaluation of certain food additives and contaminants. Geneva, World Health Organization, Joint FAO/WHO Expert Committee on Food Additives (WHO Food Additiv es Series No. 35)

Febrianti, N., Purbosari, P. P., Hertiani, T., & Moeljopawiro, S. (2018). Kandungan asam askorbat pada kulit dan daging buah naga merah (Hylocereus polyrhizus) DENGAN BERBAGAI METODE EKSTRAKSI. BioWallacea, 4(1), 41-45

Fox JG.; Cohen BJ.and Loew FM (1984). Laboratory Animal Medicine. Academic press London, U.K.: 19-120

Galaly,S. and. Mahmoud,M (2012). The protective effect of vitamin A against sodium nitrate inducedtoxicity in liver and kidney of albino rats: histological and ultrastructural study. J Am Sci 2012;8(12):293-308]. (ISSN: 1545-1003). http://www.jofamericanscience.org. 43

Gheibi S, Jeddi S, Carlström M, Gholami H and Ghasemi A. 2018, Effects of long-term nitrate supplementation on carbohydrate metabolism, lipid profiles, oxidative stress, and inflammation in male obese type 2 diabetic rats. Nitric Oxide.Vol, 75, p 27-41

Hadwan MH, kadhum Ali S. New spectrophotometric assay for assessments of catalase activity in biological samples. Analytical biochemistry. 2018 Feb 1;542:29-33.

Helal EGE. Progressive effects of the interaction of sodium nitrite and sunset yellow on different physiological parameters in albino rats. Egypt J Hospit Med, 2001; 2, 23-46

Hernawati;Setiawan, N.; A.Shintawati, R;.Priyandoko, D (2018). The role of red dragon fruit peel (Hylocereus polyrhizus) to improvement blood lipid levels of hyperlipidaemia male mice. Published under licence by IOP Publishing Ltd Journal of Physics: Conference Series, Volume 1013, 4th International Seminar of Mathematics, Science and Computer Science Education 14 October 2017, Bandung, Indonesia

Heryani, R. (2016). Pengaruh ekstrak buah naga merah terhadap profil lipid darah tikus putih hiperlipidemia. Jurnal Ipteks Terapan, 10(1), 9-17

Katan, M.B. (2009): Nitrate in foods: harmful or healthy?, Am. J. of Clin.l Nutr. 1-3, 11-12

Kim H, Choi HK, Moon JY, Kim YS, Mosaddik A, Cho SK. Comparative antioxidant and antiproliferative activities of red and white pitayas and their correlation with flavonoid and polyphenol content. Journal of food science. 2011;76(1):C38-C45.

Lefevre G, Beljean-Leymarie M, Beyerle F, Bonnefont-Rousselot D, Cristol JP, Therond P, Torreilles J. Evaluation of lipid peroxidation by assaying the thiobarbituric acid-reactive substances. InAnnales de biologie clinique 1998 May 22 (Vol. 56, No. 3, pp. 305-19).

Liaotrakoon W. Characterization of dragon fruit (Hylocereus spp.) components with valorization potential: Ghent University; 2013.

Mahdi,Ch.;Hendrawan, V.; Viestaria,Kh. (2019).The Effect of Red Pitaya Peel (Hylocereus polyrhizus Extract) on Malondialdehida Levels and Histopathology Profle in Diazinon Induced Rat (Rattus norvegicus). Indones. J. Cancer Chemoprevent., 10(2), 88-93

Mahdi,M.,(2016) Biosynthesis of Gold nanoparticles using Dragon fruit and study their biochemical properties. A Thesis submitted to The College of Science, Mustansiriyah University.

Marija Nujić*, Mirna Habuda-Stanić.2017.NITRATES AND NITRITES, METABOLISM AND TOXICITY. Food in Health and Disease, scientific-professional journal of nutrition and dietetics (2017) 6 (2) 48-89

Mihir Y P, Sachinkumar S, Tribhuvan S, Ishimo S, Nirali P. Antioxidant and Hepatoprotective Potential of Dragon Fruit Extract in 003 Opposition to Acetaminophen-Induce Liver Smash Up in Rats. Adv Res Gastroentero Hepatol. 2019; 12(5): 555846. DOI: 10.19080/ARGH.2019.12.555846

Moron M S, Depierre J W and Mannervik B (1979) Levels of glutathione, glutathione reductase and glutathione S-transferase activities in rat lung and liver. Biochimica et BiophysicaActa (BBA)-General Subjects 582(1), 67-78

Mortensen A.etal..Re-evaluation of sodium nitrate (E 251) and potassium nitrate (E 252) as food additives EFSA Journal 2017;15(6):47

Pure Sciences International Journal of Kerbala

Journal Homepage:https://journals.uokerbala.edu.iq/index.php/psijk

Ortiz Hernandez, Yolanda & Livera, Manuel & Carrillo-Salazar, J.A. & Botin, Alberto & Castillo-Martínez, R.. (2012). Agronomical, physiological, and cultural contributions of pitahaya (Hylocereus spp.) in Mexico. 60. 359-370. 10.1560/IJPS.60.3.359.

Prasetyo, B. F.;Shabrina, H.Juniantito, V.;Wientarsih, I. (2018).Activity of red dragon fruit (Hylocereus polyrhizus) juices on doxorubicin-induced nephropathy in rats IOP Conf. Series: Earth and Environmental Science 196 012037

Rangabhashiyam, S., Anu, N., Giri Nandagopal, M.S., Selvaraju, N. (2014): Relevance of isotherm models in biosorption of pollutants by agricultural byproducts, J. Environ. Chem. Eng. 2, 398-414.

Reddy, D., Reddy, G. and Mandal, P. (2018). Application of Natural Antioxidants in Meat and Meat Products-A Review. Food Nutr J: FDNJ-173. DOI, 10, 2575-7091.

Song, P., Wu, L., Guan, W. (2015): Dietary Nitrates, Nitrites and Nitrosamines Intake and the Risk of Gastric Cancer: A Meta-Analysis. Nutrients 7(12), 9872-9895

Speijers GJA et al. (1989) Integrated criteria document nitrate; effects. Appendix to RIVM Report No. 758473012. Bilthoven, National Institute for Public Health and the Environment) (RIVM Report No. A758473012) Novita Sari Harahap, Nurhayati Simatupang and Suprayitno, 2020. Potential of The Red Dragon Fruit (Hylocereus polyrhizus) as an Antioxidant in Strenuous Exercise. Biotechnology, 19: 18-22.

Suvarna K S, Layton C and Bancroft J D (2013) Bancroft's Theory and Practice of Histological Techniques. 7th edition. Elsevier Health Sciences.

Pure Sciences International Journal of Kerbala

Journal Homepage:https://journals.uokerbala.edu.iq/index.php/psijk

Occurrence, morphological, and molecular characteristics of *Trichophyton erinacei* in Iraq

Nadia N. H. AL Masaoodi1, Ban Taha Mohammed1, Jawad K. Abood Al-Janabi2*

1. 1Department of Biology, Pure Science College, University of Kerbala, Iraq, 2Department of Pathological Analysis Techniques, AL-Mustaqbal University College, Hilla, Iraq

*Corresponding author: Jawad K. Abood Al-Janabi, Department of Pathological Analysis Techniques, AL-Mustaqbal University College, Hilla, Iraq. E-mail: jka.uobsci.iq@gmail.com

P A P E R I N F O

Paper history:

Keywords:
Hylocereus polyrhizus Nitrate, histopathology, oxidative stress, kidney, Sodium Nitrate

A B S T R A C T

Background: Dermatophyte infections are caused by *Trichophyton erinacei*, which has been isolated from hedgehogs on numerous occasions. Although a variety of animal infections of this fungus have been observed in different countries, the pathogen has rarely been isolated from humans. **Aim:** This research was conducted to characterize the zoonotic isolate of *T. erinacei* through culture and molecular methods. **Materials and Methods:** An experiment was carried out on the different types of tinea identified on patients attending the Dermatology Unit at Al-Hussein Hospital in the holy city of Kerbala during the period from February to November 2018. **Results:** Based on clinical diagnoses and culture characteristics, the pathogen observed in tinea manuum, tinea faciei, and tinea corporis was identified as tinea erinaceid. The culture characteristics revealed white/cottony irregular colonies with septated elongated macroconidia and numerous pear-shaped microconidia attached along the side of the hyphae. This discovery was verified by sequencing the inner translated fungal nuclear ribosomal DNA spacers utilizing the inner translated spacer (ITS) 1-ITS4 universal primers. The fungus was recorded in the National Center for Biotechnology Information Center under entry number MK167440. The genetic tree of the fungus *T. erinacei* was shown to be related to the following global strains: The Netherlands (MH865913.1) and 96%, German (NKU257463.1) 88%, French (DQ786689.1) 88%, Iranian (1) KP789451, and Estonian (KC833522.1) 82%. **Conclusions:** This is the first report on *T. erinacei* tinea manuum infection in the Kerbala Province and, as far as is known, in the country of Iraq

INTRODUCTION

Trichophyton erinacei (J.M.B. Sm. and Marples; Quaife, 1966) is a zoophilic dermatophyte of the *Trichophyton mentagrophytes* complex.[1] It has been isolated from wild rodents[2] and from other types of animals, particularly from hunting dogs in countries that are home to hedgehogs and brown rabbits.[3,4] Certain pets have also been shown to carry the pathogen, particularly the terrestrial hedgehog, which is a natural host.[5] In addition, in Southeast Asia, skin infection caused by *T. erinacei* has been recorded after contact with an elephant.[6]

T. erinacei is believed to be responsible for human surface skin infections and causes a diffuse itchy rash on the contact area, including on the limbs. It is usually identified following exposure to a hedgehog.[7] The infection proportion of this pathogen in humans in Asia and the Middle East.[9] Infections have also been observed in New Zealand, Japan, and Western Europe and particularly in Korea and Taiwan.[1,7,10,11] It has been reported that the first infections caused by *T. erinacei* in Thailand occurred in the nails and skin and were expected to have transferred from a hedgehog.[12] Infections at other sites include kerion, tinea corporis, tinea unguium, and tinea faciei.[11] In Tunisia, the first *T. erinacei* infection case was confirmed as a separate species according to morphological and physiological features.[12]

The prevalence of hedgehogs, which are the cause of the transformation of *T. erinacei* infection into a severe zoonotic disease, is becoming an increasing concern. Prior research has shown that household hedgehog infections are growing.[13] The prevalence of hedgehogs in many parts of Iraq may be a risk factor for developing an infection caused by *T. erinacei*.[14] This organism is transmitted from hedgehogs and can cause highly inflammatory and pruritic eruptions, which typically present on the hands. This pathological

Access this article online

Website: jprsolutions.info | ISSN: 0975-7619

Pure Sciences International Journal of Kerbala

Journal Homepage:https://journals.uokerbala.edu.iq/index.php/psijk

state is known as tinea manuum.[1] However, as yet, there are no details in Iraq country about the number of infections of this tropical species that contain dermatophytes. Hedgehogs may be asymptomatic carriers of the fungus but play a key role for zoonotic transmission.[15,16] Researchers have investigated the different zoophilic fungi that cause human infections; however, to the best of our knowledge, no published research has examined *T. erinacei* as a human pathogen in Iraq. Despite the zoonotic importance of the transmission of some important pathogens and the role of this zoophilic fungus in the recent increase in the global number of human infections, this pathogen has not been documented in Iraq and there are no reports on the isolation and identification of *T. erinacei* as a human pathogen. The present study was conducted to investigate the occurrence of *T. erinacei* and characterize its zoonotic isolate through culture and molecular methods (a fragment series of the inner translated spacer [ITS] area).

MATERIALS AND METHODS

Preparation of Culture Media

Sabouraud Dextrose Agar (SDA), Potato Dextrose Broth, and Potato Dextrose Agar were prepared according to the manufactures' instructions and were fixed on their containers. All culture media were maintained at pH 5.6 with 0.05 g/l chloramphenicol and 0.5 g/l cycloheximide and were sterilized by autoclave at 15 psi/inch2 at 121°C for 15 min. A total of 15 ml sterilized medium was poured into disposable Petri dishes and incubated at 28 ± 1°C overnight to ensure sterility. The samples were subsequently stored at 4°C until being used.[17]

Specimen Collection

A total of 75 clinical specimens from skin scrapings were collected for different ages and genders from patients who attended Al-Hussein Hospital in the holy city of Kerbala for the period from February 2018 to November 2018.

Clinical and Morphological Characterization

Clinical diagnosis of tinea was made by consultant dermatologists. The patients' medical history was also discussed during a medical examination. Direct skin scrapings observations by microscope were made using 20% potassium hydroxide. The fungal structures were observed under the power objectives of ×100 and ×40.[18] The specimens were inoculated on SDA at pH 5.6 containing 0.05 g/l chloramphenicol and 0.05 g/l cycloheximide and were incubated at 28
± 1°C for 2–3 weeks.[17] *T. erinacei* was identified based on its morphological characteristics that were determined by direct analysis using cotton blue lactophenol and by holding in tubes with SDA at 4°C.[19,20] The pathogen was first examined after 7 days

followed by two examinations every 7 days for at least 21–28 days before being negative lyre ported. The distinguishing features of *T. erinacei* emerged within 10–20 days on incubating plates and the microscopic and macroscopic features were recorded. Further, growing colonies were examined for the presence or absence of pigments and for diffusion into the medium followed by topography (flat, raised, heaped) and the rate of magnification.[12]

Growth and Maintenance of *T. erinacei*

T. erinacei isolate was recultured on SDA by taking a 0.5 cm (diameter) cut from a recent colony of the fungus and placing it in the center of a petri dish (9 cm diameter) containing SDA supplemented at pH 5.6 with 0.05 g/l chloramphenicol and 0.5g/l cycloheximide. The isolate was subsequently incubated at 28 ± 1°C for 2 weeks before being kept at 4°C in a fridge. The fungus was held at 4°C on SDA pitches and was sub-cultivated each month during the experiment.

Molecular Characterizations *Genomic DNA extraction*

T. erinacei fungal cells (isolate number 3) were collected before being placed in a new sterilized 1.5 ml tube for DNA extraction. The extraction of genomic DNA from *T. erinacei* isolate was conducted with a grinder in the presence of liquid nitrogen for the initial mycelia break up. The final DNA extraction was performed with a singular purification kit (Genomic DNA Purification Kit, Zymogene, Orlando, FL, USA). A total of 6 µl DNA solution was utilized as a template for the resulting polymerase chain reaction (PCR) specimens and was subsequently quantified on 2% agarose gel using a NanoDrop spectrophotometer.

Detection of gene ITS using PCR

A molecular approach that is dependent on a sequencing analysis of the inner rRNA genes transcribed by spacer; ITS parts were utilized to verify the identification of *T. erinacei*. The PCR products of the ITS1 gene were analyzed by agarose gel electrophoresis. The ITS gene was detected using primers for amplification.
PCR primers based on the 18S rRNA gene to detect *T. erinacei* were designed in this study using data from the National Center for Biotechnology Information (*NCBI*) and the design of Primer 3 online, which was provided by Macrogen Company for DNA Technologies, South Korea. A fragment of 510 bp ITS1 was improved using a forward primer (F: 5' – GACGTTCCATCAGGGGTGAG-3 and

Pure Sciences International Journal of Kerbala

Journal Homepage:https://journals.uokerbala.edu.iq/index.php/psijk

ITS4 was improved using a reverse primer (R: 5' CTGAATTGGCTGCCCATTCG-3').
A total volume of 25 µl, consisting of 1.5 µl DNA, 5 µl Taq PCR Premix (Intron, Korea), and 1 µl, was added on a tube of every prime (10 pmol), and the water was

Pure Sciences International Journal of Kerbala

Journal Homepage:https://journals.uokerbala.edu.iq/index.php/psijk

subsequently extracted in a tube for a total volume of 25 µl. Thermal cycling conditions were followed with denaturation at 94°C for 3 min, followed by 35 cycles at 94°C for 45 s, 52°C for 1 min, and 72°C for 1 min; the final incubation was conducted with the Applied Biosystems at 72°C for 7 min. The product PCRs were isolated with 1.5% electrophoresis of agarose gel and visualized after a red stain (Intron Korea) was produced by ultraviolet (UV) exposure (302 nm).

Gene sequencing

Gene sequencing was performed at NICEM online (https://nicem.snu.ac.kr/main/?en_ skin=index. html; biotechnological laboratory and the Applied Biosystems DNA Sequencer 3730XL, Waltham, MA, USA). The basic local alignment identification tool (BLAST) was utilized with NCBI online (http://www. ncbi.nlm.nih.gov). Such studies were conducted after molecular and morphological recognition.

A maximum-likelihood tree was designed to establish the phylogenetic location of *T. erinacei*. The analysis was conducted with RAxML ver. 8.0.0. The tree bisection-reconnection procedure was applied to gain 1000 bootstrap replicates, as well as the evolutionary GTR+G model with the jModelTest 2.1.10 program utilizing the Bayesian information criterion.

RESULTS

Cultural Characteristics

The results shown in Table 1 indicate that only four dermatophyte isolates were identified as *T. erinacei* from 75 specimen samples taken from three anatomical sites. In tinea manuum (one isolate), the symptoms appeared as erythematous scaly lesions affecting the thenar of palm and surface of the index finger of both hands. Tinea faciei, which also represented one isolate, presented as erythematous lesions with multiple pustules affecting the chin, while tinea corporis (two isolates) presented as an annular patch with clearance in the center and activity at the margin.

T. erinacei is a pathogen that is mycologically caused. It was identified depending on the culture of skin scrapings for each patient. KOH examination demonstrated hyphae that were compatible with dermatophytes. *T. erinacei* grown on SDA produced fairly irregular white cottony colonies on the surface [Figure 1a] with a deep yellow to brown pigmented under-surface [Figure 1b]. *T. erinacei* had characteristic macroconidia that were elongated and were irregular in shape and

Table 1: Percentage of different types of tinea infection

Pure Sciences International Journal of Kerbala

Journal Homepage:https://journals.uokerbala.edu.iq/index.php/psijk

size, with 2–6 septa [Figure 1c1]. Numerous pear-shaped microconidia were attached along the side of the hyphae [Figure 1c2]. Morphology and microscopic examination primarily identified the characteristics of *T. erinacei*. Identification of this fungus was confirmed with molecular identification using one isolate (No. 3) based on the fully identical morphological and microscopy characteristics of the four isolates.

Molecular Identification

T. erinacei isolates IQT-No.3 ITS 1, part series; 5.8S ribosomal RNA gene, full series; and ITS 2, part series, GenBank: MK167440.1.

A series of the ITS of the fungal nuclear ribosomal DNA with uniform primary ITS1 ITS4 established the morphological characteristics of *T. erinacei* isolate. To identify the existence of a certain partial 18S ITS1 5.8S ITS2 parial28S rRNA gene, *T. erinacei* isolate was identified with the traditional PCR technique. The genomic DNAs isolated from these isolates were used as a guide to amplify the ITS1 in primary applications. The findings affirmed that the morphological amplicon size recognition equaled 665 bp after electrophoresis band and drug UV transillumination [Figure 2].

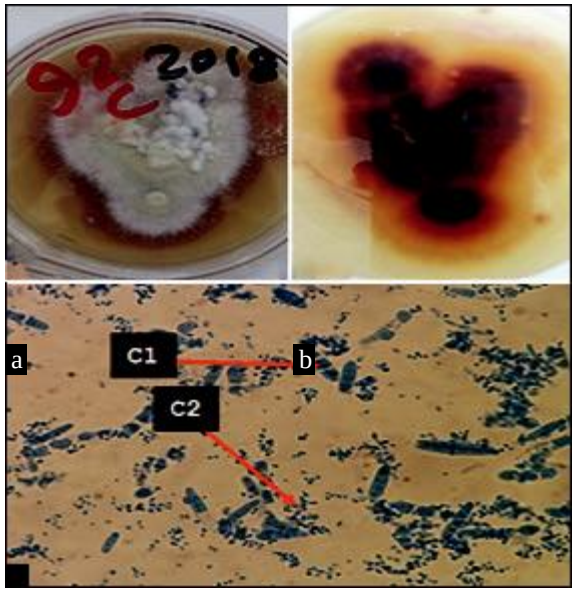

Figure 1: Macro and microscopic features of *Trichophyton erinacei* grown on an Sabouraud Dextrose Agar medium after 12 days inoculation at 28°C. Stained with lactophenol blue, a: Upper phase (white cottony colonies), b: Lower phase (dark yellow to brown pigmented under-surface), and c: Reproductive structures, c1: Macroconidia (smooth and thin wall with several septa) and c2: Microconidia was round and abundant (at ×40)

Pathogen	Tinea pedis	Tinea manuum	Tinea cruris	Tinea unguium	Tinea faciei	Tinea corporis	Tinea capitis
Trichophyton erinacei	0	1	0	0	1	2	0

Pure Sciences International Journal of Kerbala

Journal Homepage:https://journals.uokerbala.edu.iq/index.php/psijk

The results presented in Table 2 show that the local isolate *T. erinacei* (MK167440.1) was closely related to NCBI-Blast *T. erinacei* (MF153407.1) in Germany, with compatibility of 100%. Similar relationships were noted with the following strains: KJ606083.1 (USA), MN737888.1 (China), MN737936.1 (China), MF153405.2 (Germany), MK298980.1 (Belgium), MK298863.1 (Belgium), LT969629.1 (Czech Republic), LC413781.1 (Japan), KT155933.1 (the Netherlands), KT155878.1

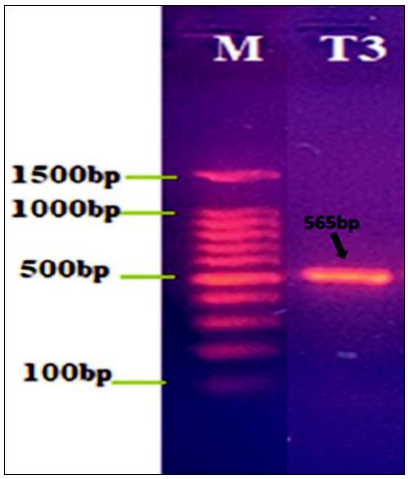

Figure 2: Polymerase chain reaction product electrophoresed in a 1.5% agarose gel at 5 volt/cm2. 1 × TBE buffer for 90 min. Where lane M (ladder of DNA)=Marker, 100–1500 bp; Lane (1). The product amplified with inner translated spacer 1 primer size was around bp 565 bp-lane

(2) of *Trichophyton erinacei* isolate (Netherlands), NR_149340.1 (USA), EF631615.1 (China), LT969625.1 (Czech Republic), MK298815.1 (Belgium), JN134091.1 (Iran), and LT969627.1 (Czech Republic). The compatibility for MH865913.1 (the Netherlands) strain was 96 and was 88% for NKU257463.1 (Germany), 88% forDQ786689.1 (France), 82% forKP789451.1 (Iran), and 82% forKC833522.1 (Estonia). *T. erinacei* isolates IQT-No. 3 ITS 1, part series; 5.8S ribosomal RNA gene, full series; and ITS 2, part series, GenBank: MK167440.1.

The idea of homology has previously suggested the presence of phylogenetically conserved regions among the tested isolates. *T. erinacei* sequence was isolated from clinical specimens of human dermatophytes in Kerbala City and was based on an 18S rRNA gene sequence submitted to GenBank. The findings of this series were analyzed and checked by qualified GenBank staff in two working days. The series was approved by GenBank and every series took the number of accessions (MK167440.1). These findings were reported and published in conjunction with the International Database of Nucleotide Sequence Collaboration. This database includes the archive of Japan's NCBI, DNA Data Bank of Japan, and European Nucleotide Archive.

Figure 3 and Table 3 show the phylogenetic tree analysis based on the part 18S ITS1 5.8S ITS2 part 28S ribosomal RNA gene sequence utilizing the unweighted pair set technique with the arithmetic average.

Pure Sciences International Journal of Kerbala

Journal Homepage:https://journals.uokerbala.edu.iq/index.php/psijk

Table 2: Homology sequence identity for local isolate MK167440.1 using the NCBI-Blast GenBank database *T. erinacei* isolate IQT-No.3

No.	Accession	Country	Source	Compatibility (%)
1	ID: MK167440.1	IRAQ	*Trichophyton erinacei*	100
2	ID: MF153407.1	Germany	*Trichophyton erinacei*	100
3	ID: KJ606083.1	USA	*Trichophyton erinacei*	100
4	ID: MN737888.1	China	*Trichophyton erinacei*	100
5	ID: MN737936.1	China	*Trichophyton erinacei*	100
6	ID: MF153405.2	Germany	*Trichophyton erinacei*	100
7	ID: MK298980.1	Belgium	*Trichophyton erinacei*	100
8	ID: MK298863.1	Belgium	*Trichophyton erinacei*	100
9	ID: LT969629.1	Czech Republic	*Trichophyton erinacei*	100
10	ID: LC413781.1	Japan	*Trichophyton erinacei*	100
11	ID: KT155933.1	Netherlands	*Trichophyton erinacei*	100
12	ID: KT155878.1	Netherlands	*Trichophyton erinacei*	100
13	ID: NR149340.1	USA	*Trichophyton erinacei*	100
14	ID: EF631615.1	China	*Trichophyton erinacei*	100
15	ID: LT969625.1	Czech Republic	*Trichophyton erinacei*	100
16	ID: MK298815.1	Belgium	*Trichophyton erinacei*	100
17	ID: JN134091.1	Iran	*Trichophyton erinacei*	100
18	ID: LT969627.1	Czech Republic	*Trichophyton erinacei*	100
19	ID: MH865913.1	Netherlands	*Trichophyton erinacei*	96
20	ID: NKU257463.1	Germany	*Trichophyton erinacei*	88
21	ID: DQ786689.1	France	*Trichophyton erinacei*	88
22	ID: KP789451.1	Iran	*Trichophyton erinacei*	82
23	ID: KC833522.1	Estonia	*Trichophyton erinacei*	82

Pure Sciences International Journal of Kerbala

Journal Homepage:https://journals.uokerbala.edu.iq/index.php/psijk

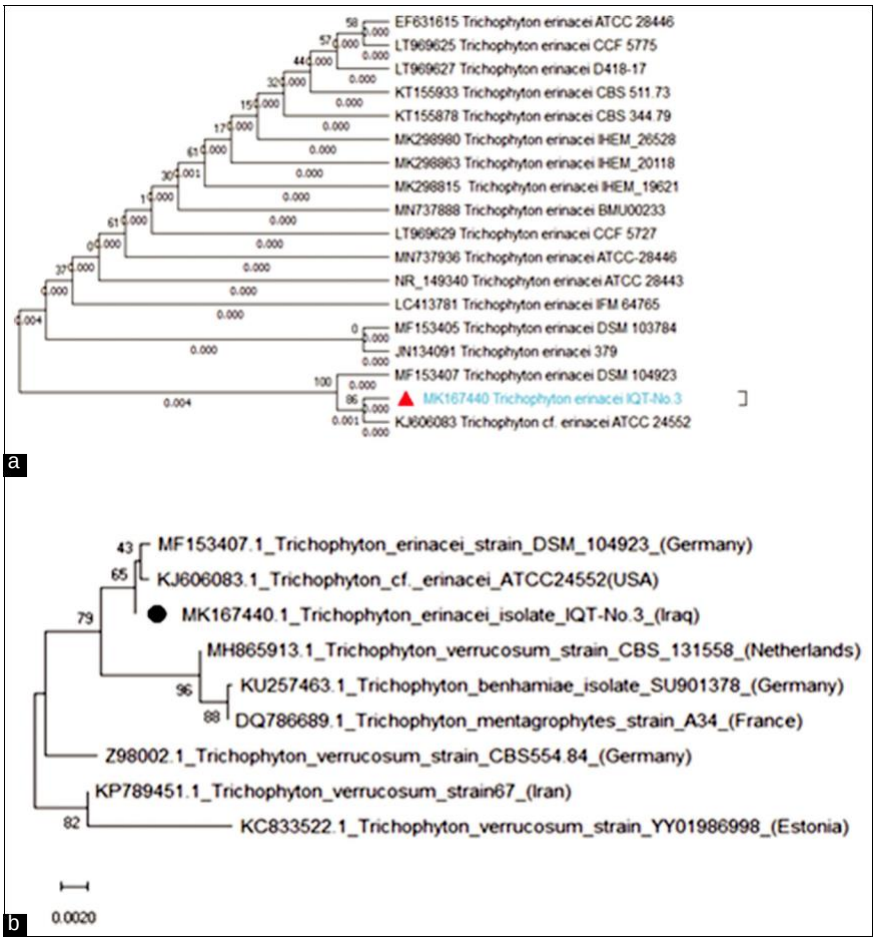

Figure 3: (a and b) Evolutionary analysis using the max probability technique

Table 3: Base composition estimations of bias-variance between series

	1	2	3	4	5	6	7	8	9	10	11	12	13	14	15	16	17	18
1. MK167440 Trichophyton erinacei IQT-No.3																		
2. MF153407 Trichophyton erinacei DSM 104923	0.000																	
3. KJ606083 Trichophyton cf. erinacei ATCC 24552	0.000	0.001																
4. MN737888 Trichophyton erinacei BMU00233	0.006	0.011	0.009															
5. MN737936 Trichophyton erinacei ATCC-28446	0.006	0.011	0.009	0.000														
6. MF153405 Trichophyton erinacei DSM 103784	0.006	0.007	0.009	0.000	0.000													
7. MK298980 Trichophyton erinacei IHEM_26528	0.006	0.012	0.010	0.000	0.000	0.000												
8. MK298863 Trichophyton erinacei IHEM_20118	0.006	0.012	0.010	0.000	0.000	0.000	0.000											
9. LT969629 Trichophyton erinacei CCF 5727	0.006	0.011	0.009	0.000	0.000	0.000	0.000	0.000										
10. LC413781 Trichophyton erinacei IFM 64765	0.006	0.011	0.009	0.000	0.000	0.000	0.000	0.000	0.000									
11. KT155933 Trichophyton erinacei CBS 511.73	0.006	0.012	0.010	0.000	0.000	0.000	0.000	0.000	0.000	0.000								
12. KT155878 Trichophyton erinacei CBS 344.79	0.006	0.012	0.010	0.000	0.000	0.000	0.000	0.000	0.000	0.000	0.000							
13. NR_149340 Trichophyton erinacei ATCC 28443	0.006	0.010	0.009	0.000	0.000	0.000	0.000	0.000	0.000	0.000	0.000	0.000						
14. EF631615 Trichophyton erinacei ATCC 28446	0.006	0.014	0.009	0.000	0.000	0.001	0.000	0.000	0.000	0.000	0.000	0.000	0.000					
15. LT969625 Trichophyton erinacei CCF 5775	0.006	0.012	0.010	0.000	0.000	0.000	0.000	0.000	0.000	0.000	0.000	0.000	0.000	0.000				
16. MK298815 Trichophyton erinacei IHEM_19621	0.006	0.012	0.010	0.000	0.000	0.000	0.000	0.000	0.000	0.000	0.000	0.000	0.000	0.000	0.000			
17. JN134091 Trichophyton erinacei 379	0.006	0.010	0.009	0.000	0.000	0.000	0.000	0.000	0.000	0.000	0.000	0.000	0.000	0.000	0.000	0.000		
18. LT969627 Trichophyton erinacei D418-17	0.006	0.012	0.010	0.000	0.000	0.000	0.000	0.000	0.000	0.000	0.000	0.000	0.000	0.000	0.000	0.000	0.000	

The background of evolution was based on the maximum-likelihood Tamura–Nei model analysis.[21] Next to the branches, the percentage of trees under which the related taxa were clustered was observed. The initial tree(s) was immediately chosen to utilize the neighbor-join and BioNJ algorithms for a vector of a pair of distances calculated using the Markov Cluster algorithm method, and the topology was chosen with a superior log probability value. The scale of the tree was determined by the branch lengths as the number of replacements per node. Eighteen nucleotide sequences were used in the study. The codon locations involved were the 1st + 2nd + 3rd + non-coding. The final dataset comprised 2550 locations. MEGA X was used for evolutionary analyses.[22]

In the table, variation in base composition variations per site can be observed;[23] the compositional gap corresponds to the number of sequence variations when the substitution patterns are homogeneous between sections. Eighteen nucleotide sequences were involved in this study. 1st + 2nd + 3rd +non-coding was included in

Pure Sciences International Journal of Kerbala

Journal Homepage:https://journals.uokerbala.edu.iq/index.php/psijk

.

the codon. The final dataset comprised 2550 places in total. MEGA X was used for evolutionary analysis.[22]

DISCUSSION

The ability of exotic animals kept as pets in the household to act as potential sources of zoonotic infections is becoming increasingly well known. Various reports have indicated the capacity of hedgehogs to transfer dermatophytes to humans.[24] *T. erinacei*, which has rarely been isolated as a human pathogen, is transferred from hedgehogs and can induce major inflammatory and pruritic eruptions, primarily on the hands.[25]

The present study is the first to record observations of three types of ringworm caused by *T. erinacei* in the Kerbala Province: Tinea manuum, tinea faciei, and tinea corporis. This has so far been seldom stated coincidentally in the same area in different countries around the world. These infections, which are thought to occur as a result of the transmission of the fungus from hedgehogs, could indicate that *T. erinacei* distribution is associated with hedgehogs and that the disease can occur wherever hedgehogs, either domesticated or wild, are present. However, transference of the disease to people is as yet not sufficiently understood. Other indirect boundary-infection sources have been identified between human and hedgehogs.[13]

The isolate obtained from four patients with tinea manuum and tinea faciei (one patient each) and with tinea corporis (two patients) was identified as *T. erinacei*. The morphological features of the SDA colonies allowed for their tentative identification. These results correlate with those of prior research that has recognized this fungus as a causative tinea agent, with various clinical manifestations.[26] The investigation distinguished the presence of inflammatory tinea of the hands, face, and body for the 1st time in Iraqi in a case whose etiology was identified by *T. erinacei* PCR-sequencing and morphology.

The present study is comparable with research by Phaitoonwattanakij *et al.*, 2019,[27] who identified the first *T. erinacei* nail and skin infections in Thailand as having been transmitted from a hedgehog.[27] The characteristic lesions were found at the extremities, particularly on the wrists and hands.[10,28] Skin infections have also been reported at other countries, including tinea corporis, tinea capitis, and tinea barbae.[10,29,30] In contrast, reports on tinea unguium, which is caused by *T. erinacei*, are rare, though cases have been recorded in the UK, Japan, Western Europe, Korea, and Mexico.[11,31] It has been reported that around 76% of cases caused by *T. erinacei* affect the extremities, particularly the wrists and hands and can occur through scratches or injuries or by direct contact with a hedgehog.[31,32]

Pure Sciences International Journal of Kerbala

Journal Homepage:https://journals.uokerbala.edu.iq/index.php/psijk

The current study refers that *T. erinacei* was identified in four patients infected with tinea faciei, tinea corporis, and tinea manuum. This correlates with the results from other research, which has progressively characterized the fungus as a causative agent of tinea, with various clinical manifestations, including scaly lesions.[12] Further molecular studies should be conducted to provide a deeper understanding of the epidemiology of the disease caused by *T. erinacei* pathogen.

In European hedgehogs (*Erinaceus europaeus*), the prevalence of *T. erinacei* was 16%; meanwhile, it was 9.5% in France and 44.7% in New Zealand. In Britain, the prevalence was 18%; this percentage ranged from 1.35–17% to 20–25%. Furthermore, in France, an infection prevalence of 13% in wild European hedgehogs and 21% in hedgehogs residing in captivity was recorded.[33]

Isolation of *T. erinacei* has been reported in other species of animals, particularly in hunting dogs in countries that are also home to hedgehogs.[2] The pathogen has also been previously identified in wild rodents.[34] A clinical case of *T. erinacei* infection of the skin was recorded in Southeast Asia after recreational contact with an elephant.[6]

A nucleotide sequence review of the ITS areas of ribosomal DNA was conducted to validate the identity of *T. erinacei*. Complete DNA was collected from *T. erinacei*, and the ITS parts were amplified using ITS1 and ITS4 primers. ITS sequencing is considered a key tool in the molecular recognition and phylogenetic analysis of dermatophytes; therefore, ITS sequences are regularly utilized by research organizations in accessible repositories.[13] It was observed that the Iraqi strain of *T. erinacei* (MK167440.1) mainly had the same ITS sequence as the other strains shown in Table 2 and 3. Utilizing this database, our strain demonstrated 100% identity with 13 international strains but only showed 96% identity with the Netherlands strain, 88% with strains from Germany and France, and 82% with Iranian and Estonian strains.

The knowledge that hedgehogs could be found nearby the areas where dogs were roaming led to the assumption that the occurrence of either direct or indirect infection with *T. mentagrophytes* var. *erinacei* originated from hedgehogs. The presence of hedgehogs infected with *T. mentagrophytes* var. *erinacei* around the walking areas of dogs was a significant risk agent of infection of the dogs and could also be a source of infection in humans who came into contact with the infected dogs, hedgehogs, or contaminated objects.[35]

There is increasing concern regarding the evolution of *T. erinacei* contamination into severe zoonotic disease due to hedgehogs' prevalence as wild animals

Pure Sciences International Journal of Kerbala

Journal Homepage:https://journals.uokerbala.edu.iq/index.php/psijk

or pets. *T. erinacei* is the most commonly isolated dermatophyte in hedgehogs and appears in 38.9–44.7% of African pygmy hedgehogs and 20–80% of European hedgehogs in an asymptomatic or periauricular formation with a lack of quills.[12]

The infection can be transmitted by infected hair and spines deposited on the ground,[9] other sources can involve touching infected people or dogs that have been in contact with hedgehogs, hedgehog nests, or contaminated soil.[1,36] Indeed, fungal spores can survive for up to 365 days in dry nests.[7] The results of the present study coincide with the results of other research, which has recognized this fungus as the causal tinea agent with various clinical manifestations.[37,38]

Preliminary observations conducted by the authors revealed that the distribution of the hedgehog population in rural areas, and sometimes in urban areas in Iraq, was relatively high. However, this fungus has not been previously identified as a potential cause of human ringworm.

CONCLUSION

Molecular identification was shown to be a significant aid in verifying morphological recognition. This study is the first to report on a case of tinea infection caused by *T. erinacei* in Iraq, which was most probably transferred from a hedgehog. This study provides insight into *T. erinacei* infections and raises awareness of the infection, which may help to minimize the spread of dermatophytosis. Maintaining personal hygiene could lessen the extent of dermatophytosis and, therefore, the burden of this disease on the population as a whole. Recognition of the source of infection is essential in preventing the risk of recurrence.

ACKNOWLEDGMENTS

The authors extend their thanks to the Biology Department, College of Education for Pure Science, Kerbala University, Iraq, for the use of its lab facilities and to Assist Professor Dr. Hussain Al-Dahmoshi, Department of Biology, University of Babylon, Iraq, for technical and scientific assistance.

CONFLICTS OF INTEREST

The authors declare no conflicts of interest.

FUNDING

The College of Education deanship financially supported this work at Pure Science, Kerbala University, Iraq. The College deanship of Pure Science, Kerbala University, offers financial support for special scientific research projects undertaken on postgraduate degrees.

CONTRIBUTION OF AUTHORS

All authors contributed greatly to this work, such as by contributing data, and in design, performance, collection, and writing.

Pure Sciences International Journal of Kerbala

Journal Homepage:https://journals.uokerbala.edu.iq/index.php/psijk

REFERENCES

1. Rhee DY, Kim MS, Chang SE, Lee MW, Choi JH, Moon KC, *et al*. A case of tinea manuum caused by *Trichophyton mentagrophytes* var. *Erinacei*: The first isolation in Korea. Mycoses 2009;52:287-90.
2. Morris P, English M. Transmission and course of *Trichophyton erinacei* infections in British hedgehogs. Sabouraudia 1973;11:4247.
3. Bond R. Superficial veterinary mycoses. Clin Dermatol 2010;28:226-36.
4. Nardoni S, Papini R, Gallo MG, Francesca M, Ranieri V. Survey on the role of brown hares (*Lepus europaeus*, pallas 1778) as carriers of zoonotic dermatophytes. Ital J Anim Sci 2010;9:126-8.
5. de Diego AM. Aspectos clínicos, diagnósticos y terapéuticos de las dermatofitosis. Enferm Infecc Microbiol Clin 2011;29:33-9.
6. Borges-Costa J, Martins ML. *Trichophyton erinacei* skin infection after recreational exposure to an elephant in Southeast Asia. Pathog Glob Health 2014;108:5859.
7. Hsieh CW, Sun PL, Wu YH. *Trichophyton erinacei* infection from a hedgehog: A case report from Taiwan. Mycopathologia 2010;170:417-21.
8. Philpot CM, Bowen RG. Hazards from hedgehogs: Two case reports with a survey of the epidemiology of hedgehog ringworm. Clin Exp Dermatol 1992;17:156-8.
9. Romano C, Gianni C, Papini M. Tinea capitis in infants less than 1 year of age. Pediatr Dermatol 2001;18:465-8.
10. Mochizuki T, Takeda K, Nakagawa M, Kawasaki M, Tanabe H, Ishizaki H. The first isolation in Japan of *Trichophyton mentagrophytes* var. *Erinacei* causing tinea manuum. Int J Dermatol 2005;44:765-8.
11. Perrier P, Monod M. Tinea manuum caused by *Trichophyton erinacei*: First report in Switzerland. Int J Dermatol 2015;54:959-60.
12. Drira I, Neji S, Hadrich I, Sellami H, Makni F, Ayadi A. Tinea manuum due to *Trichophyton erinacei* from Tunisia. J Mycol Med 2015;25:200-203.
13. Abarca ML, Castellá G, Martorell J, Cabañes FJ. *Trichophyton erinacei* in pet hedgehogs in Spain: Occurrence and revision of its taxonomic status. Med Mycol 2017;55:164-72.
14. Eabaid FA, Mallah MO. A prevalence study of ectoparasites on the long-eared hedgehog (*Hemiechinus auritus*) in AL-Muthanna province-Iraq. Al-Qadisiyah J Vet Med Sci 2017;16:55-9.
15. Donnelly TM, Rush EM, Lackner PA. Ringworm in small exotic pets. Semi Avian Exotic Pet Med 2000;9:82-93.
16. Heatley JJ, Mitchell MA, Tully TN. Manual of Exotic Pet Practice. St Louis: Saunders Elsevier; 2009. p. 433-55.
17. Obaid AJ, Al-Janabi JK, Taj-Aldin WR. Bioactivities of anethole, astragalin and cryptochlorogenic acid extracted from anise oil and *Moringa oleifera* on the keratinase gene expression of *Trichophyton rubrum*. J Pure Appl Microbiol 2020;14:615-26.
18. Koneman EW, Roberts GD, Wright SE. Practical Laboratory Mycology. USA: The Williams and Wilkins Company Baltimore; 1978. p. 139.
19. Kwon-Chung KJ, Beneet JE. Medical Mycology. Philadelphia, PA, London: Lea & Febiger; 1992.
20. Gupta AK, Cooper EA. Update in antifungal therapy of dermatophytosis. Mycopathologia 2008;166:353-67.
21. Tamura K, Nei M. Estimation of the number of nucleotide substitutions in the control region of mitochondrial DNA in humans and chimpanzees. Mol Biol Evol 1993;10:512-26.
22. Kumar S, Stecher G, Li M, Knyaz C, Tamura K. MEGA X: Molecular evolutionary genetics analysis across computing platforms. Mol Biol Evol 2018;35:1547-9.
23. Kumar S, Gadagkar SR. Disparity index: A simple statistic to measure and test the homogeneity of substitution patterns between molecular sequences. Genetics 2001;158:1321-7.
24. Rosen T. Hazardous hedgehogs. South Med J 2000;93:936-8.
25. Choi E, Huang J, Chew KL, Jaffar H, Tan C. Pustular tinea manuum from *Trichophyton erinacei* infection. JAAD Case Rep 2018;4:518-20.
26. Alejandra CA, de Lourdes PO, Leonardo MG, Jorge MR, Erika CM, Francisca HH. Inflammatory tinea manuum due to *Trichophyton erinacei* from an African hedgehog. Adv Microbiol 2018;8:1021-8.
27. Phaitoonwattanakij S, Leeyaphan C, Bunyaratavej S, Chinhiran K. *Trichophyton erinacei* onychomycosis: The first to evidence a proximal subungual onychomycosis pattern. Case Rep Dermatol 2019;11:198-203.
28. Rosen T, Jablon J. Infectious threats from exotic pets: Dermatological implications. Dermatol Clin 2003;21:229-36.
29. Jury CS, Lucke TW, Bilsland D. *Trichophyton erinacei*: An unusual cause of kerion. Br J Dermatol 1999;141:606-7.
30. Simpson JR. Tinea barbae caused by *Trichophyton erinacei*. Br J Dermatol 1974;90:697-8.
31. Lammoglia-Ordiales L, Martínez-Herrera E, Toussaint-Caire S, Arenas R, Moreno-Coutiño G. Mexican case of tinea incognito and granuloma de majocchi acquired from a hedgehog. Rev Chil Infectol 2018;35:204-6.
32. Hui L, Choo KJ, Tan JB, Yeo YW. Inflammatory tinea manuum due to *Trichophyton erinacei* from a hedgehog: A case report and review of the literature. J Bacteriol Mycol 2017;4:1057.
33. Contet-Audonneau N, Saboureau M, Percebois J. *Trichophyton erinacei* on the hedgehog. J Mycol Méd 1991;118:2932.
34. Otčenášek M, Hubálek Z, Sixl W. Survey of dermatophytes in the hair of small mammals from Austria. Folia Parasit 1980;27:83-87.
35. Kurtdede A, Haydardedeoğlu AE, Alihosseini H, Çolakoğlu EÇ. Dermatophytosis caused by *Trichophyton mentagrophytes* var. *Erinacei* in a dog: A case report. Vet Med 2014;59:349-51.
36. Takahashi Y, Sano A, Takizawa K, Fukushima K, Miyaji M, Nishimura K. The epidemiology and mating behavior of *Arthroderma benhamiae* var. *Erinacei* in household four-toed hedge- hogs (*Atelerix albiventris*) in Japan. Nihon Ishinkin Gakkai Zasshi 2003;44:31-8.
37. Tartabini ML, Bonino GS, Raccab L, Luque AG. Taxonomic study of clinic isolates of *Trichophyton* in Rosario, Argentina. Rev Argent Microbiol 2013;45:248-53.
38. Dhib I, Khammari I, Yaacoub A, Slama FH, Saïd MB, Zemni R, *et al*. Relationship between phenotypic and genotypic characteristics of *Trichophyton mentagrophytes* strains isolated from patients with dermatophytosis. Mycopathologia 2017

First Year-First Folder-Number: 0
PSIJK 184-191

Pure Sciences International Journal of Kerbala

Journal Homepage:https://journals.uokerbala.edu.iq/index.php/psijk

First Year-First Folder-Number: 0
PSIJK 184-191

Pure Sciences International Journal of Kerbala

Journal Homepage:https://journals.uokerbala.edu.iq/index.php/psijk

Biochem. Cell. Arch. Vol. 21, No. 1, pp. 1769-1775, 2021	**www.connectjournals.com/bca**	*ISSN 0972-5075*
DocID: https://connectjournals.com/03896.2021.21.1769		*eISSN 0976-1772*

EFFECT OF INDOLE ACETIC ACID AND CHELATED NANO-ZINC FOLIAR APPLICATION ON SOME WHEAT ENZYME UNDER SALINE CONDITIONS

Farah N. Al-Masoudi* and Qais H. Al-Semmak

Department of Biology, College of Education for Pure Sciences, University of Karbala, Iraq.
*e-mail : farahnassir00@gmail.com

(Received 10 November 2020, Revised 4 January 2021, Accepted 18 January 2021)

ABSTRACT : A pot experiment was carried out under field conditions at the University of Kerbala - College of Agriculture to study the effect of foliar application of auxin and Nano- chelated zinc on the activity of some antioxidant enzymes in wheat plant (*Triticum aestivum* L.) grown in sandy loam soil during the 2019-2020 agricultural season. Treatments included three factors, the first factor represented by foliar application of wheat plants with auxin at a concentration of (0, 20 mg L^{-1}) and the second factor involved the foliar application with three concentrations of Nano-chelated zinc (0, 1, 2 g L^{-1}) applied before elongation and at drain filling. The third factor was irrigation with different water quality (2, 4, 8 dS m^{-1}). This experiment included 54 experimental units arranged in CRD design in three replications. The results showed a significant effect of zinc on the activity of antioxidant enzymes (CAT, POD, SOD). While no significant effect of auxin was shown. The results also indicate the possibility of using saline water in irrigation (within this trial conditions), when plants were foliar supplied with Zn Nano - fertilizer. *Key words :* IAA, nano-zinc, wheat, salt stress. **How to cite :** Farah N. Al-Masoudi and Qais H. Al-Semmak (2021) Effect of indole acetic acid and chelated nano-zinc foliar application on some wheat enzyme under saline conditions. *Biochem. Cell. Arch*. **21**, 1769-1775. DocID: https://connectjournals.com/03896.2021.21.

INTRODUCTION

Iraq suffers from a severe shortage of water resources as a result of the lack of a proper strategy in water and soil management and the fluctuation of rainfall, as well as the various policies of the riparian countries on the Tigris and Euphrates rivers. This situation necessitates the use of poor quality water as supplementary irrigation in agricultural fields (Kubba, 2008). In Iraq, tributaries and wells water was used as a source of irrigation water, but it is characterized by a different level of salinity, which might leave negative effects on plant production (Peter, 2008). Chakraborty and Pradhan (2012) concluded that Superoxide dismutase (SOD) enzyme is the first expressive anti-stress enzyme and has a high effectiveness on most varieties of tolerant wheat. Superoxide dismutase activity was associated with increased Peroxidase (POD) efficacy. Sairam *et al* (2002) showed that there is an increase in the treatments subjected to salt stress compared to the control treatment, and that the wheat varieties that are able to maintain the activity of their antioxidant enzymes are able to withstand salt stress more. Iqbal and Bano (2009) explained that the increase in the effectiveness of POD and CAT had an effect on preserving a high amount of water in paper plant. Kirecci (2018) concluded that IAA at a concentration of 100 mg L^{-1} stimulated the activity of SOD, Catalase and ascorbate in stressed plants. Fayyad and Al-Hadithi (2011) mentioned the importance of zinc and its role as a synthetic component, cofactor and regulator for a wide range of different enzymes. Zinc is also a stimulant for various enzymes (Pandey, 2013). There are many studies that mentioned the ability to irrigate economic crops with saline water when plants foliar applied with nutrients, growth and osmotic regulators, especially wheat, which is one of the most important strategic crops in Iraq (Al-Taey, 2011; FAO, 2013). Auxins are plant hormones that were discovered early and promotes the processes of division and speeds up the elongation of cells under the developing apex,

First Year-First Folder-Number: 0
PSIJK 184-191

Pure Sciences International Journal of Kerbala

Journal Homepage:https://journals.uokerbala.edu.iq/index.php/psijk

and also contributes to the growth of roots and their branching and prevents the fall of leaves and fruits and stimulates flowering. Studies indicate that auxins help the plant to tolerant the salt stress through increasing the content of proline in leaves and dissolve sugars as well as their chlorophyll content (Afroz *et al*, 2005). Zinc is one of the trace elements necessary for normal plant growth, and it has a major role in protein metabolism for wheat crops.Studies indicate that the use of Nano-fertilizers could cause a three-fold increase in nutrient utilization efficiency and reduces the potential negative effects associated with overdose compared to bulky fertilizers as well as provides additional stress tolerance. Also, in the context of comparison, Nano-fertilizers are cheaper and are required in lesser quantities, as their use reduces the excessive consumption of ordinary (bulky) chemical fertilizers (Manjunatha *et al*, 2016; Panwar *et al*, 2012). Nano fertilizers are effective materials at lower prices compared to conventional fertilizers (Ali *et al*, 2017). Nano- fertilizers are manufactured in biological, physical or chemical ways, and the negative and toxic effects that can occur as a result of adding Nano-fertilizers are less compared to conventional fertilizers if they are added in a moderate proportion (Walpola and Yoon, 2012).

Therefore, this study was planned to find out the effect of foliar application of auxin and zinc (zinc chelated nanoparticles) and their interactions on increasing the wheat plant's tolerance to salt stress caused by irrigation with saline water through knowledge of:

1. The effect of foliar application of wheat plants with auxin in increasing its production under different salinity levels.
2. The effect of the foliar application of wheat plants with Nano-chelated zinc in increasing its tolerance, growth and production under different salinity levels.
3. The nature of the interaction of auxin and zinc chelated nanoparticles on growth, productivity and tolerance of wheat plants for irrigation with salt water.

MATERIALS AND METHODS

A pot experiment was conducted at the College of Agriculture, University of Kerbala using wheat (*Triticum aestivium* L.) (as an indicator) at 2019-2020 season. Soil materials were homogenized well and then packed in plastic pots at 15 kg of soil per pot. Some physical and chemical properties were estimated according to the standard methods shown in Page *et al* (2001) and results of analysis were shown at (Table 1). Treatments included three factors, the first factor represented foliar application

* Analyses was done at the laboratory of College of Agricultural Engineering Sciences, University of Baghdad.

of wheat plants with auxin at a concentration of (0, 20 mg L^{-1}) and the second factor involved the foliar application with three concentrations of Nano-chelated zinc (0,1,2 g L^{-1}) applied before elongation and at booting stage. The third factor was irrigation with different water quality (2, 4, 8 dSm^{-1}). This experiment included 54 experimental units arranged in CRD design in three replications. Liquid detergent (alzahi), at a rate of (0.15 cm^3 $liter^{-1}$) as a surfactant. The seeds of wheat, class IBAA 99 were sown on 25/11/2019, at a rate of 20 seeds per pot, then the seedlings were thinned to ten plants. Urea fertilizer at a rate of 150 kg N ha^{-1} and 50 kg P ha^{-1} and 80 kg K ha^{-1} using urea, TSP and potassium sulfate as fertilizers (Jadoua and Hamad, 2013).

Determination of the activity of catalase enzyme (CAT)

The effect of the enzyme was estimated by method of Aebi (1983)

$$\text{Catalase activity (unit)} = \frac{\text{Reaction volume} \times \Delta\text{bs/min}}{0.01}$$

whereas,

Δbs = the difference between absorbance (first adsorption - second absorption)

Min = reaction time

Reaction volume = 2.04 ml

0.01 = constant levels 4 and 8 dSm^{-1}, respectively, with an increase of 15.52% and 32.44%, respectively, as compared to

-1

Determination of Superoxide dismutase enzyme

First Year-First Folder-Number: 0
PSIJK 184-191

Pure Sciences International Journal of Kerbala

Journal Homepage:https://journals.uokerbala.edu.iq/index.php/psijk

treatment 2 dSm. The highest activity of CAT enzyme

(SOD)

Using the method of Markjland (1974) according to the equation :

$$I\% = \frac{C}{T}$$

$$\text{SOD activity (Units)} = \frac{I\% / 50\% \times r.v}{\text{Total time}}$$

Whereas,

I = Inhibition ratio.

C = change in absorption of control solution. T = change in absorption of plant sample.

r.v = reaction volume = 2.55 ml.

Determination of the activity of peroxidase enzyme (POD)

Using the method of Pitott (1995) according to the equation:

$$\text{Enzyme activity (U.ml}^{-1}\text{)} = \text{inclination} \times 1000 \times \frac{\text{Total size of the device cell}}{\text{Enzyme size} \times \text{Light path length} \times \text{Fixed permeability}}$$

Whereas,

- The length of optical path of the cell of the spectrometer device = 1cm.

- Molecular permeability constant of guayagol = 6.4 millimolar $^{-1}$.cm ^{2}, but required here in units the micromolar is not molar, so multiply the equation by 1000.

RESULTS

Catalase enzyme (CAT)

The results presented in Table 2 indicate that there is no significant effect of the levels of auxin on the activity of the enzyme CAT, while it is noted that there is a significant effect of the added chelated zinc levels, especially at the levels of 1 gm L^{-1} and 2 gm L^{-1} CAT enzyme: 48.14 and 48.59 unit. mg. Protein^{-1}, respectively, with an increase of 11.61% and 12.65%, compared to the comparison treatment (Z0) in the same sequence, in which the activity of the CAT enzyme reached 43.13 unit. mg. Protein^{-1}. If the CAT enzyme activity increased with increasing the salinity levels of the irrigation water, it was noted that the CAT enzyme activity increased from 40.19 unit. mg. Protein^{-1} at a salinity level of 2 dS m^{-1} to 46.43 and 53.23 unit. mg. Protein^{-1} when irrigating with was observed for the added levels of nano-chelated zinc, especially at levels (1 and 2) gm L^{-1}, as the SOD enzyme activity reached 41.63 and 44.27 unit.mg.protein^{-1}, respectively, with an increase of 0.04% and 6.39%, compared to the comparison treatment (Z0) in the same sequence in which the SOD enzyme activity reached was reached when not spraying with auxin, and the second level of chelated zinc Nano-crystalline (Z2A0) was added by 51.44 unit.mg.Protein^{-1}, while the lowest activity of CAT enzyme was at levels (Z0A0) by 37.99 unit.mg.protein^{-1}. The two-way interaction between auxin and irrigation with saline water gave a significant effect on this characteristic, through which we notice an increase in the activity of CAT enzyme at the levels (S3A1) by 54.44 unit.mg.protein^{-1}, while the lowest activity of CAT enzyme was when spraying with levels (S1A1) was 39.42 unit.mg.protein^{-1}. The two-way interaction between the levels of chelated zinc nanoparticles and the irrigation levels with salt water also had a significant effect on the activity of CAT enzyme, and the highest activity of CAT enzyme at the levels of (S3Z2) was 57.31 unit. mg. Protein^{-1} and the lowest activity of CAT enzyme at the levels (S1Z0) was 37.74 unit. mg. Protein^{-1}. The triple interference effect of the agents under study had a maximum effect of CAT in the treatment (S3Z2A0) of 58.63 unit. mg. Protein^{-1}, while the lowest activity of the CAT enzyme in the treatment S1Z0A0 was achieved by 32.94 unit.mg.protein^{-1}.

Superoxide dismutase enzyme (SOD)

The results presented in Table 3 indicate that there was no significant effect of the levels of auxin spray on the activity of the SOD enzyme, while a significant effect

First Year-First Folder-Number: 0
PSIJK 184-191

Pure Sciences International Journal of Kerbala

Journal Homepage:https://journals.uokerbala.edu.iq/index.php/psijk

41.61 unit.mg.protein^{-1}. If the activity of the SOD enzyme increased with increasing the salinity levels of the irrigation water, an increase in the SOD enzyme activity of 34.68 unit.mg.protein^{-1} was observed at the level of salinity of irrigation water S1 to 41.55 and 51.28 unit.mg.protein^{-1} when irrigating with levels (4 and 8) dSm^{-1}, respectively, with an increase of 19.80% and 47.86%, respectively, compared to the treatment of 2 dSm^{-1}.SOD, where the highest activity of SOD enzyme was achieved when not spraying with auxin, and the second level of nano- chelated zinc (Z2A0) was added by 44.47 unit.mg.Protein^{-1}, while the lowest activity of SOD enzyme was at levels (Z1A0) by 39.56 unit.mg.protein^{-1}. The bilateral interaction between auxin and irrigation with saline water gave a significant effect on this characteristic, and the highest activity of SOD enzyme was reached at the levels (S3A0)

Table 2 : The effect of adding levels of auxin and zinc chelated nanoparticles and their interactions on the activity of the CAT enzyme (unit.mg.protein^{-1}).

by 51.70 unit.mg.protein^{-1}, while the lowest activity of SOD enzyme when spraying with S1A1 levels was 33.54 unit.mg.protein^{-1}. The bilateral interaction between the levels of spraying with nano-chleated zinc and the irrigation levels with salty water also had a significant effect on the activity of the SOD enzyme and the highest activity of the SOD enzyme at the levels of (S3Z2) was 52.51 unit.mg.protein^{-1} and the lowest activity of the SOD enzyme at the levels (S1Z0) was 32.95 unit.mg.protein^{-1}

. The triple interference effect was the highest effective for (S3Z2A1) by 54.82 unit. mg. Protein^{-}

Auxin(mg L^{-1})	**Zinc(gm.L^{-1})**	**Salinity levels dSm^{-1}**			**Auxin**
		S12	**S24**	**S38**	
A0 Without added	Z0 Without added	32.94	38.02	43.02	46.14
	Z11	45.29	47.23	54.57	
	Z22	44.66	51.04	58.63	
A1 20	Z0 Without added	42.55	49.51	52.76	47.10
	Z11	37.09	50.23	45.57	
	Z22	38.62	42.60	56.00	
Salinity		40.19	46.43	53.23	
Zinc		Z0	Z1	Z2	
		43.13	48.14	48.59	
Auxin* Zinc		Z0	Z1	Z2	
A0		37.99	48.98	51.44	
A1		48.27	47.30	45.74	
Auxin* Salinity levels		S1	S2	S3	
A0		40.96	45.43	52.03	
A1		39.42	47.44	54.44	
Zinc* Salinity levels		S1	S2	S3	
Z0		37.74	43.76	47.89	
Z1		41.19	48.73	54.50	
Z2		41.64	46.82	57.31	

L..S.D. 0.05	Auxin	Zinc	Salinity	Auxin* Zinc	Auxin* Salinity levels	Zinc* Salinity levels	Auxin* Zinc salinity l
	2.9639	3.6301	3.6301	7.2145	6.3562	7.3611	8.8918

First Year-First Folder-Number: 0
PSIJK 184-191

Pure Sciences International Journal of Kerbala

Journal Homepage:https://journals.uokerbala.edu.iq/index.php/psijk

[1], while the lowest activity of SOD enzyme was achieved when treatment (S1Z0A1) was achieved by 21.20 unit.mg.protein^{-1}. Peroxidase enzyme (POD) The results presented in Table 4 indicate that there was no significant effect of the levels of auxin spray on reached 44.98 and 42.80 unit. mg. Protein^{-1}, respectively, with a decrease of 0.83% and 5.64% compared to the Z0 treatment. The comparison (Z0) in the same sequence in which the activity of the enzyme POD was 45.36 unit. mg.protein^{-1}. If the activity of the POD enzyme increased with the increase in the salinity levels of the irrigation water, it was observed that the activity of the POD enzyme increased from 42.21 unit.mg.protein^{-1} at the salinity level of S1 irrigation water to 44.66 and 46.05 unit.mg.protein^{-1} when irrigation with levels 4 and 8 (dSm^{-1} 5.80% and 9.09%) respectively, the same as compared to the treatment 2 dSm^{-1}. The results showed that there was a significant effect of the bilateral interaction between auxin and Nano- chelated Zinc in the activity of the POD enzyme, as the highest activity of the POD enzyme was reached when spraying with auxin and not adding the nano-chelated zinc (Z0A1) by 45.65 POD enzyme activity. While we notice a significant effect unit.mg.protein, while the lowest activity of the POD

of the added levels of nano-cochleate zinc, especially at enzyme was at the levels (Z2A0) by 41.81

the levels (1 and 2) gm, as the activity of the POD enzyme unit.mg.protein. The bilateral interaction between auxin

Table 3 : The effect of addition of levels of auxin and chelated zinc nanoparticles and the interaction between them on the activity of the SOD enzyme (unit.mg.protein^{-1}).

Auxin(mg L^{-1})	**Zinc(gm.L^{-1})**	**Salinity levels dSm^{-1}**			**Auxin**
		S12	**S24**	**S38**	
A0 Without added	Z0Without added	34.70	40.56	49.63	41.89
	Z1 1	29.63	38.40	50.66	
	Z22	36.30	42.29	54.82	
A1 20	Z0 Without added	21.20	42.26	51.30	43.12
	Z11	39.23	40.80	51.07	
	Z22	37.03	45.00	50.20	
Salinity		34.68	41.55	51.28	
Zinc		Z0	Z1	Z2	
		41.61	41.63	44.27	
Auxin* Zinc		Z0	Z1	Z2	
A0		41.63	39.56	44.47	
A1		41.58	43.70	44.08	
Auxin* Salinity levels		S1	S2	S3	
A0		33.54	40.42	51.70	
A1		35.82	42.68	50.85	
Zinc* Salinity levels		S1	S2	S3	
Z0		32.95	41.41	50.46	
Z1		34.43	39.60	50.86	
Z2		36.66	43.64	52.51	

L.S.D. 0.05	Auxin	Zinc	Salinity	Auxin* Zinc	Auxin* Salinity levels	Zinc* Salinity levels	Auxin* Zinc Salinity
	1.8649	2.2841	2.2841	7.588	3.5793	4.3467	5.5948

First Year-First Folder-Number: 0
PSIJK 184-191

Pure Sciences International Journal of Kerbala

Journal Homepage:https://journals.uokerbala.edu.iq/index.php/psijk

and irrigation with saline water gave a significant effect on this characteristic and the highest activity of POD enzyme was reached at The two levels (S1A0) amounted to 96.57 unit.mg.protein^{-1}, while the lowest activity of POD enzyme when sprayed with levels S3A1 was 56.35 units. unit.mg.protein^{-1}. The bilateral interaction between the levels of spraying with nano-chelated zinc and the irrigation levels with salt water also had a significant effect on the activity of the POD enzyme, and the highest activity of the POD enzyme was reached at the levels (S3Z1) by 47.23 unit.mg.protein^{-1} and the lowest activity of the POD enzyme at the levels of S1Z1, which was 41.38 unit.mg.protein^{-1}. The triple interaction of the agents under study had a significant effect on the POD enzyme activity, and the highest POD enzyme activity was reached in the treatment (S3Z1A1), which was not significantly different from the treatment (S3Z0A0), while the lowest POD enzyme activity was achieved with the two treatments(S1Z1A1) and (S1Z2A1) by 40.21 and 40.84 unit.mg.protein^{-1}, respectively. DISCUSSION

It is evident from the results shown in Tables 2, 3, 4 that the quality of irrigation water had a significant effect on the activity of SOD, CAT and POD enzymes in the wheat plant. The level of the plant cell, which led to stimulating the SOD enzyme as a first line of defense to counter ROS, and that plants have mechanisms to counter the increase resulting from increased salinity and this is what the results indicated by other researchers (Baby and Jini, 2011; Sairam and Srivastava, 2002). Likewise, the results obtained by ALyasari *et al* (2016) that the exposure of wheat plants to stress increased the efficiency of CAT in the plant and these results were similar to what was reported by Shannan (2017), where the enzyme activity increased when salinity levels increased in the wheat plant. Al Ganimi and Al-Sammak (2014) reported similar results that the exposure of the wheat plant to salt stress led to an increase in the activity of the enzyme CAT, SOD and POD and indicated the role of the enzyme CAT in protecting tissues from the

Table 4 : The effect of adding levels of auxin and zinc chelated nanoparticles and their interactions on the activity of the POD enzyme (unit.mg.protein^{-1}).

Auxin (mg L^{-1})	**Zinc (gm.Liter^{-1})**	**Salinity levels dsm^{-1}**			**Auxin modifier**
		S1	**S2**	**S3**	
A0 Without added	Z0 Without added	43.66	45.16	46.41	44.62
	Z11	42.55	45.87	46.54	
	Z22	42.04	43.57	45.76	
A1 20	Z0 Without added	43.96	45.46	47.53	43.99
	Z11	40.21	45.43	47.93	
	Z22	40.84	42.47	42.13	
Salinity		42.21	44.66	46.05	
Zinc		Z0	Z1	Z2	
		45.36	44.75	42.80	
Auxin* Zinc		Z0	Z1	Z2	
A0		45.08	44.98	43.79	
A1		45.65	44.52	41.81	
Auxin* Salinity levels		S1	S2	S3	
A0		42.75	44.86	46.24	
A1		41.67	44.45	45.86	

Pure Sciences International Journal of Kerbala

Journal Homepage:https://journals.uokerbala.edu.iq/index.php/psijk

Zinc* Salinity levels	S1	S2	S3
Z0	43.81	45.31	46.97
Z1	41.38	45.65	47.23
Z2	41.44	43.02	43.94

L.S.Dá0.05	Auxin	Zinc	Salinity	Auxin* Zinc	Auxin* Salinity levels	Zinc* Salinity levels	Auxin* Zinc Salinity l
	1.2202	1.4944	1.4944	2.5684	2.3469	2.5314	3.6606

toxic effects of hydrogen peroxide (H_2O_2). The increase in salinity levels led to a significant increase in the activity of the CAT enzyme in the wheat plant was well documented (AL-Yesari, 2017; Marklund and Marklund, 1974). An increase in antioxidant enzyme activities could be an indication of building a protective mechanism to reduce oxidative damage caused by stress (Chawla, 2013; Harinasut *et al*, 2003). The produced H_2O_2 appears to be effectively removed by POD and CAT at low salinity while zinc in these stressed plants can increase the activity of antioxidant enzymes as CAT is very sensitive to oxygen - and can be inactivated by increasing levels of superoxide (Zago, 2001). The increased activity of enzymes for SOD, POD and CAT caused by spraying with zinc when plants are subjected to salt stress can help prevent cell damage caused by ROS and reduce plant tolerance to salinity (Chawla, 2013; Abedini and Hassani, 2015) . Zinc is able to facilitate the biosynthesis of antioxidant enzymes (Cakmak, 2000) and that zinc played a role in improving the antioxidant system of plants subjected to salt stress (Tavallali *et al*, 2010; Weisany, 2012). Foliar application with fertilizer of micronutrients such as zinc improved the salt stress resulting from the presence of different levels of sodium chloride in irrigation water, which was reflected in reducing the effectiveness of these enzymes (Abedin, 2016). Nano-oxide plays an important role in the activation of some antioxidant enzymes which are of great importance in mitigating oxidative damage caused by salt stress on plant cells. The increase in enzyme activities in relation to Nano oxide may be due to stimulation of the gene expression of CAT and POD in wheat (Ghaffari and Razmjoo, 2015). The results of many studies indicated that plant growth regulators make plants more efficient in absorbing nutrients and utilizing them at a higher level in physiological processes (Baranyiovà *et al*, 2014), as they play a prominent role in increasing the ratio of roots to the shoots and accumulating antioxidants that help plants withstand stress and give better root growth (Barakat *et al*, 2013; Ghaffari and Razmjoo, 2015). So, it can be concluded that the decrease in crop plant growth caused by sodium chloride can be mitigated by foliar application with plant growth regulators and nano-chelated zinc.

REFERENCES

Abedin M (2016) Physiological responses of wheat plant to salinity under different concentrations of Zn. *Acta Biologica Szegediensis* **60**(1), 9-16.

Abedini M and Hassani D B (2015) Salicylic acid affects wheat cultivars antioxidant system under saline and non-saline condition. *Russ. J. Plant Physiol.* **62**, 604-610.

Aebi H (1983) Catalase *in vitro*. *Methods of Enzymology* **105**, 121-

126. Afroz S I, Mohammad F, Hayat S I and siddigue M (2005)

Exogenous

application of gibberllic acid counteracts the ill effect of sodium

chloridride in Mustared. *Turk. Biol.* **19**, 233-236.

Al-Ghanimi R H and Qais H A (2014) The effect of irrigation water quality and different concentrations of added gibberellin on SOD efficacy and NPK content of *Triticum aestivum* L. *Karbala University Scientific J. (in Arabic)* **12**(4), 273-281.

Ali N D H and Yawa A (2017) Applications of micro-nutrient nanotechnology in agricultural production (reference article). *Iraqi J. Agricult. Sci.* **48**(4), 984-990.

Al-Taey K A (2011) Effects of spraying acetyl salicylic acid to reduce the damaging effects of salt water stress on orange plants. *J. Kerbala Univ*. **5**(1), 192-202.

AL-Yesari J M (2017) The effect of adding potassium and calcium to a mixture of salt stress in some indicators of growth and yield of different varieties of wheat. *Master Thesis*. College of Education, University of Karbala (in Arabic).

Baby J and Jini D (2011) Development of Saltstress-tolerant plant by gene manipulation of antioxidant enzyme. *Asian J. Agric. Res*. **5**(1), 17-27 .

Barakat N, Laudadio V, Cazzato E and Tufarelli V (2013) Antioxidant potential and oxidative stress markers in wheat (Triticum aestivum) treated with phytohormones under salt stress. *Int. J. Agric. Biol.* **15**, 843–849.

Baranyiovà I, Klem K and Køem J (2014) Effect of exogenous

Pure Sciences International Journal of Kerbala

Journal Homepage:https://journals.uokerbala.edu.iq/index.php/psijk

application of growth regulators on the physiological parameters and the yield of winter wheat under drought stress. *Mendelnet* 442-446.

Cakmak I (2000) Possible roles of zinc in protecting plant cells from damage by reactive oxygen species. *New Phytol.* **146**, 185-205.

Chakraborty U and Pradhan B (2012) Oxidative stress in five wheat varieties (*Triticum aestivum* L.) exposed to water stress and study of their antioxidant enzyme defense system, water stress responsive metabolites and H_2O_2 accumulation. *Braz. J. Plant Physiol*. **24**(2), 117-130.

Chawla S, Jain S and Jain V (2013) Salinity induced oxidative stress and antioxidant system in salt-tolerant and salt-sensitive cultivars of rice (*Oryza sativa* L.). *J. Plant Biotech. Biochem.* **1**, 27-34.

FAO (2013) Food and Agriculture Organization of the United Nations Rome, Statical Yearbook. 307. pp.

Fayyad N M and Akram A L (2011) The effect of nitrogen fertilization and zinc spraying on growth and yield of yellow corn. *Anbar J. Agricult. Sci.* (in Arabic) **9**(3), 193-198.

Ghaffari H and Razmjoo J (2015) Response of durum wheat to foliar application of varied sources and rates of iron fertilizers. *J. Agr. Sci Tech.* **17**, 321–331.

Ghorbani J M, Sorooshzadeh A, Moradi F, Sanavy Seyed A M and Allahdadi I (2011) The role of phytohormones in alleviating salt stress in crop plants. *Aust. J. Crop Sci.* **5**(6), 726–734. Harinasut P, Poonsopa D, Roengmongkol K and Charoensataporn R (2003) Salinity effects on antioxidant enzymes in mulberry cultivars. *Sci. Asia* **29**, 109-113.

Iqbal S and Bano A (2009) Water stress induced changes in antioxidant enzymes, membrane stability and seed protein profile of differentwheat accessions. *Afr. J. Biotech.* **8**(23), 6576-6587.

Jadoua K A and Hamad M S (2013) Fertilizing the wheat crop. Guidance publication No. 2. Ministry of Agriculture. The National Program for the Development of Wheat Cultivation in Iraq (in Arabic).

Kirecci O A (2018) The effect of salt stress, SNP, ABA, IAA and GA application on antioxidant enzyme activities in *Helianthus annuus* L. *Fresenius Environ. Bull. J.* **27**(5), 3783-3788.

Kubba S I (2008) *Water in Iraq between reality and treatments*. Article Gilgamesh Center for Studies and Research.

Manjunatha S, Biradar D and Aladakatti Y (2016) Nanotechnology and its application in agriculture: A review. *J. Farm. Sci.* **29**(1), 1-13.

Marklund S and Marklund G (1974) Involvement of the superoxide anion radical in the autoxidation of pyrogallol and a convenient assay for superoxide dismutase. *Eur. J. Biochem*. **47**(3), 469-474.

Nadall S M, Balogy E R and Jochvic N L (2011) Hydrogen Peroxide is scavenged by antioxidant enzymes in wheat plants. *Plant Physiol.* **29**, 534-541 .

Page A L, Miller R H and Kenney D R (1982) *Method of Soil Analysis.* 2nd (ed), Agron. 9, Publisher, Madiason, Wisconsin.

Pandey B P (2013) Botany. Rajendra Ravindra ptrinters. S. Chand and Company LTD publisher. RamNagar, India.

Panwar J, Bhargya A, Akhtar M and Yun Y (2012) Positive effect of zinc oxide nanoparticles on tomato plant: A step towards developing " Nano- fertilizers". *Proc. 3rd Int. Conf. Environ. Res. Technol.* (ICERT). Penang. Malaysia.

Peter G and Postel S (2008) *Avoiding a water crisis.* Crops Soil Agronomy News. December. **53**(12).

Pitotti A, Elizalde B E and Anese M (1995) Effect of caramellzation and maillard reaction products on peroxidase activity. *J. Food Biochem*. **18**, 445-457.

Sairam R K, Rao K V and Srivastava G C (2002) Differential response of wheat genotypes to long term salinity stress in relation to oxidative stress, antioxidant activity and osmolyte concentration. *Plant Sci*. **163**(6), 1037-1047.

Shannan R G (2017) Effect of Trehalose sugar foliar application on wheat crop tolerance to salt stress. *Master thesis*. University of Karbala . pp 103.

Tavallali V, Rahemi M, Eshgi S, Kholdebarin B and Ramezanian A (2010) Zinc alleviates salt stress and increases antioxidant enzyme activity in the leaves of pistachio (*Pistacia vera* L. Badami) seedlings. *Turk. J. Agri*. **34**, 349-359.

Walpola B C and Yoon M H (2012) Prospectus of phosphate solubilizing microorganisms and phosphorus availability in agricultural soils: A review. *Afr. J. Microbiol. Res.* **6**(37), 6600-6605.

Weisany W, Sohrabi Y, Heidari G, Siosemardeh A and Ghassemi Golezani K (2012) Changes in antioxidant enzymes activity and plant performance by salinity stress and zinc application in soybean (*Glycine max* L.*). Plant Omic J*. **5**, 60-67.

Zago M P and Oteiza P I (2001) The antioxidant properties of zinc: interactions with iron and antioxidants. *Free Rad Biol Med.* **31**, 266-274.

First Year-First Folder-Number: 0
PSIJK 184-191

Pure Sciences International Journal of Kerbala

Journal Homepage:https://journals.uokerbala.edu.iq/index.php/psijk

Hormones of Maize Crop as Affected by Potassium Fertilization , Water Quality and Ascobin Foliar Application .

Qais Hussain Al-Samak Prof.
University of Kerbala, qais.hussain@uokerbala.edu.iq

Recommended Citation
Al-Samak, Qais Hussain Prof. (2020) "Hormones of Maize Crop as Affected by Potassium Fertilization , Water Quality and Ascobin Foliar Application .," Karbala International Journal of Modern Science: Vol. 6 : Iss. 3 , Article 2.
Available at: https://kijoms.uokerbala.edu.iq/home/vol6/iss3/2
https://doi.org/10.33640/ 2405-609X.1534

Abstract

A pot assay on the plastic container of the wire sunshade in the University of Kerbala's Agricultural Division was conducted to research the impact of potassium treatment, the salinity of irrigation water and ascobin sprinkling, just as their connections, on the some plant hormones activities (auxin, gibberellin and abscisic acid) in developing Zea mays crops in a soil with sandy texture during the farming fall period of 2017–2018. The trial was planned as a factorial one with three factors, Potassium adding are 0, 100 and 200 Kg K.ha^{-1} . the irrigation water salinity are 1, 3 and 6 ds.m^{-1}; and the third factor incorporates foliar application with 0, 300 and 600 mg.L^{-1} ascobin (ascorbic acid + citric acid 2:1) at two phases: the main stage at 6 leaves and 21 days after germination and the second stage at 12 leaves and 70 days after germination. This test included 81 exploratory units dependent on a complete randomized design (CRD) with three recreates. The outcomes show that variables engaged with this experiment and their associations significantly affect the some plant hormones activities , which increment when the foliar ascobin application focus increment. The outcomes likewise show the chance of utilizing saline water for Zea mays irrigation when the foliar ascobin and potassium are adding .

Keywords

Potassium, Ascobin, Salinity stress, Zea mays, Hormones

First Year-First Folder-Number: 0
PSIJK 184-191

Pure Sciences International Journal of Kerbala

Journal Homepage:https://journals.uokerbala.edu.iq/index.php/psijk

1. Introduction

Iraq experiences serious water deficiency due to precipitation variance and the various approaches of ripari-a nations on the Tigris and Euphrates, which requires scanning for water of low quality and including it for sup-plementary water system in rural fields. The nature of water system water is one of the most significant elements af-fecting crop efficiency. Populace development and eco-nomic improvement are related with an expanding requirement for water in Iraq and the comparing outcomes in this fundamental asset because of an ex-panding abuse of water assets in the neighbor-ing nations of Iraq. The saltwater issue, accordingly, isn't unavoidable; rather, it exists as of now. In this manner, it has not been managed appro-priately as per the current. Conditions in the nation, so we need to give genuine consideration to this issue in the coming decades [1]. Salinity effectsly affects plants, including direct impacts, for example, poisonous impacts, and optional impacts, for example, enzymatic, food or ionic impacts, which help order plants' vulnerability dependent on their organic exer-cises. Water deficiency owing saltiness stress can be watched, which results from the diminished procedures of division, extension and cell association, which pri-marily causes decreased leaf territories and influences plant tallness and the quantity of green branches [2, 3],. A few examinations have been led to address salt pressure and manage the issue of saltiness and salt-water use to inundate farming harvests by shower ing supplements, development controllers and assimilation controllers, as they assume a functioning job in the development and yield of yields presented to saltiness stress conditions. The substances managing assimila-tion are ascorbic corrosive and citrus extract, which assume a significant job in numerous physiological procedures in plants, for example, development, cell division, extension, biosynthesis of the cell divider and optional metabolites and stress resistance [4]. They likewise assume a job in directing maturing and creating plant guard against pests [5], just as in shielding plants from destructive burdens, for example, the impact of substantial metals, salts, herbicides and pathogens [6]. Citrus extract assumes a significant job in invigorating photosynthesis [7]. It is a non-enzy-matic cancer prevention agent in a plant that influences unpredictable food shifts, affecting the electron trans-port chain, expanding plasma layer corruption and expanding fat peroxidation [8]. Late examinations have been led to decide the impact of ascobin on the sub-stance of significant supplements and amino corrosive, particularly in creating plants under saline pressure conditions [9]. Different methods of rewarding saline water in-clude great soil and water the executives techniques to miti-entryway the unsafe impacts of sa-line water just as utilize the best salt-safe assortments to meet the developing food needs [10e13]. Zea mays L. was utilized in this examination for its monetary significance. The point of this examination is deciding the chance of utilizing saline water for water system to develop the previously mentioned crop and miti-entryway the destructive impacts of saltiness on a portion of the harvest's hormones (which have been known to direct the vari-ous physiological procedure in plant), by adding potassium compost to the dirt, showering ascobin on the plant and considering the idea of the impact of their cooperations.

2. Materials and methods

2.1. Methods of planting, treatments and

2.1.1. Collection of samples

The examination was led by planting Z. mays crop in the wire overhang at the University of Ker-bala's Agricultural Division in the fall period of 2017e2018 utilizing sandy topsoil soil. The dirt example was taken from a field in the area of Hussainiya in the territory of Kerbala at a profundity of 0e30 cm. The dirt was air-dried and gone through a 2 mm distance across strainer. It was altogether homogenized and afterward stuffed into a 30 cm plastic compartment at a tallness of 55 cm and a load of 30 kg. The physical and sub-stance properties of soile1 for every pot were assessed dependent on the standard strategies portrayed by Ref. [14], as appeared in Table 1.

The investigation was planned as a factorial one utilizing a totally randomized structure (CRD) with three variables for three repeats. The main factor (A) speaks to three degrees of potassium (0, 100, 200 kg K hae1) in the potassium sulfate compost (41% K), which was included two equivalent augmentations as indicated by the treatment (6, 12 leaves) following 21 and 70 days of agribusiness. The subsequent factor (B) speaks to three degrees of water system water saltiness (1, 3, 6 ds m^{-1}), and the third factor (C) guarantees that three convergences of ascobin (0, 300, 600 $mg.L^{-1}$)

https://doi.org/10.33640/2405-609X.1534

Pure Sciences International Journal of Kerbala

Journal Homepage:https://journals.uokerbala.edu.iq/index.php/psijk

Table 1
Some physical and chemical characteristics of soil sample used in this study.[a]

Adjective		Value	Unit
pH		7.30	
Electrical conductivity (EC)		2.31	ds.m^{-1}
Soluble cations	Ca^{2+}	2.20	C mol.Kg^{-1} Soil
Organic matter	Mg^{2+}	6.90	gm. kg^{-1} Soil
	Na^{1+}	1.12	C mol.Kg^{-1} Soil
	K^{+}	0.13	C mol.Kg^{-1} Soil
	$SO4^{-2}$	1.22	C mol.Kg^{-1} Soil
Soluble anions	$HCO3^{-1}$	0.22	C mol.Kg^{-1} Soil
	CO_3^{2-}	Nill	C mol.Kg^{-1} Soil
	Cl^{-}	2.83	C mol.Kg^{-1} Soil
Available N		35.00	gm. kg^{-1}
Available K		12.30	gm. kg^{-1}
Available P		12.39	gm. kg^{-1}
Soil separators	Sand	61.30	gm. kg^{-1}
	Silt	26.60	gm. kg^{-1}
	Clay	12.10	gm. kg^{-1}
Texture			Sandy loam

[a] Analyzes in soil analysis laboratories at the Faculty of Agriculture - University of Baghdad.

were splashed on the plants. Tween 20 was included as a treatment at the 6-and 12-leave stage to build the ingestion effectiveness of the plants. Z. mays seeds were planted on 15/7/2018 for the fall season at 10 seeds for every pot. Then the plants was reduced into two in each pot 30 days after the seedling.

Nitrogen fertilization was introduced at a rate of 320 Kg N.ha^{-1} using urea fertilizer (46% N) in four batches: the first after emergence, the second at three whole leaves, the third at six leaves and the fourth at flowering. Phosphorus was added at 200 kg P ha^{-1} using superphosphate fertilizer (20% P_2O_5), once during soil preparation for agriculture [15]. Potassium was added in two doses at three levels with spraying dates.

Plant leaves were collected dry, and plant hormones (auxin, gibberellin, abscisic acid) were estimated according to the method described by Refs. [16].

2.2. Statistical methods

The data were subjected to analysis of variance using the SAS statistical package version 9.1 th ed. at $P < 0.05$ probability level [17].

3. Results

3.1. Auxin content in leaves (mg.gm^{-1} dry weight)

The outcomes appeared in Table 2 demonstrate that potassium fertilizer, the nature of water system water and ascobin showering significantly affect auxin content in leaves.Auxin content diminished when potassium fertiliz-er and the salanity of water system water

		3 B2	0.0724	0.0649		0.0587	0.0653
		6 B3	0.0888	0.0676		0.0611	0.0625
200 A_3		1 B1	0.0687	0.0813		0.0767	0.0755
		3 B2	0.0685	0.0891		0.0832	0.0802
		6 B3	0.0669	0.0550		0.0867	0.0696
C			0.0693	0.0739		0.0791	A
A*C		A1*C	0.0604	0.0809		0.0847	0.0753
		A2*C	0.0794	0.0655		0.0693	0.0714
		A3*C	0.0680	0.0751		0.0822	0.0751
							B
B*C		B1*C	0.0647	0.0771		0.0843	0.0753
		B2*C	0.0719	0.0774		0.0744	0.0746
		B3*C	0.0713	0.0670		0.0783	0.0722
L.S.D	A	B	C	A*B	A*C	B*C	A*B*C
P < .0.05	0.00074	0.00074	0.00074	0.00013	0.00013	0.00074	0.00221

Pure Sciences International Journal of Kerbala

Journal Homepage:https://journals.uokerbala.edu.iq/index.php/psijk

Table 2
Effect of potassium fertilizer, Irrigation water and spraying of ascobin in the auxin hormone content (mg gm^{-1}dry weight) in leaves of the Zea mays under different salinity stress levels.

Potassium added kg K. ha^{-1} A	Salinity irrigation water ds. m^{-1} B				
0 A_1		$0C_1$	$300C_2$	$600C_3$	
	1 B1	0.0482	0.0859	0.0880	0.0741
	3 B2	0.0748	0.0784	0.0815	0.0783
	6 B3	0.0581	0.0785	0.0872	0.0746
100 A_2	1 B1	0.0770	0.0642	0.0881	0.0765
	3 B2	0.0480	0.0713	0.0759	0.0651
	6 B3	0.0426	0.0482	0.0521	0.0476
	1 B1	0.0750	0.0732	0.0672	0.0718
	3 B2	0.0684	0.0823	0.0695	0.0734
	6 B3	0.0420	0.0557	0.0701	0.0559
200 A_3		0.0565	0.0613	0.0654	A
		0.0625	0.0537	0.0563	0.0576
		0.0453	0.0598	0.0710	0.0587
		0.0618	0.0705	0.0690	0.0671
					B
		0.0621	0.0622	0.0687	0.0643
		0.0571	0.0663	0.0622	0.0619
		0.0503	0.0555	0.0654	0.0571
		C	A*B	A*C	B*C A*B*C
		0.0018	0.00319	0.00319	0.00319 0.00552
L.S.D	A	A1*C			
P < .0.05	0.0018	A2*C			
		A3*C			
		B1*C			
		B2*C			
		B3*C			
		B			
		0.0018			

levels expanded, yet auxin content expanded when splashing concentra-tions expanded, and the most noteworthy incentive in treatment C3 was 0.0791 mg. gme1 dry weight, contrasted and treat-ment C1, which had an estimation of 0.0693 mg. gme1 dry weight and an expansion pace of 14.14%.

The outcomes show that potassium compost and the nature of water system water significantly affect auxin content, with a most extreme estimation of 0.0802 mg.gme1 dry load in treatment A3B2, con-trasted and that in treatment A2B2, which gave the least estimation of 0.0653 mg. gme1 dry weight. The twofold cooperation between potassium treatment and ascobin splashing additionally has a significant impact on auxin, with the most noteworthy estimation of 0.0847 mg. gme1dry load in treatment A1C3 and a 40.23% expansion comparable to the treatment for which potassium compost was not included and the plants were not splashed with ascobin in treatment A1C1.

The outcomes show that the nature of water system water and ascobin showering have a critical impact. Treatment B1C3 indicated the most elevated auxin movement with an estimation of 0.0843 mg. gme1 dry weight, contrasted and the least estimation of auxin content in treatment B1C1.

The triple collaboration between potassium treat-ment, nature of water system water and ascobin splashing significantly affects auxin content. Treatment A3B2C1 indicated the most noteworthy incentive at an auxin movement of 0.0891 mg. gme1 dry weight, contrasted and the least incentive in treatment A1B1C1, which was 0.0482 mg. gm^{-1} dry weight.

3.2. Gibberellin content in leaves (mg. gme1 dry weight)

The outcomes appeared in Table 3 demonstrate that potassium manure, water system water and ascobin showering have no huge impact on gibberellin content. The outcomes show that the collaboration of potassium compost and the nature of water system water signifi-cantly affects gibberellin content, with a greatest esti-mation of 0.0734 mg. gme1 dry load in treatment A3B2, contrasted and that in treatment A1B2, which gave the most reduced an incentive at 0.0471 mg. gme1 dry weight. The twofold collaboration be-tween the potassium manure and ascobin showering addi-tionally significantly affects gibberellin, with the most noteworthy estimation of 0.0710 mg. gme1 dry load in treatment A2C3, with an expansion of 56.73% in ex-amination with that in treatment A2C1. The outcomes show a huge contrast ence between the nature of water system water and ascobin showering. Treatment B1C3 demonstrated the most noteworthy gibberellin content at 0.0687 mg. gme1 dry weight, contrasted and the most minimal substance in treatment B3C1.

Pure Sciences International Journal of Kerbala

Journal Homepage:https://journals.uokerbala.edu.iq/index.php/psijk

Table 3
Effect of potassium fertilizer and spraying of ascobin in the gibberellin hormone content (mg. gm^{-1}dry weight) in leaves of the Zea mays under different salinity stress levels.

Potassium added kg K. ha^{-1} A	Salinity irrigation water ds. m^{-1} B	Spray level of Ascobin mg. L^{-1} C	A*B		
0 A_1		$0C_1$	$300C_2$	$600C_3$	
	1 B1	0.0659	0.0535	0.0541	0.0578
	3 B2	0.0550	0.0452	0.0412	0.0471
	6 B3	0.0665	0.0624	0.0742	0.0677
100 A_2	1 B1	0.0454	0.0598	0.0849	0.0634
200 A_3	3 B2	0.0724	0.0649	0.0587	0.0653
	6 B3	0.0888	0.0676	0.0611	0.0625
C	1 B1	0.0687	0.0813	0.0767	0.0755
A*C	3 B2	0.0685	0.0891	0.0832	0.0802
	6 B3	0.0669	0.0550	0.0867	0.0696
B*C		0.0693	0.0739	0.0791	A
	A1*C	0.0604	0.0809	0.0847	0.0753
L.S.D	A	0.0794	0.0655	0.0693	0.0714
P < .0.05	0.00074	0.0680	0.0751	0.0822	0.0751
	A2*C				B
	A3*C	0.0647	0.0771	0.0843	0.0753
	B1*C	0.0719	0.0774	0.0744	0.0746
	B2*C	0.0713	0.0670	0.0783	0.0722
	B3*C	C	A*B	B*C	A*B*C
	B	0.00074	0.00013	0.00074	0.00221
	0.00074		A*C		
			0.00013		

The triple association between potassium treatment, nature of water system water and ascobin significantly affects gibberellin content. Treatment A2B1C3 demonstrated the most elevated gibberellin content at 0.0849 mg. gme1 dry weight, contrasted and the least substance in treatment A1B2C3, which was 0.0412 mg. gme1 dry weight.

3.3. Abscisic acid content in leaves (mg. gm^{-1} dry weight)

The results shown in Table 4 indicate that potassium fertilizer has no significant effect on abscisic acid content in Z. mays leaves.

The results show that irrigation water has a significant effect on this trait. Treatment B3 gave the highest value at 3.282 mg. gme1 dry weight, compared with treatment B1, which had a value of 2.854 mg. gme1 dry weight, where abscisic acid content increased by increasing salinity. Increasing the ascobin level significantly increased abscisic acid content in Z. mays leaves (3.155 and 3.506 mg. gme1 dry weight) by spraying ascobin at levels C2 and C3 sequentially, compared with level C1.

Bilateral interactions between the potassium fertilizer and irrigation water have no significant effect on this trait. In the interaction of potassium fertilization and ascobin, the highest abscisic acid content was in treatment A1C3 at 3.847 mg. gme1 dry weight, while the lowest abscisic acid content was in treatment A3C1 at 2.341 mg. gme1 dry weight. The interaction between saline water and ascobin has a significant effect on the hormone. The highest value was in treatment B1C3 at 3.576 mg. gme1 dry weight, compared with treatment B1C1, which gave the lowest value at 2.367 mg. gme1 dry weight.

The results show that the triple interaction between the factors in this study has a significant effect. Treatment A1B2C3 achieved the highest abscisic acid content at 4.220 mg. gme1 dry weight.

Table 3 shows the effect of the potassium fertilizer and ascobin spraying on gibberellin content (mg. gme1 dry weight) in Z. mays under different salinity stress levels.

4. Discussion

The results of this study show a significant differences in the content of leaf plant hormones, such as auxin, gibberellin and abscisic acid treated with the potassium fertilizer (Tables 2e4).

The results shown in Tables 2 and 3 indicate a significant differences in the plant hormones auxin and gibberellin treated with saline water at different levels. In current study, the endogenous auxin and gibberellin contents decreased with increase water salinity levels

Pure Sciences International Journal of Kerbala

Journal Homepage:https://journals.uokerbala.edu.iq/index.php/psijk

Table 4
Effect of potassium fertilizer and spraying of ascobin in the abscisic acid hormone content (mg. gm^{-1} dry weight) in leaves of the Zea mays under different salinity stress levels.

Potassium added kg K. ha^{-1} A	Salinity irrigation water ds. m^{-1} B	Spray level of Ascobin mg. L^{-1} C	A*B
0 A_1		0C_1 300C_2 600C_3	
	1 B1	2.550 2.340 3.920	2:937
	3 B2	2411 3.210 4.220	3:280
	6 B3	2.980 3.201 3.401	3:194
100 A_2	1 B1	2.680 2.680 3.410	2:923
	3 B2	3.030 3.111 2.591	2:911
	6 B3	2.631 3.911 3.781	3:441
200 A_3	1 B1	1.871 2.840 3.400	2:703
	3 B2	2.562 3.021 3.301	2:961
	6 B3	2.591 4.080 3.531	3:400
C		2.252 3.155 3.506	A
A*C	A1*C	2.647 2.917 3.847	3:137
	A2*C	2.780 3.234 3.261	3:091
	A3*C	2.341 3.314 3.411	3.847
			B
B*C	B1*C	2.367 2.620 3.576	3.411
	B2*C	2.668 3.114 3.271	3.051
	B3*C	2.544 3.731 3.571	3.345
L.S. D A	B	C A*B A*C	B*C A*B*C
P < 0.05 0.0086	0.0086	0.0086 0.0149 0.0149	0.0149 0.0258

as compared to control. It suggests that the reduction in growth under salt stress conditions is caused by reduced production of auxin and gibberellin. Table 4 shows significant differences in the estimation of plant hormones, such as abscisic acid, whose value increased by increasing salinity levels, which is attributed to the increased production of abscisic acid, which in turn stimulates the closure of the stomata. The closure of the stomata causes reduced photosynthesis, which reduces carbon dioxide content and increases oxidative stress [18].

Tables 2e4 indicate that auxin, gibberellin and abscisic acid increase when ascobin spraying concentrations increase because of the role of ascorbic acid in nutrient absorption, thus stimulating the increase of hormones. Ascorbic corrosive goes about as a cofactor for a few chemicals and directs the phytohormone-intervening flagging genius cesses and numerous physiological procedures in plants. These results are consistent with those found by Ref. [19]. Also, bilateral interactions between the potassium fertilizer and irrigation water have significant effects on the plant hormones auxin, gibberellin and abscisic acid in maize. The abscisic acid content in the leaf has a significant effects, which indicates that potassium plays a role in enhancing plants' tolerance to different salt stresses as well as in controlling plant hormones [20,21]. In this study, the bilateral interactions between ascobin spraying and irrigation water with different salinity levels show significant effects on plant hormones in the fall seasons, which positively reflects maize's improved tolerance to salt stress. These results are consistent with those found by Ref. [22] that ascobin improved salt resistance in cowpea by upgrading the gathering of nontoxic metabolites, for example, all out solvent sugars, proline and glycine betaine just as N, P and K as defensive adjustment.

References

[1] G. Peter, S. postel, Avoiding a water crisis, Crops Soil Agronomy News 53 (12) (2008). De-cember.
[2] T.K. Bose, Fruit of India. Tropical and Subtropical. Naya Prakash. India, 1985.
[3] M.E. Balibrea, M. Parra, M.C. Bolarin, F. Perez-Alfocea, Peg-Osmotic treatment in tomato seedlings induces salt-adaptation in adult plants, Funct. Plant Biol. 26 (1999) 781e786.
[4] F.A. Zeid, O.M. Elshihi, A.E. Ghallab, F.E.A. Ibrahim, Effect of exogenous ascorbic acid on wheat tolerance to salinity stress conditions, Arab J. Biotech. 12 (2009) 149e174.
[5] V. Pavet, E. Olmos, G. Kiddle, S. Mowla, S. Kumar, J. Antoniw, M.E. Alvarez, C.H. Foyer, Ascorbic acid deficiency activates cell death and disease resistance responses in Arabidopsis, Plant Physiol. 139 (2005) 1291e1303.
[6] A. Shalata, P. Neumann, Exogenous ascorbic acid (vitamin C) increases resistance to salt stress and reduces lipid peroxidation, J. Exp. Bot. 52 (2001) 2207e2211.
[7] A. Al-al, S. Fatin, Effect of urea and some organic acids on plant growth, fruit yield and its quality of sweet pepper (Capsicam annuns), Res. J. Agric. Biol. Sci. 5 (2009) 372e379.
[8] M.T. Saqr, Stress Physiology, Faculty of Agriculture, Mansoura University, 2012.
[9] E.M. A Elhamid, M.S. Sadak, M. M Tawfik, Alleviation of adverse effects of salt stress in wheat cultivars by foliar treatment with antioxidant 2dchanges in some biochemical aspects, lipid peroxidation, antioxidant enzymes and amino acid contents, Agric. Sci. 5 (2014) 1269.
[10] J. Rhoades, Use of saline water for irrigation, Calif. Agric. 38 (1984) 42e43.
[11] J.R. Al- Hadithi, Validity of Modern Wells of Agricultural Wheat, MSc Master Thesis, University of Baghdad, 1998.
[12] M.F. Yassin, A.H. Ibrahim, A. A Abed, The use of water wells in the region Halawat desert in Ramadi, J. Arab Agric 2 (1998) 14.
[13] J.K.G. Al-shammari, Effect of the Interaction between Irrigation and Irrigation Methods in Some Properties Chemical Soil

Pure Sciences International Journal of Kerbala

Journal Homepage:https://journals.uokerbala.edu.iq/index.php/psijk

and the Effectiveness of the Rice Crop, MSc MSc Thesis, Anbar University, 2004.

[14] A.L. Page, R.H. Miller, D.R. Kenney, in: 2nd, in: Agron (Ed.), Methods of Soil Analysis, vol. 9, Publisher, Madiason, Wis- consin, 1982, p. 350.

[15] K.A. Gadoua, Agriculture and service of wheat crop Republic of Iraq, Ministry of Agriculture General Authority for Agri- cultural Cooperation and Extension, 2003.

[16] N. Ergun, Ş.F. Topcuoglu, A. Yildiz, Auxin (Indole-3-acetic acid), gibberellic acid (GA_3), abscisic acid (ABA) and cyto-
kinin (zeatin) production by some species of mosses and li- chens, Turk. J. Bot. 26 (2002) 13e18.

[17] SAS , Statisical Analysis System, User,s Guide . Statistical Version 9, 1th ed ., Instiute Incorporated Cary, N.C.USA, 2012. SAS.

[18] J.K. Zhu, Salt and drought stress signal transduction in plants, Annu. Rev. Plant Biol. 53 (2002) 247e273.

[19] M.S. Sadak, S.A. Orabi, Improving thermo tolerance of wheat plant by foliar application of citric acid or oxalic acid, Int. J. ChemTech. Res. 8 (2015) 333e345.

[20] E.R. Jarret, V.J. Baird, Specific Nutrient Recommendations . Grain Production Guide No 4. Published by Center for Inte- grated Pest Management North Carolina Cooperative Exten- sion, 2001, pp. 1e6.

[21] A. Krauss, Assessing Soil Potassium in View Contemporary Crop Production . Regional IPI e LIA e LUA Workshop on Balanced Fertilization in Contemporary Plant Production . IPI, 2003.

[22] A.A. Zinab, Improving growth and yield of salt-stressed cowpea plants by exogenous application of ascobin, Life Sci. J. 11 (2014) 11.

First Year-First Folder-Number: 0
PSIJK 184-191

Pure Sciences International Journal of Kerbala

Journal Homepage:https://journals.uokerbala.edu.iq/index.php/psijk

Effect of nano-silvers, nano-zinc oxide and benomyl pesticide on some physiological properties of *Sclerotinia sclerotiorum*

Husham A. Mehdi[1] , Ban T. Mohammed*[2], Abbas M. Bashy [3]**

[1,2]*Department of Biology, University of Kerbala, Iraq.*

[3] *Department of Chemistry, Applied Medical Sciences, University of Kerbala, Iraq*

[*]*E-mail: Bantmh@gmail.com*

***** A part of PhD. thesis***

Abstract: Laboratory experiments were conducted in the laboratory of graduate studies in the Department of Biology - College of Education for Pure Sciences / Kerbala University to study the effect of silver nanoparticles with glucose, sodium bicarbonate, ascorbic acid and formaldehyde, as well as the zinc oxide and compared their results with the fungicide Benomyl on the *Sclerotinia sclerotiorum* (Lib.) De Bary, which affects a large number of plants. The aim of this study was to reduce using a conventional chemical pesticide and to reduce pollution. A series of experiments were carried out which included the use of fungal isolate previously isolated and diagnosed as *sclerotinia sclerotiorum*(MMBIRAQ), recorded for the first time in Iraq at the National Center for Biotechnology Information (NCBI) under the entry numbers Accession number (MF167296) at GenBank. The nanocompounds and Benomyl were prepared volumes of 2ml, 1ml, 0.7 ml, 0.5 ml, 0.3 ml, 0.1 ml, 50 µ ml, 25 µ ml to 50 ml from the medium. The results of the treatment were obtained with nanocompounds and fungicide in terms of the diameter of the fungal colony grown on the potato dextrose agar (PDA) medium and the biomass of the fungus grown on the medium of the potato dextrose broth (PDB), according to the average number , mass of the sclerotia , the shape of growth in Petri dishes , as well as the preparation of microscopic slices for the purpose of measuring the length , width and shape of the fungus under the microscope using the microscope ocular.The effect of nanocompound and fungicides on the production of oxalic acid, which is the main factor in fungal pathology, was also studied. The effect of these nanocompounds and fungicides on subsequent generations was studied after subsequent experiments. The results showed that all, nanocompound had a significant effect on the diameter of the fungal colony (cm) after 5 days of inoculation at 0.3 ml and the highest volumes compared with the comparison sample which recorded 9 cm diameter. After 12 days of inoculation, it was 0.7 ml and larger volumes compared with the comparison sample. Nanocompound also caused the disappearance of sclerotia ranging from 25 micrometers to 2 millimeters compared with the comparison sample of 15.57 sclerotia. The mass of sclerotia for all samples was 0.042 g. The effect of nanoparticles on the biomass of fungi was significant from 0.1 ml, and the towards higher volumes, when the sclerotia were produced.

Keywords: *Sclerotinia sclerotiorum*, fungal nanotechnology.

Pure Sciences International Journal of Kerbala

Journal Homepage:https://journals.uokerbala.edu.iq/index.php/psijk

Sclerotinia sclerotiorum (Lib) De Bary conditions and can survive more than eight years under laboratory conditions (Mohammed 2012). Sclerotia can be survived after the soil is ploughed and deeply buried, so the buried of sclerotia reduces the chances of survival(Imolehin & Grogan 1980). The fungus produces oxalic acid, which is an important factor in virulence, the acid is affected by a variety of environmental and chemical factors(Mohammed, and Almothafer 2013). Benomyl is one of the pesticides that can control the *S.sclerotiorum* (Gossen et al. 2001). Benomyl has an inhibitory role on cell division in fungus, but it has negative effects on the environment through its effect on fungal mycorrhiza fungi(Clement & Jarrett 1994). It also affects the process of nitrification through its effect on the bacteria that have a role in this process (Chen et al. 2001). Recently, attention has been focused on alternatives to the use of chemical pesticides and being environmentally friendly, including the use of silver nanocompound that inhibits fungi and pathogenic bacteria (Clement and Jarret, 1994). The silver nanoparticle has a stronger effect as an antimicrobial agent when compared with silver ion in the mineral formula (Morones et al. 2005). The role played by nanocompound as an antimicrobial agent was due to its large surface area, size , physical and chemical properties, which allowed to increase contact with microorganisms and to penetrate into cells (Kim et al. 2012). Silver nanocompounds have the ability to attack vital microorganisms, including cell membrane structure, and thus will be damaged and lose function(Sondi & Salopek-Sondi 2004). Other nanocompounds are zinc oxide, which has important properties such as size, shape, structure, crystalline design and exterior appearance, because of the high and unique ionic oxide of the zinc oxide used in high surface areas and because of its high stability properties, therefore, it was used as an antimicrobial (Kolodziejczak-Radzimska & Jesionowski 2014). Studies have shown that produces sclerotia resistant to adverse zinc oxide is an optional toxic effect of bacteria with little effect on human cells, and is recommended for future use in agriculture and food industry(Zhang et al. 2007).

MATERIAL AND METHODS:

Samples Collection: The stems of the infected eggplant plants were collected from farms close to the Technical college of Musayyib, Babylon city ,Iraq, and where the sclerotia were taken. Based on the phenotypic symptoms and initial diagnosis. The sclerotia were washed with normal water and then sterile by immersing them for 3 minutes with 6% commercial chlorax solution, washed several times with sterile distilled water and dried on sterile filter sheets (Mohammed, 2001). The fungal isolation was recorded in the name *S.sclerotiorum* MMBIRAQ fungi as the first time in Iraq at the National Center for Biotechnology Information (NCBI) under the Accession number MF167296 in GenBank . The results revealed that the isolated S.sclerotiorum MMBIRAQ isolated in this study is a new isolation previously unknown in the world.(Husham *et.al* unpublished).

Cultivation of the sclerotia S. sclerotiorum: One sclerotia was planted in the middle of a petri dish containing a medium of chloramphenicol 250 mg / L. After five days of incubation at 20 + 2 ° C, and before the new sclerotia formation, the dish was divided into cubed pieces for the propagation of fungus on the wheat grain media as described in Mohammed, (2001), to produce as many sclerotia as possible.

Preparation of silver nanoparticles with the presence of the reduced agent glucose(Ag with glucose): Silver nanotubes are prepared according to the modified (El-Kheshen & El-Rab 2012) method as follow: Two grams of glucose dissolved in 50 ml distilled water and cooled until the temperature reached 60C ° ---- (Solution No. 1).Take 1 g of silver nitrate and dissolved in 50 ml distilled water ---------- (Solution No. 2).Take 1 g of starch and

Pure Sciences International Journal of Kerbala

Journal Homepage:https://journals.uokerbala.edu.iq/index.php/psijk

dissolved in 2 ml distilled water ---------- (Solution No. 3) .At first, solution No. 1 was placed on the Magnetic stirrer with heating until it reached 60 ° C, then solution 3 was added to solution 1, then solution 2 was added to the product solution drop by drop, with a shift in color from light yellow to light purple. Then the color turned to light orange, and the solution is the result of a stock of nanocompound, the concentration of silver nanoparticles in which 9.8 mg / ml, and from it attended the subsequent concentrations, by adding different volumes of it ,2 ml, 1 ml, 0.7 ml, 0.5 ml, 0.3 ml, 0.1 ml, 50 µml, 25 µml to 50 ml to the PDA media as in Table 1.

Preparation of silver nanocompound with the presence of the reduced agent Sodium Citrate (Ag with Sodium Citrate): - Silver nanocompound has been prepared in sodium phosphate by El-Kheshen and El-Rab (2012 modified method. The process is as follows:

One and a half gram of PVA material and dissolved in 50 ml distilled water ---------- (1)

Two gram of silver nitrate , dissolved in 100 ml distilled water, then 10 ml taken - --- No. (2)

Weight of 0.387 g of tri-sodium citrate and dissolved in 50 ml distilled water and 1.1were taken ---------- No. (3)

The PVA was added to the water with magnetic stirrer at 60 ° C, and then the solution 3 was added. Silver solution 2 was added as distillation until the solution was converted to light yellow, with the continued heat for two hours. the pH was adjusted at 9-11 and then turn to brown or black light after adding drops of NaOH, and considered the solution is the result of a stock of nanocompound concentration of silver nanoparticles in which 10 mg / ml, by adding different volumes of it, 2 ml, 1 ml, 0.7 ml, 0.5 ml, 0.3 ml, 0.1 ml, 50 µml, 25 µml to 50 ml to the PDA media as in Table 1.

Table 1: Concentrations of nanocompound (Ag/Zn) mg / ml) based on the volume used in the medium

Concentration of Nano compounds and Benomyl (mg / ml)	volume used in media							
	25 µml	50 µml	0.1 ml	0.3 ml	0.5 ml	0.7 ml	1 ml	2 ml
Ag + glucose	0.245	0.490	0.980	2.940	4.900	6.860	9.800	19.600
Ag + sodium bicarbonate	0.250	0.500	1.000	3.000	5.000	7.000	10.000	20.000
Ag + ascorbic acid	0.105	0.210	0.420	1.260	2.100	2.940	4.200	8.400
Ag + formaldehyde	0.0075	0.015	0.030	0.090	0.150	0.210	0.300	0.600
zinc oxide	0.725	1.450	2.900	8.700	14.500	20.300	29.000	58.000
Benomyl	o.oooo3	0.00006	0.0012	0.0036	0.0060	0.0084	0.0120	0.0240

Preparation of Silver nanocompound is prepared with the presence of the reduced agent Ascorbic acid (Ag with Ascorbic acid):

The silver nanocompounds were prepared by a reduced agent, ascorbic acid according to (El-Kheshen & El-Rab (2012) modification method, as follows:Weight of 2 g of silver nitrate , dissolved in 100 ml distilled water, 40 ml were taken ---------- (No. 1).Weight of 5 g of Polyvinyl pyrrolidone (PVP) added to

Pure Sciences International Journal of Kerbala

Journal Homepage:https://journals.uokerbala.edu.iq/index.php/psijk

solution 1 --- (No. 2).
Weight of 1.7 g ascorbic acid, dissolved in 150 ml distilled water -------- (No. 3). PVP was added to 40 ml of silver nitrate solution with magnetic stirrer. The solution 1 + 3 was added to solution 2 at 80 ° C, then the heat was stopped with Continues stirrer, by adding solution 3, and the color shift of the solution is monitored until the red color appears. The resulting solution is a stock of nanocompound. The concentration of nanocompound is 4.2 mg / ml and the subsequent concentrations by adding different volumes of it, 2 ml, 1 ml, 0.7 ml, 0.5 ml, 0.3 ml, 0.1 ml, 50 µml, 25 µml to 50 ml to the PDA media as in Table 1.

Preparation of nanocompound with the presence of the reduced factor Formaldehyde (Ag with formaldehyde): According to(Sarkar et al. 2007) .Dissolved of 0.17 g silver nitrate in 50 ml distilled water ------ No. (1). Dissolved of 0.288 g of SDS in 50 ml distilled water---------- No. (2). to fixed nano- silver. And to produce ammoniac silver complex, add 20 ml ammonia ---------- No. (3). For reduction added 20 ml formaldehyde ---------- No. (4). Solution 3 was added to 20 mL of solution 1, with stirring, then add 20 ml solution 2 was with the stirring for 5 minutes and then 20 ml of Solution No. 4 with stirring and raise the temperature to about 82 ° C until the color is shift to dark yellow. The resulting solution is a stock of nanocompound. The concentration of nanoparticles is 0.3 mg / ml, by adding different volumes of it, 2 ml, 1 ml, 0.7 ml, 0.5 ml, 0.3 ml, 0.1 ml, 50 µml, 25 µml to 50 ml to the PDA media as in Table 1.

Preparation of Zinc oxide Nanocompound (ZnO):was prepared according to (Kunde et al. 2016) modification method as follows :
Dissolved of 29.728 g of zinc nitrate Zn (NO_3) in a solution of 1000 ml of distilled water with a quantity of starch and stirring with a magnetic mixer until melting zinc nitrate.
Solution of 25 ml of NaOH 0.2M was added in the form of a droplet beaker and continued for 2 hours after adding NaOH.The solution was centrifuged at 10000 rpm for 5 minutes .The precipitate was taken, washes with distilled water three times, and then dried at 80 ° C. The precipitate formed was put in an oven at 450C ° to burn the remaining materials after the formation of the zinc oxide.The dilution was done for zinc nanocompound by adding distilled water 100 ml to the 0.1 g nanocompound powder. The resulting solution is a stock of nanocompound. The concentration of nano-zinc oxide is 29 mg / ml and the subsequent concentrations were obtained by adding different volumes of it, 2 ml, 1 ml, 0.7 ml, 0.5 ml, 0.3 ml, 0.1 ml, 50 µml, 25 µml to 50 ml to the PDA media as in Table 1

Preparation of Benomyl: The benomyl pesticide has been prepared as the manufacturer of the pesticide, dissolves 60 g of benomyl pesticide powder in 100 liters of distilled water. The resulting solution is a stock .The concentration of the benomyl pesticide is 0.6 mg / ml and the subsequent concentrations were obtained. By adding different volumes of it , 2ml, 1 ml, 0.7 ml, 0.5 ml, 0.3 ml, 0.1 ml, 50 µml, 25 µml to 50 ml to the PDA media as in Table 1

Properties Study of Nanocompound Prepared by FTIR Infrared Spectrometer ,AFM Atomic Force Microscopy, SEM, Electron Microscope Scanner, U.V.visibale Spectroscopy of Visible and Ultraviolet Radiation Spectroscopy.

Nanocompound and benomyl were evaluated for growth of the *sclerotinia sclerotiorum* using different volume 2 ml, 1 ml, 0.7 ml, 0.5 ml, 0.3 ml, 0.1 ml, 50 µml, 25 µm to 50 ml of the medium.

On the PDA was measured:

The vegetative growth of *Sclerotinia sclerotiorum* based on diameter of the fungal colony was determined (cm) after 5and 12 days of inoculation **(**Husham et.al 2018). The following equation was used as in Kim and his group (2012) to find the percentage of inhibitory. Inhibition Rate (%) = R-r/ R, Where

Pure Sciences International Journal of Kerbala

Journal Homepage:https://journals.uokerbala.edu.iq/index.php/psijk

R and r represent the growth of control and treatment respectively.

The number and mass (g) of sclerotia grown on PDA after 12 days of inoculation.

Microscopic study of mycelium after treatment with nanocompound and benomyl after 12 days of inoculation.

The vitality of the pathogen in generations resulting from the treatment of nanocompound and benomyl on PDA with a measurement of the number and weight of the resulting sclerotia.

On liquid PDB was measured:

The rate of the biomass of the fungi grown on the liquid medium (g)was adopted after 12 days of inoculation, using the modified Augustine et al. (2006) method of Navale and its group (2015).

Estimation of oxalic acid produced by fungi in liquid media estimated at mg / l after 12 days of inoculation (Bateman & Beer 1965).

Statistical analysis: completely randomized design(C.R.D.) was adopted and means were compared by L.S.D. at 0.05 probability level.(Steel et al. 1997)

RESULTS AND DISCUSSIONS:

Study of properties of nanocompound: -

By infrared spectrometer: Noted in Figure 1, the conversion of silver from ion to metal after taking the electrons and comes the role of the installer to be formed balls shaped . the package between 703-666 represents the vibration of nanocompound to demonstrate the composition of nanocompound on the difference of the reduced factor, silver nanoparticles appear in different sizes and diameters (Sun 2013;Rycenga et al. 2011; (Sakamoto et al. 2009). By Atomic Force Microscope AFM: The results of the microscopic examination by the atomic force microscope in Fig. 2 ,the characteristics of the nanoparticles through the rise of the nanoparticle and its fear. This is shown by the microscopic atomic force, where the heights and volumes of nanoparticles varied according to the reduced factor) Van Hyning & Zukoski 1998.(

Electron microscopy scanner SEM: The nanocompound of different diameters according to the reduced factor (figure 3). The nanoparticle mix with the zinc oxide is shown in the shape of its silver heart and its zinc form (da Silva et al. 2011; Rogers et al. 2012; Alarcon et al. 2012.(

Optical and ultraviolet radiation spectroscopy. U.V.visibale: Figure 4 appears a Package location for nanoparticle by the wavelength of maximum absorption, showing the wavelength of light falling on the surface of nanoparticles with their free electrons orbiting the surface of the nanoscale to show us what is called Plasmon, which turns the metal surface electrons to give a bundle in the ultraviolet light (Aslan et al. 2005)

Pure Sciences International Journal of Kerbala

Journal Homepage:https://journals.uokerbala.edu.iq/index.php/psijk

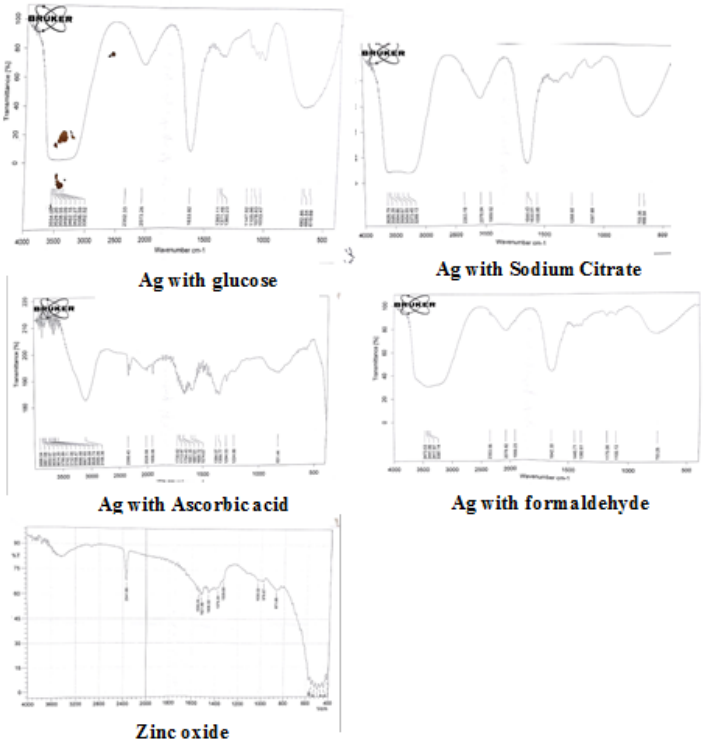

Figure 1: Properties of nanoparticles prepared by FTIR

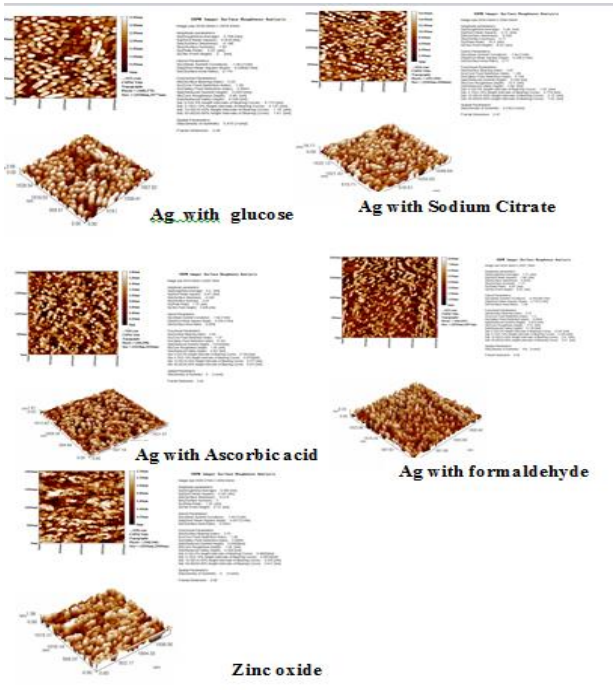

Figure 2: Properties of nanoparticles prepared by AFM

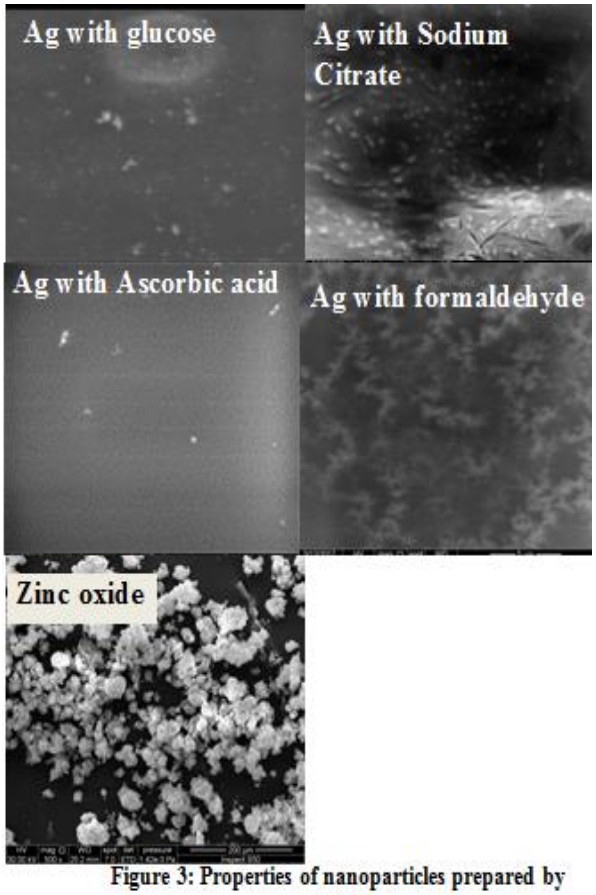

Figure 3: Properties of nanoparticles prepared by SEM

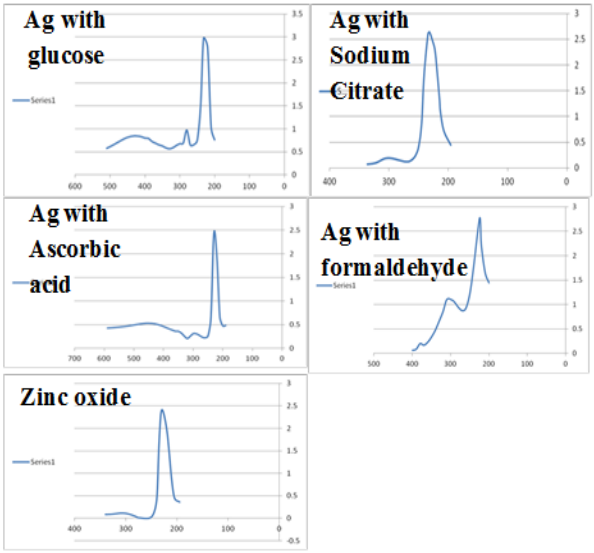

Figure 4: Properties of nanoparticles prepared by Optical and ultraviolet radiation spectroscopy. U.V.visibale.

Evaluation of nanoparticles and benomyl

Pure Sciences International Journal of Kerbala

Journal Homepage:https://journals.uokerbala.edu.iq/index.php/psijk

pesticide on the PDA medium:

Evaluation of nanoparticles and benomyl in the growth of the fungus *Sclerotinia sclerotiorum* after 5 days of inoculation: Figure 5 shows that nanocompound silver with formaldehyde gave the lowest growth rate in terms of diameter of the fungal colony, and it was not significant with benomyl pesticide. So it was clear that with increasing the volume of nanocompound decreased diameter of the fungal colony. In the same figure shows that there was a significant interaction between all nanocompound and volumes with the silver with formaldehyde at 0.3 ml and the larger volumes were completely inhibited the growth. In the Fig. 6 shows although no colony diameter was inhibited, but there were changes in the growth of fungal mycelium , including the disappearance of the cotton appearance of the fungal mycelium and appearance of transparent hypha. The effect of nano-silver on formaldehyde showed significant differences in inhibition of fungal growth ranging from 0.3 ml to 2 ml. Inhibition of formaldehyde which was completely inhibited. No gradient was observed and total inhibition was obtained as previous forms. In cultural appears Cottony fungal were similar and did not differ from control. The lowest inhibitory rate was at 0.5 ml and was estimated at 11% and highest inhibition at 2 ml. By 38%. As for the benomyl pesticide, the results showed significant differences between the different volume and the comparison sample started from 0.1 ml to 2 ml. For the 25 and 50 µml volumes, the cotton pattern appeared in the 0.1ml and the percentage of inhibition is 68% and the highest inhibitory rate was in the volumes that followed 0.3 ml and estimated at 100% and the differences in these volumes disappear (Fig. 6). These results prove the ability of silver nanoparticles in various forms as well as the alkaline oxide of nitrogen to inhibit the growth of fungal and this inhibition varies depending on the volume and method of preparation and the results showed that increase in volume gave an increase in the rate of inhibition. By Kim et al. (2012) of the study of the impact of nanocompound on plant pathogens, which inhibited their growth in every of the concentrations used. This effect may be due to increased saturation and absorption of nanoparticles by fungal hypha leads to a decrease in the activity of plant pathogenic fungi because of the effect of silver on the DNA microorganisms that is loss their ability to multiply, because of the silver and high tendency towards sulfur and phosphate thus inhibit the expression of proteins by ribosome units and enzymes necessary for energy production(Yamanaka et al. 2005; Feng et al., 2000). These results were identical to those of Kim et al (2012).

Pure Sciences International Journal of Kerbala

Journal Homepage:https://journals.uokerbala.edu.iq/index.php/psijk

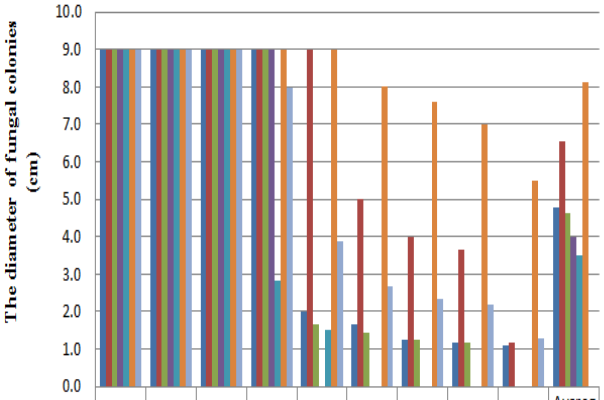

	control	25 µml	50 µml	0.1 ml	0.3 ml	0.5ml	0.7 ml	1 ml	2 ml	Average
Ag + glucose	9.0	9.0	9.0	9.0	2.0	1.7	1.3	1.2	1.1	4.8
Ag + sodium bicarbonate	9.0	9.0	9.0	9.0	9.0	5.0	4.0	3.7	1.2	6.5
Ag + ascorbic acid	9.0	9.0	9.0	9.0	1.7	1.4	1.3	1.2	0.0	4.6
Ag + formaldehyde	9.0	9.0	9.0	9.0	0.0	0.0	0.0	0.0	0.0	4.0
zinc oxide	9.0	9.0	9.0	2.8	1.5	0.0	0.0	0.0	0.0	3.5
Benomyl	9.0	9.0	9.0	9.0	9.0	8.0	7.6	7.0	5.5	8.1
Average	9.0	9.0	9.0	8.0	3.9	2.7	2.4	2.2	1.3	

$LSD_{0.05}$	Interaction=0.955	Size= 0.302	Nanocompound and benomyl =0..288

Figure 5: Effect of different sizes nanocompound and benomyl on the diameter of fungal colonies (cm) at the age of 5 days of inoculation on the PDA at 20 ± 2 ° C.

Each number represents three replicates

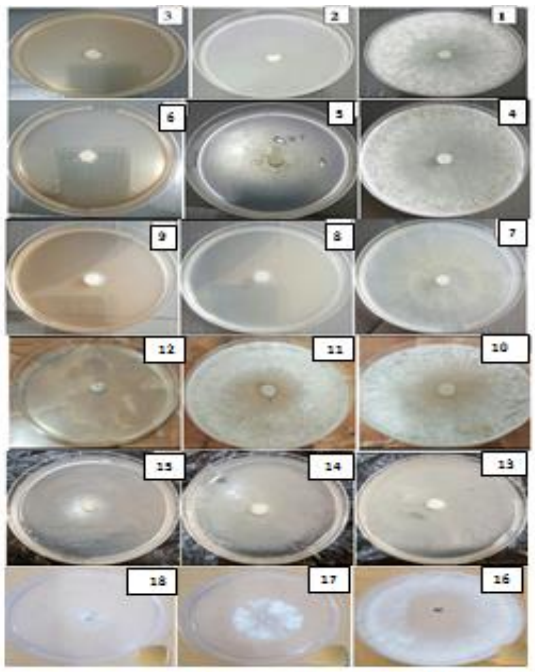

Figure 6 : Effect of different sizes nanocompound at benomyl on the diameter and shape of colonies (cm) : the age of 5 days of inoculation on the PDA at20 ± 2 °

1= control	2 = 0.1ml Ag with glucose	3 = 0.5ml Ag with glucose
4= 0.1ml Ag with Sodium Citrate	5= 0.5ml Ag with Sodium Citrate	6 = 2 ml Ag with Sodium Citrate
7= 0.1ml Ag with Ascorbic acid	8= 0.3ml Ag with Ascorbic acid	9 = 0.7ml Ag with Ascorbic acid
10=25µml Ag with formaldehyde	11=0.1ml Ag with formaldehyde	12=0.5ml Ag with formaldehyde
13=25µml Zinc oxide	14=0.1ml Zinc oxide	15=0.5ml Zinc oxide
16=0.1ml Benomyl	17=0.7ml Benomyl	18=2ml Benomyl

Evaluation of nanocompound and benomyl effect on the growth of the fungus *Sclerotinia sclerotiorum* after 12 days of inoculation: Figure 7 shows that there were differences in the effect of nanocompound and benomyl on the rate of fungal colony diameter grown on the PDA medium after 12 days of inoculation at 20 ± 2 ° C. There were increases average diameter of the fungal colony compared with 5 days of inoculation, so the average colony diameter of ZnO was 9.0 cm, indicating the full growth of the fungus, may be evidence of the impact of nanocompound and their lack of effectiveness due to re-aggregation or loss of some of their properties (Mahdizadeh et al. 2015) .The same figure showed that with the increase in the volume of nanocompound and benomyl pesticides there was a decrease in the diameter of the fungal colony. The volume of 2 ml was significant compared to the control treatment and the rest of the higher volumes. The volume 25µml did not cause any significant differences in the diameter of the colony. The same table showed the effect of interaction of different nanocompound and benomyl on the growth of *S. sclerotiorum* after 12 days of inoculation. Interactions showed inhibition of growth of the fungus. The volume of 2 ml was shown to be 66% and 72% inhibition with glucose and sodium citrate respectively. Zinc oxide had no effect and the rest showed a 100% inhibition ratio at 2 ml. The decreased effect at was at on these two volumes 0.3 ml and 0.5 ml, which had a significant effect in 5 days of incubation, and the lowest inhibitory rate was 50% at 0.7 ml and 66%. The fungal mycelium

Pure Sciences International Journal of Kerbala

Journal Homepage:https://iournals.uokerbala.edu.iq/index.php/psijk

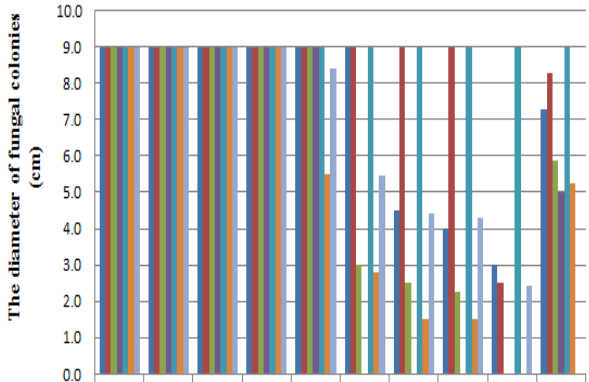

	control	25 µml	50 µml	0.1 ml	0.3 ml	0.5ml	0.7 ml	1 ml	2 ml	Average
Ag + glucose	9.0	9.0	9.0	9.0	9.0	9.0	4.5	4.0	3.0	7.3
Ag + sodium bicarbonate	9.0	9.0	9.0	9.0	9.0	9.0	9.0	9.0	2.5	8.3
Ag + ascorbic acid	9.0	9.0	9.0	9.0	9.0	3.0	2.5	2.3	0.0	5.9
Ag + formaldehyde	9.0	9.0	9.0	9.0	9.0	0.0	0.0	0.0	0.0	5.0
zinc oxide	9.0	9.0	9.0	9.0	9.0	9.0	9.0	9.0	9.0	9.0
Benomyl	9.0	9.0	9.0	9.0	5.5	2.8	1.5	1.5	0.0	5.3
Average	9.0	9.0	9.0	9.0	8.4	5.5	4.4	4.3	2.4	

$LSD_{0.05}$ Interaction=0.502 Size= 0.159 Nanocompound and benomyl =0.151

Figure 7: Effect of different sizes nanocompound and benomyl on the diameter of fungal colonies (cm) at the age of 12 days of inoculation on the PDA at 20 ± 2 ° C.

Each number represents three replicates

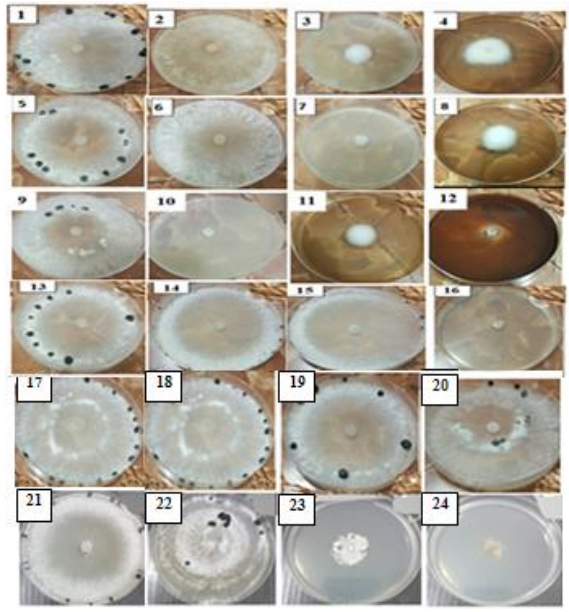

Figure 8: Effect of different sizes nanocompound and benomyl on the diameter and shape of colonies (cm) at the age of 12 days of inoculation on the PDA at20 ± 2 ° C.

1= control
2 = 50 µml Ag with glucose
3 = 0.3ml Ag with glucose
4= 2.0ml Ag with glucose
5= 25 µml Ag with Sodium Citrate
6 = 0.1 ml Ag with Sodium Citrate
7= 0.5ml Ag with Sodium Citrate
8=2.0ml Ag with Sodium Citrate
9 =25 µml Ag with Ascorbic acid
10== 0.1ml Ag with Ascorbic acid
11=0.7ml Ag with Ascorbic acid
12=2.0 ml Ag with Ascorbic acid
13=25 µml Ag with formaldehyde
14=0.1ml Ag with formaldehyde
15=0.3ml Ag with formaldehyde
16=0.5ml Ag with formaldehyde
17= control
18=control
19=0.1ml Zinc oxide
20=0.3ml Zinc oxide
21=25 µml Benomyl
22= 0.1ml Benomyl
23=0.5ml Benomyl
24=1.0ml Benomyl

was spread out in the form of a scattered hypha away from the center of the plate in a radial white color and lost the normal cotton shape of the fungus (Figure 8). In silver with sodium citrate, the results showed that the fungal growth filled the dish in all volumes except with 2 ml, The fungal growth in figure 8 shows the hypha in the volumes 25 µml, 50 µml and 0.1 ml was cotton shape as the shape of the control dish, while the other volumes were transparent hypha filled the dish. This may be the reason for the inability of the fungus to form initiation of sclerotia, and showed transparent growth due to treatment with nanoparticles and benomyl pesticide. The fungal pattern did not change under the effect of different sizes of zinc oxide from the control .These results were identical to those of Mahdizadeh and others (2015)who mentioned that the effect of silver nanoparticles decreases with time , in addition of some resistance or adaptation to pathogenic fungi(Arciniegas-Grijalba et al. 2017; Petica et al. 2008) noted that nanocompound initially showed high antifungal ability, which decreased over time without losing completely, as well as the the stable colloidal solution containing nanocompound has the antifungal properties are effective against *Aspergillus, Penicillium* and *Trichoderma*.

Evaluation of nanocompound and benomyl on the number of sclerotia of the fungus *Sclerotinia sclerotiorum* after 12 days of inoculation: The results in figure 9 showed significant differences in the number of sclerotia. Silver with glucose was the lowest in comparison to other nanocompound and benomyl, while the highest number of sclerotia was in zinc oxide and Benomyl. As for the effect of the size of the nanocompound and the benomyl pesticide on the number of Sclerotia, the results showed that there were significant differences between the different volume number of sclerotia in the size of 25 µml and the lowest in the 1 and 2 ml. The same figure

Pure Sciences International Journal of Kerbala

Journal Homepage:https://journals.uokerbala.edu.iq/index.php/psijk

showed significant interaction between nanocompound and benomyl (nano-silver, nano-zinc and benomyl). Nanocompound silver with glucose showed a complete inhibitory effect on the appearance of sclerotia on different volume of nanocompound, the inhibition of 100%. Sclerotia has not been shown compared to control, this achieves the desired goal of reducing the number of sclerotia and the minimum volume of the inhibitor. The mycelium growth on petri dishes was

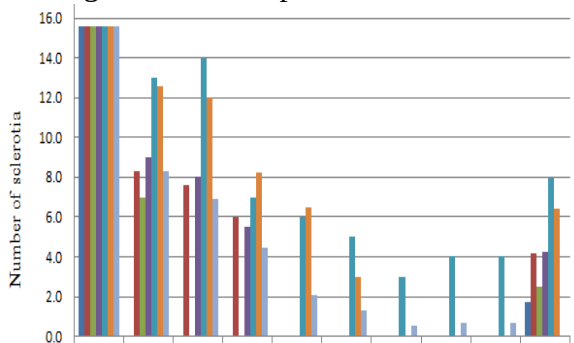

	control	25 µml	50 µml	0.1 ml	0.3 ml	0.5ml	0.7 ml	1 ml	2 ml	Average
Ag + glucose	15.6	0.0	0.0	0.0	0.0	0.0	0.0	0.0	0.0	1.7
Ag + sodium bicarbonate	15.6	8.3	7.6	6.0	0.0	0.0	0.0	0.0	0.0	4.2
Ag + ascorbic acid	15.6	7.0	0.0	0.0	0.0	0.0	0.0	0.0	0.0	2.5
Ag + formaldehyde	15.6	9.0	8.0	5.5	0.0	0.0	0.0	0.0	0.0	4.2
zinc oxide	15.6	13.0	14.0	7.0	6.0	5.0	3.0	4.0	4.0	8.0
Benomyl	15.6	12.6	12.0	8.3	6.5	3.0	0.0	0.0	0.0	6.4
Average	15.6	8.3	6.9	4.5	2.1	1.3	0.5	0.7	0.7	

LSD 0.05 Interaction=2.315 Size= 0.732 Nanocompound and benomyl=0.698

Figure 9: Effect of different sizes nanocompound and benomyl on the number of sclerotia of the *.Sclerotinia sclerotiorum* after 12 days of inoculation on the PDA at 20 ± 2 ° C
Each number represents three replicates

nanocompound, (Shyla et al. 2014) reported that nanocompound caused deformities fungal hypha and degradation lead to defects in sclerotia and lack of composition.

Evaluation of nanocompound and benomyl effect on the mass of the *sclerotinia sclerotiorum* after 12 days of incubation:

The results showed in Figure 10 that there were significant differences between nanocompound and benomyl in terms of the mass of sclerotia. The lowest mass of Sclerotia in nano-silver with

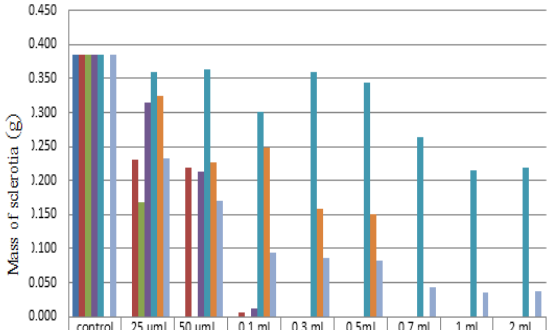

	control	25 µml	50 µml	0.1 ml	0.3 ml	0.5ml	0.7 ml	1 ml	2 ml
Ag + glucose	0.386	0.000	0.000	0.000	0.000	0.000	0.000	0.000	0.000
Ag + sodium bicarbonate	0.386	0.230	0.220	0.006	0.000	0.000	0.000	0.000	0.000
Ag + ascorbic acid	0.386	0.168	0.000	0.000	0.000	0.000	0.000	0.000	0.000
Ag + formaldehyde	0.386	0.315	0.213	0.011	0.000	0.000	0.000	0.000	0.000
zinc oxide	0.386	0.360	0.364	0.301	0.360	0.345	0.264	0.216	0.220
Benomyl	0.000	0.324	0.226	0.248	0.159	0.150	0.000	0.000	0.000
Average	0.386	0.233	0.171	0.094	0.087	0.083	0.044	0.036	0.037

LSD 0.05 Interaction=0.074 Size= 0.023 Nanocompound and benomyl =0.022

Figure10: Effect of different sizes nanocompound and benomyl on the mass of sclerotia (g) of the *.Sclerotinia sclerotiorum* after 12 days of inoculation on the PDA at 20 ± 2 ° C
Each number represents three replicates

transparent and has a spread to the top away from the PDA and
therefore the absence of cotton shape may be indicative and absence of the sclerotia initiation. The same figure showed that the effect of benomyl pesticide had significant differences in 25 µml. The mycelium shape on 25 µml to 0.5ml was regular growth, cotton shape, thus forming sclerotia. The highest rate of production of sclerotia was 25 µml with a rate of 8.3 after the control while the minimum volume of sclerotia products of 1 and 2 ml at 0.7 sclerotia, this may be due to the effect of various sugar. There were no significant differences in the mass of sclerotia. The effect of different volumes showed significant differences between them and control. These results were similar to those of G et al. 2016 Which showed that nanocompound have an effect on sclerotia formation , emergence , the appearance of deficiency and deformities of sclerotia.

Evaluation of nanocompound and benomyl effect of the length and width of fungal cell *Sclerotinia scleroterium* after 12 days of inoculation:

Figure 11 shows that different nanocompounds

Pure Sciences International Journal of Kerbala

Journal Homepage:https://journals.uokerbala.edu.iq/index.php/psijk

and benomyl significantly affected the rate of fungal cell length compared to the control sample. The effect of different volumes on fungal cell length had a significant effect on all volumes from 25 µml to 2 ml. The shorter cell was 2 ml and the longest cell was 25 µml after the comparison sample, suggesting changes in the fungal growth. The conditions that are no longer suitable for the growth due to the addition of different compounds(Christias & Lockwood 1973) . As for the cell width rate, there were significant differences in the effect of nanocompound and benomyl on the fungal cell width rate. The fungus may be trying to formation sclerotia and to escape from unsuitable conditions for its vegetative growth. The treatments causes a significant decrease on the cell width rate from the comparison sample, nanocompound in different components, as well as the benomyl pesticide on the width and length of the fungal cells of the *sclerotinia sclerotiorum*. The effect was varied due to type of substance. It was highly effective in the all Ag treatments and as low in effect as on the zinc oxide.

nanocompound and benomyl on volume, as well as the effect of interaction between the type of material and the size in the width and length of the fungal isolates. The effect of silver nanoparticles on glucose showed significant differences in length of fungal cells from control, in the volume 0.1 ml and higher volumes, while the effect of silver nanoparticles on width appears in the volume of 0.7 ml and larger volumes. The longest cell fungus appeared in the size of 25 µml and the smallest cell fungus in 2 ml, in the width was to display fungal cell at the volume of 0.7 ml and higher volumes, the thinnest cell was in 0.1 ml and the lower volumes till the comparison sample, may be explained by the result of physiological changes within the fungus cells and perhaps the production of some compounds that act as a kind of protection for fungi, as well as changes that may lead to the loss of fungus of its vital processes , the aggregation of protoplasm ,shrinkage , destruction of the cell and collapse.(Figure 12) . The results showed that there were significant differences in the length and width of fungal cells. The least affected was

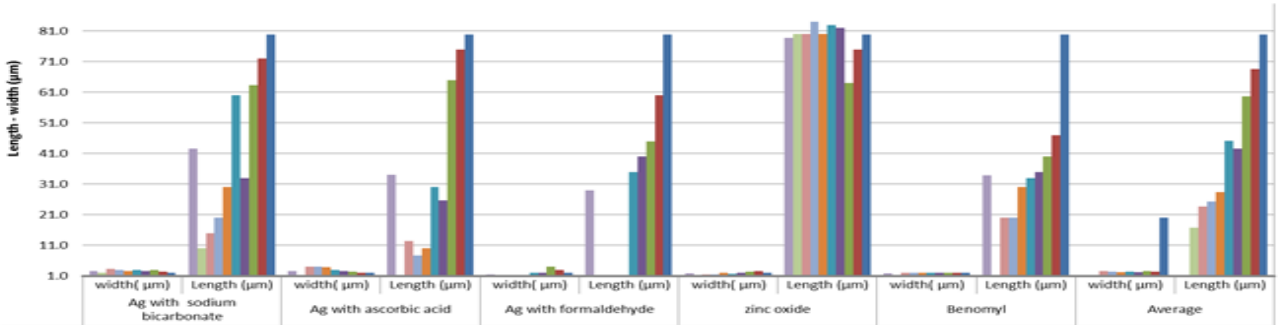

	Ag with sodium bicarbonate		Ag with ascorbic acid		Ag with formaldehyde		zinc oxide		Benomyl		Average	
	width(µm)	Length (µm)	width(µm)	Length (µm)	width(µm)	Length (µm)	width(µm)	Length (µm)	width(µm)	Length (µm)	width(µm)	Length (µm)
control	2.0	79.9	2.0	79.9	2.0	79.9	2.0	79.9	2.0	79.9	20.0	79.9
25 µml	2.3	72.0	2.0	75.0	3.0	60.0	2.5	75.0	2.0	47.0	2.3	68.5
50 µml	3.0	63.3	2.3	65.0	4.0	45.0	2.3	64.1	2.0	40.0	2.6	59.6
0.1 ml	2.5	33.0	2.5	25.6	2.0	40.0	2.0	82.0	2.0	35.0	2.2	42.6
0.3 ml	3.0	60.0	3.0	30.0	2.0	35.0	1.7	83.0	2.0	33.0	2.4	45.2
0.5ml	2.6	30.0	3.8	10.0	0.0	0.0	2.0	80.0	2.0	30.0	2.2	28.3
0.7 ml	3.0	20.0	4.0	7.6	0.0	0.0	1.5	84.0	2.0	20.0	2.4	25.3
1 ml	3.3	15.0	4.0	12.3	0.0	0.0	1.5	80.0	2.0	20.0	2.5	23.7
2 ml	2.0	10.0	0.0	0.0	0.0	0.0	1.0	80.0	0.0	0.0	1.2	16.7
Average	2.6	42.6	2.6	33.9	1.4	28.9	1.8	78.7	1.8	33.9		

LSD $_{0.05}$ Length		Interaction=13.568	Size= 4.291	Nanocompound and benomyl =4.091
	width	Interaction=1.430	Size= 0.452	Nanocompound and benomyl =0.431

Figure11: Effect of different size nanocompound and benomyl on the length and width of mycelium (µm) after 12 days of inoculation on the PDA at 20 ± 2 ° C
Each number represents three replicates

The figure indicates a significant effect of the zinc oxide, and showed a rate of cells in

Pure Sciences International Journal of Kerbala

Journal Homepage:https://journals.uokerbala.edu.iq/index.php/psijk

silver with glucose sugar and the thinnest cell rate was in silver with formaldehyde. These

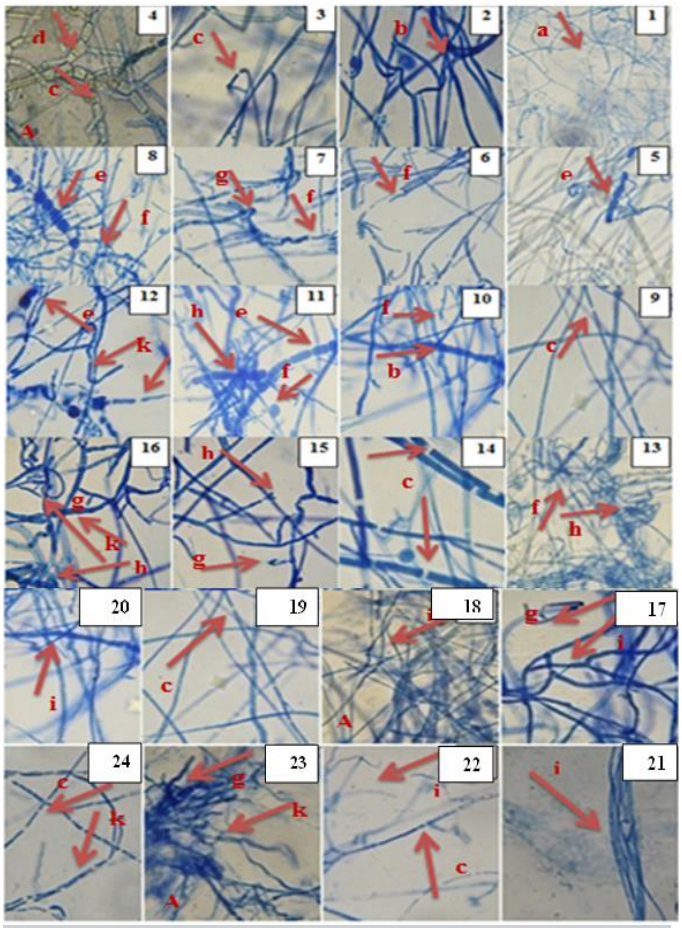

Figure 12: Effect of nanocompound and benomyl in different sizes on the length and width of the fungal cell after 12 days of inoculation on the PDA medium at 20 ± 2 ° C and with a 40X magnification force.

1= control	2 = 0.3ml Ag with glucose	3 = 0.5ml Ag with glucose
4= 0.1ml Ag with glucose	5= 50µml Ag with Sodium Citrate	6 = 0.3 ml Ag with Sodium Citrate
7= 0.7ml Ag with Sodium Citrate	8= 2.0ml Ag with Sodium Citrate	9 = 50µml Ag with Ascorbic acid
10=0.3µml Ag with Ascorbic acid	11=0.5ml Ag with Ascorbic acid	12=0.5ml Ag with formaldehyde
13=25µml Ag with formaldehyde	14=50µml Ag with formaldehyde	15=0.5ml Zinc oxide
16=0.3ml Ag with formaldehyde	17=25µml Zinc oxide	18=0.3ml Zinc oxide
19=1.0ml Zinc oxide	20=2ml Benomyl	21=50µml Benomyl
22=0.1ml Benomyl	23=0.5ml Benomyl	24=1.0ml Benomyl

a= Normal hypha
b= The appearance of the protoplasmic material and increased density of the protoplasm
c= Septa appears clearly as a result of the splitting of the plasma membrane and the aggregation of the protoplasm in the cell
d= Increase in cell thickness with increased appearance of septa as a starting point for the formation of sclerotia initiation.
A= Coloration of fungal hypha with melanin is evidence of resistance.
e= Protoplasm collection and cell wall separation.
f= The weakness of the fungal hypha and its breakdown as a result of the emergence of protoplasmic components, as well as elongation of the cell before the crash.
g= Deviation in the pathway of the protoplasmic material towards the intact hypha to prepare the formation of sclerotia initiation.
h= Swollen the fungal cells and shorten their length with increased septa and increased cell thickness
i= The fungal hyphae are Long and slim where no septa was shown on the strength of the magnification used
k= The emergence of septa with the survival of fungi maintains cell strength and no abnormalities.

results came close to other studied that used nanocompound , such as zinc oxide and the cause of abnormalities in the form of swilling fungal cells, which were usually smooth in the case of *Botrytis cinerea*, and in the case of *Penicillium expansum* caused distortions in the conidia (He et al. 2011). Nanocompound with the *Colletotrichum gloeosporioides* caused damage and overlap in the fungal hypha and have been malformed in the growth of fungal filaments and the shape of cellular walls (Lamsal et al. 2011).

Evaluation of nanoparticles and benomyl effect on the biomass of *Sclerotinia sclerotiorum* after 12 days of inoculation: on the liquid medium PDB: Figure 12 shows that the *Sclerotinia sclerotiorum* biomass was affected by nanocompound and benomyl. The effect of the volume ratio was significant differences with the control sample. The most significant volume in biomass was in 2 ml and the lowest was 25 µml. Nanomaterials in their liquid state showed a significant effect on fungal growth when compared with growth of fungi in dishes or in solid media This increase in effect was due to the free movement of liquid nanocompound in liquid media and decreased in solid.(Navale et al. 2015) where nanocompound caused a reduction in biomass may disappeared in the high concentrations of nanocompound used, and the role played by nanocompound can be attributed to the generation of oxidative stress that can be caused by the formation of free roots and therefore can affect the growth of microorganisms.

Evaluation of nanocompound and benomyl pesticide effect on the production of oxalic acid of *sclerotinia sclerotiorum* after 12 days of inoculation:The results in figure 14 indicate that nanocompound and benomyl had a significant effect on the rate of oxalic acid in the PSB compared with the control sample, the lowest oxalic acid in the benomyl , as for the volume ratio, there was a significant difference

Pure Sciences International Journal of Kerbala

Journal Homepage:https://journals.uokerbala.edu.iq/index.php/psijk

in oxalic acid when compared to the control sample and between them, where the size of 1.0 and 2.0 ml gave the lowest amount of oxalic acid and the amount of acid in the size of 25 µml. The maximum amount of acid after the comparison sample was 25 µml and the lowest quantity was 0.3 ml and the higher volumes .

These results were based on experiments that measured the amount of oxalic acid under the effect of inhibitors. There was a direct correlation between the rate of growth of the fungus and its production of acid, as the production of acid increases directly by increasing the vegetative growth of fungi, and the production of this acid is directly affected by the same factors that affect fungal growth(Beaulieu 2008; Beaulieu 2008; Mohammed, Al-Muzaffar, 2013 and Jubouri, 2013)

Evaluation of nanocompound and benomyl effect on the subsequent generation of *sclerotinia sclerotiorum* after 12 days of inoculation on the PDA after 12 days of inoculation: The results of this experiment showed in figure 15. The obtained data from previous experiment and despite of the weak growth of fungi, it gave a complete hypha similar to the control. This has been confirmed in previous experiments with regard to the microscopic interpretation of the fungal isolates(figure 12), which remain part of the sclerotia, may be the reason for overcome the conditions that are not suitable for the growth of fungi (Joboury & Mohammed 2013) . Results showed that although the cell wall was damaged due to an imbalance of the osmotic pressure between and outside the fungus, the results showed that, Low pH will in turn to inhibit the work of the enzymes of the wall, but at the same time, there are areas marked in Figure 12 indicate that the primers of the initiated sclerotia that are inappropriate conditions, with the survival of densely collected areas, have the ability to re-growth of the fungus when removing the inappropriate external effect. The production of sclerotia was uneven in the rate of dimension, and therefore was based on the rate of diameter of sclerotia as well as number .Table 15, the lowest number of sclerotia was after treatment with silver formaldehyde and did not differ significantly between them, while giving the largest number of sclerotia after treatment with silver with ascorbic acid, indicating the possibility of transformation of nanocompound and may have

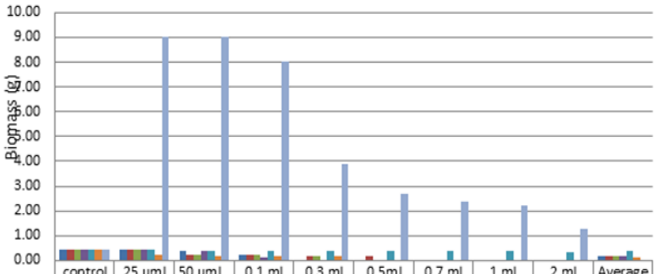

	control	25 µml	50 µml	0.1 ml	0.3 ml	0.5ml	0.7 ml	1 ml	2 ml	Average
Ag with glucose	0.46	0.42	0.38	0.21	0.00	0.00	0.00	0.00	0.00	0.16
Ag with sodium bicarbonate	0.46	0.43	0.23	0.21	0.16	0.17	0.00	0.00	0.00	0.18
Ag with ascorbic acid	0.46	0.43	0.23	0.23	0.17	0.00	0.00	0.00	0.00	0.17
Ag with formaldehyde	0.46	0.42	0.41	0.14	0.00	0.00	0.00	0.00	0.00	0.16
zinc oxide	0.46	0.45	0.40	0.41	0.41	0.38	0.38	0.37	0.35	0.40
Benomyl	0.46	0.21	0.20	0.17	0.16	0.00	0.00	0.00	0.00	0.13
Average	0.46	9.00	9.00	8.00	3.90	2.70	2.40	2.20	1.30	

LSD $_{0.05}$ Interaction=0.119 Size= 0.038 Nanocompound and benomyl =0.036

Figure 13: Effect of nanocompound and benomyl pesticide in biomass (g) for *Sclerotinia sclerotiorum* after 12 days of inoculation on liquid PDB medium at 20 ± 2 ° C
Each number represents three replicates

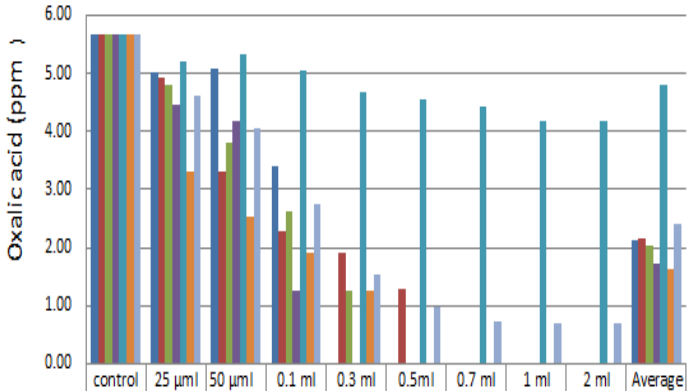

	control	25 µml	50 µml	0.1 ml	0.3 ml	0.5ml	0.7 ml	1 ml	2 ml	Average
Ag with glucose	5.68	5.01	5.08	3.41	0.00	0.00	0.00	0.00	0.00	2.13
Ag with sodium bicarbonate	5.68	4.93	3.31	2.29	1.90	1.30	0.00	0.00	0.00	2.16
Ag with ascorbic acid	5.68	4.81	3.80	2.61	1.27	0.00	0.00	0.00	0.00	2.02
Ag with formaldehyde	5.68	4.44	4.18	1.27	0.00	0.00	0.00	0.00	0.00	1.73
zinc oxide	5.68	5.20	5.31	5.06	4.69	4.55	4.43	4.18	4.18	4.81
Benomyl	5.68	3.30	2.53	1.90	1.27	0.00	0.00	0.00	0.00	1.63
Average	5.68	4.62	4.04	2.76	1.52	0.98	0.74	0.70	0.70	2.41

LSD 0.05 Interaction=1.134 Size= 0.358 Nanocompound and benomyl =0.342

Figure14: Effect of different sizes nanocompound and benomyl on oxalic acid (ppm) that produced after 12 days of inoculation on PDB at 20 ± 2 ° C
each number represents three replicates.

Pure Sciences International Journal of Kerbala

Journal Homepage:https://journals.uokerbala.edu.iq/index.php/psijk

a different effect of course on the carriers between the impact remains influential for generations to come and encourage the production of sclerotia and the completion of life cycle in a natural way.The same table shows that the effect of nanocompound (silver with zinc) and benomyl benzene on later generations (number and diameter of sclerotia) was at different levels, it had a clear effect on some materials such as ZnO and sometimes disappears some compounds that affected in the growth of fungus previously, as in the compound of silver nanocompound with sodium bicarbonate and ascorbic acid and sometimes the effect disappears as in the case of zinc oxide. This experiment may open up horizons for the effect of other nanocompound that may have an effect in later generations of the second generation, or that repeated treatment with nanocompound may conceal the sclerotia of the fungus without fear of a mutation, due to the effect of silver on several vital processes in the fungus making the role of mutation or nanocompound resistance is completely excluded (Herrera et al. 2001; Wright et al. 1999) .

CONCLUSIONS: Experiments have shown that nanomaterials and benomyl pesticide have affected the fungus with different effects, but have not continued their effects for the first

generation and may need extensive studies to identify useful and environmentally friendly nanoparticles.(Beaulieu 2008)

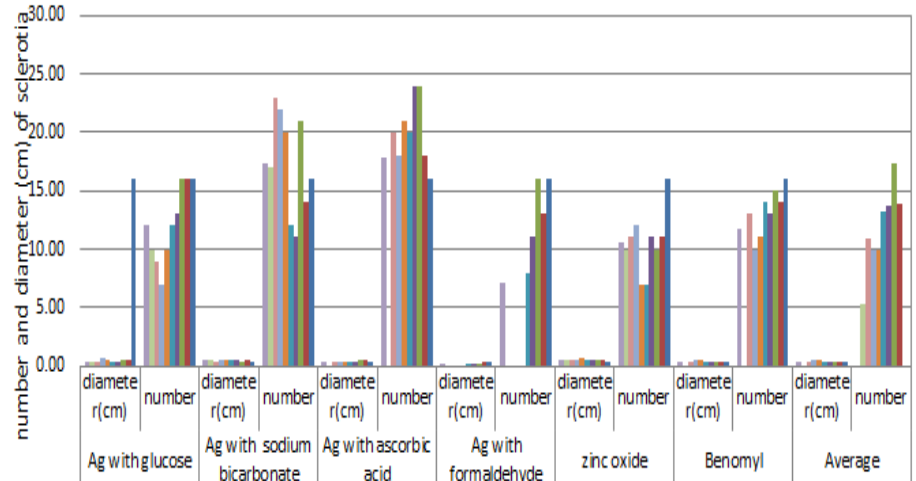

	Ag with glucose		Ag with sodium bicarbonate		Ag with ascorbic acid		Ag with formaldehyde		zinc oxide		Benomyl		Average	
	diameter(cm)	number	diameter(cm)	number	diameter(cm)	number	diameter(cm)	number	diameter(cm)	number	diameter(cm)	number	diameter(cm)	number
control	16.00	16.00	0.44	16.00	0.44	16.00	0.44	16.00	0.44	16.00	0.44	16.00	0.44	
25 µml	0.50	16.00	0.55	14.00	0.50	18.00	0.30	13.00	0.55	11.00	0.30	14.00	0.30	13.85
50 µml	0.50	16.00	0.35	21.00	0.50	24.00	0.20	16.00	0.52	10.00	0.30	15.00	0.30	17.42
0.1 ml	0.40	13.00	0.53	11.00	0.30	24.00	0.20	11.00	0.55	11.00	0.33	13.00	0.33	13.71
0.3 ml	0.35	12.00	0.45	12.00	0.35	20.00	0.20	8.00	0.45	7.00	0.40	14.00	0.40	13.28
0.5ml	0.45	10.00	0.46	20.00	0.35	21.00	0.00	0.00	0.62	7.00	0.50	11.00	0.50	9.85
0.7 ml	0.70	7.00	0.46	22.00	0.35	18.00	0.00	0.00	0.52	12.00	0.50	10.00	0.50	9.85
1 ml	0.30	9.00	0.40	23.00	0.30	20.00	0.00	0.00	0.50	11.00	0.40	13.00	0.40	10.85
2 ml	0.30	10.00	0.50	17.00	0.00	0.00	0.00	0.00	0.50	10.00	0.00	0.00	0.00	5.28
Average	0.43	12.11	0.47	17.33	0.35	17.88	0.14	7.11	0.52	10.55	0.34	11.77	0.34	

$LSD_{0.05}$ Number	Interaction=1.48	Size= 0.46	Nanocompound and benomyl =0.44
Diameter	Interaction=0.54	Size= 0.17	Nanocompound and benomyl =0.16

Figure15: Effect of different sizes nanocompound and benomyl on number and diameter (cm) of sclerotia to the second generation that produced after 12 days of inoculation on PDA at 20 ± 2 ° C
each number represents three replicates.

Pure Sciences International Journal of Kerbala

Journal Homepage:https://journals.uokerbala.edu.iq/index.php/psijk

REFERANCES:

Augustine, A., Imelda, J. & Paulraj, R., 2006. Biomass estimation of Aspergillus niger S, 4 a mangrove fungal isolate and A. oryzae NCIM 1212 in solid-state fermentation. *Journal of the Marine Biological Association of India*, 48(2), pp.139–146.

Bateman, D.F. & Beer, S. V, 1965. Simultaneous production and synergistic action of oxalic acid and polygalacturonase during pathogenesis by Sclerotium rolfsii. *Phytopathology*, 55(11), pp.204–211.

Beaulieu, R.A., 2008. Oxalic acid production by Sclerotinia homoeocarpa: the causal agent of dollar spot.

Chen, S.-K., Edwards, C.A. and Subler, S., 2001. Effects of the fungicides benomyl, captan and chlorothalonil on soil microbial activity and nitrogen dynamics in laboratory incubations. *Soil Biology and Biochemistry*, 33(14), pp.1971–1980.

Christias, C. & Lockwood, J.L., 1973. Conservation of mycelial constituents in four sclerotium-forming fungi in nutrient-deprived conditions. *Phytopathology*.

Clement, J.L. & Jarrett, P.S., 1994. Antibacterial Silver. *Metal-Based Drugs*, 1(5–6), pp.467–482. Available at: http://www.hindawi.com/archive/1994/707103/abs/.

El-Kheshen, A.A. & El-Rab, S.F.G., 2012. Effect of reducing and protecting agents on size of silver nanoparticles and their anti-bacterial activity. *Der Pharma Chemica*, 4(1), pp.53–65.

G, D.K., N, N. & S, N., 2016. Antifungal activity of nanofungicide Trifloxystrobin 25% + Tebuconazole 50% against Macrophomina phaseolina. *African Journal of Microbiology Research*, 10(4), pp.100–105. Available at: http://academicjournals.org/journal/AJMR/article-abstract/0BCFC7656959.

Gossen, B.D., Rimmer, S.R. & Holley, J.D., 2001. First report of resistance to benomyl fungicide in Sclerotinia sclerotiorum. *Plant Disease*, 85(11), p.1206.

He, L. et al., 2011. Antifungal activity of zinc oxide nanoparticles against Botrytis cinerea and Penicillium expansum. *Microbiological research*, 166(3), pp.207–215.

Imolehin, E.D. & Grogan, R.G., 1980. Factors affecting survival of sclerotia, and effects of inoculum density, relative position, and distance of sclerotia from the host on infection of lettuce by Sclerotinia minor. *Phytopathology*, 70(12), pp.1162–1167. Available at: https://www.cabdirect.org/cabdirect/abstract/19811371910.

Joboury, M.N.N.A.- & Mohammed, B.T., 2013. Effect of Some Agricultural Media and pH on the Growth of Sclerotinia sclerotiorum and Oxalic Acid Production . , pp.44–49.

Kim, S.W. et al., 2012. Antifungal effects of silver nanoparticles (AgNPs) against various plant pathogenic fungi. *Mycobiology*, 40(1), pp.53–58.

Kolodziejczak-Radzimska, A. & Jesionowski, T., 2014. Zinc oxide-from synthesis to application: A review. *Materials*, 7(4), pp.2833–2881.

Kunde, S.P. et al., 2016. Synthesis and characterization of nanostructured Cu-ZnO: An efficient catalyst for the preparation of (E)-3-styrylchromones. *Arabian Journal of Chemistry*. Available at:http://dx.doi.org/10.1016/j.arabjc.2016.12.015.

Lamsal, K. et al., 2011. Application of silver

Pure Sciences International Journal of Kerbala

Journal Homepage:https://journals.uokerbala.edu.iq/index.php/psijk

nanoparticles for the control of Colletotrichum species in vitro and pepper anthracnose disease in field. *Mycobiology*, 39(3), pp.194–199.

Mahdizadeh, V., Safaie, N. & Khelghatibana, F., 2015. Evaluation of antifungal activity of silver nanoparticles against some phytopathogenic fungi and Trichoderma harzianum. *Journal of Crop Protection*, 4(3), pp.291–300.

Mohammed, Ban Taha ; Almothafer, Haider A.M., 2013. Diagnosis of Sclerotinia sclerotiorum by using PCR and determination of oxalic acid produced under different ecological and chemical conditions. , 1093.

Mohammed, B.T., 2012. The Effect of Storage Period of Sclerotia Viability which are Produced by the Fungus Sclerotinia sclerotiorum(Lib.)de Bary and Accompanied Fungi. Ban. , 2012(February 2009), pp.180–189.

Morones, J.R. et al., 2005. The bactericidal effect of silver nanoparticles. *Nanotechnology*, 16(10), p.2346.

Navale, G.R., Late, D.J. & Shinde, S.S., 2015. JSM Nanotechnology & Nanomedicine Antimicrobial Activity of ZnO Nanoparticles against Pathogenic Bacteria and Fungi. *JSM Nanotechnol Nanomed*, 3(1).

Petica, A. et al., 2008. Colloidal silver solutions with antimicrobial properties. *Materials Science and Engineering: B*, 152(1–3), pp.22–27.

Rycenga, M. et al., 2011. Controlling the synthesis and assembly of silver nanostructures for plasmonic applications. *Chemical reviews*, 111(6), pp.3669–3712.

Sakamoto, M., Fujistuka, M. & Majima, T., 2009. Light as a construction tool of metal nanoparticles: Synthesis and mechanism. *Journal of Photochemistry and Photobiology C: Photochemistry Reviews*, 10(1), pp.33–56.

Sarkar, S. et al., 2007. Facile synthesis of silver nano particles with highly efficient anti-microbial property. *Polyhedron*, 26(15), pp.4419–4426.

Shyla, K.K., Natarajan, N. & Nakkeeran, S., 2014. Antifungal activity of zinc oxide, silver and titanium dioxide nanoparticles against Macrophomina phaseolina. *J. Mycol. Plant Pathol*, 44(3), pp.269–274.

Sondi, I. & Salopek-Sondi, B., 2004. Silver nanoparticles as antimicrobial agent: a case study on E. coli as a model for Gram-negative bacteria. *Journal of colloid and interface science*, 275(1), pp.177–182.

Steel, R.G.D., Torrie, J.H. & Dickey, D.A., 1997. Principles and procedures of statistics: a biometrical approach., 3rd edn (McGraw-Hill: New York).

Wright, J.B. et al., 1999. Efficacy of topical silver against fungal burn wound pathogens. *American journal of infection control*, 27(4), pp.344–350.

Yamanaka, M., Hara, K. & Kudo, J., 2005. Bactericidal actions of a silver ion solution on Escherichia coli, studied by energy-filtering transmission electron microscopy and proteomic analysis. *Applied and environmental microbiology*, 71(11), pp.7589–7593.

Zhang, L. et al., 2007. Investigation into the antibacterial behaviour of suspensions of ZnO nanoparticles (ZnO nanofluids). *Journal of Nanoparticle Research*, 9(3), pp.479–489.

First Year-First Folder-Number: 0
PSIJK 184-191

Pure Sciences International Journal of Kerbala

Journal Homepage:https://journals.uokerbala.edu.iq/index.php/psijk

Effect of Silver and Zinc oxide Nanocompound Mixture on Growth and Some Physiological Properties of *Sclerotinia sclerotiorum*

Husham A. Mehdi, Ban T. Mohammed and Abbas M. Bashi [1]
Department of Biology, University of Kerbala, Iraq.
[1]Department of Chemistry, Applied Medical Sciences, University of Kerbala, Iraq
E-mail: Bantmh@gmail.com

Abstract: Laboratory experiments were carried out in at Kerbala University, Iraq to study the effect of silver and zinc oxide nanocompound (Ag/ZnO) on the *sclerotinia sclerotiorum* (Lib.) De Bary. A series of experiments were carried out, which included the isolation and diagnosis of *Sclerotinia sclerotiorum*, phenotypic and laboratory, and then molecularly using the polymerase chain reaction technique, using ITS4 , ITS1 (Internal transcribed spacer), and the fungal isolates *S.sclerotiorum* (MMBIRAQ) were recorded for the first time in Iraq National Center for Biotechnology Information (NCBI) under Entry Numbers (MF167296) at GenBank. the highest percentage of genetic similarity was with the isolated from Italy, amounting to 99%, while the more distant isolated was from Canada, accounting to 96%.The mixture between Silver and Zinc oxide nanocompound (Ag/ZnO) was present in the laboratory in terms of 1 nanocompound volume / 50 the volume of the potato dextrose agar solution before solidation). The results showed that Ag/ZnO had a significant effect on the fungal colony diameter in Potato dextrose agar (PDA) after 5 and 12 days of inoculation at 50 µml and the highest volumes. The Ag/ZnO compound caused the disappearance of sclerotia ranging from 25µml to 2 ml. The sclerotia mass was 0.04 g. The effect of Ag/ZnO on biomass of Potato dextrose broth (PDB) was significant at 25µml and the highest volumes. The effect was significant on cell length at 25 µml and the highest volumes, while the thickness was at 50µml. The effects of Ag/ZnO on cell decomposition and destruction were caused by cell wall rupture. The significant difference in the production of oxalic acid was at the volume of 25 µml and the highest volumes. The average number of sclerotia in the subsequent generation was 8.88 sclerotia with a diameter of 0.16 cm.

Keywords: *Sclerotinia sclerotiorum*, fungal nanotechnology.

Sclerotinia sclerotiorum (Lib) De Bary is a plant pathogen that affects more than 400 plant species in different stages of growth (Boland and Hall 1994). It is considered that the fungus is difficult to eliminate because of its production of sclerotia that is resistant to inappropriate conditions (Mohammed 2012) . The sclerotia can resist drought, heat , fungicides and can remain active. Species belonging to the *Sclerotinia* are closely related to the external appearance and can be distinguished by microscopic examination or by genetic material DNA (Malvarez *et al* 2007). Polymerase chain reaction (PCR), is characterized by rapid, high resolution and sensitivity (Qin *et al* 2011).Pesticides are one of the important methods of controlling and managing plant diseases, which are chemical methods used for the elimination of various plant pathogens, but this method has effects due to the continuous

Pure Sciences International Journal of Kerbala

Journal Homepage:https://journals.uokerbala.edu.iq/index.php/psijk

use of pesticides, large amounts of them or their products have deteriorated or accumulated in the ecosystem, and not all the applied chemical pesticides reach their targets, but the rest remain in the soil. Al-Naser (2006) found that the benomyl pesticide with the recommended concentration or the double concentration had an effect on the fungal groups found in the rhizosphere area of the bean roots, the effect lasted for two weeks for the recommended concentration and three weeks for the multiplier concentration. Nanotechnology has been introduced as an advanced technology based on the study and understanding of nanoscience and basic science with the technological ability to synthesize nanomaterials and control their internal structure by restructuring and arranging atoms and molecules to ensure unique and unique products, so the nanotechnology is one of the most important and in the forefront fields and fields in chemistry, physics, engineering and biology (Fouda 2012) . The transformation from micro-particles to nanoparticles occurs in a number of changes in physical properties, the one of this applications is controlling plant pathogens, and it has shown many forms of impact on or against microbes and microscopic organisms(Clement and Jarrett ,1994). Silver ion showed a safe control of plant pathogens compared with the pesticides(Park *et al*., 2006). Transgenic nanoparticles have also been used to control pathogens properly compared to fungicides, such as nanoparticles of Ag-SiO_2, which have the inhibitory activity of *Botrytis cinerea* (Yamamoto, 2001). Zinc oxide powder showed an inhibitory effect on fungi and bacteria (Sawai and Yoshikawa ,2004). The aim of this study was to reduce using a conventional chemical pesticide and to reduce pollution.

MATERIAL AND METHODS:

Samples Collection: The stems of the infected eggplant plants were collected from farms GPS 32°47'25.9"N 44°23'57.5"E based on the phenotypic symptoms and initial diagnosis. The sclerotia were washed with normal water and then sterile by immersing them for 3 minutes with 6% commercial chlorax solution, washed several times with sterile distilled water and dried on sterile filter sheets (Mohammed, 2001).

Diagnosis the fungus *S. sclerotiorum* according to metod of earlier workers (Kohn 1979, Tariq *et al* 1985, Saharan and Mehta 2008).The DNA was extracted using the Cat No: FAPGK100 extraction kit processed by Taiwan-China Favorgen. DNA purity was determined by applying the following formula described by William and others (1997): DNA purity= the amount of absorbance at wavelength of 260 nm. The amount of absorbance at wavelength of 280 nm. The polymerase chain reaction test (PCM PreMix, Cat. No. K-2012) was conducted by the Korean company Bioneer. The polymerase chain reaction was performed with a volume of 20 microliter and containing 1 microliter of all the frontal initiators (5'-TCCGTAGGTGAACCTGCGG-3': ITS1) and posterior (5'-TCCTCCGCTTATTGATATGCI-3': ITS4) . After completing the specimen transfer on gel layer, examine the gel containing the DNA packets under UV trans illumination and take photos. The PCR products were sent to the Korean company Microgen for the determination of the nucleotide sequence and in the front and rear directions of the multiply products of the fungal isolates. The nucleotide sequences are analyzed using the Basic Local Alignment Search Tool (BLAST) to compare the data available at the National Center for Biotechnology Information (NCBI), which belong to the same isolate and internationally recognized.

Cultivate the sclerotia *S. sclerotiorum*: One sclerotia was planted in the middle of a petri dish containing a medium of chloramphenicol 250 mg / L. After five days of incubation at 20 ±2 ° C , and before the new sclerotia formed, the dish was divided into cubed pieces for the propagation of fungus on the wheat grain media as described in Mohammed (2001) to produce as many sclerotia as possible.

Preparation of Ag/ZnO: The compound was prepared according to the modified Kunde *et al*(2016) method. The compound consists of the

Pure Sciences International Journal of Kerbala

Journal Homepage:https://journals.uokerbala.edu.iq/index.php/psijk

combination of silver nanoparticles with zinc nanoparticles, as the followings:-
Solution 1: Weight of 29.7 g of zinc nitrate, and add 167 ml of ethanol to zinc nitrate and 2 ml of ethylene chloral to the solution made of zinc and ethanol
Solution 2: Weight of 4.2 g of silver nitrate and dissolved in 100 ml distilled water ----------
Solution 3: Add 0.6 ml of HNO3 to 26 mL distilled water
Weight of 5 g of Polyvinylpyrrolidone (PVP).
The solution 1 was placed on the magnetic mixer and shaking well, then the solution 3 was added to it with the continues shaking. After that, solution No. 2 was distilled into the solution of 1 +3, after which 5 g of PVP was added, At 120 ° C until obtained a third of the solution. The resulting solution is a stock of nanoparticle. The concentration of Nano-silver is 32.8mg / ml and the concentration of Nano-zinc oxide is 323 mg / ml, from which the subsequent concentrations are obtained by adding different volumes of 1, 2, 0.7, 0.5, 0.3 and 0.1 ml, 50 µ ml, 25 µ ml to 50 ml from the medium, as in Table 1.

Nanocompound are evaluated for the growth of the *sclerotinia sclerotiorum* using different sizes using the following media:
Solid PDA: The following characteristics were studied: The vegetative growth of *Sclerotinia sclerotiorum* in term of diameter of the fungal colony (cm) after 5and 12 days from inoculation, the percentage of inhibition using the equation of Kim and his group (2012). [Inhibition Rate (%) = R-r/ R, R=the growth in the control dish, r= the growth in the treatment], the number and mass (g) of sclerotia grown on PDA after 12 days of inoculation, the Microscopic parameters of mycelium treatment with Ag/ZnO after 12 days of inoculation and the vitality of the pathogen produce from Ag/ZnO treated fungus in terms of number and weight of resulting sclerotia .
Liquid PDB: The following characteristics were studied: The mean of fungal biomass (g) after 12 days of inoculation, using the modified Asha *et al.* (2006) and Navale *et al.* (2015) ,Estimation of oxalic acid produced by fungi in liquid media (mg / l)after 12 days of inoculation (Bateman and Beer (1965).

RESULTS AND DISCUSSIONS:
The fungus is microscopically dependent on the nature and form of sterile mycelium as applied

Table 1: Concentrations of nanocompound (Ag/Zn) mg / ml) based on the volume used in the medium

Concentration of Nano-compound Ag/Zn) mg / (ml	volume used in media							
	25 µml	50 µml	0.1 ml	0.3 ml	0.5 ml	0.7 ml	1 ml	2 ml
Ag	0.820	1.640	3.280	9.800	16.400	22.960	32.800	65.600
ZnO	8.075	16.150	32.300	96.900	161.500	226.100	323.000	646.000

Attributes studied:
Sclerotinia sclerotiorum diagnosis using traditional method and molecular properties as well as sequencing of fungi and its registration in the World Genomic Bank was done. .
The properties of nanoparticles prepared by FTIR Infrared Spectrometer ,AFM Atomic Force Microscopy, SEM, Electron Microscope Scanner, U.V.visibale Spectroscopy of Visible and Ultraviolet Radiation Spectroscopy. Ag/Zn

to the taxonomic keys contained in Saharan and Mehta (2008), Tariq and his group (1985) and Kohn, (1979). As identified by Mohammed and Almothafer (2013) and ALmasody (2015). The results of DNA extraction of *S. sclerotiorum* isolation and the use of polymerase chain reaction, used internal transcribed spacer (ITS4) and ITS1, showed that it is similar to the same

Pure Sciences International Journal of Kerbala

Journal Homepage:https://journals.uokerbala.edu.iq/index.php/psijk

isolates identified by Mohammed and Almothafer (2013) and ALmasody (2015), although the sequence of the prefixes used in the two studies are different, but they are similar to the same isolates (Figure 1).

The fungal isolation was recorded in the name *S.sclerotiorum* MMBIRAQ fungi the first time in Iraq at the National Center for Biotechnology Information (NCBI) under the Accession number MF167296 in GenBank. The results revealed that the isolated *S.sclerotiorum* MMBIRAQ isolated in this study is a new isolation previously unknown in the world. The results of the Nucleotide Sequence Analysis of the amplification DNA bundle and using the BLAST program and comparing them with the data available at the National Center for Biotechnology Information (NCBI), showed that isolating the *S. Sclerotiorum*. is the highest genetic resemble isolated from *S.sclerotiorum* isolated from Japan (Accession number: LC318723) of 99%, while the most genetically divergent isolated was from *S.sclerotiorum* isolated from Canada (KF859935: Accession number number) of 96%. Other isolates gave homozygous ratios ranging from 96-99% with isolated *S.sclerotiorum* isolates in this study from Babylon (Figure 2, Table 2).

```
....|....| ....|....| ....|....| ....|....| ....|....|
10         20         30         40         50
CAGAGTTCAT GCCCGAAAGG GTAGACCTCC CACCCTTGTG TATTATTACT
....|....| ....|....| ....|....| ....|....| ....|....|
60         70         80         90        100
TTGTTGCTTT GGCGAGCTGC TCTCCGGGGC CTTGTATGCT CGCCAGAGAA
....|....| ....|....| ....|....| ....|....| ....|....|
110        120        130        140        150
TATCAAAACT CTTTTTATTA ATGTCGGTCT GAGTATTATA TAATAGTTAA
....|....| ....|....| ....|....| ....|....| ....|....|
160        170        180        190        200
AACTTTCAAC AACGGATCTC TTGGTTCTGG CATCGATGAA GAACGCAGCG
....|....| ....|....| ....|....| ....|....| ....|....|
210        220        230        240        250
AAATGCGATA AGTAATGTTG AATTGCAGAA TTCAGTGAAT CATCGAATCT
....|....| ....|....| ....|....| ....|....| ....|....|
260        270        280        290        300
TTGAACGCAC ATTGCGCCCC TTGGTATTCC GGGGGGCATG CCTGTTTCGA
....|....| ....|....| ....|....| ....|....| ....|....|
310        320        330        340        350
GCGTCATTTC AACCCTCAAG CTCAGCTTGG TATTGAGTCC ATGTCATGTA
....|....| ....|....| ....|....| ....|....| ....|....|
360        370        380        390        400
ATGGCAGGCT CTAAAATCAG TGGCGGCGCC GCTGGGTCCT GAACGTAGTA
....|....| ....|....| ....|....| ....|....|
410        420        430        440
ATATCTCTCG TTACAGGTTC TCGGTGTGCT TCTGCCAAAA
```

Figure 2: The nucleotide sequence of the DNA (PCR-amplified product) from S.sclerotiorum isolated from some farms in Babylon province, which is characterized by PCR.

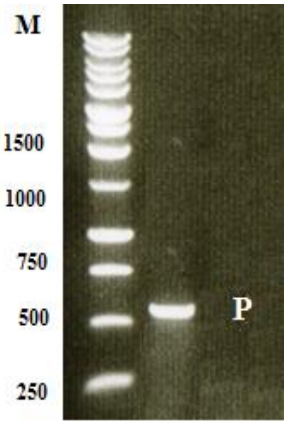

Figure1: Electrolysis of Cellulose Gel for DNA Complications by PCR of *S. sclerotiorum* isolated from Babylon province.
M = DNA ladder marker 1Kpb
P= product

Table2: Comparison of the neoclutidosis ratios of *S.sclerotiorum* isolates from Babylon province and other isolates of the same fungus registered globally at the National Biotechnology Information Center (NCBI).

Pure Sciences International Journal of Kerbala

Journal Homepage:https://journals.uokerbala.edu.iq/index.php/psijk

Fungus	Isolate or strain name	Origin	The most similar sequences in GenBank database	
			GenBank Accession Number	Sequence similarity (%)
S.sclerotiorum	*MMBIRAQ	Iraq	MF167296	100
S.sclerotiorum	MuNi-339	Japan	LC318723	99
S.sclerotiorum	3Scl	Italy	EU627005	99
S.sclerotiorum	SSAG01	India	KT281863	99
S.sclerotiorum	1	Chile	KF148604	99
S.sclerotiorum	CAF-11011	Republic of Korea	KX951645	99
S.sclerotiorum	SS5	USA	KF545319	98
S.sclerotiorum	DB 090720091	Italy	GQ375746	98
S.sclerotiorum	CR 45	Iran	KY694474	98
S.sclerotiorum	SQC-000	China	KY750530	98
S.sclerotiorum	CXL14041906	China	KX781301	98
S.sclerotiorum	SK-8	China	KJ576850	98
S.sclerotiorum	CBS:537.77	Japan	AB926090	97
S.sclerotiorum	wb560	Austria	AF455413	97
S.sclerotiorum	F0675	Japan	AB693927	97
S.sclerotiorum	wb560	Austria	AF455413	96
S.sclerotiorum	-	Canada	KF859934	96
S.sclerotiorum	-	Canada	KF859935	96

* Isolation of *S.sclerotiorum* isolated in this study from a farm in Babylon province

Ag / ZnO characteristics of prepared compound:

By FTIR: The Nano-silver at package 875 after the dissociation of glucose as a result of giving electrons of the material reduces the conversion of silver from ion to metal after taking the electrons and comes the role of the installer to be formed in the form of balls. Note that the package between 703-666 represents the vibration of nanoparticles To demonstrate the composition of nanoparticles on the difference of the reduced factor, silver nanoparticles appear in different sizes and diameters (Sun 2013; Rycenga *et al* 2011; Sakamoto *et al* 2009).

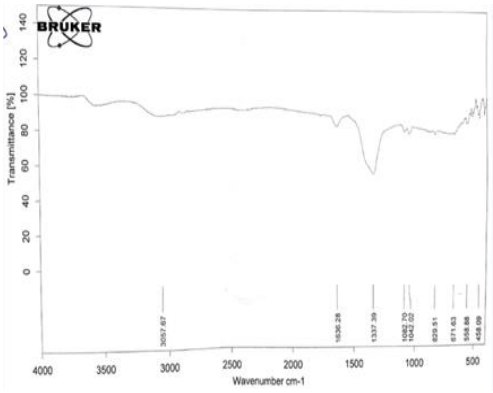

Figure 3: Ag/ZnO characteristics compound by FTIR.

By AFM: The results of the microscopic examination by the atomic force microscope in Fig. 4, show that the obtained compounds are nanoparticles and possess the characteristics of the nanoparticles through the rise of the nanoparticle and its fear. This is shown by the microscopic atomic force, where the heights and sizes of nanoparticles varied according to the reduced factor (Van Hyning and Zukoski1998).

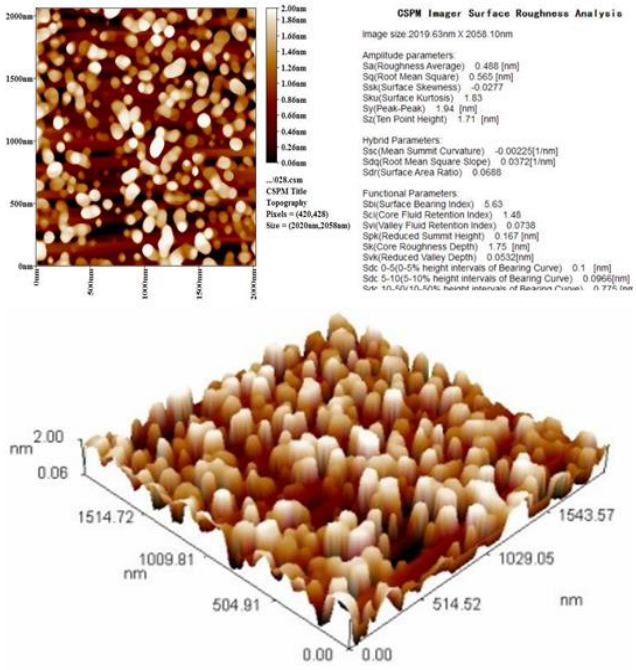

Figure 4:Ag / ZnO characteristics of prepared

Pure Sciences International Journal of Kerbala

Journal Homepage:https://journals.uokerbala.edu.iq/index.php/psijk

compound by AFM

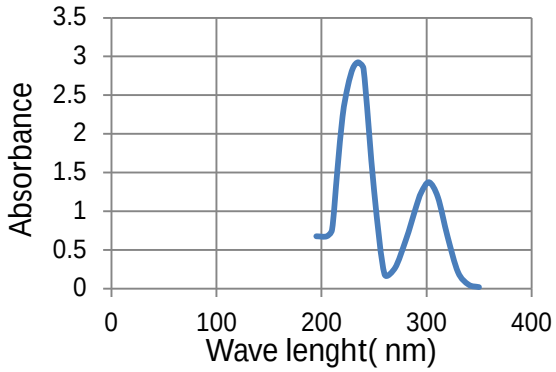

Fig 6: Ag/ZnO characteristics of prepared compound by means of the optical and ultraviolet radiation spectroscopy U.V.visible.

By electron microscope SEM scanner: The electron microscopy shows forms of nanoparticles of different diameters according to the reduced factor (Fig 5). The nanoparticle mix with the zinc oxide is shown in the shape of its silver heart and its zinc form (Ferreira da Silva *et al* 2011; Rogers *et al* 2012; Alarcon *et al* 2012).

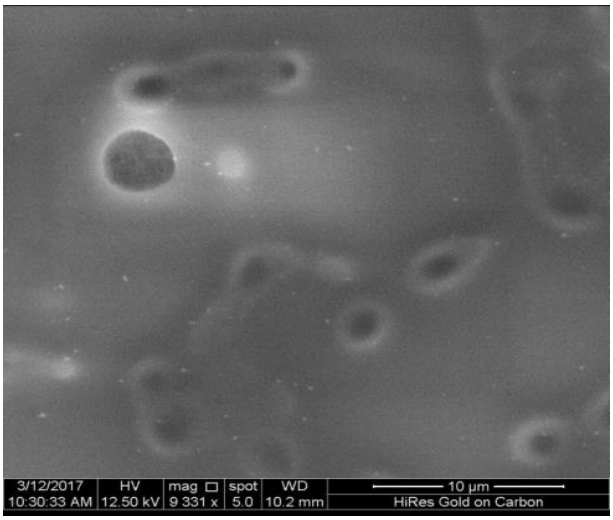

Figure 5:Ag / ZnO characteristics of prepared compound by SEM scanner

Optical and ultraviolet radiation spectroscopy: By examining the resulting nanoparticles with ultraviolet-visible light, Figure 6 appears package locations for nanotubes by the wavelength of maximum absorption. Thus, showing the wavelength of the wavelength of light falling on the surface of nanoparticles with their free electrons orbiting the surface of the nanoscale to show Plasmon, which turns the metal surface electrons to give a bundle in the ultraviolet light (Kadir *et al*. 2005).

E**valuation of the Ag / ZnO nanocompound on the PDA:** The Ag / ZnO nanocompound affected the fungus in terms of growth and phenotypic shape of the fungal colony (Table 3). That the Ag / ZnO nanocompound had a significant effect on the fungal colony diameter. After 5 and 12 days of inoculation at 50 µml the highest volumes, leading to slow and distorted growth (Fig 7). The shape of the colony in the

Pure Sciences International Journal of Kerbala

Journal Homepage:https://journals.uokerbala.edu.iq/index.php/psijk

media was characterized by its distorted shape and uneven growth, as well as irregular and curvilinear edges (Fig7). The growth distinguished by 25 µml being close to the control form, 50 µml was a distorted and irregular growth, so at 0.1 ml and 0.3 ml, the spinning form was spread out and far from the PDA. The Ag / ZnO nanocompound compound was not affected by the time, 50 µml in the 5 days and 12 days was not different. The increase in the size of the Ag / ZnO nanocompound increases the inhibition rate (Table 4). This effect may be caused by an increase in the saturation and absorption of nanoparticles by fungal mycelium leading to a decrease in the activity of plant pathogenic fungi due to the effect of silver on microscopic, microorganisms DNA replication ability and inhibition of protein expression by ribosomes and enzymes necessary for energy production (Yamanaka *et al*. 2005; Feng *et al*. 2000). These results were identical to Kim's *et al*. (2012). The effect was significant on mycelium length at 25 µml and the highest sizes, while the width was at 50µml (Table 4).

Figure 8 and table 4 , showed that the effect of different sizes of Ag / ZnO nanocompound on fungal cells after 12 days of inoculation on a PDA, this effect is between separation of the cellular wall , aggregation of the protoplasm , cell collapse, disintegration in cells , cell deformation and path deflection and began initiation of sclerotia ,is the important phenomenon to survival the fungus over inappropriate circumstances ,and this is the main cause to regrowth the fungus during the subsequent generation. The average number of sclerotia in the subsequent generation was 8.77 sclerotia with a diameter of 0.35 cm (Table 5). This experiment may open up horizons for the effect of other nancompounds that may have an effect on later generations of the second generation, or that repeated treatment with nanoparticles may conceal the sclerotia of the

Table 3: Effect of different sizes of Ag / ZnO nanocompound on the diameter of fungal colonies (cm) the number and weight of sclerotia at the age of 5 and 12 days of inoculation on the PDA at 20 ± 2 ° C.

Size of Ag/ZnO Age of the colony (Day)	Control	25µml	50µml	0.1ml	0.3ml	0.5ml	0.7ml	1.0ml	2.0ml	The average
5	9.000	9.000	2.500	1.000	0.000	0.000	0.000	0.000	0.000	2.389
12	9.000	9.000	3.000	2.500	2.000	0.000	0.000	0.000	0.000	2.833
	*(15) **(0.360)	0.000	0.000	0.000	0.000	0.000	0.000	0.000	0.000	
The average	9.000	9.000	2.750	1.750	1.000	0.000	0.000	0.000	0.000	
LSD0.05	Interaction=0.862			Size= 0.609				Days=0.287		

Each number represents three replicates
*= Average number of sclerotia
**= Average weight of sclerotia.

Pure Sciences International Journal of Kerbala

Journal Homepage:https://journals.uokerbala.edu.iq/index.php/psijk

After 5 days of inoculation

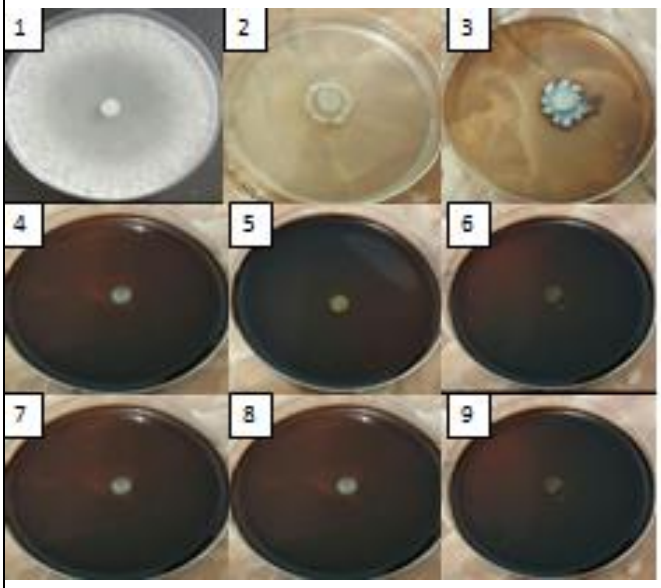

After 12 days of inoculation

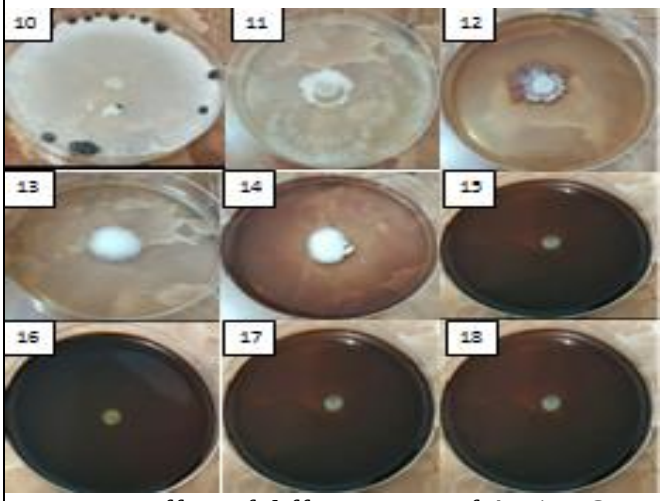

Figure 7: Effect of different sizes of Ag / ZnO nanocompound on the diameter of fungal colonies(cm) the number and weight of sclerotia at the age of 5 and 12 days of inoculation on the PDA at 20 ± 2 ° C.

1,10=control	2.11= 25µml	3,12=50 µml
4,13=0.1ml	5,14=0.3ml	6,15=0.5ml
7,16=0.7ml	8,17=1ml	9,18=2ml

fungus without fear of a mutation, due to the effect of silver on several vital processes in the fungus making the role of mutation or nanoparticle resistance is completely excluded (Herrera *et al*. 2001, Wright *et al* .1999).

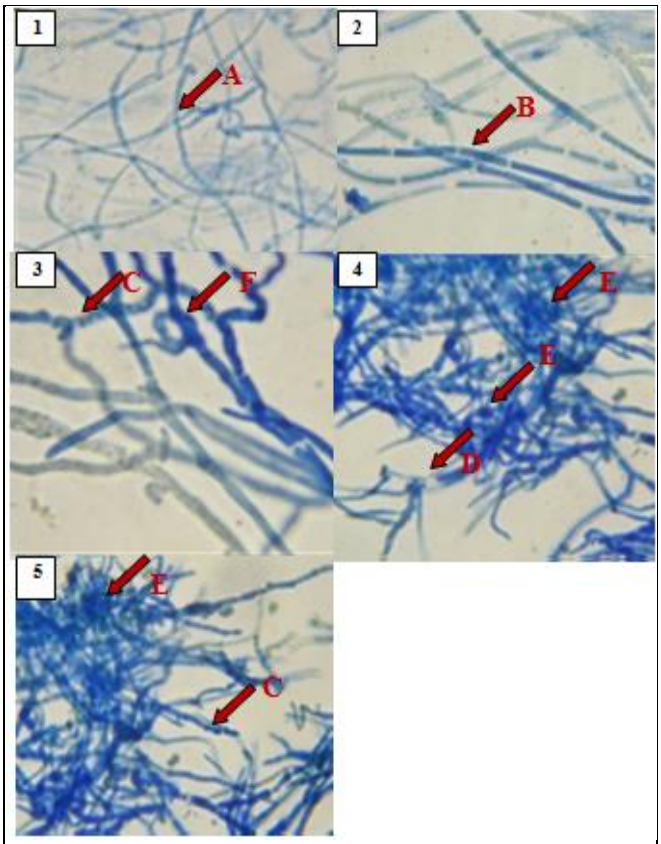

Figure 8: Effect of different sizes of Ag / ZnO nanocompound on fungal cells after 12 days of Inoculation on the PDA at 20 ± 2 ° C. (40X).
1= control , 2 = 25µml , 3=50 µml, 4= 0.1ml, 5= 0.3ml.
A= Normal growth, B= Separation of the cellular all and the aggregation of the protoplasm , C= The aggregation of the protoplasm and cell collapse, D = Disintegration in cells, E= The aggregation of the protoplasm and began initiation of sclerotia. F= Cell deformation and path deflection.

Evaluation of the Ag / ZnO nanocompound on the PDB: There was a significant at 25µml the highest volumes until 0.5ml Ag / ZnO

Pure Sciences International Journal of Kerbala

Journal Homepage:https://journals.uokerbala.edu.iq/index.php/psijk

nanocompound and the highest there were no growth (Table 6) .The Ag / ZnO nanocompound caused the significant decrease number of sclerotia, and disappear in the volumes ranging from 0.5 ml to 2 ml. The Ag / ZnO nanocompound effects in cell decomposition and destruction were caused by cell wall rupture. The production of oxalic acid also showed a significant decrease in the production of acid with increasing sizes of Ag / ZnO nanocompound. However, it is shown increase in acid production with volume increase except in size 25, Which indicates some of the anomalous behavior of the fungus against some external influences (Cessna *et al* 2000).

Table 4: Effect of different sizes of Ag / ZnO nanocompound on the length and width of the mycelium (µm) at the age of 12 days of inoculation on the PDA at 20 ± 2 ° C.

volume of Ag/ZnO Characteristic study	Control	25µml	50 µml	0.1 ml	0.3ml	0.5ml	0.7ml	1ml	2ml	Average	$LSD_{0.05}$
Average length of hypha (mµ)	80.000	32.500	27.000	10.000	10.000	0.000	0.000	0.000	0.000	17.720	9.34
Average width of hypha (mµ)	2.000	3.000	4.000	2.000	2.000	0.000	0.000	0.000	0.000	1.440	1.139
LSD0.05	length=9.340		width=1.139								

Each number represents three replicates.

Table 5: Effect of different sizes of Ag / ZnO nanocompound on the Average number of Sclerotia and Average diameter of sclerotia (cm) in the subsequent generation at the age of 12 days of inoculation on the PDA at 20 ± 2 ° C.

volume of Ag/ZnO Characteristic study	Control	25µml	50µml	0.1ml	0.3ml	0.5ml	0.7ml	1.0ml	2.0ml	The average
number of sclerotia	15.000	11.000	20.000	13.000	20.000	0.000	0.000	0.000	0.000	8.770
12	0.330	0.300	0.230	0.330	0.300	0.000	0.000	0.000	0.000	0.350
$LSD_{0.05}$	Average number of sclerotia=2.491			Average diameter of = 0.118 sclerotia(cm)						

Each number represents three replicates

Table 6: Effect of different sizes of Ag / ZnO nanocompound on the fungal biomass rate (gm), the number, diameter of the sclerotia (mm), and the rate of oxalic acid (ppm) production at 12 days of inoculation on PDB at 20 ± 2° C.

volumes of Ag/ZnO Characteristic study	Control	25µml	50 µml	0.1 ml	0.3ml	0.5ml	0.7ml	1ml	2ml	Average	$LSD_{0.05}$
Average of Biomass (gm)	0.460	0.240	0.180	0.160	0.150	0.000	0.000	0.000	0.000	0.132	0.127
Average number of sclerotia	15.000	11.000	20.000	13.000	20.000	0.000	0.000	0.000	0.000	8.770	2.491
Average diameter	0.330	0.300	0.230	0.330	0.300	0.000	0.000	0.000	0.000	0.350	0.118

Pure Sciences International Journal of Kerbala

Journal Homepage:https://journals.uokerbala.edu.iq/index.php/psijk

of sclerotia (mm)											
Average product of oxalic acid (ppm)	5.580	3.180	2.790	2.280	1.265	0.000	0.000	0.000	0.000	1.677	1.127

Each number represents three replicates

CONCLUSION: The fungal isolates *S.sclerotiorum* (MMBIRAQ) were first recorded in Iraq at the National Center for Biotechnology Information (NCBI) under the entry number (MF167296) at the GenBank Genomic Bank. By comparison, the highest genetic similarity was isolated with isolates isolated from Italy, 99%, while the most isolated from isolated from Canada. Nanocompound influenced fungi on the growth, biomass and number of sclerotia, and showed their effect on the phenotype in the dish as well as on the microscopic level of mycelium. . They varied according to the incubation period between 5 to 12 days, and in the solid and liquid media.The effect of nanomaterials on the first generation after treatment has not continued.

Acknowledgements:
We would like to thank Dr. Aqeel Nazzal Al Abedy for his role in facilitating the use of the PCR technology in the college of Agriculture / Kerbala University .

REFERENCES:

Alarcon E I, Udekwu K, Skog M , Pacioni NL, Stamplecoskie KG, Gonzalez-B M , Polisetti N , Wickham A, Richter-Dahlfors A, Greffith M and Scaiano J 2012, The biocompatibility and antibacterial properties of collagen-stabilized, photochemically prepared silver nanoparticles. *Biomaterials* **33**(19): 4947–4956.

ALmasody , N N 2015. Physiological Study on Sclerotia of *Sclerotinia sclerotiorum* under different conditions Msc. thesis, Faculty of Education for Pure Sciences, Karbala University.(in Arabic).

Al-Naser Z 2006. The effect of certain fungicides on mycoflora in the bean plant rhizosphere. Damascus university, *Journal of The Agricultural Sciences* **22** (1): 156-180. (in Arabic) .

Asha A, Imelda J and Paul R 2006. Biomass estimation of *A. niger* S14 a mangrove fungal isolate and A. oryzae NCIM 1212 in solid-state fermentation. *Journal of the Marine Biological Association of India***48**: 139-146.

Bateman D F and Beer S V 1965. Simultaneous production and synergistic action of oxalic acid and poly galacturonase during pathogenesis by *Sclerotium rolfsii* . *Photo Pathology Indian Agricultar* . Research Institute. New Delhi. **55**: 204-211.

Boland GJ and Hall R 1994. Canadian journal of plant pathology index of plant hosts of *Sclerotinia sclerotiorum* Index of plant hosts of *Sclerotinia sclerotiomm*. *Canadian Journal of Plant Pathology* **16**:93–108 .

Cessna SG, Sears V E, Dickman M B and Low P S 2000, Oxalic Acid, A Pathogenicity

Pure Sciences International Journal of Kerbala

Journal Homepage:https://journals.uokerbala.edu.iq/index.php/psijk

Factor for *Sclerotinia sclerotiorum* , Suppresses the Oxidative Burst of the Host Plant. *The Plant Cell*, 12(11),:.2191–2199.

Clement J L and Jarrett P S 1994. Antibacterial silver. Metal-based drugs, **1**(5–6): 467–482.

Ferreira da Silva B, Perez S, Gardinalli P, Singhal R, K,Mozeto A and A,Barcelo D2011 Analytical chemistry of metallic nanoparticles in natural environments. *TrAC, Trends in Analytical Chemistry*. **30**(3): 528–540 .

Feng Q L, Wu J, Chen G O, Cui F Z, Kim T N and Kim J O 2000, A mechanistic study of the antibacterial effect of silver ions on *Escherichia coli* and *Staphylococcus aureus. Journal of Biomedical Materials Research* ,**52**: 662-668.

Fouda M M G 2012. Antibacterial modification of textiles using nanotechnology. In A Search for Antibacterial Agents. In INTECH.

Herrera M , Carrion P, Baca P, Liebana J, and Castillo A 2001,In vitro untibacterial activity of glass- ionomer cements *Microbios*.**104** : 141-148.

Kadir A, Joseph R, Lakowiez and Geddes CD, 2005 , Rapid Deposition of Triangular Silver Nanoplates on Planar Surfaces: Application to Metal-Enhanced Fluorescence,*The Journal of Physical Chemistry B*, **109**, 6247-6251

Kim S W, Jung J H, Lamsal K, KimYS, Min J S and Lee YS, 2012. Antifungal Effects of Silver Nanoparticles (AgNPs) against various plant pathogenic fungi. *Mycobiology* **40**(1): 53-58.

Kohn L M, 1979.Amonographic revision of genus *Sclerotinia*,*Mycotaxon*, **9**: 365-444.

Kunde S P, Kanade K G , Karale B K , Akolkar H N , Randhavane P V and Shinde S T, 2016 . Synthesis and characterization of nanostructured Cu-ZnO: An efficient catalyst for the preparation of (E)-**3**-styrylchromones. *Arabian Journal of Chemistry*.

Malvarez G , Carbone I , Grünwald N J , Krishnamurthy V S , Schafer M , Kohn L M 2007. New populations of *Sclerotinia sclerotiorum* from lettuce in California and peas and lentils in Washington, *The American Psychopathological Society* **97**:470-483 .

Mohammed B T 2012. The Effect of Storage Period of Sclerotia Viability which are Produced by the Fungus *Sclerotinia sclerotiorum*(Lib.)de Bary and Accompanied fungi. *Al - Furat Journal of Agricultural Sciences* **4**(2) p.180–189. (In Arabic)

Mohammed B T 2001. The biological study of *Sclerotinia sclerotiorum* (lib.) the bar and use of solar pasteurization for its control, PhD thesis philosophy, faculty science, University of Babylon 87 pages. (in Arabic).

Mohammed BT and Almothafer H A 2013. Diagnosis of *Sclerotinia sclerotiorum* by

Pure Sciences International Journal of Kerbala

Journal Homepage:https://journals.uokerbala.edu.iq/index.php/psijk

using PCR and determination of oxalic acid produced under different ecological and chemical conditions. *Al - Furat Journal of Agricultural Sciences*,**5**(3), p. 179 -192.(in Arabic).

Navale GR, Thripuranthaka M , Late DJ and Shinde S S, 2015 , Antimicrobial Activity of ZnO Nanoparticles against Pathogenic Bacteria and Fungi. JSM *Nanotechnol Nanomed* ,**3**(1): 1033.

Park HJ ,Kim S H, Kim H J and Choi S H 2006. A new composition of nanosized silica-silver for control of various plant diseases. *The plant pathology journal*, **22**(3), pp.295–302.

Qin L, Fua Y, Xiea J, Chenga J, Jiangab D, Liab G, Huanga J. 2011.A nested-PCR method for rapid detection of Sclerotinia sclerotiorum on petals of oilseed rape (Brassica napus).*Plant Pathology* (60): 271–277.

Rogers K R, Bradham K, Tolaymat T, Thomas DJ, Hartmann T and Ma L, et al., 2012Alterations in physical state of silver nanoparticles exposed to synthetic human stomach fluid. *Science of the Total Environment*, **420**: 334-339

Rycenga M, Claire M, Cobley Jie Zeng, Weiyang Li, Christine H, Moran Qiang Zhang, Dong Qin, and Younan Xia et al, 2011.Controlling the synthesis and assembly of silver nanostructures for plasmonic applications. *Chemical . Reviews* . **111**(6), 3669–3712 .

Saharan G S and Mehta N 2008 .Sclerotinia diseases of crop plants: biology, ecology and disease management, *Department of Scientific and Industrial Research*, New Zealand :531 pp.

Sakamoto M, Fujistuka M, and Majima T, 2009,Light as a construction tool of metal nanoparticles: synthesis and mechanism. *Journal of Photochemistry and Photobiology C* **10**(1), 33–56 .

Sawai J and Yoshikawa T 2004. Quantitative evaluation of antifungal activity of metallic oxide powders (MgO, CaO and ZnO) by an indirect conductimetric assay. *Journal of applied microbiology*, **96**(4), pp.803–809.

Sun Y 2013. Controlled synthesis of colloidal silver nanoparticles in organic solutions: empirical rules for nucleation engineering. *Chemical Society Reviews* **42**: 2497–2511

Tariq V N, Gutteridge CS and Jeffries P 1985. Comparative studies of cultural and biochemical characteristics used for distinguishing species within *Sclerotinia*, *Transactions of the British Mycological Society*, **84**(3), pp.381–397.

Van Hyning DL and Zukoski CF, 1998.Formation mechanisms and aggregation behavior of borohydride reduced silver particles. *Langmuir* ,**14**, 7034–7040 .

William WW, Mackey K and Chomczynski P 1997. Effect of pH and ionic strength on the spectrophotometric assessment of

Pure Sciences International Journal of Kerbala

Journal Homepage:https://journals.uokerbala.edu.iq/index.php/psijk

nucleic acid purity. *Biotechniques*,**22**: 474-481.

Wright J B, Lam K, Hansen D and Burrell RE, 1999. Efficacy of topical silver against fungal burn wound pathogens ,*American journal of infectus control* , **27** , 344-350.

Yamanaka M, Hara K and Kudo J, 2005,.Bactericidal actions of a silver ion solution on *Escherichia coli*, studied by energyfiltering transmission electron microscopy and proteomic analysis. *Applied Environ Microbiol* ,**71**:7589-93.

Yamamoto O, 2001. Influence of particle size on the antibacterial activity of zinc oxide. *International Journal of Inorganic Materials*, **3**(7), pp.643–646.

First Year-First Folder-Number: 0
PSIJK 184-191

Pure Sciences International Journal of Kerbala

Journal Homepage:https://journals.uokerbala.edu.iq/index.php/psijk

Evaluation of mineral- , nano -zinc, and fluconazole interaction on some growth characteristics of *Trichophyton rubrum and Microsporum canis*

Shrook Gany Yassin Sh.gani.2671@gmail.com

Ban Taha Mohammed Bantmh@gmail.com

Department of Biology / college of Education for pure Science / Kerbala University / Iraq.

Abstract

This study was conducted in the postgraduate laboratory at the College of Education for Pure Science at the University of Kerbala in collaborating with Center for Manuscript Preservation, Restoration and Care of Researchers at the Imam Hussain Holy Shrine in Kerbala for the period from 17-3-2019 to 20-9-2020 . In order to evaluate the virulence of fungal isolates *Trichophyton rubrum* isolate IQT-No.1 *and Microsporum canis* isolate IQM-No1. registered in the Global Genebank that accession numbers MK167434 and MK167435 respectively , in a previous study in their production of protease, lipase and keratinase during 3, 6 and 9 days incubation periods at 25 ° C. and evaluation of the efficacy of different concentrations at twelve combinations of mineral –zinc or nano-zinc and fluconazole antifungal. and the interaction between zinc in its two forms with the fluconazole antifungal on a biomass dry weight of colony (mg) on grown the liquid sabouraud dextrose broth media, as well as the phenotypic characteristics of fungal colonies developing on sabouraud dextrose agar media as a colony diameter (mm), and the microscopic features of mycelium and conidia after 14 days of incubation. The results showed that both fungi have the ability to produce the enzymes protease, lipase, and keratinase , the fungus *Trichophyton rubrum* was higher in its production of the protease and lipase on the ninth day of incubation, which was significantly different from the *Microsporum canis*, while the *Microsporum canis* recorded a significant superiority in its production of the keratinase on the ninth day of incubation compared to the *Trichophyton rubrum* . The results indicated that using the combination of 30 mg zinc with 10 mg flucanazole was the best combination in the low dry weight of *T.rubrum*, while the *M.canis* was affected by the combination of 10.0mg zinc and 10.0mg flucanazole, and it did not significantly differ from 15.0 mg zinc and 5.0 mg flucanazole compared with the control . The two fungi also differed with each other in the average dry weight of the biomass, and the *M.canis* was less dry weight compared to *T.rubrum* . All the combinations of nano zinc and fluconazole were positive in decreasing the dry weight of the biomass of the *T.rubrum*, except for treatments 7.5 and 15.0 nano zinc to 22.5 and 15.5 respectively , which did not differ from the control. Likewise, the *M.canis* was affected by the combinations and gave a significant decrease over the control, especially in treatment, 30 nano zinc and 10 flucanozol. *T.rubrum*, 5.0mg mineral zinc and 5.0mg flucanozol , recorded the lowest rate of colony diameter over the solid Sabouraud's dextrose agar medium, while two treatments 22.5m zinc with the 7.5mg fluconazol and 20mg zinc with 20mg fluconazol respectively showed the lowest average for the *M.canis* colony diameter (mm), and all the treatments recorded a significant decrease compared to the control. The best combination was 15.0 mg nano zinc with 5.0 mg only fluconazol in decreasing the diameter colony of *T.rubrum*, Likewise, the *M.canis* was affected by the combinations and gave a significant decrease over the control, especially in treatment 7.5mg nano zinc and 22.5mg flucanozol. The inhibition of the average diameter of the fungal culture in terms of phenotypically and grow vertically tend toward the cover plate . As for the microscopic aspect, deformation occurred in the

Pure Sciences International Journal of Kerbala

Journal Homepage:https://journals.uokerbala.edu.iq/index.php/psijk

fungal hypha, separation of protoplasm from the cell wall and aggregation of protoplasm, in addition to the disappearance of the conidia, compared to the control. **Conclusions**: This is fungal growth and deformation of conidia formation . Tests showed that nano zinc has more effective effect than mineral zinc and has an important role in reducing the amount of antifungal used.

KEY WORDS: *Trichophyton rubrum* ,*Microsporum canis* .Nano-zinc , Fluconazole antifungal.

Introduction: Superficial fungal infection is a major global public health problem affecting 20-25% of the world's population. (Asticcioli *et al*. 2008) Among these diseases dermatomycosis, or ringworm, is one of the most frequent fungal infections. This infection is caused by the dermatophytes of the genera *Trichophyton, Microsporum, or Epidermophyton.* (Yehia *et al.* 2010) .These dermatophytes usually invade different areas of keratin in the body, causing tinea corporis, facial tinea, tinea pedis, tinea capitis, and tinea corporis (Degreef 2008). Dermatophytosis infection can lead to mild or severe symptoms, depending on the immune response of the host (Almeida *et al.* 2017). It also appears that many patients are particularly at risk of developing the infection, including individuals with diabetes, AIDS, Kidney disease, psoriasis, and immunodeficiency types, such as transplant recipients and patients on long-term corticosteroid therapy (Piérard 2001). The incidence of skin fungi and the causative types varies according to where they appear in the body, in a study conducted by Al-Masaoodi *et al*. (2020a) report on a case of tinea infection caused by *T. erinacei* in Iraq, which was most probably transferred from a hedgehog .Dermatophytes cause infections of the skin, hair, and nails, obtaining nutrients from keratinized material (Midgley *et al* .1994) . The organisms colonize the keratin tissues causing inflammation as the host responds to the first report on *T. rubrum and M.canis* tinea were treated with the combination between mineral zinc or nano zinc with fluconazole antifungal to reduce the pathogenic metabolic byproducts. Colonies of dematophytes are usually restricted to the nonliving cornified layer of the epidermis because of their inability to penetrate viable tissue of an immunocompetent host. Invasion does elicit a host response ranging from mild to severe. Acid proteinases (proteases) elastase, keratinase s, and other proteinases reportedly act as virulence factors. Additionally, the products of these degradative enzymes serve as nutrients for the fungi (Goldsmith *et al.*2012*)* . Dermatophytes can digest keratin and other proteinaceous substrates present in skin and its appendages, such as nail, hair, and feather, and use it as its sole source of carbon and nitrogen. Proteolytic and keratinolytic activities of dermatophytes have been a subject of interest for several years to understand the pathogenicity of infection (Venkatesan *et al* .2010). Different studies suggest proteases as major determinants of fungal virulence (Mohammed *et al.* 2018; Jasim *et al*.2019 ; Al-Masaoodi *et al*.2020b). Azole antifungals consist of two primary classes: imidazoles and triazoles. Both classes are fungistatic agents and share similar mechanisms of action. The azoles interfere with the synthesis and permeability of fungal cell membranes by inhibiting cytochrome P450-dependent 14-alpha-sterol demethylase. This enzyme is required for the synthesis of ergosterol, the major sterol of most fungal cell membranes. The loss of cell membrane integrity inhibits cell division by causing intracellular swelling and interferes with cellular adhesion and epithelial penetration by allowing the protrusion of cytoplasm through the membrane. Currently available imidazoles include clotrimazole, miconazole, ketoconazole, econazole, and butoconazole. The triazoles used most widely

Pure Sciences International Journal of Kerbala

Journal Homepage:https://journals.uokerbala.edu.iq/index.php/psijk

are fluconazole, itraconazole, and terconazole.. (Ghannoum and Rice 1999). Nanomaterials are not new, and not all of them are manufactured. They are found in nature everywhere, but what is new is the ability of humans to engineer them from common materials for functional purposes. Nanomaterials appear in nature in the and mechanical processes. Nanomaterials are designed and manufactured for specific electronic, mechanical, optical, enzymatic and medical applications using a range of micro-manufacturing methods. Today, nanomaterials are widely used in many fields such as agriculture, food, cosmetics, personal care products, disinfectants, clothing, electronic devices and antimicrobial materials (Sharma *et al.* 2015;). In the field of biology, zinc oxide nanoparticles have taken great interest due to its antimicrobial activity, which has opened new horizons for biological sciences (Allahverdiyev *et al.* 2011). Ravishankar Rai (2011) explained that zinc oxide has a significant and clear effect as an anti-microbial, and therefore it has been exploited in industrial fields, including water treatment, dyes, and cosmetics. Nanoparticles are characterized by being active and effective with biological systems due to their different shapes, and a large surface area.Charge and surface absorption capacity is high (Kasemets *et al.* 2009) attributed the inhibitory activity of zinc oxide towards pathogens that may come through the formation of free radicals on the surface, which leads to damage to the lipids of the cell membrane of microbes through the interaction of free radicals with fats, and thus leads to breakdown of the cell membrane of microbial cells.(Brayner *et al*. 2006;Reddy *et al*. 2007). Various mechanisms have been proposed to discuss the effect of nanoparticles on the growth of fungi. The first is the formation of an H_2O_2 root on the surface of ZnO NP due to the possibility of forming a hydrogen bond between a hydroxyl group of cellulose molecules with the oxygen atom of ZnO NP, leading to inhibition. Fungal growth, structures of coral reefs and marine plankton, and in birds' beaks, feathers, and leaves of some plants(Hochella *et al.* 2015). Natural nanomaterials are generally considered to be products of chemical, photochemical, thermal, biological

the second mechanism is the release of Zn^{+2} ions that cause damage to the cell membrane and interact with the contents reacting with (Moraru *et al.* 2003) Zinc nanoparticles form free radicals such as the hydroxyl radical and a single oxygen root that stimulates cell death (Lipovsky. *et al*. 2011; Mehdi , *et al*.2018a). Recently, many of the fungi accompanying the manuscripts have been inhibited by the use of nanoscale zinc oxide (Jasim.2019). Therefore, the study aimed to use , mineral- zinc or nano -zinc with anti-fungal fluconazole to form a combination between them in inhibiting the growth of the fungi *Trichophyton rubrum and Microsporum canis*.

[redacted]

[redacted] The two fungal isolates used in this study were *Trichophyton rubrum* isolate IQT-No.1 and *Microsporum canis* isolate IQM-No.3, obtained by Prof. Ban Taha Mohammad from the Postgraduate Laboratory at the College of Education for Pure Sciences at the University of Kerbala . The two isolates were diagnosed and recorded in Global GenBank under serial numbers MK167434.1 and MK167439.1 respectively in the previous study (Al-Masaoodi *et al*.2020c) isolates were activated and cultured on SDA medium, and their phenotypic and microbiological properties were studied before and after subsequent treatments (Mehdi , *et al*.2018b).

[redacted]) :They was Prepared according to the manufacturer's instructions

Pure Sciences International Journal of Kerbala

Journal Homepage:https://journals.uokerbala.edu.iq/index.php/psijk

Skimmed - milk Agar: The medium was prepared according to Jasim *et al*., (2018) and Hankin and Anagnostakis (1975).

Keratin agar: Chicken feathers were used as a source of keratin, where a large amount of chicken was collected, cut to a size of 1 cm, washed with chloroform and methanol alcohol, with a volume ratio of 1: 1, and then washed with distilled water , dried in the sun (Mini *et al*. 2012). The feathers were placed in 10 ml of a solution of dimethyl sulfoxide (DMSO) for 24 hours, and then 10 ml of acetone was added to it and left for 30 minutes. Then it was filtered with filter paper and the filtrate was taken and added to the medium of the mineral salt pellets containing K_2HPO_4 1.5 g / liter. ; $MgSO_4.7H_2O$ 0.05 g / l; $CaCl_2$ 0.025 g / l; $FeSO_4.7H_2O$ 0.015 g / l; $ZnSO_4.7H_2O$ 0.005 g / l; 2 agar, 100 ml distilled water and the pH was neutralized to 7.5, where it was inferred that the ability of fungi to produce keratin enzyme is effective aclear halo zone around the fungal colony (Wawrzkiewicz *et al*. 1991)**.**

To all of the above Media, 250 mg/l of Chloramphenicol antibiotic was added before sterilization, and then sterilized by autoclave at 121 ^{0}C under 1.5 pressure for 20 min. Mineral zinc and Zinc nanoparticles were used us a double combination with Fluconazole according the table 1. The Bi combinations were used to determine their effect on the weight of the *Trichophyton rubrum* and *Microsporum canis* in a broth media, as well as their effect on the phenotypic properties of the fungi and the average diameter of the fungal colonies on the solid media and to study the micro properties in terms of hyphal shape and the number of conidia under microscopy.

Average dry weight (mg) for growth on the liquid Sabouraud dextrose media: In order to test the effect of the mineral zinc or nano zinc on the dry weight of fungi, the mineral zinc or nano zinc were mixed with the sterile Sabouraud dextrose broth after removing it from the autoclave at a temperature of 50 ° C

Tween 80 Agar: This medium was prepared according to Sierra, (1957) .

and twelve combinations as below table, of three replicates for each one, in addition to the control treatment (culture medium only without any addition). Put 20 ml of the culture media into glass tubes with a capacity of 70 ml. The tubes were inoculated with different combinations of mixture , inoculation by implanting a tablet with a diameter of 7 mm. Incubation at 25^{0}C for 14 days , then filtering the liquid cultures through a known weight filter paper. Then the filter papers were dried with the mass of the fungi in an oven at 40 ° C for a period of 24 hours(Mehdi, *et al* , 2018b) . The dry weight of the fungi was calculated using a sensitive electrical balance using the following equation (Arey 2010).

Weight of mycelium = (Weight of filter paper + Weight of Mycelium) - (Weight of filter paper)

Average colony diameter (mm) grown with the Sabouraud dextrose agar SDA medium: The method of Jasim et al. (2019) was followed, in which mineral zinc or nano zinc with Fluconazole antifungal , with different combinations with the cultivar medium Sabouraud dextrose agar before solidification, three replicates for each, in addition to the control treatment (cultivated medium only without any addition). After hardening the medium, a hole was made in the center of each plate by means of a cork borer of 7 mm diameter. The plates were inoculated with the studied and developed fungi vaccine on SDA medium at 14 days of age for each by implanting a 7 mm disc for each of them in the hole that worked in the center of the plate. All plates were incubated at 25 ° C for two weeks. The diameter of the growing colony was measured average of two perpendicular diameters and the results were recorded

Pure Sciences International Journal of Kerbala

Journal Homepage:https://journals.uokerbala.edu.iq/index.php/psijk

(Mohammed, *et al*., 2018 ; Khanzada *et al.*

Statistical analysis: Factorial experiment within Completely Randomized Design (CRD) was adopted. The means of tretments were compared using the Least Significant Difference (LSD) at a probability level of 0.05 (Steel and Torrie 1981). Genstat software was used in the statistical analysis.

RESULTS : The phenotypic and microbiological characteristics of the two fungi *Trichophyton rubrum* isolate IQT-No.1 *and Microsporum canis* isolate IQM-No1. registered in the Global Genebank that accession numbers MK167434 and MK167435 respectively were completely identical to what was mentioned in Al-Masaoodi, *et al*., (2020) Fig 1.

The results showed in Figures 2 , 3 and the ability of fungi to produce protease, lipase, and keratinase enzymes during 3, 6 and 9 days incubation periods at 25 ° C., the *T. rubrum* was higher in its production of the protease and lipase on the ninth day of incubation, which was significantly different from the *M. canis*, while the *M. canis* recorded a significant superiority in its production of the enzyme keratinase on the ninth day of incubation compared to the *T. rubrum* .

It is evident from Figure 3 that the fungi differed in their production of enzymes and the *T.rubrum*was superior in its production of protease and lipase enzymes compared to the *M.canis*, while the *M.canis* recorded an superiority in its production of keratinase. In addition, the production of the three enzymes increased with the increase in the incubation period, with significant differences, While the *M.canis* showed a higher production of enzymes on the ninth day of incubation compared to the *T.rubrum*, while the *T.rubrum* showed a superiority in its production of enzymes on the third day of incubation , and the differences were not significant on the sixth day. The differences were not significant between the two fungi in their production of enzymes. Likewise, the ninth day of incubation is the most productive of enzymes, as well as the protease is the most productive enzyme, followed by lipase and then keratinase .

The results in (Fig. 4) indicated that using the combination (treatments 12,1,2,4)respectively of 30 mg zinc with 10 mg flucanazole was the best combination in the low dry weight of *T.rubrum*, which was not significantly different from the combination of 2.5mg zinc with 7.5 mg flucanazole, as well as the combination of 5.0 mg zinc with 5.0mg flucanazole and 5.0mg zinc with 15.0mg flucanazole compared with the control, while the *M.canis* was affected by the combination (treatments 5,6)of 10.0mg zinc and 10.0mg flucanazole, and it did not significantly differ from 15.0 mg zinc and 5.0 mg flucanazole compared with the control . The Figure indicates that treatment 12 represented by the combination 30mg zinc and 10mg flucanozole was the best combination in dry weight of fungi, and it was significantly different from control, whereas the combination in treatment 11, which consisted of 20mg zinc and 20mg flucanozol, did not significantly differ from the control in dry weight of fungi. The two fungi also differed with each other in the average dry weight of the biomass, and the *M.canis* was less dry weight compared to *T.rubrum*.

The results in Fig.(5) indicate the effect of different combinations of nano zinc on the average dry weight of the fungi. All the combinations were positive in decreasing the dry weight of the biomass of the *T.rubrum*, except for treatments 7 and 8, which did not differ from the control. Likewise, the *M.canis* was affected by the combinations and gave a significant decrease over the control, especially in treatment 12, which is about 30 nano zinc and 10 fluconazol. The Figure 5 indicates that

Pure Sciences International Journal of Kerbala

Journal Homepage:https://journals.uokerbala.edu.iq/index.php/psijk

all treatments by all combinations was significantly different from control. The two fungi also differed with each other in the *T.rubrum*, in Treatment 2 (5.0mg zinc and 5.0mg flucanozol) , recorded the lowest rate of colony diameter over the solid Sabouraud's dextrose agar medium and was significantly different from the other treatments, which differed from the contol except for treatment 12(30 zinc and 10 flucanozol), which did not show a significant difference from the control, while the two treatments 9 and 11 represented to the 22.5m zinc with the 7.5mg fluconazol and 20mg zinc to 20mg fluconazol respectively showed the lowest average for the *M.canis* colony diameter (mm), and all the treatments recorded a significant decrease compared to the control.

All the combinations prepared from meniral zinc and flucanozole showed a significant decrease in the rate of diameter of fungal colonies and the best of them was treatment 2 in which 5mg meniral zinc with 5mg flucanozol (Figure 6). The two fungi also differed with each other in the average of colony diameter (mm), and the *M.canis* was less diameter colony compared to *T.rubrum* (Figure 6).

The results in Fig.(7) indicate the effect of different combinations of nano zinc and fluconazole on the average diameter of the colony . The best combination in treatment was 6 which contained 15.0 mg nano zinc with 5.0 mg only fluconazol in decreasing the diameter colony of *T.rubrum*, except for treatments 2 and 3, which did not differ from the control. Likewise, the *M.canis* was affected by the combinations and gave a significant decrease over the control, especially in treatment 7, which is about7.5mg nano zinc and 22.5mg flucanozol. The Figure indicates that all treatments by all combinations was significantly different from control and the best treatment was 10 . The two fungi also differed with each other in the average of diameter average dry weight of the biomass, and the *M.canis* was less dry weight compared to *T.rubrum*.

colony , and the fungus *M.canis* was less diameter compared to *T.rubrum* (Figure 7). Figure 8indicates an inhibition of the average diameter of the fungal culture in terms of phenotypically and grow vertically tend towarde the cover plate . As for the microscopic aspect, deformation occurred in the fungal hypha, separation of protoplasm from the cell wall and aggregation of protoplasm, in addition to the disappearance of the conidia, compared to the control.

Discussion : The results showed that *Trichophyton and Microsporum* were able to produce enzymes that degrade keratin, fats and protein, and that the high activity of the enzyme was represented by the diameter of the aura, where the protase was the most effective among the enzymes, and that the enzyme activity increased with the increase of the incubation period, as dermatophytes produce and secrete the Protease enzyme in response to extracellular components such as keratin as it invades the epidermis. Protease may contribute to the ability of dermal cells to degrade components of the deep layers of the dermis in patients with dermatomycosis (Nir-Paz *et al.* 2003). A study presented by Al-Masaoodi *et al.* (2020b) showed the ability of Trichophyton rubrum to produce the protease enzyme and increased gene expression of this enzyme when treated with fungus leaches *Marasmius palmivorus.*It is believed that, in addition to the mechanical penetration of fungal elements, proteolytic enzymes lead to the degradation of the components of the skin tissue. The degradation of keratin by proteins is an important aspect of fungal pathogenesis, providing a source of nutrition on the keratinocyte layer, which is an obstacle to pathogens (Kaufman *et al*. 2007)

Pure Sciences International Journal of Kerbala

Journal Homepage:https://journals.uokerbala.edu.iq/index.php/psijk

The results showed that the concentrations of nano- mineral- zinc, zinc, the antibiotic and the synergistic action between them significantly affected the growth rates (diameters and weights) of *Trichophyton* and *Microsporum* by fungal colony. The small size of the nanoparticles and their large surface area (the smaller the size, they accumulate in greater numbers on the surface of the cells, which leads to an increase in their toxicity to the microorganisms), which leads to an effect on the permeability of the plasma membrane of the cell and thus cell death (Lin *et al*. 2014). The mechanism in which the nanoparticles interact with the micro-organisms is that these organisms carry negative charges while the nanoparticles and their oxides carry positive charges, which creates an electromagnetic attraction between the cell and the surface of the minute particles and that the surface of the minute releases ions that interact with the thiol group of protein transporting nutrients that emerge from The cell membrane, which reduces the permeability of the membrane and thus the death of the cell (Zhang and Chen 2009). The nanocomposites have a role in disrupting the transport systems and this is reflected in respiration, cellular representation and interaction between organelles in addition to that zinc ions and nanoparticles are known to produce free radicals that act on Destruction of amino acids, fats, and protein (Brayner *et al*. 2006; Reddy *et al*. 2007; Hwang *et al*. 2008). Various factors have been proposed responsible for the antifungal activity of ZnO-NPs: one of which is the formation of H_2O_2 hydrogen peroxide on the surface of ZnO-NPs due to the possibility of hydrogen bonding between the hydroxyl group of cellulose molecules of fungi with the oxygen atom of ZnO-NPs leading to inhibition The growth of fungi, or it may be the release of Zn ++ ions, which causes damage to the cell membrane and interacts with the contents of the cell (Moraru *et al.* 2003), or it may be due to the interaction of ZnO-NPs with the fungal cell membrane, causing inhibition of DNA replication, breakdown of proteins and enzymes. Breaking down the cytoplasmic structure, inhibiting the activity of cell division (Matai *et al*. 2014), or by generating active oxygen species (ROS) (Dutta *et al*. 2011), all of these factors lead to rupture of the fungal cell membrane, causing leakage of the fungal cell contents, which results (Padmavathy and Vijayaraghavan 2011) reported shrinkage in plasma membrane size and cell death. These results are in agreement with (Hassan *et al.* 2013) where he observed that the effect of ZnO nanoparticles on treated fungi at (8 mg / mL) caused damage to the conidial cell membrane of the fungus and A spergillus and the formation of perforations in the cell wall and the occurrence of some spaces between cells, which led to the leakage of cell components and their eventual death. And it agrees with El-Diasty *et al*. (2013) when studying the effect of ZnO-NPs on a number of dermatophytes Trichophyton mentagrophyte, Microsporum canis, Candida albicans and Aspergillus fumigatus in inhibiting their growth and that the increase in inhibition rate was strongly associated with increased concentration and the highest rate of inhibition of ZnO. -NPs was at concentration (40 mg / mL).

The antifungal Fluconazole had a significant effect in the diameters and weights of the fungal colonies, and the rate of inhibition rate increased by increasing the concentration. This membrane is the main component of the

Pure Sciences International Journal of Kerbala

Journal Homepage:https://journals.uokerbala.edu.iq/index.php/psijk

secretory vesicles, and this complex has an important role in the mitochondrial respiration process (Bossche, *et al.* 2003), as Azol antagonists act on the target enzyme 14 α - demethylase sterol, which is responsible for *al*. 1988) which is encoded by the gene CYP51, and as a result of interfering with this gene, there is a decrease in the arctrol complex and an accumulation of 14 α-demethylase, thus a defect occurs in the functioning of the fungal cell and may lead to its death and that the antagonist works to inhibit Germination of large conidia spores that are characterized by a thick wall and are resistant to antifungal agents and also interfere with the construction of the microtubules and thus the formation of the spindle and the accuracy of the normal division occurrence (Bossche *et al*. 2004) .Also, Azol compounds affect the activity of chitin building, which leads to an irregular distribution of chitin in the cell wall. (Bossche 1985). This result In agreement with Suchodolski , *et al*. (2020) in their study of the effect of the antifungal fluconazole on the plasma membrane of *Candida albicans* in that Azol compounds inhibit the formation of arctrolytes by inhibiting the enzyme 14 methyl sterol demethylase (P450 cytochrome) encoded by the ERG11 gene.

The results of the microscopic examinations showed that there are internal abnormalities that can be observed during the microscopic examination, and this may be the reason for the occurrence of physiological changes within the cells of the fungus and perhaps the production of some compounds that act as a kind of protection for the fungus, as well as changes that may lead to the fungus losing its vital processes, gathering protoplasm, shrinkage and collapse The cell collapse, and it may be attributed to the presence of some toxic converting lanostol into arctrol, which is the predominant compound in the membrane. Plasmapheresis of fungal cells (Van den Bossche *et al*. 1978 ; Isaacson *et*

substances that poison the cell or increase its osmotic pressure, which leads to the breakdown of the mycelium. This is reflected in the growth and development of conidia .Some studies have suggested that ZnO NPs may cause changes in the fungal cell membrane, causing cytoplasmic leakage and consequently cell death (Brayner *et al*. 2006). In another study He *et al*. (2011) demonstrated that the effect of ZnO NPs on fungal cells during his study of the fungi Botrytis Cinerea. Penicillium Expansum is a deformation and breakdown of the cell wall. The plasma membrane is also severely damaged, leading to leakage of the cell contents, the disappearance of the konides, leading to cell death. This is in agreement with Ghannoum *et al.* (2012) when he explained that treating T. rubrum with TDT 067 containing terbinafine led to deformations and rupture of the fungal thread and shrinkage of the protoplasm, which led to the formation of vacuoles.

.**CONCLUSIONS:** This is the first study in Iraq deals with *T. rubrum and M.canis* tinea were treated with the combination between mineral zinc or nano zinc with fluconazole antifungal to reduce the pathogenic fungal growth and deformation of conidia formation . This may be the key to future studies to reduce the use of antifungal drugs and replace them or reduce their dose through the use of environmentally friendly materials. In all of the above, nano zinc has more effect than mineral zinc when mixed with the anti-fungal fluconazole.

Pure Sciences International Journal of Kerbala

Journal Homepage:https://journals.uokerbala.edu.iq/index.php/psijk

Table (1): Bi combination between Mineral zinc and zinc nanoparticles with Fluconazole (mg)

Tretments	Combination	
	Fluconazole(mg)	mineral zinc or Nanozinc*(mg)
Control	0.0	0.0
1	7.5	2.5
2	5.0	5.0
3	2.5	7.5
4	15.0	5.0
5	10.0	10.0
6	5.0	15.0
7	22.5	7.5
8	15.0	15.0
9	7.5	22.5
10	30.0	10.0
11	20.0	20.0
12	10.0	30.0

*Specifications of zinc Nanopowder by Provider US Research Nanomaterials, Inc

Appearance	Stook	Pratical size	purity	BET specific surface area	Product Origin
Grey powder	US1167 CAS:7440-66-6	35-45nm (metal Basis)	99.99%	7 g/ 30-50 m^2	USA

.us-nano.com WWW.us-nano.com

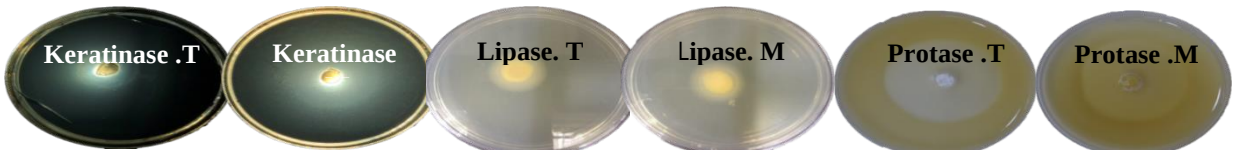

Figure (2): Enzyme production by *Trichophyton rubrum and Microsporum canis* on the appropriate culture media for each enzyme at a temperature of 25 ^{0} C and an age of 9 days.

Keratinase T = Keratinase production from *Trichophyton rubrum* on the medium of keratin agar
Keratinase. M = Keratinase production from *Microsporum canis* on keratin agar medium
Lipase. T = Lipase production from *Trichophyton rubrum* on Tween 80 agar medium
Lipase. M = Lipase production from *Microsporum canis* on Tween 80 agar medium
Protase T = Protase production from *Trichophyton rubrum* on medium skimmed milk agar.
Protase.M = Protase production from *Microsporum canis* on medium skimmed - milk agar

First Year-First Folder-Number: 0
PSIJK 184-191

Pure Sciences International Journal of Kerbala

Journal Homepage:https://journals.uokerbala.edu.iq/index.php/psijk

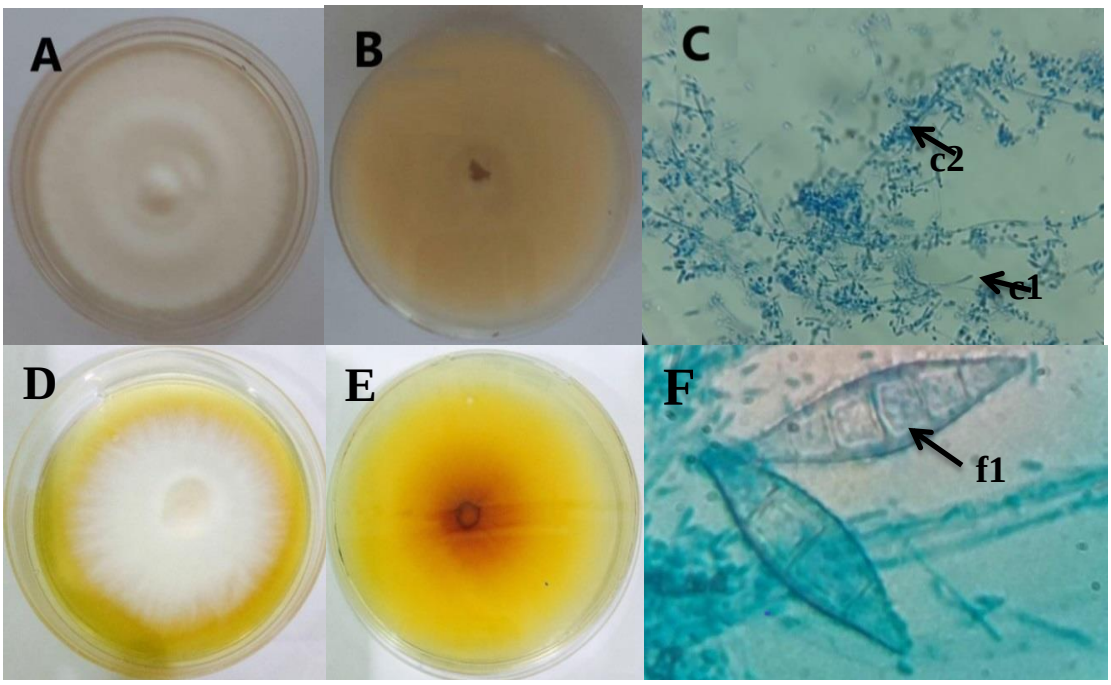

Figure (1): Phenotypic and microscopic features of *Trichophyton rubrum* and *Microsporum canis*. on SDA medium at a temperature of 25 ^{0} C at age of 14 days.
A = The upper surface of the colony of *Trichophyton rubrum* ,B = Posterior face of the colony of *Trichophyton rubrum* ,C = the microscopic form of *Trichophyton rubrum*, Macroconidia (c1), and Microconidia (c2) appear after staining their mycelium structures with a stain blue lacto phenol with 40X magnification ,D = the upper surface of the colony of the *Microsporum canis* ,E = posterior face of the colony of the fungus *Microsporum canis* ,F = the microscopic shape of the *Microsporum canis* ,(F1) Macroconidia and mycelium , structures with. blue lacto phenol , magnification = 100X

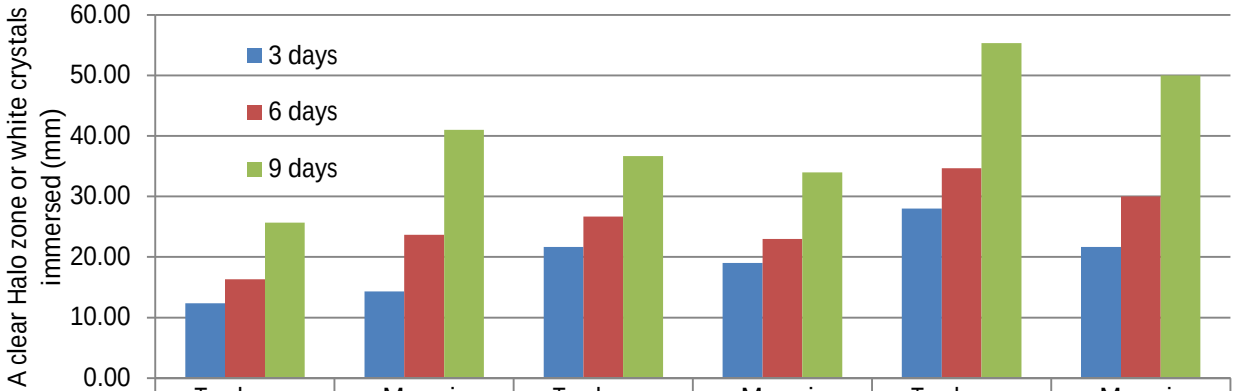

	T.rubrum	M.canis	T.rubrum	M.canis	T.rubrum	M.canis
	Keratinase		Lipase		Protease	
3 days	12.33	14.33	21.67	19.00	28.00	21.67
6 days	16.33	23.67	26.67	23.00	34.67	30.00
9 days	25.67	41.00	36.67	34.00	55.33	50.00

Figure 3: A clear halo zone (mm) resulting from the activity of the enzymes, protease and keratinase , and white crystals immersed from the activity of lipase of the fungi *Trichophyton rubrum and Microsporum canis* in 3,6,9 days of incubation at 28^{0}C.

L.S.D.0.05 The interaction between fungal type, period of incubation and types of enzymes =2.458

Pure Sciences International Journal of Kerbala

Journal Homepage:https://journals.uokerbala.edu.iq/index.php/psijk

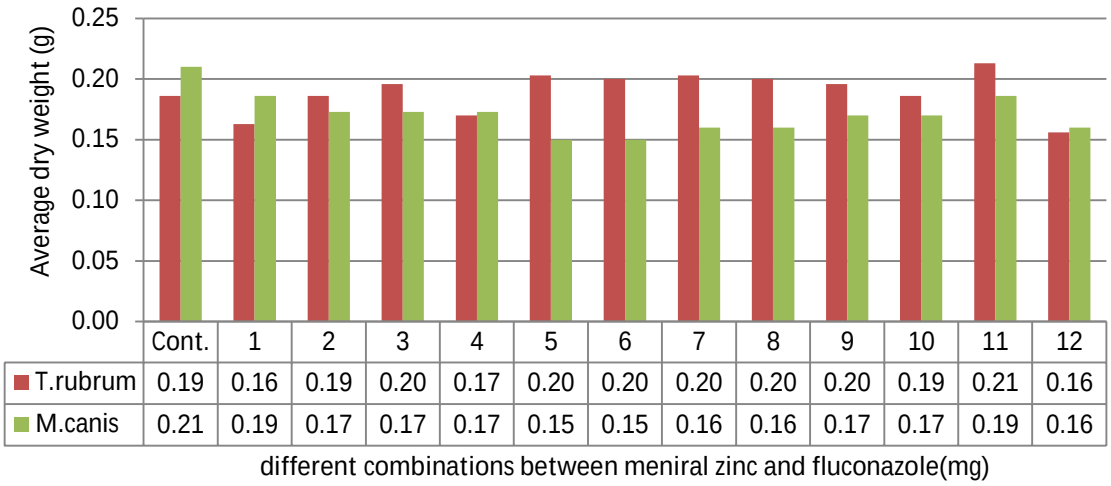

	Cont.	1	2	3	4	5	6	7	8	9	10	11	12
T.rubrum	0.19	0.16	0.19	0.20	0.17	0.20	0.20	0.20	0.20	0.20	0.19	0.21	0.16
M.canis	0.21	0.19	0.17	0.17	0.17	0.15	0.15	0.16	0.16	0.17	0.17	0.19	0.16

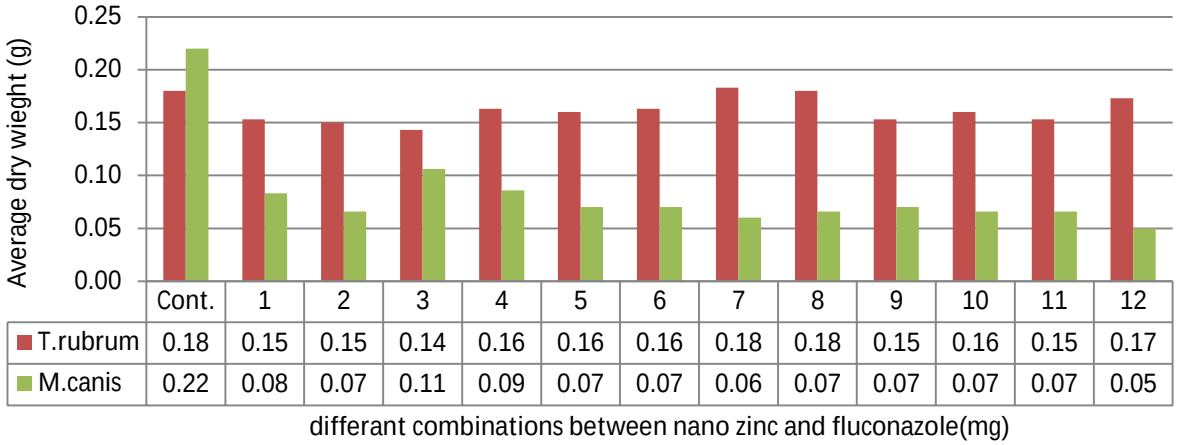

	Cont.	1	2	3	4	5	6	7	8	9	10	11	12
T.rubrum	0.18	0.15	0.15	0.14	0.16	0.16	0.16	0.18	0.18	0.15	0.16	0.15	0.17
M.canis	0.22	0.08	0.07	0.11	0.09	0.07	0.07	0.06	0.07	0.07	0.07	0.07	0.05

Figure (5): The interaction between fungal type and different combinations between nano zinc and Fluconazole on average dry weight for *Trichophyton rubrum and Microsporum canis* on sabrouaud dextrose broth at 28^0C for 14 days .

L.S.D.0.05=: The interaction between fungal type and different combinations between nano zinc and Fluconazole=0.01

The effect of different combinations of nano zinc and Fluconazole =0.01

The effect of Fungal types,= 0.003

Pure Sciences International Journal of Kerbala

Journal Homepage:https://journals.uokerbala.edu.iq/index.php/psijk

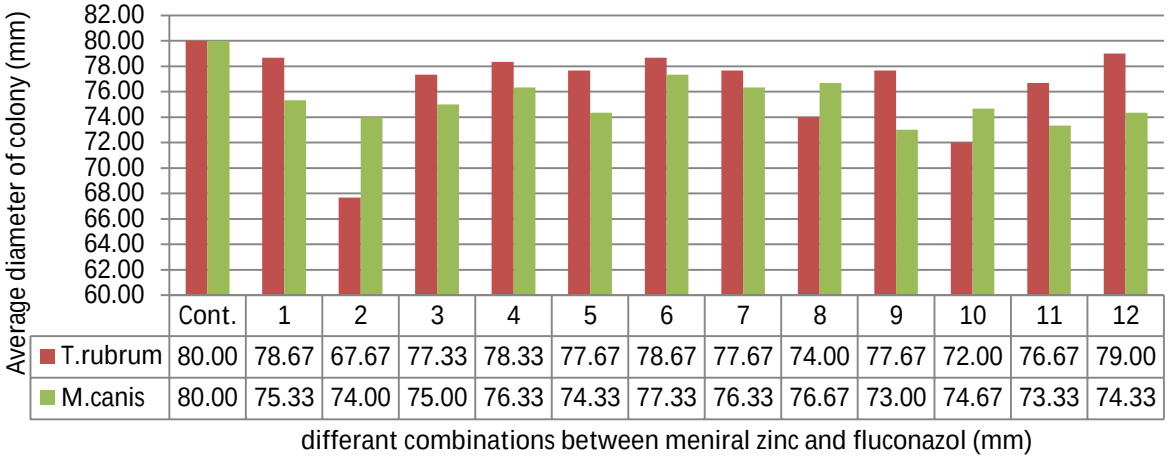

Figure (6: The interaction between fungal type and different combinations between mineral zinc and Fluconazole on average diameter of colony (mm) *Trichophyton rubrum. and Microsporum* canis on sabrouaud dextrose agar at 28^0C for 14 days.

L.S.D.0.05 The interaction between fungal type and different combinations between mineral zinc and Fluconazole=2.55

The effect of different combinations of mineral zinc and Fluconazole= 1.083

The effect of Fungal types= 0.707

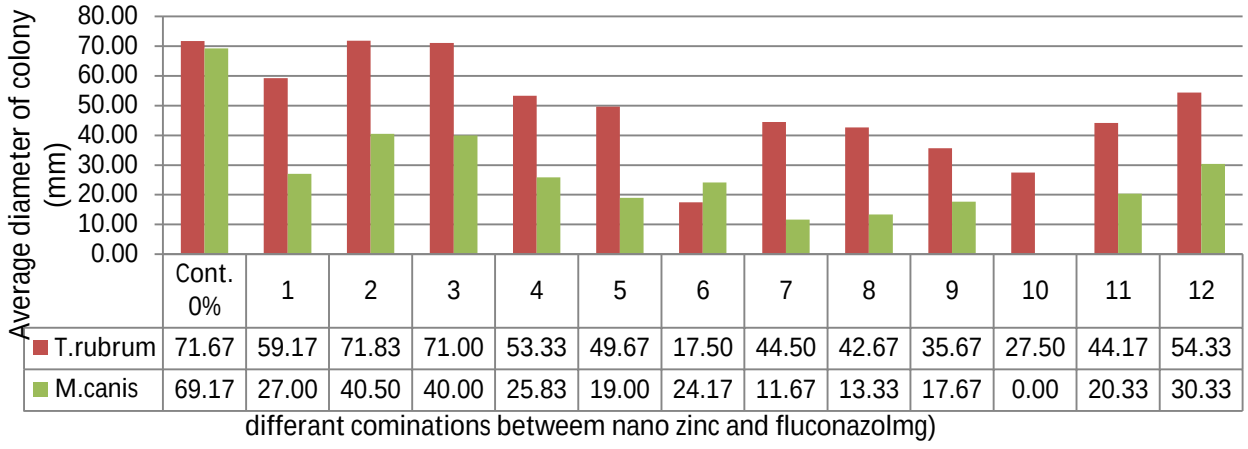

Figure (7): The interaction between fungal type and different combinations between nano zinc and Fluconazole on average diameter of colony (mm) *Trichophyton rubrum and Microsporum canis* on sabrouaud dextrose agar at 28^0C for 14 days.

L.S.D0.05 The interaction between fungal type and different combinations between nano zinc and Fluconazole=6.73

The effect of different combinations of nano zinc and Fluconazole= 4.76

The effect of Fungal types=1.86,

Pure Sciences International Journal of Kerbala

Journal Homepage:https://journals.uokerbala.edu.iq/index.php/psijk

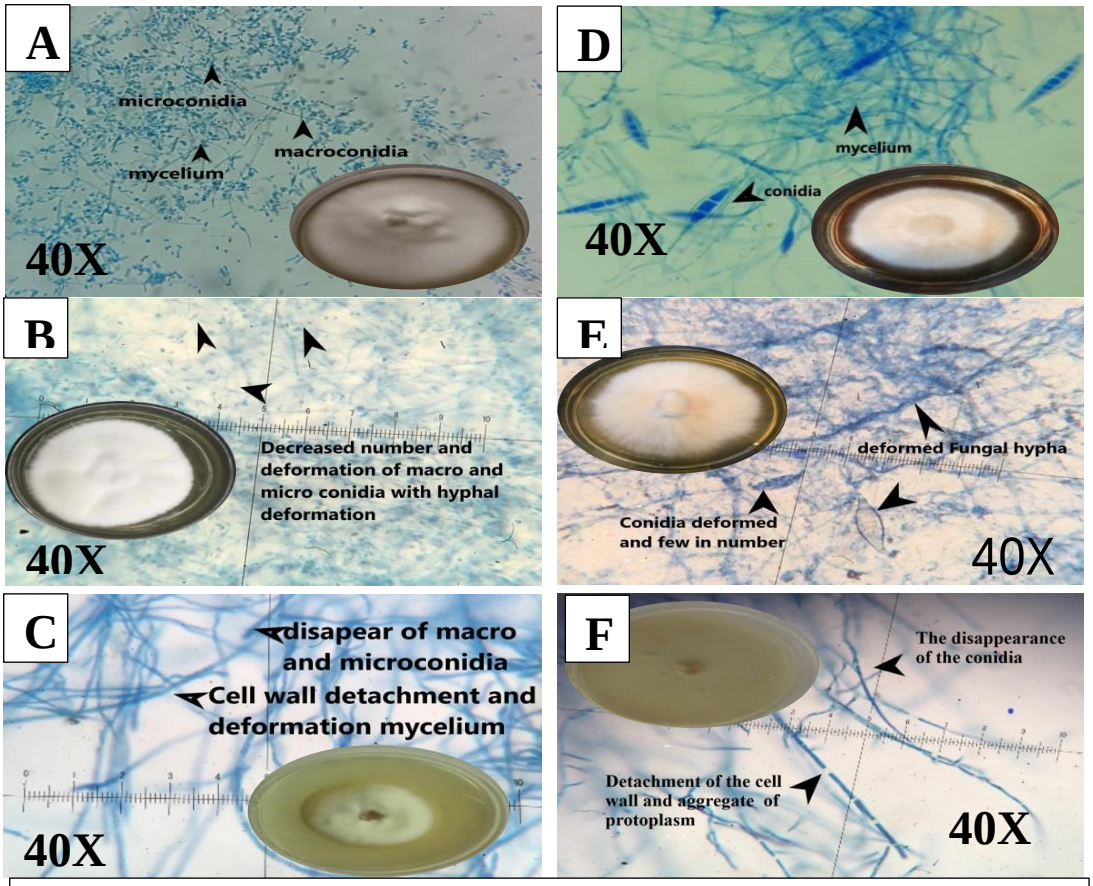

Figure (8): The interaction between mineral zinc or nano zinc and Fluconazole on average diameter of colony (mm) on sabrouaud dextrose agar at 28^0C for 14 days

A : *T. rubrum* morphology and microscopic features.

B: *T. rubrum* :The combinations between mineral zinc and Fluconazole

C: *T. rubrum*.: The combinations between nano zinc and Fluconazole

D : *M. canis* morphology and microscopic features

E: *M. canis* :The combinations between mineral zinc and Fluconazole

F= *M. canis* :The combinations between nano zinc and Fluconazole

Pure Sciences International Journal of Kerbala

Journal Homepage:https://journals.uokerbala.edu.iq/index.php/psijk

Referances :

Allahverdiyev, Adil M., Kateryna Volodymyrivna Kon, Emrah Sefik Abamor, Malahat Bagirova, and Miriam Rafailovich. 2011. "Coping with Antibiotic Resistance: Combining Nanoparticles with Antibiotics and Other Antimicrobial Agents." *Expert Review of Anti-Infective Therapy* 9(11):1035–52.

Al-Masaoodi, Nadia. N. H., Abood Al-Janabi, and Ban T. Mohammed (2020 b). Molecular characterization and gene expression profiling of Trichophyton rubrum treated with a Marasmius palmivorus filtrate. Drug Invention Today, 14(6), 877–888.

Al-Masaoodi, N. N. H. (2020) . Morphological and Molecular properties of some dermatophytes present in Kerbala province and evaluation of Marasmius palmivorus filtrate and Moringa oliefera leaves extract on the growth and gene. Expression of *Trichophyton rubrum*. . Ph.D.thesis . College of Education for Pure Science.University of Kerbala.Iraq. 100pp .(In Arabic)

Al-Masaoodi, Nadia N. H., Ban T. Mohammed, and Jawad K. Abood Al-Janabi. (2020a)."Occurrence, Morphological, and Molecular Characteristics of Trichophyton Erinacei in Iraq." *Drug Invention Today* 14(6).

Almeida, Débora de Fátima, Thais F. Fraga-Silva, Amanda R. Santos, Angela C. Finato, Camila M. Marchetti, Marjorie de Assis Golim, Vanessa S. Lara, Maria S. P. Arruda, and James Venturini. 2017. "TLR2−/− Mice Display Increased Clearance of Dermatophyte Trichophyton Mentagrophytes in the Setting of Hyperglycemia." *Frontiers in Cellular and Infection Microbiology* 7:8.

Arey NC. 2010. Manual Of Environmental Analysis,Ane Books Pvt Ltd, New Delhi, India, , 424.

Asticcioli, Sara, Adriano Di Silverio, Laura Sacco, Ilaria Fusi, Luca Vincenti, and Egidio Romero. 2008. "Dermatophyte Infections in Patients Attending a Tertiary Care Hospital in Northern Italy." *New Microbiol* 31(4):543–48.

Bossche, H. Vanden, M. Engelen, and F. Rochette. 2003. "Antifungal Agents of Use in Animal Health–Chemical, Biochemical and Pharmacological Aspects." *Journal of Veterinary Pharmacology and Therapeutics* 26(1):5–29.

Bossche, Hugo Vanden, Jannie Ausma, Hilde Bohets, Karen Vermuyten, Gustaaf Willemsens, Patrick Marichal, Lieven Meerpoel, Frank Odds, and Marcel Borgers. 2004. "The Novel Azole R126638 Is a Selective Inhibitor of Ergosterol Synthesis in Candida Albicans, Trichophyton Spp., and Microsporum Canis." *Antimicrobial Agents and Chemotherapy* 48(9):3272–78.

Bossche, Hugo Vanden. 1985. "Biochemical Targets for Antifungal Azole Derivatives: Hypothesis on the Mode of Action." Pp. 313–51 in *Current topics in medical mycology*. Springer

Brayner, Roberta, Roselyne Ferrari-Iliou, Nicolas Brivois, Shakib Djediat, Marc F. Benedetti, and Fernand Fiévet. 2006. "Toxicological Impact Studies Based on Escherichia Coli Bacteria in Ultrafine ZnO Nanoparticles Colloidal Medium." *Nano*

Pure Sciences International Journal of Kerbala

Journal Homepage:https://journals.uokerbala.edu.iq/index.php/psijk

Letters 6(4):866–70.

Degreef, Hugo. 2008. "Clinical Forms of Dermatophytosis (Ringworm Infection)." *Mycopathologia* 166(5–6):257.

Dutta, Ranu K., Prashant K. Sharma, and Avinash C. Pandey. 2011. "Assessing the Conformational and Cellular Changes of ZnO Nanoparticles Impregnated Escherichia Coli Cells through Molecular Fingerprinting." *Adv Mat Lett* 2:268–275.

El-Diasty, EMAN M., M. A. Ahmed, NAGWA Okasha, SALWA F. Mansour, SAMAA I. El-Dek, H. M. A. El-Khalek, and MARIAM H. YOUSSIF. 2013. "Antifungal Activity of Zinc Oxide Nanoparticles against Dermatophytic Lesions of Cattle." *Romanian j. Biophys* 23(3):191–202.

Ghannoum, M., N. Isham, W. Henry, H. A. Kroon, and S. Yurdakul. 2012. "Evaluation of the Morphological Effects of TDT 067 (Terbinafine in Transfersome) and Conventional Terbinafine on Dermatophyte Hyphae in Vitro and in Vivo." *Antimicrobial Agents and Chemotherapy* 56(5):2530–2534.

Ghannoum, Mahmoud A., and Louis B. Rice. 1999. "Antifungal Agents: Mode of Action, Mechanisms of Resistance, and Correlation of These Mechanisms with Bacterial Resistance." *Clinical Microbiology Reviews*.

Goldsmith, Lowell A.; Fitzpatrick, Thomas B. 2012 . Fitzpatrick's dermatology in general medicine (8th ed.). New York: McGraw-Hill Medical

Hankin, Lester, and S. L. Anagnostakis. 1975. "The Use of Solid Media for Detection of Enzyme Production by Fungi." *Mycologia* 67(3):597–607.

Hassan, A. A., M. E. Howayda, and H. H. Mahmoud. 2013. "Effect of Zinc Oxide Nanoparticles on the Growth of Mycotoxigenic Mould." *SCPT* 1(4):66–74.

He, Lili, Yang Liu, Azlin Mustapha, and Mengshi Lin. 2011. "Antifungal Activity of Zinc Oxide Nanoparticles against Botrytis Cinerea and Penicillium Expansum." *Microbiological Research* 166(3):207–215.

Hochella, Michael F., Michael G. Spencer, and Kimberly L. Jones. 2015. "Nanotechnology: Nature's Gift or Scientists' Brainchild?" *Environmental Science: Nano* 2(2):114–19.

Hwang, Ee Taek, Jin Hyung Lee, Yun Ju Chae, Yeon Seok Kim, Byoung Chan Kim, Byoung- In Sang, and Man Bock Gu. 2008. "Analysis of the Toxic Mode of Action of Silver Nanoparticles Using Stress- specific Bioluminescent Bacteria." *Small* 4(6):746–50.

Isaacson, D. M., E. L. Tolman, A. J. Tobia, M. E. Rosenthale, J. L. McGuire, H. Vanden Bossche, and P. A. J. Janssen. 1988. "Selective Inhibition of 14α-Desmethyl Sterol Synthesis in Candida Albicans by Terconazole, a New Triazole Antimycotic." *Journal of Antimicrobial Chemotherapy* 21(3):333–343.

Jasim, A. A., 2019 . Estimating the effectiveness of someNanoparticles in Control contamination by Fungi isolated from some Historical Manuscripts on the at the Al-Hussein Holy . Athesis . College of Education for Pure Science.University of Kerbala.Iraq. 101 pp.(In Arabic)

Pure Sciences International Journal of Kerbala

Journal Homepage:https://journals.uokerbala.edu.iq/index.php/psijk

Jasim, A. A., Mohammed, Ban. T., & Lahuf, A. A. (2019). Molecular and enzymatic properties of fungi isolated from historical manuscripts preserved at the Al-Hussein. Biochem. Cell. Arch, 19(2), 4295–4305.

Kasemets, Kaja, Angela Ivask, Henri-Charles Dubourguier, and Anne Kahru. 2009. "Toxicity of Nanoparticles of ZnO, CuO and TiO2 to Yeast Saccharomyces Cerevisiae." *Toxicology in Vitro* 23(6):1116–22.

Kaufman, Gil, Benjamin A. Horwitz, Lea Duek, Yehuda Ullman, and Israela Berdicevsky. 2007. "Infection Stages of the Dermatophyte Pathogen Trichophyton: Microscopic Characterization and Proteolytic Enzymes." *Medical Mycology* 45(2):149–55.

Lin, Xiuchun, Jingyi Li, Si Ma, Gesheng Liu, Kun Yang, Meiping Tong, and Daohui Lin. 2014. "Toxicity of TiO 2 Nanoparticles to Escherichia Coli: Effects of Particle Size, Crystal Phase and Water Chemistry." *PloS One* 9(10):e110247.

Lipovsky, Anat, Yeshayahu Nitzan, Aharon Gedanken, and Rachel Lubart. 2011. "Antifungal Activity of ZnO Nanoparticles—the Role of ROS Mediated Cell Injury." *Nanotechnology 22(10):105101.*

Matai, Ishita, Abhay Sachdev, Poornima Dubey, S. Uday Kumar, Bharat Bhushan, and P. Gopinath. 2014. "Antibacterial Activity and Mechanism of Ag–ZnO Nanocomposite on S. Aureus and GFP-Expressing Antibiotic Resistant E. Coli." *Colloids and Surfaces B: Biointerfaces* 115:359–67.

Mehdi, Husham A., Ban T. Mohammed, and Abbas M. Bashi. 2018a. "Effect of Silver and Zinc Oxide Nanocompound Mixture on Growth and Some Physiological Properties of Sclerotinia Sclerotiorum." *Indian Journal of Ecology* 45(2):358–366.

Mehdi, H. A., Mohammed, Ban T., & Bashy, A. M. 2018b. Effect of nano-silvers, nano-zinc oxide and benomyl pesticide on some physiological properties of Sclerotinia sclerotiorum. Biochemical and Cellular Archives, 18(2), 2181–2196.

Midgley, G; Moore, M. K.; Cook, J. C.; Phan, Q. G. 1994. "Mycology of nail disorders". Journal of the American Academy of Dermatology. **31** (3 Pt 2): S68-74.

Mini, K. D., K. P. Mini, and Jyothis Mathew. 2012. "Screening of Fungi Isolated from Poultry Farm Soil for Keratinolytic Activity." *J Advanced Appl Sci Res* 3:2073-2077.

Mohammed, Ban. T., Dakhil, M. H., & Almutairy, T. M. (2018). Manuscripts preserved at the Al-Hussein Holy shrine: Isolation and diagnosis of fungi causing potential damage. *Indian Journal of Ecology*, *45*(1).

Moraru, Carmen I., Chithra P. Panchapakesan, Qingrong Huang, Paul Takhistov, Sean Liu, and Jozef L. Kokini. 2003. "Nanotechnology: A New Frontier in Food Science Understanding the Special Properties of Materials of Nanometer Size Will Allow Food Scientists to Design New, Healthier, Tastier, and Safer Foods." *Nanotechnology* 57(12).

Moraru, Carmen I., Chithra P. Panchapakesan, Qingrong Huang, Paul

Pure Sciences International Journal of Kerbala

Journal Homepage:https://journals.uokerbala.edu.iq/index.php/psijk

Takhistov, Sean Liu, and Jozef L. Kokini. 2003. "Nanotechnology: A New Frontier in Food Science Understanding the Special Properties of Materials of Nanometer Size Will Allow Food Scientists to Design New, Healthier, Tastier, and Safer Foods." *Nanotechnology* 57(12).

Nir-Paz, Ran, Hila Elinav, Gerald E. Pierard, David Walker, Alexander Maly, Mervyn Shapiro, Richard C. Barton, and Itzhack Polacheck. 2003. "Deep Infection by Trichophyton Rubrum in an Immunocompromised Patient." *Journal of Clinical Microbiology* 41(11):5298–5301.

Padmavathy, Nagarajan, and Rajagopalan Vijayaraghavan. 2011. "Interaction of ZnO Nanoparticles with Microbes—a Physio and Biochemical Assay." *Journal of Biomedical Nanotechnology* 7(6):813–22.

Piérard, Gérald. 2001. "Onychomycosis and Other Superficial Fungal Infections of the Foot in the Elderly: A Pan-European Survey." *Dermatology* 202(3):220–24.

Ravishankar Rai, V. 2011. "Nanoparticles and Their Potential Application as Antimicrobials."

Reddy, Kongara M., Kevin Feris, Jason Bell, Denise G. Wingett, Cory Hanley, and Alex Punnoose. 2007. "Selective Toxicity of Zinc Oxide Nanoparticles to Prokaryotic and Eukaryotic Systems." *Applied Physics Letters* 90(21):213902.

Sharma, Virender K., Jan Filip, Radek Zboril, and Rajender S. Varma. 2015. "Natural Inorganic Nanoparticles–Formation, Fate, and Toxicity in the Environment." *Chemical Society Reviews* 44(23):8410–23.

Sierra, Gonzalo. 1957. "A Simple Method for the Detection of Lipolytic Activity of Micro-Organisms and Some Observations on the Influence of the Contact between Cells and Fatty Substrates." *Antonie van Leeuwenhoek* 23(1):15–22.

Steel, R. G.D., and Torrie ,J. H. 1981. *Principles and Procedures of Statistics: A Biometrical Approach*. Second edition . McGraw-Hill.

Suchodolski, Jakub, Daria Derkacz, Jakub Muraszko, Jarosław J. Panek, Aneta Jezierska, Marcin Łukaszewicz, and Anna Krasowska. 2020. "Fluconazole and Lipopeptide Surfactin Interplay During Candida Albicans Plasma Membrane and Cell Wall Remodeling Increases Fungal Immune System Exposure." *Pharmaceutics* 12(4):314.

Van den Bossche, H., G. Willemsens, W. Cools, W. F. J. Lauwers, and L. Le Jeune. 1978. "Biochemical Effects of Miconazole on Fungi. II. Inhibition of Ergosterol Biosynthesis in Candida Albicans." *Chemico-Biological Interactions* 21(1):59–78.

Venkatesan G, Ranjitsingh1 AJA, Murugesan AG, Gokulshankar S, Ranjith MS . 2010. Is the difference in keratinase activity of dermatophytes to different keratinaceous substrates an attribute of adaptation to parasitism. Egyptian Dermatol Online J 6: 6.

Wawrzkiewicz, Krystyna, Tadeusz Wolski, and Jerzy Łobarzewski. 1991. "Screening the Keratinolytic Activity of Dermatophytes in Vitro." *Mycopathologia*

Pure Sciences International Journal of Kerbala

Journal Homepage:https://journals.uokerbala.edu.iq/index.php/psijk

114(1):1–8.

Yehia, Mostafa A., Tarek S. El-Ammawi, Khairia M. Al-Mazidi, Mahmoud A. Abu El-Ela, and Hejab S. Al-Ajmi. 2010. "The Spectrum of Fungal Infections with a Special Reference to Dermatophytoses in the Capital Area of Kuwait during 2000–2005: A Retrospective Analysis." *Mycopathologia* 169(4):241–46.

Zhang, Huanjun, and Guohua Chen. 2009. "Potent Antibacterial Activities of Ag/TiO2 Nanocomposite Powders Synthesized by a One-Pot Sol− Gel Method." *Environmental Science & Technology* 43(8):2905–10.

First Year-First Folder-Number: 0
PSIJK 184-191

Pure Sciences International Journal of Kerbala

Journal Homepage:https://journals.uokerbala.edu.iq/index.php/psijk

Evaluation of Nano - silver and zinc particles in fungi accompanying historical manuscripts at the Husseini shrine in Karbala

Ban Taha Mohammed [a)] and Alaa Aqeel Jasim [b)]

a) Department of Biology, University of Kerbala, Iraq.

b) Al-Furat Al-Awsat Technical University

*E-mail: Bantmh@gmail.com

Abstract. This study was conducted in the postgraduate laboratory at the College of Education for Pure Sciences at the University of Kerbala in collaboration with Center for Manuscript Preservation and Restoration and Care of Researchers at the Imam Hussain Holy Shrine in Karbala, for the period from 20-11-2018 to 20-1-2019. In order to preserving manuscripts within the series of isolation and diagnosis of fungi accompanying ancient manuscripts. Controlling fungi that cause damage to the manuscripts using silver and zinc nanoparticles of different concentrations 0,5,10,15, 20 and 25 mg/L to inhibit the growth of *Alternaria atra* , *Aspergillus ustus*, *Cladosporium exasperatum*, *Chaetomium globosum Microdochium nivale* , *Penicillium tardochrysogenum -1*, *Penicillium tardochrysogenum -2*. The fungi were registered in pervious study in the International Genbank and had accession numbers : MK503427 و MK503428و MK504425و MK504424و MK503439و MK504426و MK504427 respectively [1]. The results were obtained as the diameter of colony on the PDA medium after 14 days of incubation as well as studying the shape of the fungal colonies on the culture media as well as prepare microscopic slides. The manuscripts damaged by fungi were treated with these two nanomaterials in the dough prepared for the purpose of restoring and preserving the manuscripts. Silver and zinc nanoparticles, showed a significant effect on the mean of colony diameter and the growth morphology that tends towards to decrease colony diameter with increase in the concentration of the nanoparticles . The *Alternaria atra* and *Penicillium tardochrysogenum-1*, gave the highest mean value of inhibition represented by the average fungal colony diameter of 10 mm when treated with Nano zinc at a concentration of 25 mg / L from the PDA culture medium , which were not significantly different from both *Microdochium nivale* and *Penicillium tardochrysogenum- 1*. The *Alternaria atra* and *Penicillium tardochrysogenum -2* showed the highest inhibition value represented by the average fungal colony diameter of 13.33 mm when treated with silver nanoparticles at a concentration of 25 mg / L on the PDA culture medium. The microscopic examinations of the fungal hypha showed that it was affected by the nanoparticles with an increase in the concentration, and this effect ranged between the complete destruction of the fungal hypha and its explosion, especially in the high concentrations, and the aggregation of the protoplasm of the fungal cell, especially in the medium concentrations of the nanoparticles , or a deviation in the course of the fungal flow and its attempt avoidance of the toxic substance by agglomeration in a specific place in the microscopic space under examination, especially in low concentrations, as well as the reduction of the conidia, its small size or its deformation depending on the type of fungus, the concentration of the nanomaterial and its type. The culture tests of samples taken by swabs from ancient manuscripts after being treated with the treated material in the presence of a high concentration of 25 mg /L of paste prepared for the purpose of restoration were for each of the nano silver and zinc nanoparticles separately by reducing the number of fungi compared to the manuscript prior to restoration.

INTRODUCTION

The fungi that cause damage to the manuscripts have met the interest of researchers, and many fungi have been isolated, the most frequent of them were *Aspergillus .flavus*, *A. fumigatus*, and *A. niger* had the highest rate of occurrence compared to other fungi, and had high enzymatic efficacy in analyzing the components of the manuscripts [2].

The ability of Nano silver to interact with sulfur and phosphorous prevents it from reaching the DNA necessary for the vital processes of the cell [3]. The study presented by Mehdi and his group [4] demonstrated that effect of silver nanoparticles on

First Year-First Folder-Number: 0
PSIJK 184-191

Pure Sciences International Journal of Kerbala

Journal Homepage:https://journals.uokerbala.edu.iq/index.php/psijk

the fungal hypha of the *Sclerotinia sclerotiorum*, showed an effect represented by deformations of the fungal hypha, the separation of the plasma membrane from the cell wall, the occurrence of a collection of protoplasm and the shrinkage of the fungal cell, as well as the deviation of the flow of nutrients of the fungus and the acceleration. In the formation of sclerotia primordia . Nano zinc showed a change in the form *Fusarium graminearum* hypha , where they appeared thinner and tended to clump together, in which the wall was shattered, more gaps and cytoplasmic fluidity appeared, and there is an inhibition of fungal growth compared to normal zinc oxide, although both of them liberated the same levels of soluble zinc, which confirms that the toxicity of zinc depends on the particle size, the smaller it is, the more effective and inhibitory, which is represented by nanostructured zinc oxide [5]. He and his group [6] suggested that zinc oxide nanocomposites can be used as a fungicide for plant pathogenic fungi. They studied its effect on the *Botrytis cinerea* and *Penicillium expansum* found that the concentration of 3 mol / cm was effective in inhibiting the fungi, and the particle size 15-70. nm, inhibiting the growth of *Botrytis cinerea* by affecting cellular functions and deforming the mycelium and *Penicillium expansum* due to lack of development and deformed carriers of conidia, causing the death of fungal hypha . In another study, the effect of zinc and silver nanoparticles on some skin fungi(*Trichophyton rubrum* and *Microsporum canis*) was shown that the treated with the combination between mineral zinc or nano zinc with fluconazole antifungal to reduce the pathogenic fungal growth and deformation of conidia formation [7] .

METERIAL AND METHODS

Fungi used in the study: Seven fungal isolates used in this study namely : *Alternaria atra* , *Aspergillus ustus*, *Cladosporium exasperatum*, *Chaetomium globosum Microdochium nivale* , *Penicillium tardochrysogenum -1*, *Penicillium tardochrysogenum -2*. The fungi registered in a pervious study in the International Genbank were obtained by Prof. Ban Taha Mohammad from the Postgraduate Laboratory at the College of Education for Pure Sciences at the University of Kerbala . All isolates were diagnosed and recorded in Global GenBank under serial numbers MK503427 و MK503428و MK504425و MK504424و MK503439و MK504426و MK504427 respectively in the previous study [1] . Isolates were activated and cultured on PDA medium, and their phenotypic and microbiological properties were studied before and after subsequent treatments .

Potato dextrose agar (PDA): Prepare the (PDA) medium by dissolving 39g of the medium powder in 1000ml of distilled water, according to the manufacturer's instructions.

Preparation of silver and nano-zinc concentrations: After carrying out a number of preliminary experiments in preparing concentrations of nanomaterials, the method of adding the solvent DMSO Dimethyl sulfoxide ($CH3)_2SO$ was chosen to the PDA culture as followings :-

1. Add 10 ml of dimethyl sulfoxide (DMSO) to 2.5 mg of nanoparticles and placed on the thermal heater and magnetic stirrer for 120 minutes. The stock solution was considered as nanoparticles. The control was prepared without adding the nanoparticles
2. Different concentrations of silver and zinc nanoparticles were prepared from stock solution: 5, 10, 15, 20 and 25 mg / L as well as a control treatment.
3. Before the medium solidified, it was poured into Petri dishes for the purpose of studying the effect of nanoparticles.

Effect of Zinc and Silver Nanoparticles on Isolated Fungi: - Potato Dextrose Agar medium was prepared, substitution of distilled water with the specific concentration of nanomaterials (silver and zinc nanoparticles separately) (MIC) in addition to a treatment without nanomaterials (PDA) as a control treatment poured into plastic petri dishes. The plates were inoculated with 5 mm disc of the pure colony growing at the age of 3 days at a temperature of 26 ± 2 ° C with three replications. After complete growth the plates were incubated with control. All cultures were examined and the following traits were recorded:-

1- The effect on the average diameter of fungal colonies (percentage of inhibition): -

Pure Sciences International Journal of Kerbala

Journal Homepage:https://journals.uokerbala.edu.iq/index.php/psijk

The inhibition percentage was calculated according to the formula provided in Abbott, (1925), That add in [1]as:

Inhibition ratio% = Fungal growth rate at control - Fungal growth rate per treatment x 100
Fungal growth rate in control

2- Study the phenotypic shape of the developing colonies with the presence of the nanomaterial compared with the control

Test of inhibitory concentration of nanomaterial with old material in manuscript restoration: After knowing the concentration in which the fungi were inactivated, a substance used in manuscript restoration was prepared from methyl hydroxyethyl cellulose MH6000, the trade name Tylose, was prepared at 1%. Parchment paper was coated with this prepared material. After 3 days, a swab was taken from the manuscript using sterile cotton swabs and then cultivated in the PDA recorded data were either depending on the appearance and growth of the fungus or not.

Statistical analysis Completely Randomized Design (C.R.D) was used. GenStat was used to analyze the data and compare the averages with the least significant difference (L.S.D.) at 0.05p level.

RESULTS AND DISCUSSION

Effect of zinc and silver nanoparticles on the average diameter of fungal colonies (percentage of inhibition):

Table 1, indicates that there are significant differences in the amount of fungi growth, as the fungus was most inhibited by nanostructured zinc was the fungus *Alternaria atra*, with the mean of 17.56, while the least effect of nano zinc was the fungus *Cladosporium exasperatum* with a rate of 45.84. The concentration 25 mg / L was more effective on fungi as it reached 18.90 and the concentration 5 mg / L was the least conc. able to inhibit fungi, reaching 34.05compared to the control treatment. As for the relationship between fungi and concentrations, the concentration 25 mg / L was more inhibitory for the fungus *Penicillium tardochrysogenum*-2 by 10.00, while the concentration of 5 mg / L was less effective on the *Aspergillus ustus* by 56.67. This was in agreement with previous studies of nanocomposites that play a role in disrupting transport systems and this was reflected by the cellular representation, respiration and interaction between organelles in addition to that zinc and nano silver ions are known to produce free radicals that destroy proteins, fats and nucleic acids [8, 9], and these results were consistent with findings by Mehdi and his group[10], when they used different nanoparticles including zinc oxide at different concentrations that affected the growth of the fungus *Sclerotinia sclerotiorum* (as the pathogen of the plant).

Table (1): The different concentrations of nanoparticles zinc in the average diameter of the fungi isolated from the manuscripts (percentage of inhibition(mm)) growing on PDF medium at a temperature of 26 ± 2 ° C for 5-7 days.

No.	Fungi	(Nano Zinc Concentration (mg / L)*						
		Control	5	10	15	20	25	Average of Fungi diameter (mm)
1	*Alternaria atra*	36.67	23.67	11.00	11.67	12.33	10.00	17.56
2	*Aspergillus ustus*	55.00	56.67	31.67	53.33	19.67	23.33	39.94
3	*Chaetomium globosum*	43.33	41.67	38.33	32.33	36.67	20.00	35.39
4	*Cladosporium exasperatum*	55.00	45.00	41.67	50.00	38.33	45.00	45.83

Pure Sciences International Journal of Kerbala
Journal Homepage:https://journals.uokerbala.edu.iq/index.php/psijk

5	*Microdochium nivale*	30.00	21.67	11.67	19.33	15.67	11.67	18.33
6	*Penicilliu tardochrysogenum1*	25.00	26.33	15.00	21.67	12.00	10.00	18.33
7	*Penicillium tardochrysogenum2*	27.00	23.33	19.67	19.00	15.00	12.33	19.39
	Average of the nano zinc concentrations	38.86	34.05	24.14	29.62	21.38	18.90	

L.S.D $_{0.05}$ Fungi = 2.90 Concentrations= 3.16 Interaction =7.75
*= Each number in the table represents the average of three replicates

The percentage of inhibition of fungi isolated from manuscripts at 26 ± 2 ° C and on PDA medium at 5, 10, 15, 20, 25 mg / ml Nano-zinc particles

		(Nano Zinc Concentration (mg / L)				
No.	Fungi	5	10	15	20	25
1	*Alternaria atra*	40%	68.5%	66 %	66%	97%
2	*Aspergillus ustus*	5%	36%	3.6%	60%	54%
3	*globosum Chaetomium*	24%	50%	8.5%	10%	42%
4	*Cladosporium exasperatum*	18%	24%	9.0%	31%	18%
5	*Microdochium nivale*	27%	60%	36.6%	47%	60%
6	*Penicilliu 1tardochrysogenum*	17%	25%	12%	60%	67%
7	*Penicillium 2tardochrysogenum*	8%	23%	26.9%	50%	60%

Table (2) indicates that *Alternaria atra* was more affected by silver nanoparticles, while *Aspergillus ustus* was less affected with significant differences. Concerning silver nanoparticles, the concentration of 25 mg / L was more effective in inhibiting the growth of isolated fungi, while the concentration of 5 mg / L was less effective compared to the control treatment. It was more effective while the concentration of 15.5 mg / L with *Aspergillus ustus* was less effective. The reason for the decrease in the diameter of the colony as a result of the increase in the concentration of the nanoparticles was due to the increase in the saturation and absorption of the nanoparticles by the fungal hypha [11]. It is also to its react with sulfur and thus inhibit protein expression processes by ribosomes units and enzymes necessary for energy production [12and 13]. The nanoparticles acted as a poison to the cells on the membrane permeability leading to cell death [14].

Table (2): Different concentrations of silver nanoparticles in fungi isolated from manuscripts (mm) (percentage of inhibition) and growing on PDF medium at a temperature of 2 ± 26 ° C for 5-7 days.

No.	Fungi	(Nano silver Concentration (mg / L)*						
		Control	5	10	15	20	25	Average of Fungi diameter (mm)

Pure Sciences International Journal of Kerbala

Journal Homepage:https://journals.uokerbala.edu.iq/index.php/psijk

1	*Alternaria atra*	35.00	20.00	11.67	13.33	13.33	13.33	17.78
2	*Aspergillus ustus*	48.33	43.33	35.00	45.33	21.67	33.33	37.83
3	*Chaetomium globosum*	40.00	31.67	33.33	18.33	26.67	25.67	29.28
4	*Cladosporium exasperatum*	46.67	36.67	30.00	38.33	28.33	21.67	33.61
5	*Microdochium nivale*	33.33	25.00	22.33	21.00	21.67	20.00	23.89
6	*Penicilliu tardochrysogenum1*	31.67	23.33	23.33	28.33	25.00	18.33	25.00
7	*Penicillium tardochrysogenum2*	28.33	18.33	18.33	18.33	21.67	13.33	19.72
Average of the nano silver concentrations		38.86	37.62	28.33	24.86	26.14	22.62	20.18

L.S.D. $_{0.05}$ Fungi =3.30 Concentrations= 3.56 Interaction =8.73

*= Each number in the table represents the average of three replicates

The percentage of inhibition of fungi isolated from manuscripts at 26 ± 2 ° C and on PDA medium at 5, 10, 15, 20, 25 mg / ml Nano-silver particles

(Nano Zinc Concentration (mg / L)

No.	Fungi	5	10	15	20	25
1	*Alternaria atra*	25%	66%	62%	56%	49%
2	*Aspergillus ustus*	4.4%	42%	25%	43%	33%
3	*Chaetomium globosum*	29%	26%	49%	40%	35%
4	*Cladosporium exasperatum*	40%	23%	37%	30%	45%
5	*Microdochium nivale*	38%	27%	30%	45%	33%
6	*Penicilliu 1tardochrysogenum*	8%	25%	20%	43%	49%
7	*Penicillium 2tardochrysogenum*	10%	55%	48%	27%	35%

Effect on the phenotype of colonies developing by the presence of the nanomaterial

It is evident from figure (1), that the fungi varied in the type of inhibition response due to the action of nano-zinc, and this response was represented by a deformation in growth compared to the control, as the fungal culture tended away from the toxic effect of nanoparticles and preferred to grow vertically for some fungal species according to the concentration. Thus, some fungal cultures treated with nano-zinc tended to rise towards the plate cover. The other change was the production of some dyes that changed the natural color of the culture medium, as happened to the *Penicillium tardochrysogenum2*, for example it is added a black substance, likely melanin, and this

Pure Sciences International Journal of Kerbala

Journal Homepage:https://journals.uokerbala.edu.iq/index.php/psijk

happened with other fungi, and this result is close to what was described by Mehdi and his group [10], although the fungi were different. There was also a change in the color of the culture medium in some fungi to pink, dark pink and orange, as it is shown in the same figure.

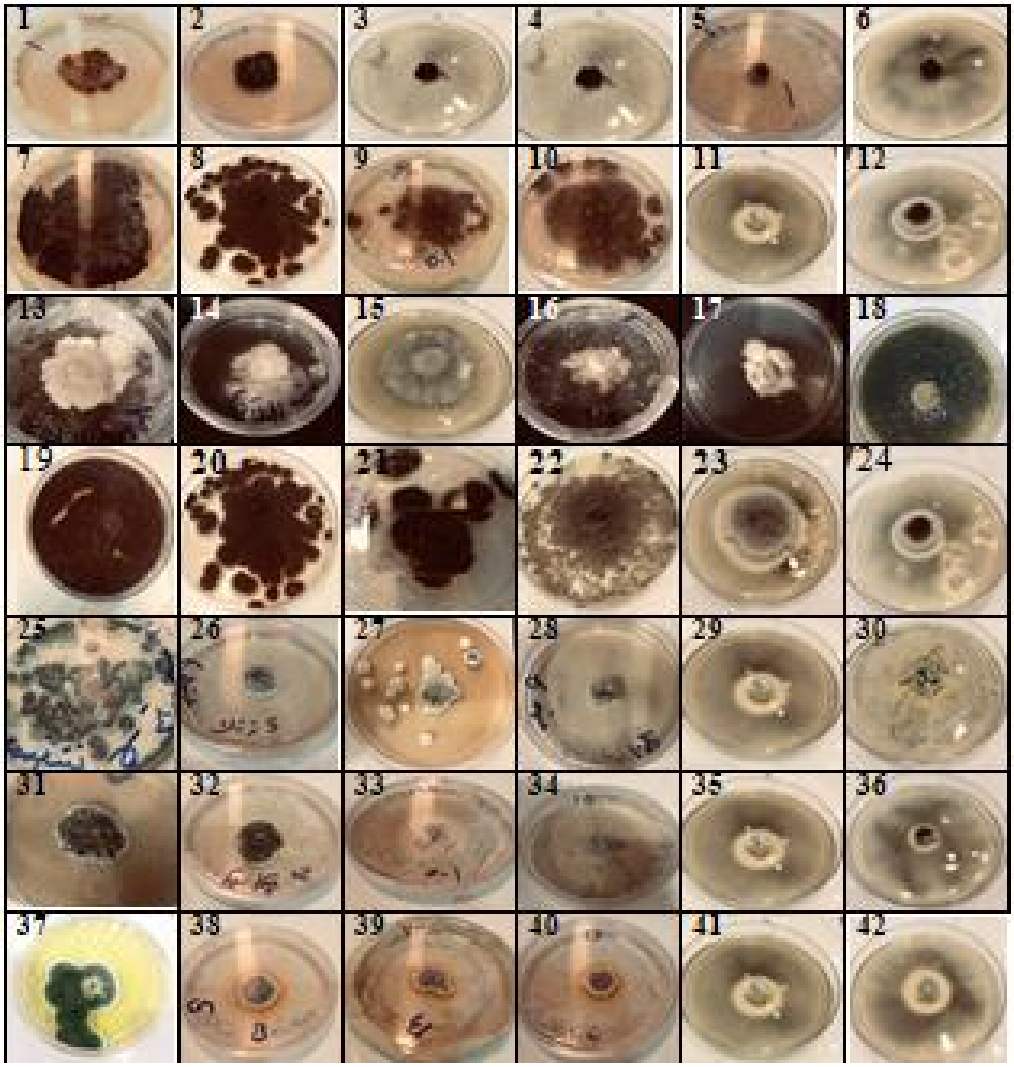

Figure 1.: Different concentrations of zinc nanoparticles in growth for fungal colonies on PDA medium at temperature 26 ± 2 0 m, for a period of 5-7 days.

Pure Sciences International Journal of Kerbala

Journal Homepage:https://journals.uokerbala.edu.iq/index.php/psijk

1=Control Alternaria atra
2=Add 5 mg nanozinc to Alternaria atra
3 =Add 10 mg nanozinc to Alternaria atra
4=Add 15 mg nanozinc to Alternaria atra
5=Add 20 mg nanozinc to Alternaria atra
6=Add 25 mg nanozinc to Alternaria atra
7= Control Aspergillus ustus
8=Add 5 mg nanozinc to Aspergillus ustus
9 =Add 10 mg nanozinc to Aspergillus ustus
10=Add 15 mg nanozinc to Aspergillus ustus
11=Add 20 mg nanozinc to Aspergillus ustus
12=Add 25 mg nanozinc to Aspergillus ustus
13=Control Chaetomium globosum
14=Add 5 mg nanozinc to Chaetomium globosum
15=Add 10 mg nanozinc to Chaetomium globosum
16=Add 15 mg nanozinc to Chaetomium globosum
17=Add 20 mg nanozinc to Chaetomium globosum
18=Add 25 mg nanozinc to Chaetomium globosum
19=Control Cladosporium exasperatum
20=Add 5 mg nanozinc to Cladosporium exasperatum
21=Add 10 mg nanozinc to Cladosporium exasperatum
22=Add 15 mg nanozinc to Cladosporium exasperatum
23=Add 20 mg nanozinc to Cladosporium exasperatum
24=Add 25 mg nanozinc to Cladosporium exasperatum
25=Control Microdochium nivale
26=Add 5 mg nanozinc to Microdochium nivale
27=Add 10 mg nanozinc to Microdochium nivale
28=Add 15 mg nanozinc to Microdochium nivale
29=Add 20 mg nanozinc to Microdochium nivale
30=Add 25 mg nanozinc to Microdochium nivale
31=Control Penicillium tardochrysogenum1
32=Add 5 mg nanozinc to Penicillium tardochrysogenum1
33=Add 10 mg nanozinc to Penicillium tardochrysogenum1
34=Add 15 mg nanozinc to Penicillium tardochrysogenum1
35=Add 20 mg nanozinc to Penicillium tardochrysogenum1
36=Add 25 mg nanozinc to Penicillium tardochrysogenum1
37=Control Penicillium tardochrysogenum 2
38=Add 5 mg nanozinc to Penicillium tardochrysogenum 2
39=Add 10 mg nanozinc to Penicillium tardochrysogenum2
40=Add 15 mg nanozinc to Penicillium tardochrysogenum 2
41=Add 20 mg nanozinc to Penicillium tardochrysogenum2
42=Add 25 mg nanozinc to Penicillium tardochrysogenum2

The effects of silver nanoparticles on the phenotype of the fungal cultures were directed in the same direction and the cases were described in the effect of zinc nanoparticles. Figure (2) represents a model for some of these effects. Figure2- A, it is noticed that the addition of 25 mg of silver nanoparticles to *Alternaria atra* reduces the size of growth and the direction of growth of the fungus upward with the coloration of the culture medium in a dark brown color. Either in shape B, adding 15 mg of silver nanoparticles to *Aspergillus ustus* notes a decrease in the growth of the fungus compared to the control, with no growth abnormalities or stains added to the culture medium by the fungus In C, the addition of 15 mg silver nanoparticles to the *Chaetomium globosum* notes a decrease in the growth of the fungus compared to the control, with the presence of deformations in the growth and the upward direction and the non-pigmentation of the culture medium by the fungus compared to control, with the slow formation of spores that stain the surface of the culture in a dark brown to black color, and the culture medium was not stained by the fungi. E also shows the addition of 20 mg of silver nanoparticles to the *Microdochium nivale*. There was a decrease in the growth of the fungus compared to the control and the height of the culture due to the growth of the fungus upward, with the slow formation of spores that colored the surface of the culture in dark turquoise to dark brown, and the culture medium was not stained by the fungus. F when adding 20 mg silver nanoparticles to *Penicillium tardochrysogenum -1*. There was a decrease in the growth of the fungus compared to the control and the height of the culture due to the growth of the fungus towards the top irregularly, and the yellowing of the culture medium by the fungus. Finally, the addition of 15 mg Nano silver to the *Penicillium tardochrysogenum*- 2 reduced the growth of the fungus compared to the control, the growth was not deformed, and the culture medium was not stained by the fungus.

First Year-First Folder-Number: 0
PSIJK 184-191

Pure Sciences International Journal of Kerbala

Journal Homepage:https://journals.uokerbala.edu.iq/index.php/psijk

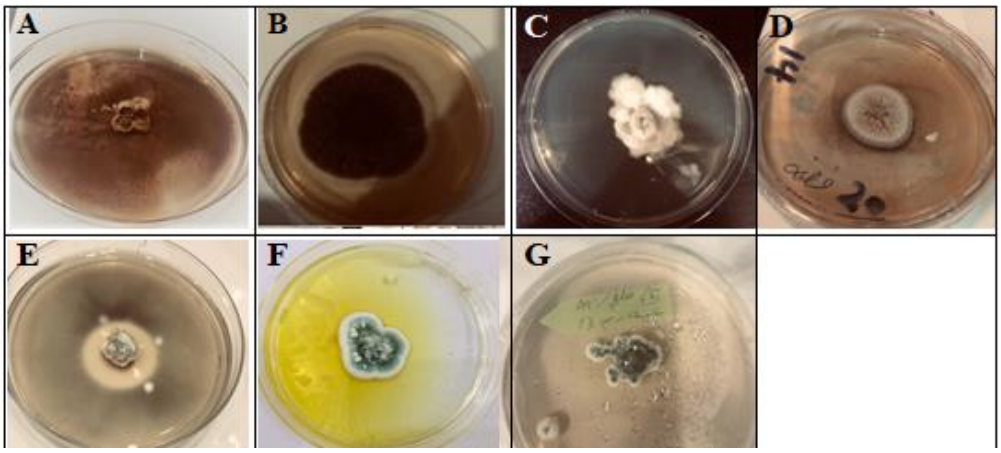

Figure 2: Different concentrations of silver nanoparticles in growth for fungal colonies on PDA medium at temperature of 26 ± 2 ° C for a period of 5-7 days.

A = Addition of 25 mg silver nanoparticles to Alternaria atra

B = Addition of 15 mg nanoparticles to Aspergillus ustus

C = Addition of 15 mg nanoparticles to Chaetomium globosum

D = Addition of 20 mg nanoparticles to Cladosporium exasperatum

E = Addition of 20 mg nanoparticles to Microdochium nivale

F = Addition of 20 mg silver nanoparticles to Penicillium tardochrysogenum -1

G = Addition of 15 mg nanoparticles to Penicillium tardochrysogenum -2

Influence on the microscopic properties of fungi

The results in figures (3and 4) showed that, silver and zinc nanoparticles had an effect on the growth and integrity of fungal cells, and the occurrence of this depended on the concentration of the nanoparticles and the period of exposure of the fungus to the materials until it reaches the states of its destruction and the appearance of deformations in the fungal hypha and their effect on the cell walls [15]. The microscopic examinations of the fungal hypha showed that it was affected by the nanoparticles with an increase in the concentration of the nanoparticles, and this effect ranged between the complete destruction of the fungal hypha and its explosion, especially in the high concentrations of the nanoparticles . The accumulation of the protoplasm of the fungal cell, especially in the high concentrations of the nanoparticles , or a deviation in the flow of the fungus and its attempt to move away from the toxic substance by clumping in a specific place in the microscopic space under examination, especially at low concentrations, as well as the reduction of conidia. Its small size or deformation was depending on the type of fungus, the concentration of the nanomaterial and its type. This result was similar to what Mehdi and his group mentioned [4 and 10], cell wall separation from the plasma membrane of *Alternaria atra* treated with 10 mg / L silver nanoparticles may occur or deformation and atrophy of conidia occurs with silver nanoparticles at a concentration of 10 mg / L. The conidial head and the hypha of the *Aspergillus ustus*, with a concentration of Nano silver 10 mg / L, also showed deformation while , the conidiophore was deformed, and the fungal hypha of *Chaetomium globosum* gets cut with losing its shape at a concentration of 10 mg / L . Note the emergence of terminal chlamydospore and the occurrence of swelling of mycelium without presence of conidia at a concentration of 10 mg / L, in addition to the aggregation of protoplasmic material in one of the fungal hypha at a concentration of 10 mg / L accompanied by discharging of the other hypha from the protoplasm as well as a deformed conidiophore with loss of the fungal hypha and its damage at a

First Year-First Folder-Number: 0
PSIJK 184-191

Pure Sciences International Journal of Kerbala

Journal Homepage:https://journals.uokerbala.edu.iq/index.php/psijk

concentration of 10 mg / L. The occurrence of a deformed conidial head with a concentration of 10 mg / L was deformed at concentration 10 mg / L . In N with a denatured conidia carrier with fungal hypha loss and damage at concentration of 10 mg / L for the latter fungus (Fig. 4).

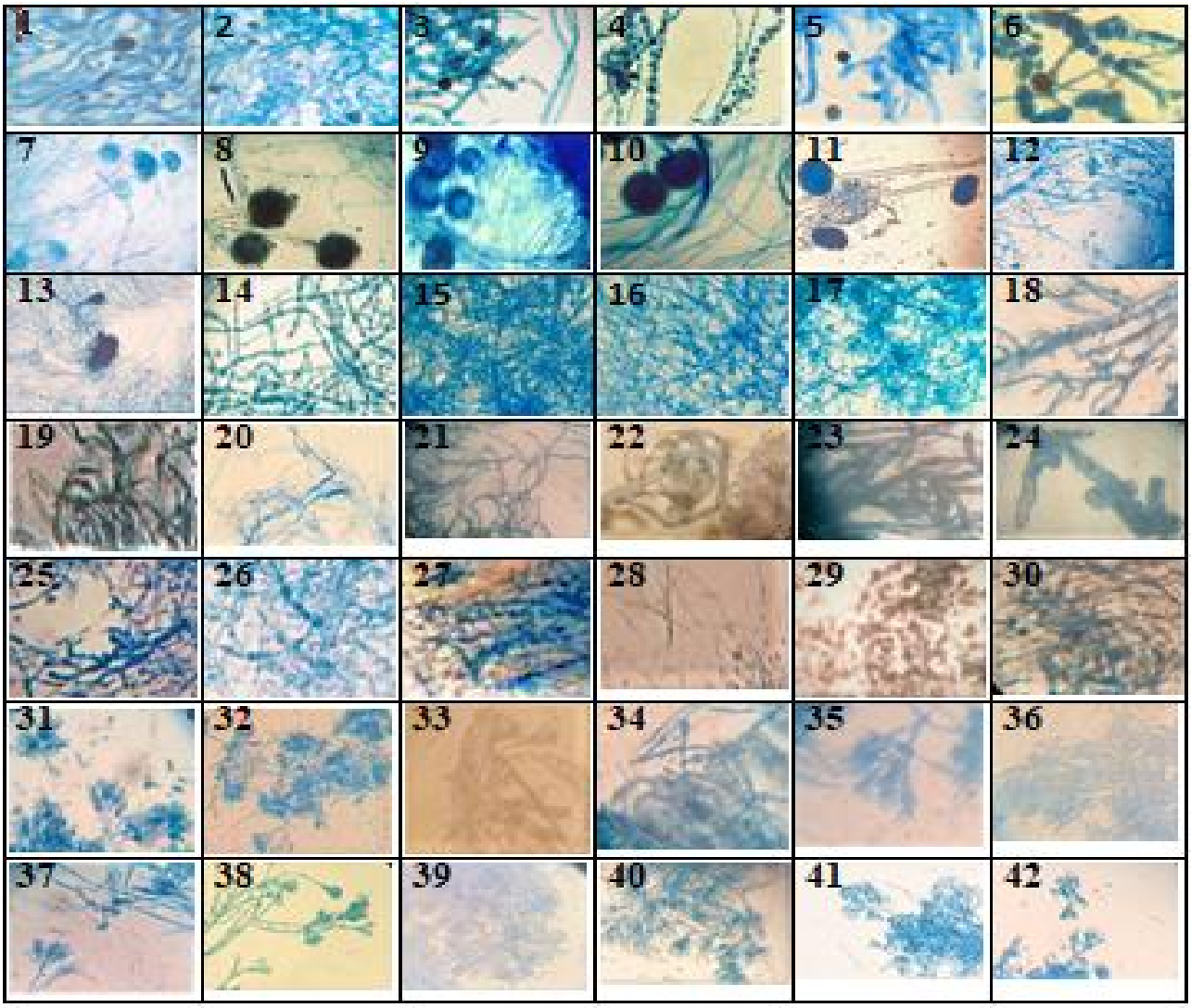

Figure 3: The effect of different concentrations of zinc nanoparticles in the microscopic shape of fungal cultures on PDA medium at a temperature of 25 ± 2 0 C. for a period of 5-7 days. With 40X magnification

Pure Sciences International Journal of Kerbala

Journal Homepage:https://journals.uokerbala.edu.iq/index.php/psijk

1=Control Alternaria atra
2=Add 5 mg nanozinc to Alternaria atra
3 =Add 10 mg nanozinc to Alternaria atra
4=Add 15 mg nanozinc to Alternaria atra
5=Add 20 mg nanozinc to Alternaria atra
6=Add 25 mg nanozinc to Alternaria atra
7= Control Aspergillus ustus
8=Add 5 mg nanozinc to Aspergillus ustus
9 =Add 10 mg nanozinc to Aspergillus ustus
10=Add 15 mg nanozinc to Aspergillus ustus
11=Add 20 mg nanozinc to Aspergillus ustus
12=Add 25 mg nanozinc to Aspergillus ustus
13=Control Chaetomium globosum
14=Add 5 mg nanozinc to Chaetomium globosum
15=Add 10 mg nanozinc to Chaetomium globosum
16=Add 15 mg nanozinc to Chaetomium globosum
17=Add 20 mg nanozinc to Chaetomium globosum
18=Add 25 mg nanozinc to Chaetomium globosum
19=Control Cladosporium exasperatum
20=Add 5 mg nanozinc to Cladosporium exasperatum
21=Add 10 mg nanozinc to Cladosporium exasperatum
22=Add 15 mg nanozinc to Cladosporium exasperatum
23=Add 20 mg nanozinc to Cladosporium exasperatum
24=Add 25 mg nanozinc to Cladosporium exasperatum
25=Control Microdochium nivale
26=Add 5 mg nanozinc to Microdochium nivale
27=Add 10 mg nanozinc to Microdochium nivale
28=Add 15 mg nanozinc to Microdochium nivale
29=Add 20 mg nanozinc to Microdochium nivale
30=Add 25 mg nanozinc to Microdochium nivale
31=Control Penicillium tardochrysogenum1
32=Add 5 mg nanozinc to Penicillium tardochrysogenum1
33=Add 10 mg nanozinc to Penicillium tardochrysogenum1
34=Add 15 mg nanozinc to Penicillium tardochrysogenum1
35=Add 20 mg nanozinc to Penicillium tardochrysogenum1
36=Add 25 mg nanozinc to Penicillium tardochrysogenum1
37=Control Penicillium tardochrysogenum 2
38=Add 5 mg nanozinc to Penicillium tardochrysogenum 2
39=Add 10 mg nanozinc to Penicillium tardochrysogenum2
40=Add 15 mg nanozinc to Penicillium tardochrysogenum 2
41=Add 20 mg nanozinc to Penicillium tardochrysogenum2
42=Add 25 mg nanozinc to Penicillium tardochrysogenum2

Pure Sciences International Journal of Kerbala

Journal Homepage:https://journals.uokerbala.edu.iq/index.php/psijk

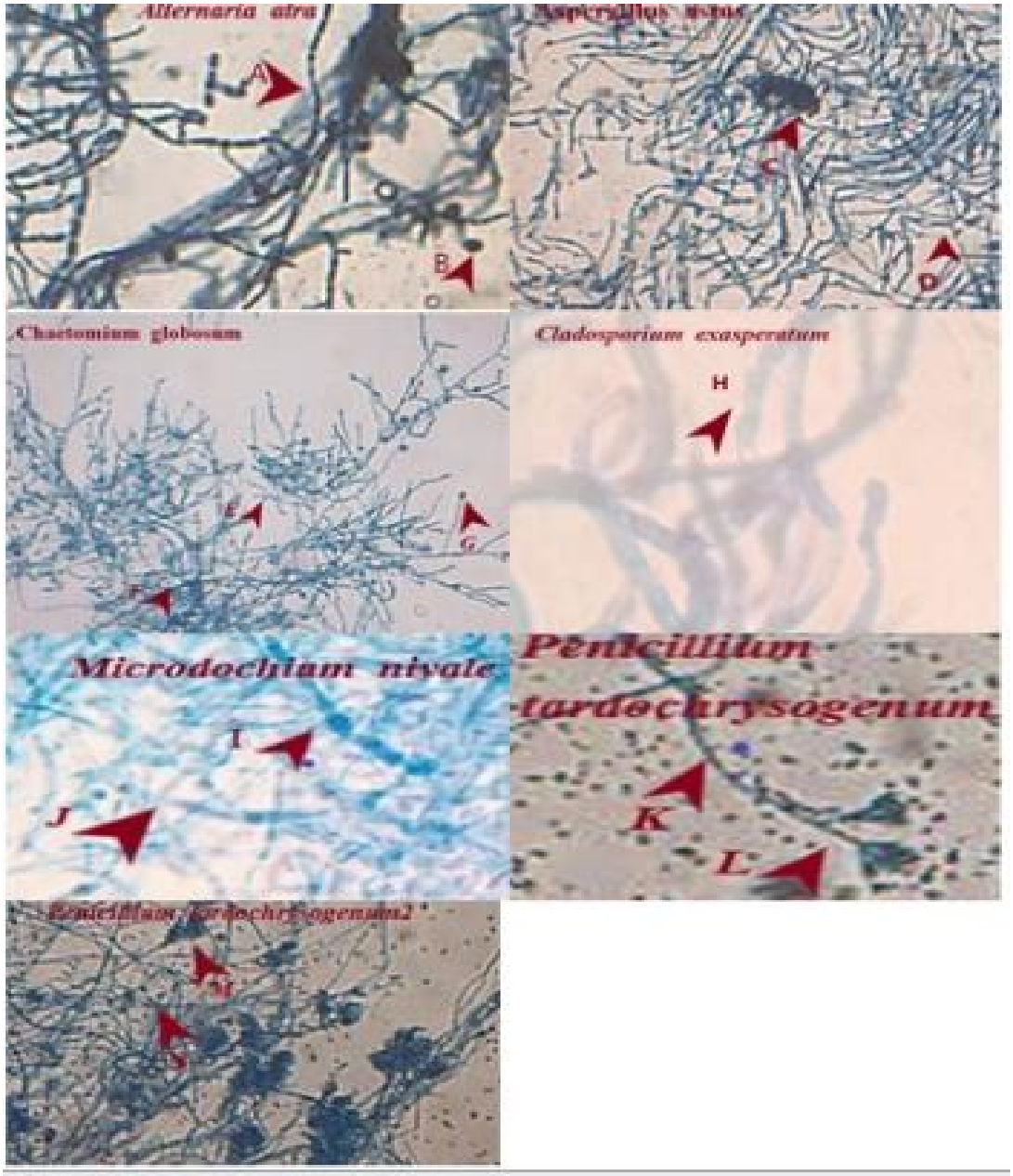

Figure4: The effect of different concentrations of nanoparticles in the microscopic shape of the fungal cultures on the PDA medium at a temperature of 25 ± 2 0 C. for a period of 5-7 days. With 40X magnification

A=separation of the cell wall from the plasma membrane of *Alternaria atra* with silver nanoparticles of 10 mg/ L.

B = deformation and atrophy of the conidia with silver nanoparticles of 10 mg / L.

C = the conidial head of the *Aspergillus ustus* at a concentration of 10 mg / L silver nanoparticles

D = cut the fungal hypha, with the deformation of the conidia carriers

E = fungal hypha of *Chaetomium globosum* with losing its shape at a concentration of 10 mg / L

F = The fungus could not produce perithecium fruiting bodies

Pure Sciences International Journal of Kerbala

Journal Homepage:https://journals.uokerbala.edu.iq/index.php/psijk

G = terminal chlamydospore appearance.

H = mycelial hypha swelling and no conidia present at a concentration of 10 mg / ml

I = a grouping of protoplasmic material in one of the fungal hypha at a concentration of 10 mg / L

J = discharging the other Hypha from protoplasm at a concentration of 10 mg / L

K = a deformed conidial carrier with the loss of the fungal yarn and its damage at a concentration of 10 mg / L

L = a deformed conidial head at a concentration of 10 mg / ml

M = Conidial head deformed at concentration 10 mg / L

N = denatured conidia carrier with fungal hypha loss and degradation at concentration of 10 mg / L.

Test of inhibitory concentration of nanomaterial with old material in the manuscript restoration

The combination of individual nanoparticles to the restoration material (1% methyl hydroxyethyl cellulose MH6000) had a good efficacy in inhibiting the growth of fungi on manuscript, as the number of fungi was reduced compared to the manuscript before treatment . The emergence of fungi of different genera, in very small numbers and at very cheap prices, which indicates the effectiveness of nanoparticles in controlling their neighboring areas[11].

CONCLUSION

Zinc Nanoparticles had proved its ability to inhibit the growth of fungi more than silver nanoparticles, especially at a concentration of 25 mg / L.

The presence of Zinc nanoparticles or silver nanoparticles in the manuscript conservation paste contributes to Inhibiting the fungi that cause spoilage and speeding up manuscript obsolescence.

ACKNOWLEDGMENTS

We would like to express our thanks to Center for Manuscript Preservation and Restoration and Care of Researchers at the Imam Hussain Holy Shrine in Karbala for boilable assistance during period of experimental work.

REFERENCES:-

[1] A. A. Jasim, B. T. Mohammed, and A. A. Lahuf, “Molecular and enzymatic properties of fungi isolated from historical manuscripts preserved at the Al-Hussein Holy Shrine,” *Biochem. Cell. Arch.*, vol. 19, no. 2, 2019.

[2] B. T. Mohammed, M. H. Dakhil, and T. M. Almutairy, “Manuscripts preserved at the Al-Hussein Holy shrine: Isolation and diagnosis of fungi causing potential damage,” *Indian J. Ecol.*, vol. 45, no. 1, 2018.

[3] J. R. Morones *et al.*, “The bactericidal effect of silver nanoparticles,” *Nanotechnology*, vol. 16, no. 10, pp. 2346–2353, 2005.

[4] H. A. Mehdi, B. T. Mohammed, and A. M. Bashy, “EFFECT OF NANO-SILVERS, NANO-ZINC OXIDE AND BENOMYL PESTICIDE ON SOME PHYSIOLOGICAL PROPERTIES OF SCLEROTINIA SCLEROTIORUM,” *Biochem. Cell. Arch.*, vol. 18, no. 2, pp. 2196–2018, 2018.

[5] C. O. Dimkpa, J. E. McLean, D. W. Britt, and A. J. Anderson, “Antifungal activity of ZnO nanoparticles and their interactive effect with a biocontrol bacterium on growth antagonism of the plant pathogen Fusarium graminearum,” *BioMetals*, vol. 26, no. 6, pp. 913–924, 2013.

[6] L. He, Y. Liu, A. Mustapha, and M. Lin, “Antifungal activity of zinc oxide nanoparticles against Botrytis cinerea and Penicillium expansum,” *Microbiol. Res.*, vol. 166, no. 3, pp. 207–215, 2011.

[7] K. Yassin,Shrook and B. T. Mohammed, “Evaluation of mineral, nano-zinc, and fluconazole interaction on some growth characteristics of Trichophyton rubrum and Microsporum canis,” *Biochem. Cell. Arch.*

[8] R. Brayner, R. Ferrari-Iliou, N. Brivois, S. Djediat, M. F. Benedetti, and F. Fiévet, “Toxicological impact studies based on *Escherichia coli* bacteria in ultrafine ZnO nanoparticles colloidal medium,” *Nano Lett.*, vol. 6, no. 4, pp. 866–870, 2006.

[9] E. T. Hwang *et al.*, “Analysis of the toxic mode of action of silver nanoparticles using

Pure Sciences International Journal of Kerbala

Journal Homepage:https://journals.uokerbala.edu.iq/index.php/psijk

stress-specific bioluminescent bacteria," *Small*, vol. 4, no. 6, pp. 746–750, 2008.

[10] H. A. Mehdi, B. T. Mohammed, and A. M. Bashi, "Effect of Silver and Zinc oxide Nanocompound Mixture on Growth and Some Physiological Properties of Sclerotinia sclerotiorum," *Indian J. Ecol.*, vol. 45, no. 2, pp. 358–366, 2018.

[11] S. W. Kim, J. H. Jung, K. Lamsal, Y. S. Kim, J. S. Min, and Y. S. Lee, "Antifungal effects of silver nanoparticles (AgNPs) against various plant pathogenic fungi," *Mycobiology*, vol. 40, no. 1, pp. 53–58, 2012.

[12] J. O. K. Q.L. Feng, J.Wu, G. Q. Chen, F.Z. Cui, T.N. Kim, "A mechanistic study of the antibacterial effect of silver ions on Escherichia coli and Staphylococcus aureus," *Jhon Wiley sons. INC.*, vol. 52, no. 4, pp. 662–668, 2000.

[13] S. Pal, Y. K. Tak, and J. M. Song, "Does the antibacterial activity of silver nanoparticles depend on the shape of the nanoparticle? A study of the gram-negative bacterium Escherichia coli," *Appl. Environ. Microbiol.*, vol. 73, no. 6, pp. 1712–1720, 2007.

[14] X. Lin *et al.*, "Toxicity of TiO 2 nanoparticles to Escherichia coli: effects of particle size, crystal phase and water chemistry," *PLoS One*, vol. 9, no. 10, p. e110247, 2014.

[15] K. Lamsal, S. W. Kim, J. H. Jung, Y. S. Kim, K. S. Kim, and Y. S. Lee, "Application of silver nanoparticles for the control of Colletotrichum species in vitro and pepper anthracnose disease in field," *Mycobiology*, vol. 39, no. 3, pp. 194–199, 2011.

Pure Sciences International Journal of Kerbala

Journal Homepage:https://journals.uokerbala.edu.iq/index.php/psijk

Manuscripts Preserved at the Al-Hussein Holy Shrine: Isolation and Diagnosis of Fungi Causing Potential Damage

Ban T. Mohammed *[1], Mohammed H. Dakhil [2], Thikra M. ALmutairy [3]

[1,2]*Department of Biology, University of Kerbala, Iraq.*
[3]*Imam Hussein Medical City of Kerbala, Iraq*
[*]*E-mail: Bantmh@gmail.com*

Abstract: A total of 110 samples were collected, 60 samples of manuscripts preserved in the Al-Hussein Holy shrine, and 50 samples of the internal and external air of the fortified (the place where the manuscripts are kept). Fungal species were isolated and identified. The results showed dominance *Aspergillus* spp. on the other genus and ranked first in terms of occurrence, frequency and distribution density coefficient followed by *Penicillium* spp. in the second rank in terms of occurrence, frequency and distribution intensity, while the other genus *Mucor, Rhizopus*, Yeast and white mycelium recorded the lowest rank. The degradation of cellulose, protein, starch and fat because the activity of fungi on the manuscripts were detected for the purpose of identifying the effects of fungi and their damage to manuscripts. The fungi were isolated from the internal and external air of the fortified and showed the results of the fungus *Aspergillus* spp. with different types on the rest of the fungal species and dominated in terms of occurrence and frequency and density of distribution followed by Yeast second rank, while. *Penicillium* spp. was the third and the remaining fungi *Mucor*, white mycelium and *Rhizopus* recorded the lowest rank. The existence of some fungal species on the manuscripts may be the main cause of damage, as well as there were similarity and relationship between fungi isolated from the manuscripts and fungi isolated from the internal and external air of the fortified, where the manuscripts kept in, which confirms the contamination and the need to address for the purpose of conservation and preservation of the legacy of civilization.

Keywords: Opportunistic fungi, Manuscripts fungi, air fungi, Fungal enzymes.

Manuscripts and books are of raw materials of organic origin (plant or animal) such as paper, skin, papyrus, cloth and sometimes wood. These materials have a characteristic hydroscopic nature that the internal water content changes with the changing ambient humidity. As the relative humidity increases in the surrounding environment, organic matter absorbs water, thus increasing the water content of the materials, making the manuscripts and books susceptible to decomposing fungi and also facilitating the adhesion of dust and other suspensions into the air. The dust and pendants found in the air have the role in the injury of manuscripts and the benefits of fungus because it carries the fungi that grow very quickly, especially if the availability of moisture and heat where the fungus plays the role of sovereignty in the destruction of manuscripts compared to bacteria and actinomycetes, because of its ability to withstand the wide range of temperatures and lack of moisture. It has been documented that fungi can grow down to 0 ° C (cold fungus) and can tolerate more than 60 ° C (thermophilic fungus), while the fungi grows well at relative humidity of more than 60%, saprophytic fungi are characterized by introduction of fungi in many buildings used by humans (Youssef, 2012).

Because of lack of studies on the fungus of manuscripts, this study is targeted to isolate and diagnose the fungus associated with the manuscripts and causes the damage, and study the effectiveness of enzymatic analysis of the components of the manuscripts, as well as study the relationship of fungi associated with the internal and external air surrounding them in places saved.

MATERIAL AND METHODS

Agricultural media were used

Sabouraud's dextrose agar medium: This medium, as reported in Kwon-Chung and Bennett (1992), melted 65 g of Sabouraud's dextrose agar powder with liter of distilled water and pH was adjusted at 6.5.

Czapex agar (CA): It was given by Ramirz (1982), which included the following composition: 1 g K_2HPO_4, 0.5 g KCl, 2 g $NaNO_3$, 0.5 g $MgSO_4.7H_2O$, 0.05 g $FeSO_4.7H2O$, 20 g Sucrose, 18 g Agar then added to a liter of distilled water.

Potato dextrose agar (PDA): Prepare the PDA by Collee and his group (1996) by pouring 39 g of medium powder per liter of distilled water.

Cellulose agar medium: Baath and Sodarstrow (1980) method which included the following materials: 2 g $NaNO_3$, 1 g $NH_4(2SO_4)$, 1 g KH_2PO_4, 0.5 g $MgSO_4.7H_2O$, 0.5 g KCl , 0.05 $CaCl_2$, 0.01 g $FeSO_4.7H_2O$, 0.01 g $CaSO_4.5H_2O$, 0.005 g $MnSO_4.4H2O$, 0.001 g $ZnSO_4$ $7.H_2O$, 15 g Agar. Dissolved in a liter of distilled water and added to the 5 g of pure cellulosic acid 85% (Tansey 1971). The medium was used to detect the susceptibility of fungi to the production of cellulose enzyme.

Milk skimmed medium: Five grams of skimmed -milk was poured in the 50 ml distilled water. Dissolved 10 g of sugar in 450 ml distilled water in another flask. Equilibrate the pH to 7. Sterilize the two solutions separately and then cool to 45 ° C. Then mixed together, (Aaronson 1973). This medium was used to detect the susceptibility of fungi to protease production.

Starch agar medium: A fifteen gram of starch, 1 g K_2HPO_4, 0.5 g of $MgSO_4.7H_2O$ and 15 g of sugar in a litter of distilled water (Sarhan 2012) modified (delete the yeast extract).

Tween 80 agar medium: This medium was prepared from the following ingredients, 10 g peptone, 5 g NaCl and 0.1 g $CaCL_2$, per litre of distilled water , 5 ml of Tween 80 was add and the pH was adjusted at 6.8. This medium was used to investigate the susceptibility of fungi and yeasts to production of lipase enzymes (Slifkin 2000).

Pure Sciences International Journal of Kerbala

Journal Homepage:https://journals.uokerbala.edu.iq/index.php/psijk

To all of the above mentioned Media, 250 mg / L of Chloramphenicol antibiotic was added before sterilization, and then sterilized by autoclave at 121 ° C under 1.5 pressure for 20 min. After cooling, the sterile medium was poured into plastic Petri dishes.

Collection of samples: The study included the collection of 110 samples; 60 samples of manuscripts and 50 samples of the internal and external air of the fortified (25 samples each) . The samples were taken from the manuscripts by smear and planted on special media, and then transferred to the laboratory. Samples were also taken from the inner and outer air of the fortified, using an open dish technique to isolate air fungus.

Manuscripts at the center for the maintenance and restoration of manuscripts of the Al-Hussein holy shrine: Some of the fungi were isolated from ancient manuscripts and preserved in the center for the maintenance and restoration of manuscripts, taking isolates by sterile cotton swabs from three locations of the manuscript, represented by the beginning, middle and end of the manuscript. The inoculations were planted in Sabouraud's Dextrose Agar medium (SDA). Direct isolation was done in the Streaking method. They were placed in the incubator for growth at 28 ° C and for 5-7 days. The dishes were examined first for the purpose of counting the growing colonies on the growing media. The fungal species were purified onto the SDA and incubated at 28 ° C for 5-7 days to obtain pure colonies. The fungus was also re-grown on Czapex Dox Agar and Potato Dextrose Agar medium. The fungi were identified according to their morphological and colony colors. The following sources were used in diagnosis (Ellis 1971; Barnett and Bary 1972; Pitt Moubasher 1993 and Hocking 1997).

The total number of isolates and fungal species isolated from each manuscript and percentage of occurrence calculated from the following equation:

$$\text{Occurrence\%} = \frac{\text{Number of specimens that appeared genus or species}}{\text{The total number of samples during the study}} \times 100$$

The percentage of frequency calculated from the following equation:

$$\text{Frequency\%} = \frac{\text{Number of single isolates}}{\text{Total number of isolates}} \times 100$$

Distribution Intensity Index (DII) according to the distribution density coefficient of all fungi isolated from the following equation:

$$\text{DII} = \%\ \text{occurrence} \times \sqrt{\%\text{Frequency}}$$

(Booth *et al.,* 1988).

Detection of analyzing fungi: In order to investigate the activity of fungi and at their damage to the manuscripts, fungi were studied. Analyzing enzymes of Cellulose, Protein, Starch and lipids were examined .Each experiment included two replicates for each fungal species and each enzyme type in addition to the control (without inoculation).

The center of selective media was inoculated with 6 mm tablet of pure fungus that have been developed on PDA medium, three days age, at 28^{o}C for 72 hours.

Cellulose: Use the medium agar- cellulose media. Cellulose decomposition was detected by using the HCl-Iodine reagent. Add the detector to the dish and leave for 5 minutes, then pour the solution and leave the dish for 10 minutes.

The appearance of a translucent circle around the fungal colonies showed that cellulose was transformed into simple sugars by the enzyme cellulose. The diameter of the circle, means the higher activity of the fungus in the production of the enzyme (Yoeh *et al*., 1985).

Protein: Use the medium Skimmed milk- agar media. Protein breakdown (casein in milk) was detected when a translucent circle appeared around the colonies. The higher diameter of circle means higher activity of the fungus in the production of the enzyme (Aaronson, 1973).

Starch: Use the medium starch agar. Detection of starch decomposition using reagent. Add the detector to the dish and left for 5 minutes and then poured the solution and left the dishs for 5 minutes. The appearance of a transparent circle around the fungal colonies indicates the production of the enzyme amylase and the greater the diameter of the circle whenever evidence of fungal activity in the production of the enzyme (Pandey *et al.*, 2006).

Lipase enzyme: Use the medium Tween 80-supported peptide. The results were recorded by observation of white sediments around the colonies or by the appearance of a transparent circle around the colony of fungi (Tako *et al.,* 2012).

Isolation of fungi from the air: The air samples were collected from inside and outside the fortified, where the 50 samples of air were stored, 25 samples of the inside of the fortified and 25 samples of the outside of the fortified by exposing the SDA into the air for three minutes. Closed the dishes tightly and transferred to the laboratory. Incubator at 28 ° C for a period of 3 - 5 days and then previewed the colonies and calculate them. The method of work was completed as mentioned in the isolating fungi from the above manuscripts.

RESULTS AND DISCUSSION

Isolation and diagnosis of fungi isolated from manuscripts .Ten species of fungus belonging to six genera were isolated from three sites of the manuscript representing the beginning, middle and end of the manuscript, as well as the isolation of the sterile white fungus (Table 1). *Aspergillus* was 76.7%, followed by *Penicillium*, *Mucor*, and *Rhizopus.*

Pure Sciences International Journal of Kerbala

Journal Homepage:https://journals.uokerbala.edu.iq/index.php/psijk

Table 2: Percentage of total occurrence, percentage of frequency and distribution density coefficient of fungi isolated from manuscripts.

isolates of fungal	Percentage of Occurrence	Percen-tage of Frequ-ency	Distribu-tion Intens-ity coefficient
A.niger	%80	19.97	357.5
A.flavus	%70	17.62	293.8
A.fumigauts	%61	15.40	239.4
A.terrus	%53	13.45	194.4
A. versicolor	%41	10.26	131.3
Penicellium	%35	8.74	103.5
Mucor	%20	5.13	45.3
Rhizopuse	%17	4.44	35.8
yeast	%11	2.77	18.3

The *Aspergilluse* spp. recorded the highest percentage of appearance of the five types and *A. niger*, accounted for 80% followed by a *A.flavus* with 70%, followed by *A. fumigatus* with 61% The highest per cent frequency value was for *A.niger* (19.97) followed by *A. flavus* (17.62) , *A. fumigates and A. terreus* 13.45, *A. versicolor* (10.26) , *Penicillium* (8.74) , *Mucor* (5.13) and *Rhizopuse* (4.44) while the lowest frequencywas of Yeast and White sterile mycelium (2.77 and 2.22%, respectively) . Species *A. fumigatus, A. terreus, A. flavus. niger, A., Penicillium spp., A. versicolor* were the most intense in distribution ,while the less dense species were *Mucor, Rhizopuse*, and Yeast, as well as sterile white mycelium (Table 2). The current study showed that *Aspergillus* spp., which was the most visible and recombinant, and the distribution density coefficient are 80%,70% ,61% ,53% and 41% for *A. niger , A. flavus , A. fumigatus , A. terreus and A. versicolor* respectively .

The reason for *Aspergillus* spp. occurs in all samples is to suit the different environmental conditions for its growth and reproduction. The fungus also has the ability to form large numbers of asexual reproduction in addition of sexual and sclerotia are more resistant to adverse environmental conditions and most species have high enzymatic ability to use different organic matter and protein as food sources. As well as growth in broad ranges of heat and humidity. *Aspergillus* species are characterized by growing in temperatures ranging from 45-5 ° C or higher .These fungi also have the ability to grow at low moisture levels and with moisture content ranging between 18-15% (Rustum 1997). Some species also have the ability to compete and inhibit the growth of other species by producing effective bioactive toxins such as Aflatoxin. The second rank of fungus is listed after *Aspergillus spp*. is *Penicillium* spp. (35%), and it is present in all places and is an opportunistic fungi and has the potential to grow on many materials under different conditions (Pitt and Hocking 1997).

The *Aspergillus* species were the densest in the manuscript samples followed by *Penicillium*. These fungi have special life strategies that enable them to tolerate environmental conditions, making them more viable than other genus and species. The rest of the fungal species

Table 1: Number of isolates and fungal species isolated from the three sites of the manuscript during the study period.

isolates of fungal	manuscripts			Number of species
	Beginning	Center	End	
A. niger	48	54	42	144
A. flavus	42	48	37	127
A. fumigatus	36	43	32	111
A. terreus	31	38	28	97
A. versicolor	23	30	21	74
Penicillium	20	25	18	63
Mucor	15	10	12	37
Rhizopus	12	10	10	32
yeast	8	7	5	20
White sterile mycelium	6	5	5	16
Total	241	270	210	721

appeared in one or two species and differed in their appearance and frequency between the beginning, center and end of the manuscript, as well as differences in appearance and frequency of the site during the study months. This may be due to variations in environmental conditions of temperature, humidity, etc. or the nature of the manuscript and its components.

Detection of fungi analyzed:

Cellulose: The five fungal isolates of *Aspergilluse* spp. had the ability to produce cellulose degradation enzyme at different efficiencies (Table 3). *A. versicolor* and *A. terreus* were very effective, with a transparent halo diameter greater than 15 mm, and *A.fumigatus, A. flavus* were moderately effective, with a transparent halo diameter of 10-15 mm, (Fig1).

Table 3: degradation of cellulose by fungus on the cellulose agar at 28 ° C and for a period of 3 days incubation

isolates of fungal	diameter of analysis zone (mm)	cellulose activity
A. niger	*>15*	+++
A.terrus	*>15*	+++
A. versicolor	*>15*	+++
A.flavus	*15 – 10*	++
A.fumigatus	*15 – 10*	++

+++ Highly effective
++ Medium effective

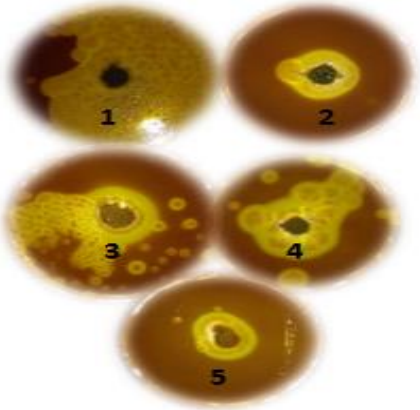

Figure 1: Effect of fungus in the analysis of cellulose on the center of cellulose agar at 28 ° C after three days of incubation
1- *Aspergillus niger* 2- *A. flavus*
3-*A. terreus* 4- *A. versicolor*
5-*A.fumigatuse*

Pure Sciences International Journal of Kerbala

Journal Homepage:https://journals.uokerbala.edu.iq/index.php/psijk

The rest of the fungal species tested were not effective. This result is consistent with the fact that most of the true fungi have the ability to analyze natural cellulose for the purpose of growth and durability of life through the production of cellulose degradation enzymes. In nature, fungi are effective in the analysis of crystalline cellulose, mainly *Trichoderma viride. ,T. lignorum, T. koningii , penicillium verrucosum, P. funiculosum, Chrysosporium lignorum*, and *Chaetomium* , Sharif (2012), reported that. many fungi possess cellulose degradation enzymes, which can attack cellulose industrial products such as paper, cardboard, cotton products, and wood products. Differences were also observed between isolates of the genus *Aspergillus* spp. from weak to good. The weakness of some isolates can be explained by the secretion of cellulose for several reasons, including insufficient incubation duration to stimulate secretion and difference in the ability to exploit the plant medium or the inappropriate pH of these isolates (Abdel-Hadi, 2011; Luiza, 2000). The results of the study suggest that the presence of these fungi on the manuscripts may be due to their ability to secrete the cellulose enzyme on the tissue paper, which is the fiber of cellulose, its constituent component.

Protein: *A. flavus, A. fumigatus, Penicillium* spp. were highly effective, where the diameter of the transparent halo was greater than 15 mm (Table 4, Fig. 2)

Table 4: Protein degradation by fungus on skimmed milk at 28 ° C and for a period of 3 days.

isolates of fungal	diameter of analysis zone(mm)	effectiveness of casein degradation
Penicillium	*>15*	+++
A.fumigatus	*>15*	+++
A.terrus	*>15*	+++
A.flavus	*>15*	+++
A. niger	*10-15*	++

+++ Highly effective
++ Medium effective

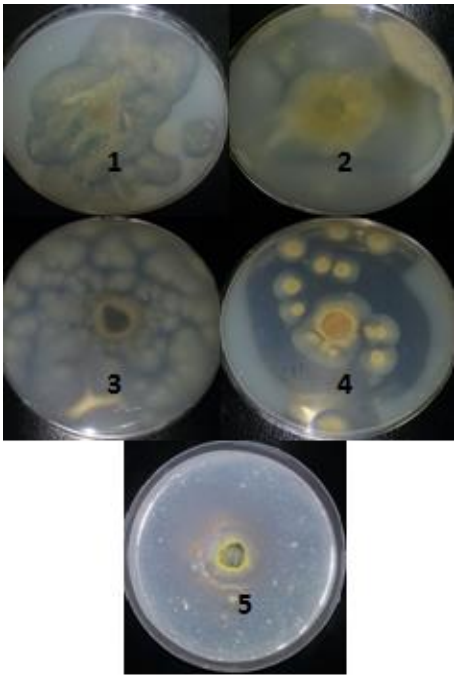

Figure 2: Effect of fungus in the analysis of protein on skimmed milk media at 28 ° C after three days of incubation.
1- *penicillum* 2- *A. fumigatuse*
3-*A. niger* 4-*A. Terruse*
5- *A. flavus*

A.niger was the medium effective, the diameter of the transparent halo was between 10- 15 mm. The results were similar to those of Al-Amiri (2014), where the fungi *A. niger, A. flavus, A. terreus,* and other fungi were not able to produce protease. Protease enzymes have been widely produced in the industry using *Aspergillius* spp.and bacteria sush as some species of *Bacillius*. Nieves (2003) confirmed that fungi attacked skins because leather is an organic substance that contains fats, carbohydrates and proteins in their composition, this confirms our results caused by the presence of fungi on the covers of manuscripts. This is due to the use of leather in the packaging of printed books and the manuscript and the chemical composition of the skin is the same as the installation of paper and parchment, as the parchment and parchment protein materials extracted from the skin and the majority of fungi specialized in the analysis of skins and parchment attributed to the genotypes *Penicillium, Aspergilluse, Alternaria* and *Helminthosprium* .These races play a role in the analysis of cellulosic materials.

Starch: *A. fumigatus, , .Penicillium* spp. were highly effective where the diameter of the transplant halo was greater than 15 mm (Table 5, Figure 3), while *A. niger A. flavus* and *Mucor* was less effective, the diameter of the transplant halo was lower than 10 mm either the rest of the fungal species were not analyzed, and this confirm that the presence of these fungi on the manuscripts may be due to the presence of starch, which is a material included in the installation of manuscripts, leaflets, lattice, and the heels of

Pure Sciences International Journal of Kerbala

Journal Homepage:https://journals.uokerbala.edu.iq/index.php/psijk

Table 6 : Number of isolates and fungal species isolated from the sites inside and outside the fortified during the period of study.

Number of total isolates external and internal air Fungal species	indoor air	outdoor air	total isolates
A. flavus	*23*	*25*	*48*
A. niger	*21*	*22*	*43*
A. fumigatus	*20*	*18*	*38*
A.nidulans	*10*	*15*	*25*
A.oryzae	*7*	*12*	*19*
Penicillium	*11*	*14*	*25*
Yeast	*13*	*18*	*31*
White sterile mycelium	*7*	*9*	*16*
Mucor	*4*	*6*	*10*
Rhizopus	*3*	*5*	*8*
Total	*119*	*144*	*263*

anuscript books. This may also be used in various restoration processes inside the manuscript,, as the starch is a complex compound of glucose there are some fungus specializing in the analysis and feeding on its components through the secretion of secrete enzymes.

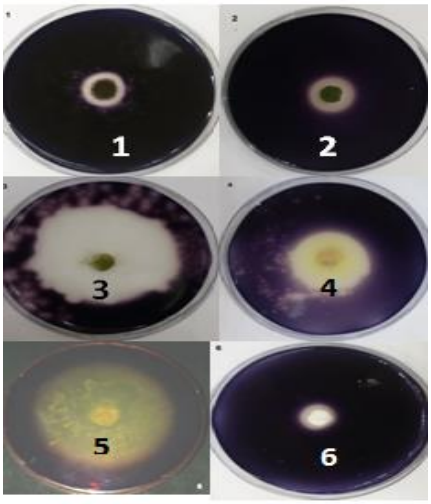

Figure 3: Highly effective fungi in the production of amylase on Agar pure starch at 28 ° C and incubation for 3 days
1-*A.niger* 2 - *A. flavus*
3- *A.fumigatuse* 4- *A.terreuse*
5- *penicillium* 6-*Mucor*

Fat: The results of the lysis test for the fungus isolates isolated from the manuscripts were found in the center of the lipase (Table 6) .The test results showed that most fungal isolate species have the ability to secrete the lipase enzyme. *A. flavus, A.fumigatus, A.niger, A. versicolor, A.terreus, Mucor* spp., *Rhizopuse* spp., and White sterile mycelium. Sumathy and his group, (2012) reported that

Table 5: Starch degradation by fungus on starch at 28 ° C for 3 days incubation.

isolates of fungal	Diameter of analysis zone(mm)	effectiveness of starch degradation
Penicillium	>15	+++
A.fumigatus	>15	+++
A.terreus	>15	+++
A.niger	10<	+
A. flavus	10<	+
Mucor	10<	+

+++ Highly effective
+ week effective

Aspergillus, Fusarium, Geotrichum and *Penicillium* had the ability to produce Lipase-enzyme. The results were in accordance with that found by Bramono and his co-workers (2010) studying the susceptibility of some fungi to the secretion of lipase. The rest of the fungal species, i.e. *Penicillium* and Yeast which they had not any activity of analyzing (Figure 4).

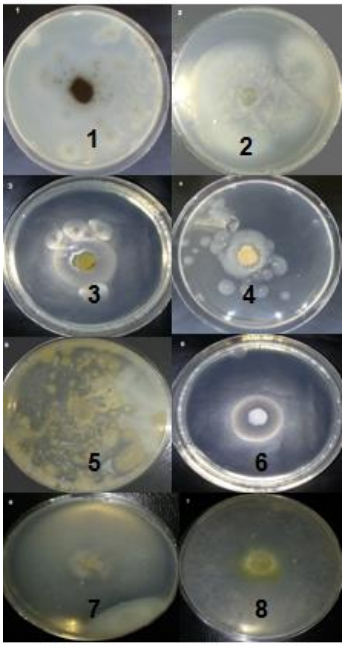

Figure 4: The fungi lysis on lypaes media at 28 ° C for 3 days incubation. Show that is a white deposit is visible around the colony.
1- *A. niger* 2- *A.flavuse*
3-*A. terreus* 4-*A. versicolor*
5- *A. flavus* 6-*Mucor*
7- *Rhizopuse* 8- White mycelia

Isolation and diagnosis of fungi isolated from the air inside and outside the fortified: The results showed that there are differences in the occurance of fungal species during the study at different locations (Table 6).

Pure Sciences International Journal of Kerbala

Journal Homepage:https://journals.uokerbala.edu.iq/index.php/psijk

Table 7: Percentage of total appearance, percentage of frequency and distribution density coefficient of fungi isolated from indoor and outdoor air the fortified.

Fungal isolates	Percentage of total occurance		percentage of frequency		distribution density coefficient of fungi isolated	
	indoor air	outdoor air	indoor air	outdoor air	indoor air	outdoor air
A.flavus	*92*	*100*	*19.33*	*17.36*	*404.5*	*416.7*
A.fumagatus	*80*	*88*	*16.81*	*15.28*	*328.0*	*343.1*
A.niger	*84*	*72*	*17.65*	*12.5*	*352.9*	*254.6*
Yeast	*52*	*72*	*10.92*	*12.5*	*171.8*	*254.6*
A.nidulanse	*40*	*60*	*9.24*	*10.42*	*115.9*	*193.7*
Penicellium	*44*	*56*	*8.40*	*9.72*	*133.7*	*174.6*
A.oryzae	*28*	*48*	*5.88*	*8.33*	*67.9*	*138.5*
White sterile mycelium	*28*	*36*	*5.88*	*6.25*	*67.9*	*90.0*
Mucor	*16*	*24*	*3.36*	*4.17*	*29.3*	*49.0*
Rhizopus	*12*	*20*	*2.53*	*3.47*	*19.1*	*37.3*

Concering the air inside the fortified, *Aspergilluse* spp. were dominant. The percentages of occurance were *A. flavus* (92) followed by *A. niger* (84) , *A. fumigatus* (80) , *A. nidulans* (40) , As for the other sites, an air outside the fortified the results showed, the highest recorded percentage of occurance was of *A. flavus* (100), followed by *A. fumigatus*, (88), *A. niger*(72) and *A. nidulans* (60) (table 6). Six of isolates and fungal species isolated from the sites inside and outside the fortified during the study period. The results of the fungal percentage of frequency showed a clear variance for both sites (Table 7). The frequency of fungal species of the internal air of the fortified, the highest value of the frequency was *Aspergillus* spp. followed by Yeast. *A. flavus* recorded the highest frequency of 19.33percent followed by *A.niger, A.fumigatus, A. nidulans, A.oryzae,* Yeast and *Penicillum,* while the *Mucor* and *Rhizopus* were 3.36 and 2.53 percent, respectively. Concerning outside the fortified *Aspergillus* spp. the highest percent frequency was *A.flavus*, (17.36) followed by *A. fumigatus, A.niger A. nidulans* and by *A.oryzae*. Yeast ranked second with a frequency of 12.5, followed by *Penicillium* with a frequency of 9.72. The fungi of white mycelium, *Mucor* and *Rhizopus* were the last and lowest frequencies giving 6.25, 4.17 and 3.47 percent, respectively. The results of the determination of the density coefficient of the isolated fungi from the air and both the inside and outside of the fortification showed that there is a difference between the distribution density coefficient (Table 7).The results of the site within the fortification showed that *A. fumigatus, A.flavus,. A. niger, Penicillium* spp*, A. nidulans*, Yeast were the most intense in distribution, while the less dense species were *Mucor, A.oryzae, Rhizopus*, and white sterile mycelium.

The results of the outside the fortified species showed that *A. fumigatus, flavus. A. niger, Penicillium* spp, *A. nidulans, Yeast* and *A.oryzae* were the most densely distributed while the less intense species were *Mucor, Rhizopus*, and white sterial mycelium. The *Aspergillus* spp. in air samples, ranked first in terms of occurance, frequency and distribution intensity coefficient for both sites inside and outside the fortified, and this result is similar to what were mentioned by Mohammad and Mohammed (2007) on the dominance of *Aspergillus* spp. in the air. The reason is that this fungus is an aerobic fungus. The speed of the wind has led to the transmission of this fungus from the areas of its propagation and propagation by means of plant and soil residues and carried into the buildings (Latge 1999). The fungus also has the ability to form large numbers of asexual breeding units, some of which are sexually active and sclerotia that are more resistant to adverse environmental conditions. Most of these species have high enzymatic potential to help them use various organic substances and protein as food sources .These reasons made *Aspergillus* spp. this superiority is similar to that having of Menezes *et al*. (2004). In the same fungus role in the air, the number of isolates of *A. fumigatus* was observed in the outer air than in the internal air, while the increase of *A. niger* isolates was observed in the indoor air than in the outside air. This may be due to the possibility of various fungal species each other as appropriate conditions (Mohammad and Mohammed 2007).

The species *A.flavus, A. fumigatus*, and *A. niger* had the highest rate of occurance compared to other fungi, as well as the highest frequency ratio and the most distributed factor between the internal and external air of the fortified. This result is in consistent with several studies of air inside and outside buildings (Shelton et al. 2002; Macura and Gniadek 2000). The Yeast was the second rank beyond the *Aspergillus* spp. both in terms of percentage of occurance, frequency, and distribution density coefficient. Su *et al.,* (2001) reported that yeasts fall within the dominant group of indoor air samples. Ismail *et al*., (2000) noted that yeast is predominant in air samples inside and outside buildings. *Penicillium* spp. was ranked as the third common source of occurance, frequency and distribution density. The reason for this widespread is its ability to produce large numbers of breeding units that are unsuitable for adverse environmental conditions (Faris and Wardlaw 2010). Semenov *et al*., (2003) shows that *Penicillum* is present in the air and in the internal dust of homes and buildings and is supported by Faris and Wardlaw 2010. The air fungus recorded in the study is mostly due to the saprophytic and this sovereignty has already been recorded in the Al-Bader 1995 study of external air fungus in the city of Basra as shown in Al-Ani and Al-Hamdani 2000. Many studies around the world have shown that saprophytic fungi predominate in the air fungal community (Abdulrahman *et al.*, 1999; Rainer *et al.,* 2001; Valeria and Airaudi, 2001 and Zhiguo *et al.,* 2005).

Pure Sciences International Journal of Kerbala

Journal Homepage:https://journals.uokerbala.edu.iq/index.php/psijk

This is due to the nature of the fungus feeding, its presence in the soil, on plant surfaces and animal skins, and mostly for large, open, dry, easy to volatilize units and spread as dominant plankton in the microbial community. There are no global or local standards to assess atmospheric pollution in indoor or outdoor air. However, most studies on air pollution tend to compare the innate content of the air inside the buildings with the outside air. If there are indoor types not found in the outside air, this may give an indication that the source of contamination was inside the building rather than outside air(Brian et al 2002).

REFERENCE

Aaronson S 1973. Enrichment culture, In: "CRC - Hand of Microbiology" . The Chemical Rubber Co. press book. *Cleveland, U.S.A*. **1**. PP: 725 – 735.

Abdel – Hafez S I 1982. Osmophilic fungi of desert soil in Saudi Arabia . *Mycopathologia* . **80**:9 - 14 .

Abdel Hadi and Sha Younis 2011. Determination of the efficiency of fungal isolates in the production of cellulose enzyme. *Tikrit University of Pure Sciences* **16** (2): 167-174.(Arabic).

Abdulrahman S A, Hasanain SM, and Bahkali A H 1999. Viable airborne fungi in Riyadh.*Saudi Arabia Aerobiologia* **15**(2):121-130.

Al-Ani S and Al-Hamdani F M 2000. Occurrence of indoor aeromycota in the homes of Basrah city, Iraq. *Basrah J. Sci–B*.**18**:33-38.(Arabic)

Al-Bader S M 1995. The fungal airspora at Basrah, Iraq. *Basrah J. Sci*.**13**,11-18. (Arabic)

Baath E and Sodarstrow B 1980 . Degradation of macromolecules by microfungi isolated from different podzolic soil horizons . *Can .J. Bot.* **58** : 422 - 425 .

Barnett HL and Bary BH 1972 . Illustrated Genera of imperfect fungi . 3rd . *Burgess pubilishing com* .

Beguin H and Noland N 1994. Molds biodiversity in homes, air and surface analysis of 130 dwelings. *Aerobiology.* **10**: 2-3.

Booth T, Gorrie S and Mabsin TM. 1988 . Life Strategies among fungal , assemblages on Salicornia europase agg . *Mycologia* . **80** : 176 - 191 .

Bramono K, Yamazaki M, Tsuboi R and Ogawa H. 2006. Comparison of proteinase, lipase and alphaglucosidase activities from the clinical isolates of Candida species. *Jpn J. Infect. Dis*. **59**:73-76

Brian G, Shelton BG, Kirkland K H, Flanders W D and Morris G K .2002 . Profiles of Airborne Fungi in Buildings and Outdoor Environments in the United States. *Appl Environ Microbiol.* **68** (4) : 1743–1753.

Christov L P, Szakacs G and Balakrishnan H. 1997 . Production , Partial characterization and use of fungal Cellulase – free xylanase in pulp leaching . *Process . Bioch* .**32** : 511 - 517 .

Collee JG, Fraser AG, Marmion BP, and Simmons A. 1996. *Practical medical microbiology thed .Churchill living stone .* pp:695-717

Domsch K H and Anderson T H 1980. "Compendium of Soil Fungi*". Academic press. London*. **1**:859p.

Dunil P 1980 . The current Status of enzymes technology . In : "Enzymiz and non - enzymic catalysis"Ellis Horwood 1td . *C. chichester . England.*

Ellis M B 1971 . Dematiaceous by phomycetes common weather mycological Institute . *Kew , Surrey , England.*

Fairs A and Wardlaw A 2010.Guideli-nes on ambient intramural airborne fungal spores .Journal of Investigational *Allergology and clinical Immunology* **20**:90-98.

Sharif F M 2012. Medical fungi. *Memory for printing and publishing.* 468 pages.(Arabic)

Flannigan B and Sellars PN 1977 . Amylase , Betaylucosidase and Beta – xylosidase activityof thermotolerant and thermophilic fungi isolated from barley . *Trans . Br. Mycol . Soc* . **69** : 316 – 327.

Ismail M A, Chebon S K and Nakamya R .2000. Preliminary survey of outdoor and indoor aeromycobiotain uganda . *Mycopathologia*. **148**: 41-51.

Khan Z U, Khun M A, Chandy R and Sharma P N. 1999. Aspergillus and other molds in the air of Kuwait. *Mycopathologia*. **146**: 25-32.

Kwon-Chung K J and Bennett J E . 1992 . Medical Mycology . Lea and Febiger *, Philadelphia , London.*

Latge JP 1999. Aspergillus fumigatus and Aspergillosis. *Clin. Microb. Rev*. **12**: 310-350.

Luiza J 2000 .Solid-state fermentation of agricultural wastes for endogluconaes production. *Industrial Crops and Products*, **11**: 1-5.

Macura A B.and Gniadek A 2000. Fungi present in the indoor environments of a social welfare home. *Primelanary Study Mikal Lek*. **7**: 13-17.

Mandels M, Sternberg P and Andeott E 1975 . Growth and cellulase production by Trichoderma , symposium on enzymatic hydrolysis of cellulose . *Aulanko , Finland* ; **14** : 81 - 109 .

Markanen LT and Enari 1977. Enzyme activity of *Penicillium* sp. *Food Microbiol J.* **29** : 281 – 295.

Menezes E A,Emerson C,Trindade P Costa M M,Freirc C C F, Caval cantc M de S and Cunha F A 2004. Airborne fungi isolated from Fortaleza city, State of Ceara Brazil Rev.Inst..*Med trop.S.Paulo*.**46** (3):133-. 137.

Mishra R R and Kanaujia R S 1973 . Observation on soil fungistasis in relation to soil depth , Seasonal changes soil Amendment and physico – *chemical characteristics of the soil plant and soil* . **38** : 321 – 330 .

Mohammed B T and Mohammed L T 2007. A Comparative Study of Aerial Air Pollutants of the City of Karbala, Karbala University. *Journal of Science.(Arabic)* :**5,** *263-267.*

Moubasher A H , Abdel-Hafez S I I, Abdel-fattah H M and Mohrran 1982 . Fungi of wheat and broad-bean staw composts . *Mycopathology.* **78**:161-168.

Moustafa A F and Kamel S M 1976 . A study of fungal spore population in the atmosphere of Kuwait. *Mycopathlogia.* **59 :**(1), 29-35.

Nakagowa Y 1970. Alkaline proteinase from *Aspergilluse* In : " Methods in enzymology " . Acadmic press , *Newyork and London* ; **19** : PP : 583 – 585 .

Nieves V 2003.Microbial Contamin-ation and Insect infestation in organic materials .Internate (yahoo). Coalition .**6**(1),February 2003 http://www.geomic.uni–Oldenburg–delprojekt /coalition .

Pandey A ,Nigamp V T ,Socco L, Singh, D and Mohan R 2006. Advances in microbial amylases, *Biochem*, **31**. 35-152

Pitt J I and Hoching A D 1997 . Fungi and food Spoilage . Blackie academic and professional . 2nd ed . London . Newyork . Tokyo . Melbourne .

Pugh G J F 1980 . Strategies in fungal ecology . *Trans Br . Mycol . Soc* ; **75 :**1 -14 .

Ramirz C 1982 . Manual and atlas of the Pencillia . Elsevier biomedical press. *Oxford* . PP : 874.

Rustum Y S I 1997. Aflatoxin in food and feed \occurance, Legistatation an activation by physical methods. *Food chemistry* .**59:**57-67.

Sarhan T A 2012. Mycology practical. Printed book by the City College of Science University of Baghdad, first edition, p 62. .(Arabic)

Semenov S A , Gumargalieva K Z and Zaikov G E 2003.Biodegradation and Durability of material under the effect of microorganism (New concepts in polymer scince).

Shelton B G , Kirkland K H , Flanders W D and Morris G K 2002. Profile of airborne fungi in building and outdoor environments in the United State. *Appl Envirn Microbial.* **68:**1743- 53.

Pure Sciences International Journal of Kerbala

Journal Homepage:https://journals.uokerbala.edu.iq/index.php/psijk

Slifkin M 2000 . Tween 80 test responses of various Candida species. *J Clin Microbiol* **38:** 4626-4628.

Su H J, Wu C, Chen H L, Lee F C and Lin L L 2001. Exposure assessment of indoor allergens, endotoxin and airborne fungi for homes in southern Taiwan. *Environ Res*. **85**: 135–44.

Sumathy R, Vijayalakshmi M and Deecaraman M 2012. Studies on Lipase production from fungal strains by different inducers at varied concentrations Acomparative study. *International Journal of Enviromental Science*. **3:** (3).

Tako M, Papp T, Kotogan A.,Nemeth B and Vagvolgyi Cs 2012 . Extracellular lipase production of Zygomycetes fungi isolated from soil, *Rev. Agric. Rural. Dev*. **1**(1): 62-66.

Tansey M R 1971 . Agar diffusion assay of cellulolytic ability of thermophilic fungi . *Arch . Microbiol* . **77 :** 1- 11 .

Valeria F M and Airaudi D 2001. Temporal trends of the airborne fungi and their function relation with environment in suburban site. *Mycologi*. **93:** (5), 831-840.

Yeoh H H and Khew E and Lim G 1985 . A simple method of screening cellulolytic fungi.*Mycologia,***77**(1):161-162

Youssef M El Sayed 2012 . Maintenance of the manuscripts Note and Act, *Dar al-Arab writer for printing and publishing.*

Zhigho F, Zhiyun, Lifeng H U, Yioke W, Hua Z and Xeuqiang L 2005 . Culturableairborne fungi in outdoor in Beiging. China. *Science of Environment*. **350:** (1-3), 47-58.

First Year-First Folder-Number: 0
PSIJK 184-191

Pure Sciences International Journal of Kerbala

Journal Homepage:https://journals.uokerbala.edu.iq/index.php/psijk

Molecular and Chemical properties of a common medicinal plants in Iraq.

Shrook Gany Yassin 1*, Ban Taha Mohammed 1
1 Department of Biology, College of Education for Pure Science, Kerbala University, IRAQ
***Corresponding author: Sh.gani.2671@gmail.com**

Abstract

This study was conducted in the Postgraduate Laboratory at the College of Education for Pure Sciences at the University of Kerbala in collaborated with Center for Manuscript Preservation and Restoration and Care of Researchers at the Imam Hussain Holy Shrine in Kerbala for the period from 3/17/2019 to 9/20/2020 with the aim of studying the active compounds of Five plants are *Conocarpus erectus, Eucalyptus globulus, Salvia rosmarinus, Thymus vulgaris and Zingibar officinale*. A series of experiments were conducted that included the molecular diagnosis of medicinal plants under study, and the plant species were recorded in the Genbank of the National Center for Biotechnology Information (NCBI), the first registration of these Iraqi plant species in the Global Genebank and the study of the convergence and similarity between the recorded plants. The serial numbers were carried by *Conocarpus erectus* MT444957, *Eucalyptus globulus* MT444955, *Salvia rosmarinus* MT444956, *Thymus vulgaris* MT444978 and *Zingiber officinale* MT495786 in the genebank .Some chemical tests were performed for the plants selected in the experiment, such as the diagnosis of the active compounds using the qualitative analysis of the chemical compounds in the plant samples using the GCMASS technique.

Introduction

Medicinal plants can be defined as those plants that have therapeutic properties for various diseases or have a physiological effect on the human or animal body and affect the performance of the organs in the human or animal body, whether it has a stimulant or inhibitory effect, and it also has an effect on the parasitizing effect on living organisms. The human being or animal externally or internally, either by activation, inhibition, killing or expulsion (Srivastava 2018). These plants are either those types of wild plants that grow spontaneously in self-sustaining groups in natural ecosystems or the types of domesticated plants that arose through human actions such as selection or breeding and depend on the management of their existence (Calixto 2000). Herbal medicines have proven to be the main treatment in the traditional medicine system, and they have been widely used since ancient times, and this has prompted the use of medicinal plants and their biological benefits in the production of drugs and medicines , the active substances used in traditional

Pure Sciences International Journal of Kerbala

Journal Homepage:https://journals.uokerbala.edu.iq/index.php/psijk

medicinal treatment are obtained from whole plants or their parts such as roots, leaves, bark, or seeds (de Sousa Araújo *et al.* 2016).

Medicinal plants have occupied an important place in traditional medicine and herbal remedies in various countries of the world, and 80% of the world's population still depends on them for their availability, ease of access, low costs and promising efficacy, in order to avoid the negative effects resulting from the use of synthetic drugs. Most medicinal plants are non-toxic, but some of them are severe. Toxicity to both humans and animals (Okoye et al. 2014).

The extraction of biologically active compounds depends on the extraction solvent used and the temperature of extraction or mixing with the presence of three techniques that are considered classic, namely, saxolite, soaking and aqueous distillation (Azmir et al. 2013)

The phytochemical contents can be divided into two parts primary and secondary metabolites (Seigler 2012).

Conocarpus erectus this plant is widely spread on the coasts in tropical and subtropical regions, and the original home of plant cultivation is East Africa, Eritrea, Somalia, Yemen, and Djibouti. Its cultivation has also been introduced to Saudi Arabia, Kuwait, the Emirates, Oman and Iraq, and it is found in the south of the Arabian Peninsula, Sudan, India, Pakistan and Australia (Al-Surrayai *et al*. 2009), Active substances: Phenols are the main compounds of secondary metabolites that are found in the carpis plant (Abdel-Hameed et al. 2012). It contains many chemical compounds with an anti-microbial effect such as alkaloids, glycosides, phenols and tannins (Barnabas and Nagarajan 1988). *Eucalyptus globulus* the original home of eucalyptus trees is in Australia and Tasmania and is cultivated today in many regions of Africa and South America, and in southern Europe and Asia (Fleming 2000), Active substances: volatile oils (1,8-cineol, p-cymene, alpha-pinenes, limonene, geraniol and camphene), flavonoids, coumarins, tannins and a number of phenolic acids (Boland et al. 1991). *Salvia rosmarinus the original home for plant cultivation is the Mediterranean basin. It grows in Algeria, France, Spain and Portugal (Crozier et al. 2008). It is also grown in India, Central Asia, America, South Africa, Southeast Africa, the United States, Brazil and in many countries of the world. Its cultivation is suitable in fields, farms and in home gardens. (Boix et al. 2010), Active substances: Caffeic acid, Diterpenes, Flavonoids, Triterpenes, Volatile oil (Houlihan et al. 1985). Thymus vulgaris the original home of thyme growth in the countries of the Mediterranean basin and is cultivated in many regions around the world, especially in temperate regions such as the Levant, Turkey, North African countries and southern European countries (Madaus 1979), Thyme is a natural source*

Pure Sciences International Journal of Kerbala

Journal Homepage:https://journals.uokerbala.edu.iq/index.php/psijk

of antioxidants (Nakatani 2000), as it contains a high percentage of thymol and carvacrol and contains basic antioxidants such as phenols, flavonoids, saponins, resins, gumes and coumarines (Association and Committee 1976). Zingiber officinale the original home of the plant is from Southeast Asia, and it is one of the most widespread plants in Southeast Asia and in China and in tropical Asia regions, where it grows abundantly in India, the Philippines and Pakistan, and the best types are those grown in Jamaica and India is the first country producing it in the world (Tyler et al 1988), Active substances: volatile oils containing zingerone, shogaols and gingerols (An et al. 2016).

Therefore, the study aimed to qualitative analysis of chemical compounds in medical plant samples using GCMASS technology in the local environment, molecular diagnosis of medical plants , determination of nitrogenous bases sequences, bioinformatics analysis, and phylogeny genetic tree , and to register them in the global genebank.

Material and Methods

Collect medicinal plants

Thymus vulgaris and *zingiber officinale* were obtained from the local market in Kerbala province. *Eucalyptus globulus and Conocarpus erectus* were obtained from a home garden in Karbala province, and *Salvia rosmarinus* was obtained from a home garden in Babelon province. In April of 2019, the used plant parts were washed by plain water, then with distilled water, dried by air, and then milled by an electric grinder for the purpose of obtaining vegetable powder.

Preparation of alcoholic extracts

Fifty gm of dry powder were weighed for each of the plant samples and mixed with 500 ml of 70% ethyl alcohol in a 1000 ml glass beaker closed with cotton and aluminum paper placed in a vibrating incubator and left for 24 hours at room temperature after which the mixture was filtered using several layers of medical gauze for disposal. Then the extract was filtered using Whatman NO0.1. the extract was dried using the oven at 40 ° C, then store in the refrigerator until use (Hernández-Pérez et al. 1994) using the GC-MAAS technique.

Qualitative analysis of chemical compounds in plant samples using the GCMAAS technique

Determination of the leaves' content of the active substances using a gas chromatography-mass spectrometry device.

Plant samples were extracted and analyzed using the modified method Vijisaral et al (2014), by taking 1 g of dried

Pure Sciences International Journal of Kerbala

Journal Homepage:https://journals.uokerbala.edu.iq/index.php/psijk

leaves for each of thyme, carpies, ginger, eucalyptus, rosemary from each treatment and adding 5 ml of 96% ethyl alcohol with continuous stirring for 10 After that, it was left in a dark place for 6 hours at laboratory temperature, and then filtered with a 0.45 5m diameter filter (of Spanish origin) connected to a 10 ml syringe to speed up the filtration process, Then the filtrate was taken. The precipitate was extracted with 5 ml of chloroform in the same way, the second filtrate was combined with the first and concentrated at a temperature of 40 ° C and dried, and then the dry matter was dissolved in 5 ml of hexane. One ml of the resulting extract was taken

and then injected 2 µl of it into the GCMS-QP2010 Ultra device, which includes an automatic identification unit for compounds based on mass spectra according to the following conditions:

1. The separation column is composed of 100% dimethyl polysilocan .

2. The helium gas carrier with a flow rate of 1 ml. Min -1imensions of 30nm × 30 0.25nm × 1µm.

3-The temperature of the injector is 250 ° C and the temperature of the ion source is 200 ° C, and the oven temperature is programmed automatically to obtain a thermal gradient, as it starts from 40 ° C (an equal temperature for 3 minutes) and increases to 15 ° C every one minute down to 180 ° C. Then it increases 10 ° C every 3 minutes, reaching 300 ° C, after which the temperature stabilizes at 300 ° C.

4. Total time for each sample is 28 minutes.

Diagnose active compounds

The components were identified using the National Institute of Standards and Technology (NIST) database by comparing the resulting spectrum of the unknown component with those known stored in the NIST library. This analysis was performed in the laboratory of gas chromatography related to mass spectrometry / in the Environment and Water Department of the Ministry of Science and Technology.

Analysis of the sequence of nitrogenous bases of the double DNA

1-The multiplexed PCR-amplified products from the polymerase chain reaction of plant samples with anterior and posterior primers (ITS1 and ITS4) which were used in the complete duplication of the ribosomal internal transcribed spacer (ITS) region task in plant diagnostics were sent to a company. Macrogene in South Korea for the purpose of determining the sequence of nitrogenous bases. The diagnosed plants were registered in the Global Genebank 2-

3- Phylogenetic tree analysis: and symmetry of the studied plants: The genetic tree of the plants under study was determined using the Chromas program, for the purpose of knowing the similarity between the plants under study and the globally registered plants. DNA replication using the Basic Local Alignment Search Tool (BLAST) program of the National Center for Biotechnology Information (NCBI) website of the same globally diagnosed plants.

Results

Pure Sciences International Journal of Kerbala

Journal Homepage:https://journals.uokerbala.edu.iq/index.php/psijk

Qualitative analysis of chemical compounds in plant samples using GCMASS technology

Chemical compounds in the alcoholic 1-extract of *Conocarpus erectus* leaves

Table (1) and figure(1) show the chemical compounds present in the alcoholic extract of carpis leaves *Conocarpus erectus,* which were detected by the gas chromatography technique with mass spectrometry as the detection showed the presence of 9 compounds in the carpis plant and that the highest peak area of the carpis extract was 2.17 per minute for n-Hexane and the lowest peak area was 22.50 per minute for Hexadecane. The compounds varied in their appearance time and there were compounds that appeared repeatedly in different time periods

Table (1) GCMASS analysis of the alcoholic extract of *Conocarpus erectus*

Peak	R.T(min)	Area%	Compound name	Molecular Formula
1	2.17	55.06	n-Hexane	C_6H_{14}
2	2.38	15.22	unknown	
3	2.50	19.77	Ethyl Acetate	$C_4H_8O_2$
4	2.92	3.11	unknown	
5	17.48	0.43	Tetradecane	$C_{14}H_{30}$
6	20.02	0.44	Pentadecane	$C_{15}H_{32}$
7	22.50	0.38	Hexadecane	$C_{16}H_{34}$
8	27.06	0.61	Benzene, 1,1'-(1,2-cyclobutaned...	$C_{16}H_{16}$
9	35.96	4.97	Dibutyl phthalate	$C_{16}H_{22}O_2$

Pure Sciences International Journal of Kerbala

Journal Homepage:https://journals.uokerbala.edu.iq/index.php/psijk

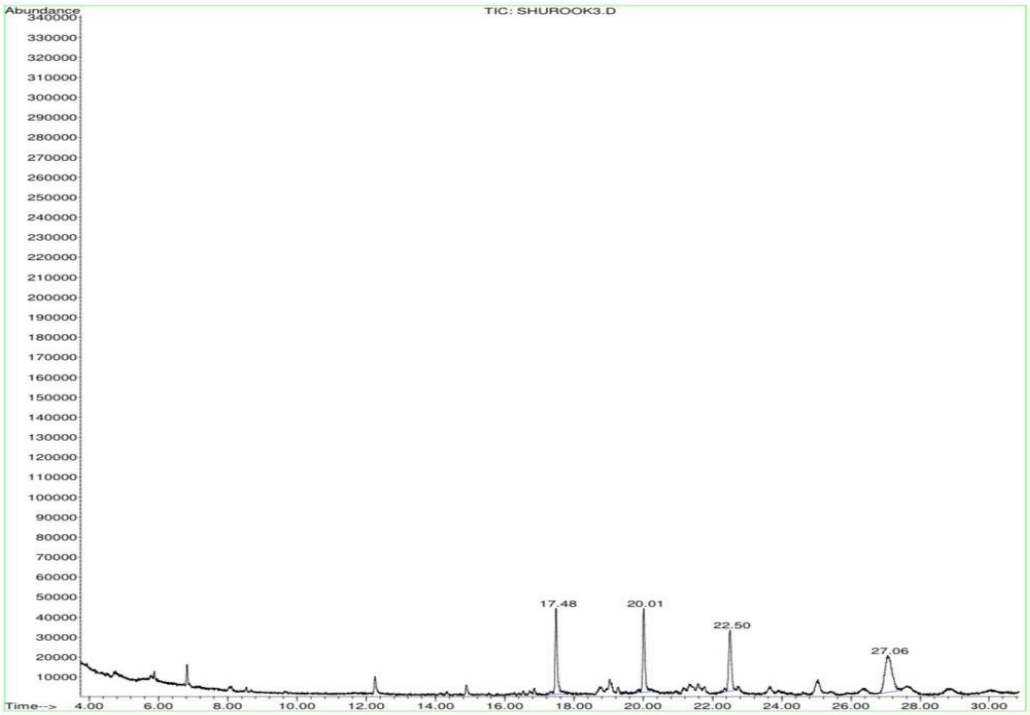

Figure (1) **GCMASS analysis of the alcoholic extract of *Conocarpus erectus***

Chemical compounds in the alcohol extract of 2-*Eucalyptus globulus* leaves

Table (2) figure (2) show the chemical compounds present in the alcoholic extract of *Eucalyptus globulus* leaves that were detected by the gas chromatography technique with mass spectrometry as the detection showed the presence of 15 compounds for eucalyptus and the highest peak area of eucalyptus extract was 2.13 per minute for n-Hexane and the lowest peak area was 17.7 per minute for the copaena compound. The compounds varied in the time of their appearance and there are compounds that reappear at different time periods

.

Table(2): GCMASS analysis of the alcoholic extract of *Eucalyptus globulus*

Peak	R.T(min)	Aerea%	Compound name	Molecular Formula
1	2.13	31.83	n-Hexane	C_6H_{14}
2	2.40	12.57	Pentane, 3-methyl	C_6H_{14}
3	2.65	43.08	Cyclopentane, methyl-	C_6H_{12}
4	8.10	1.63	Eucalyptol	$C_{10}H_{18}O$

Pure Sciences International Journal of Kerbala

Journal Homepage:https://journals.uokerbala.edu.iq/index.php/psijk

5	11.14	0.34	Bicyclo[3.1.1]heptan-3-ol, 6,6-...	$C_{10}H_{16}O$
6	12.61	0.74	2-Pinene	$C_{10}H_{16}$
7	17.07	0.19	Copaene	$C_{15}H_{24}$
8	17.47	0.54	Tetradecane	$C_{14}H_{30}$
9	18.78	0.65	Aromandendrene	$C_{15}H_{22}$
10	19.32	0.41	Alloaromadendrene	$C_{15}H_{24}$
11	19.99	0.70	Pentadecane	$C_{15}H_{32}$
12	22.13	0.99	3,7-Cyclodecadiene-1-methanol,	$C_{15}H_{26}O$
13	22.45	0.50	Hexadecane	$C_{16}H_{34}$
14	22.90	1.06	1H-Cycloprop[e]azulen-7-ol, dec...	$C_{15}H_{24}O$
15	25.15	4.76	2-Naphthalenemethanol, decahydr	$C_{15}H_{26}O$

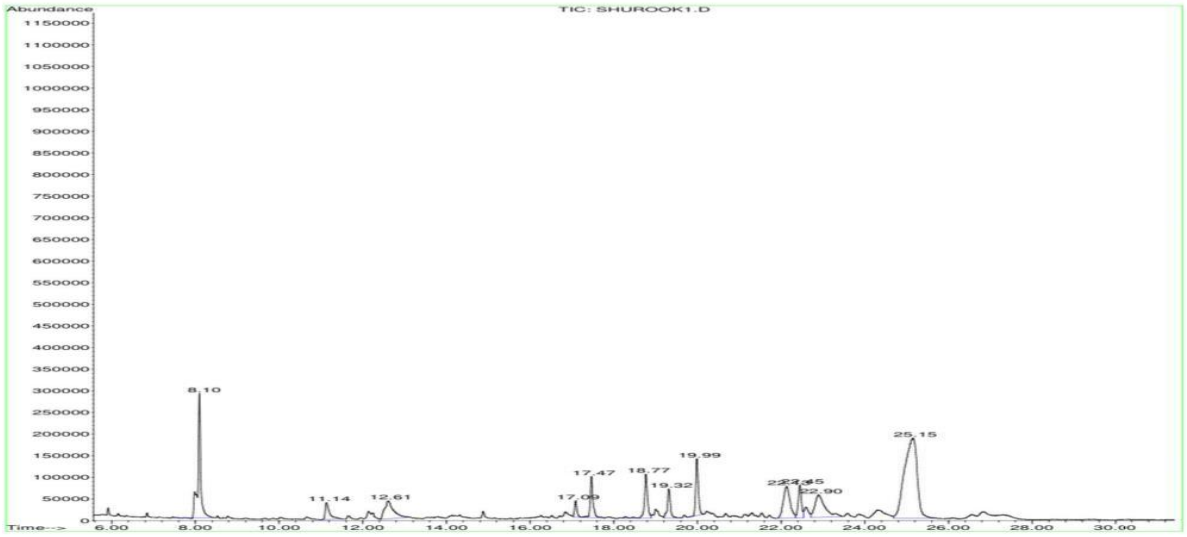

Figure(2) GCMASS analysis of the alcoholic extract of *Eucalyptus globulus*

3-Chemical compounds in alcoholic extract of *Salvia rosmarinus* leaf

Table (3) and figure(3) show the chemical compounds present in the alcoholic extract of *Salvia rosmarinus* leaves, which were detected by the gas chromatography technique with mass spectroscopy, as the detection showed the presence of 40 compounds for rosemary plant and the highest peak area for the extract. Rosemary was 2.11 per minute for n-Hexane and the

Pure Sciences International Journal of Kerbala

Journal Homepage:https://journals.uokerbala.edu.iq/index.php/psijk

lowest peak area was 6.34 per minute for Bicyclo [3.1.0] hex-2-ene, 4-meth. The compounds varied in the time of their appearance and there are compounds that appeared repeatedly at different time periods.

Table (3): GCMASS analysis of the alcoholic extract of *Salvia rosmarinus*

Peak	R.T(min)	Area%	Compound name	Molecular Formula
1	2.11	38.31	n-Hexane	C_6H_{14}
2	2.56	37.82	Cyclopentane, methyl	C_6H_{12}
3	5.73	0.27	Bicyclo[3.1.0]hex-2-ene, 2-meth	$C_{10}H_{16}$
4	6.34	0.11	Bicyclo[3.1.0]hex-2-ene, 4-meth	$C_{10}H_{14}$
5	6.73	0.12	Bicyclo[3.1.0]hexane, 4-methyle..	$C_{10}H_{14}$
6	7.45	0.13	Bicyclo[3.1.0]hex-2-ene, 2-meth...	$C_{10}H_{14}$
7	7.74	0.17	Cyclohexene, 1-methyl-4-(1-meth...	C_6H_{10}
8	8.0.	0.69	Eucalyptol	$C_{10}H_{18}O$
9	11.15	1.11	(+)-2-Bornanone	$C_{10}H_{16}O$
10	11.92	1.49	endo-Borneol	$C_{10}H_{18}O$
11	12.14	0.36	Terpinen-4-ol	$C_{10}H_{18}O$
12	12.64	0.85	Terpineol	$C_{10}H_{18}O$
13	13.04	2.41	Bicyclo[3.1.1]hept-3-en-2-one	$C_{10}H_{14}O$
14	14.77	0.83	Acetic acid, 1,7,7-trimethyl-bi...	$C_2H_4O_2$
15	26.21	0.20	Tricyclo[2.2.1.0(2,6)]heptane,	$C_{10}H_{16}$
16	16.49	2.13	Cyclohexene, 1-methyl-3-(1-meth...	$C_{10}H_{16}$
17	16.99	0.12	p-Cymen-7-ol	$C_{10}H_{14}O$
18	17.11	0.25	alfa.-Copaene	$C_{15}H_{24}$
19	17.50	0.53	Tetradecane	$C_{14}H_{30}$
20	18.15	0.15	(3R,3aR,7R,8aS)-3,8,8-Trimethyl	$C_{15}H_{24}$
21	18.30	0.27	Caryophyllene	$C_{15}H_{24}$
22	18.54	0.18	(1R,2S,6S,7S,8S)-8-Isopropyl-1-.	C15H24
23	19.07	0.13	Octadecane, 1-chloro	$C_{18}H_{37}CL$
24	19.20	0.18	1,4,7,-Cycloundecatriene, 1,5,9.	$C_{15}H_{24}$
25	19.46	0.38	Bicyclosesquiphellandrene	$C_{15}H_{24}$
26	19.75	1.04	gamma.-Muurolene	$C_{15}H_{24}$

Pure Sciences International Journal of Kerbala

Journal Homepage:https://journals.uokerbala.edu.iq/index.php/psijk

27	20.05	0.37	Pentadecane	$C_{15}H_{32}$
28	20.20	0.24	gamma.-Muurolene	$C_{15}H_{24}$
29	20.36	0.30	.alpha.-Muurolene	$C_{15}H_{24}$
30	20.75	0.62	Naphthalene, 1,2,3,4,4a,5,6,8a	$C_{15}H_{24}$
31	20.39	1.00	Naphthalene, 1,2,3,5,6,8a-hexah...	$C_{10}H_{8}$
32	21.37	0.32	Epizonarene	$C_{15}H_{24}$
33	21.56	0.24	1-(p-Methylphenyl)-1H-isoquinol	$C_{15}H_{11}N$
34	21.96	0.23	Naphthalene, 1,2,3,4,4a,5,6,8a-...	$C_{10}H_{18}$
35	22.57	0.56	Hexadecane	$C_{16}H_{34}$
36	22.78	0.74	Caryophyllene oxide	$C_{15}H_{24}O$
37	23.03	0.10	salvial-4(14)-en-1-one	$C_{4}H_{6}O_{2}$
38	23.56	0.54	(1R,3E,7E,11R)-1,5,5,8-Tetramet..	$C_{15}H_{24}O$
39	23.90	3.78	Cedrol	$C_{15}H_{26}O$
40	25.13	0.42	unknown	

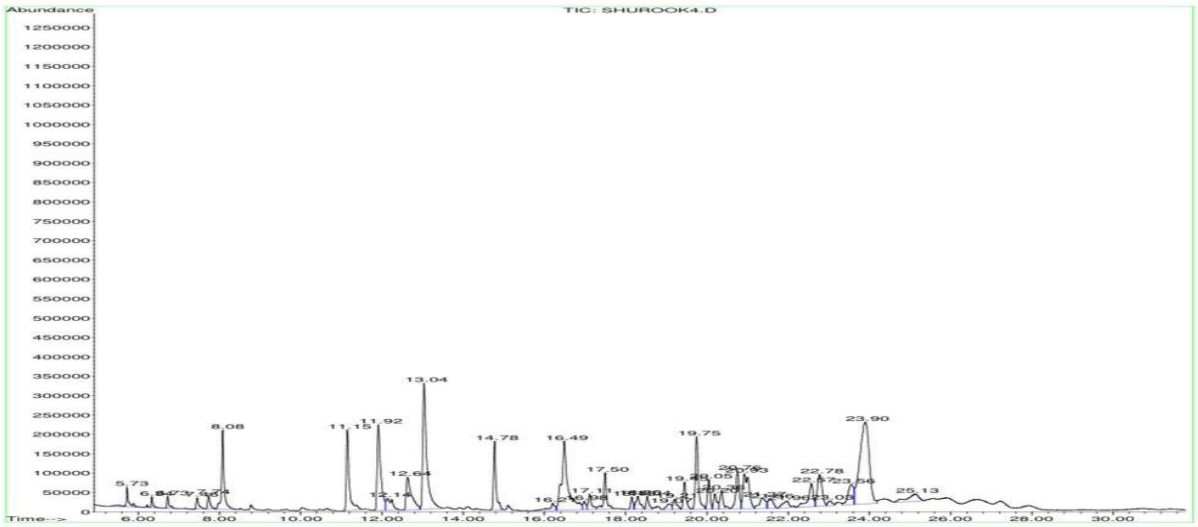

Figure (3): GCMASS analysis of the alcoholic extract of *Salvia rosmarinus*

4 Chemical compounds in the alcoholic extract of *Thymus vulgaris* leaf

Table (4) and figure(4) show the chemical compounds present in the alcoholic extract

Pure Sciences International Journal of Kerbala

Journal Homepage:https://journals.uokerbala.edu.iq/index.php/psijk

of thyme leaves, *Thymus vulgaris*, which were detected by the gas chromatography technique with mass spectrometry, as the detection showed the presence of 8 compounds of the thyme plant and the highest peak area of the thyme extract was per minute. 2.27 for n-Hexane and lowest peak area was 7.17 for Decan،

Table (4): GCMASS analysis of the leaf alcoholic extract of *Thymus vulgaris*

No.peak	R.T(min)	Area%	Compound name	Molecular Formula
1	2.27	40.46	n-Hexane	C_6H_{14}
2	2.37	31.67	2-Ethyl-oxetane	$C_5H_{10}O$
3	2.45	26.89	Cyclopentane, methyl	C_6H_{12}
4	7.17	0.10	Decane	$C_{10}H_{22}$
5	12.26	0.32	Dodecane	$C_{12}H_{26}$
6	17.48	0.28	Tetradecane	$C_{14}H_{30}$
7	20.01	0.15	Pentadecane	$C_{15}H_{32}$
8	22.50	0.14	Hexadecane	$C_{10}H_{14}O$

Pure Sciences International Journal of Kerbala

Journal Homepage:https://journals.uokerbala.edu.iq/index.php/psijk

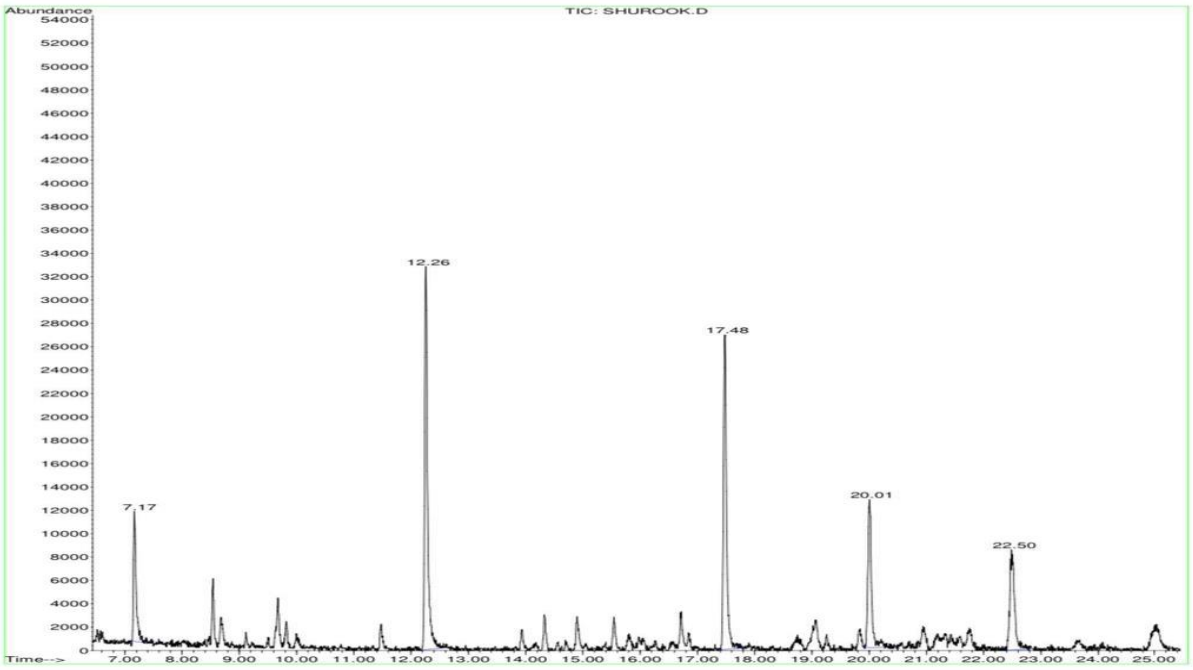

Figure (4): GCMASS analysis of the leaf alcoholic extract of *Thymus vulgaris*

5- Chemical Compounds in Alcoholic Extract of *Zingiber Officinale* rhizomes

Table (5) figure (5) show the chemical compounds in the alcohol extract of *Zingiber Officinale*, which were detected by gas chromatography with mass spectroscopy, as the detection showed the presence of 33 compounds of ginger extract and that the highest peak area was in minute 2. 08 for n-Hexan and the lowest peak area per minute was 6.04 for R (-) 3,7-Dimethyl-1,6-octadiene،

Table (5): GCMASS analysis of the alcoholic extract of *Zingiber Officinale* rhizomes

Peak	R.T(min)	Area%	Compound name	Molecular Formula
1	**2.08**	**14.03**	**n-Hexane**	**C_6H_{14}**
2	2.26	6.39	unknown	
3	2.67	18.76	Cyclopentane, methyl-	C_6H_{12}
4	4.37	0.21	Benzene, 1,3-dimethyl	C_8H_{10}
5	5.30	0.47	Styrene	C_8H_8

Pure Sciences International Journal of Kerbala

Journal Homepage:https://journals.uokerbala.edu.iq/index.php/psijk

6	6.04	0.08	R(-)3,7-Dimethyl-1,6-octadiene	$C_{10}H_8$	
7	11.90	0.33	Bicyclo[2.2.1]heptan-2-ol, 1,7,...	$C_8H_{12}O$	
8	12.24	0.09	Dodecane	$C_{10}H_{22}$	
9	12.62	0.23	L-.alpha.-Terpineol	$C_{10}H_{18}O$	
10	17.10	0.14	alfa.-Copaene	$C_{15}H_{24}$	
11	17.47	0.63	Tetradecane	$C_{14}H_{30}$	
12	17.76	0.12	cis-.alpha.-Bergamotene	$C_{15}H_{24}$	
13	18.56	0.11	Bicyclo[3.1.1]hept-2-ene, 2,6-d...	C_7H_{10}	
14	19.05	0.75	Caryophyllene	$C_{15}H_{24}$	
15	19.27	0.71	(1R,4R,4aS,8aR)-4,7-Dimethyl-1-..	$C_{15}H_{22}O_2$	
16	19.92	9.09	Benzene, 1-(1,5-dimethyl-4-hexe	$C_{15}H_{22}$	
17	20.19	6.67	1,3-Cyclohexadiene, 5-(1,5-dime.	$C_{15}H_{24}$	
18	20.48	5.90	.beta.-Bisabolene	$C_{15}H_{24}$	
19	20.94	6.71	Cyclohexene, 3-(1,5-dimethyl-4-...	$C_{15}H_{24}$	
20	21.74	0.63	4,4-dimethyltricyclo[6.3.2.0(2,.	$C_{15}H_{24}$	
21	22.24	2.76	1,6,10-Dodecatrien-3-ol, 3,7,11...	$C_{15}H_{26}O$	
22	22.45	0.35	Hexadecane	$C_{16}H_{34}$	
23	23.10	0.98	Benzene, 1-(1,5-dimethylhexyl)-...	$C_{15}H_{22}$	
24	23.33	0.95	7-epi-cis-sesquisabinene	$C_{15}H_{24}$	

Pure Sciences International Journal of Kerbala

Journal Homepage:https://journals.uokerbala.edu.iq/index.php/psijk

			hydrate		
25	23.86	2.65	(1S,2R,5R)-2-Methyl-5-((R)-6-me.	$C_{15}H_{26}O$	
26	24.19	1.50	1,5-Cyclodecadiene, 1,5-dimethy	$C_{15}H_{24}$	
27	24.62	2.68	Bicyclo[8.1.0]undeca-2,6-diene,	$C_{15}H_{24}$	
28	25.29	6.11	(-)-Globulol	$C_{15}H_{26}O$	
29	26.82	6.01	METAMITRON	$C_{10}H_{10}N_4O$	
30	29.29	0.96	unknown		
31	30.59	0.64	unknown		
32	32.03	0.89	(E)-1-(6,10-Dimethylundeca-5,9-...	$C_{13}H_{22}O$	
33	35.22	1.48	1,2-Benzenedicarboxylic acid, b...	$C_{20}H_{22}O_{10}$	

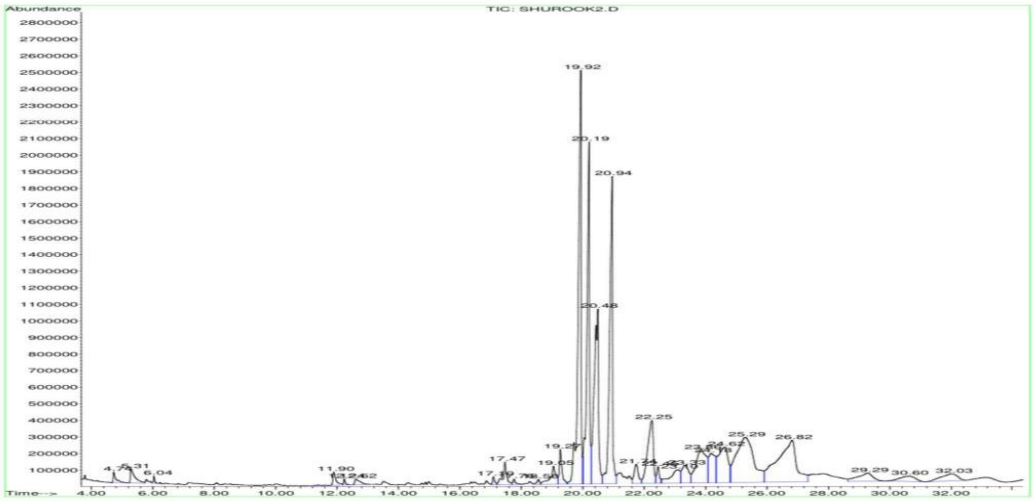

Figure(5) : GCMASS analysis of the alcoholic extract of *Zingiber Officinale* rhizomes

Molecular Diagnosis of Medical Plants

Pure Sciences International Journal of Kerbala

Journal Homepage:https://journals.uokerbala.edu.iq/index.php/psijk

The results of the Polymerase Chain Reaction (PCR) showed that all medicinal plants used in this study, which were phenotypically diagnosed, contained a single bundle of extracted DNA and its purity was measured using a visible spectrophotometer at wavelengths of 260 and 280 nanometers, and that the results of the analysis for the gene 18S ribosomal RNA of an ITS positive region for all plants Figure(6) .

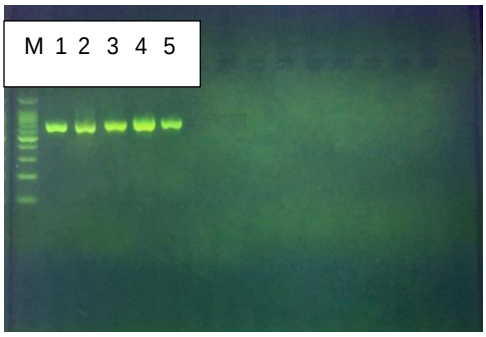

Figure (6): Electrophoresis on agarose gel of studied plants
M =Ladder
1 =*Conocarpus erectus*
2= *Eucalyptus globulus*
3=*Salvia rosmarinus*
4= *Thymus vulgaris*
5=*Zingiber officinale*

The results also showed in Table (6) that the medicinal *plants Conocarpus erectus, Eucalyptus globulus, Salvia rosmarinus, Thymus vulgaris, Zingiber Officinale*. , their genomes interacted with the initiator and matched their counterparts, 99-98% .

The plant species were registered in the Genbank of the National Center for Biotechnology Information (NCBI), and it is considered the first registration of these Iraqi plant species in the Global Genebank, according to what is shown in the registration information and the study of convergence and similarity between the recorded plants..

Table (6) shows that sample No. 1 of *Conocarpus erectus* contains two transition variants at sites 456 and 433, and the percentage of match was 99% with the sample AY050562.1. It carried the sequence MT444957 in the genebank, while sample No. 2 of *Eucalyptus globulus* was It contained 4 variants, one of them was Transvertion and the rest was a transition at

Pure Sciences International Journal of Kerbala

Journal Homepage:https://journals.uokerbala.edu.iq/index.php/psijk

sites 574, 482, 470 and 347, respectively, and the match rate was 99% with the sample KC952021.1. It carried the sequence MT444955 in the genebank, sample 3 of *Salvia rosmarinus* had five variants, two of them Transvertion and three transition at sites 661, 588, 585, 504 and 474 respectively, and the percentage of match was 99% with the sample EU796893.1 and carried the serial number MT444956 in the Global Genebank. 371, 365, 339 and 114 and the match was 98% with the sample LS999887.1 and carried the serial number MT444978 in the genebank. Sample number 5 of *Zingiber officinale* contained three transition variants. At locations 342, 152 and 151, with a 99% match to the sample KR816711.1 and loaded serial number MT495786 in the genebank.

Table (6) The percentage of genetic similarities between the local isolates under study with global isolates For plants diagnosed and registered with the World Genebank and their sequence numbers

Type of substitution	Location	Nucleotide	Sequence ID	GenBank Accession Number	Identities	Source
Transition						*ocarpus*
Transition						*ectus*
Transvertion	574	C>A	ID: KC952021.1	MT444955	99%	*Eucalyptus globulus*
Transition	482	G>A				
Transition	470	A>G				
Transition	347	G>A				
Transition	661	G>A	ID: EU796893.1	MT444956	99%	*Salvia rosmarinus*
Transvertion	588	G>C				
Transition	585	G>A				
Transvertion	504	A>T				
Transition	474	R>A				
Transition	371	C>T	ID: LS999887.1	MT444978	98%	*Thymus vulgaris*
Transition	365	G>A				
Transvertion	339	A>T				
Transvertion	114	G>C				
Transition	342	T>C	ID: KR816711.1	MT495786	99%	*Zingiber officinale*
Transition	152	A>G				
Transition	151	A>G				

Determination of nitrogenous bases sequence, bioinformatics analysis, and phylogeny genetic tree

The results of the analysis of the Nucleotide sequence of the double stranded DNA using the Mega / 6 and NSBI program and comparing them with the data

Pure Sciences International Journal of Kerbala

Journal Homepage:https://journals.uokerbala.edu.iq/index.php/psijk

available in the National Center for Biotechnology Information (NCBI) and of the isolate *Conocarpus erectus* diagnosed and recorded in the genebank are identical with the global isolates of each From China and South Africa by 99%, and the Chinese isolation coincided with the isolation of South Africa by 100% figure (7) .

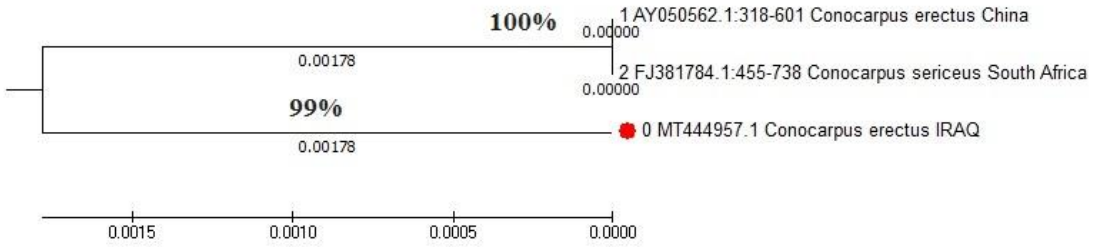

Figure (7) a phylogenetic tree in *Conocarpus erectus* with other strains. The bar indicates the genetic distance due to the sequence difference

Figure (8) show the analysis of the genetic tree of the sample *Eucalyptus globulus* shows that it matches the Indian sample by 99%

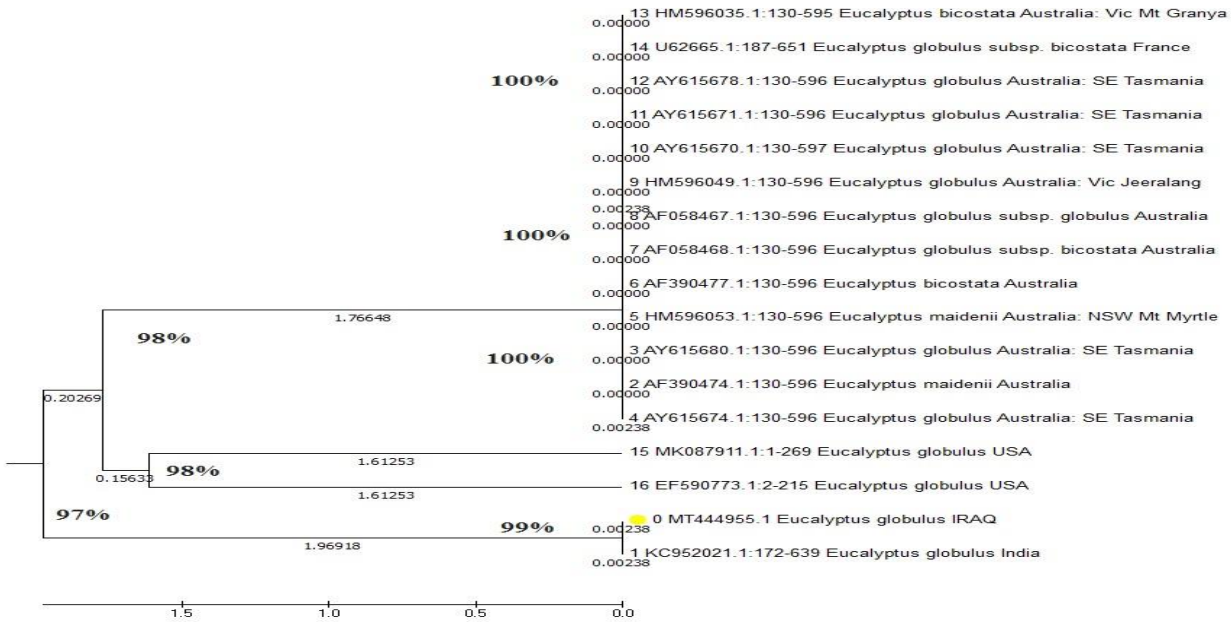

Figure (8) a phylogenetic tree, *Eucalyptus globulus*, with other strains. The bar indicates the genetic .distance due to the sequence difference

Figure (9) shows the results of the analysis of the genetic tree. The sample of *Salvia rosmarinus* matches with each of the samples from Holland, America, Germany and Iran by 99% and it matches another sample from Germany by 98%

Pure Sciences International Journal of Kerbala

Journal Homepage:https://journals.uokerbala.edu.iq/index.php/psijk

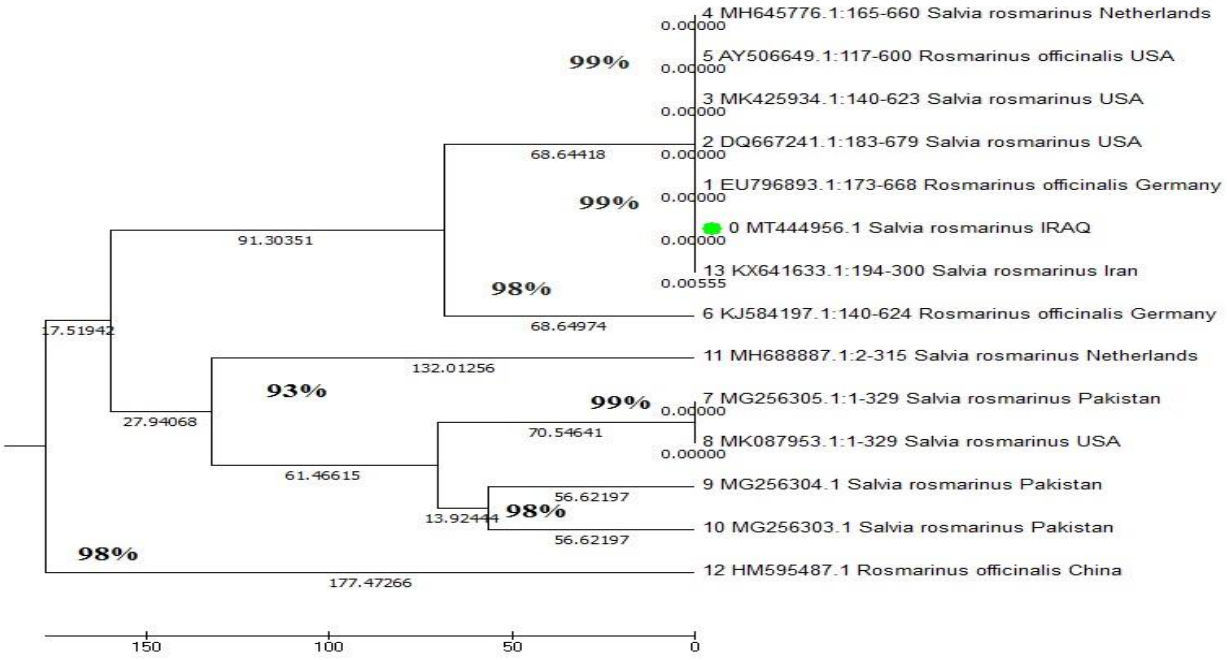

Figure (9) a phylogenetic tree *Salvia rosmarinus* with other strains. The bar indicates the genetic .distance due to the sequence difference

Figure (10) shows the analysis of the genetic tree of the sample, *Thymus vulgaris*, with 98% conformity with Iran, Germany, Italy and America, and 97% with the USA and the Netherlands.

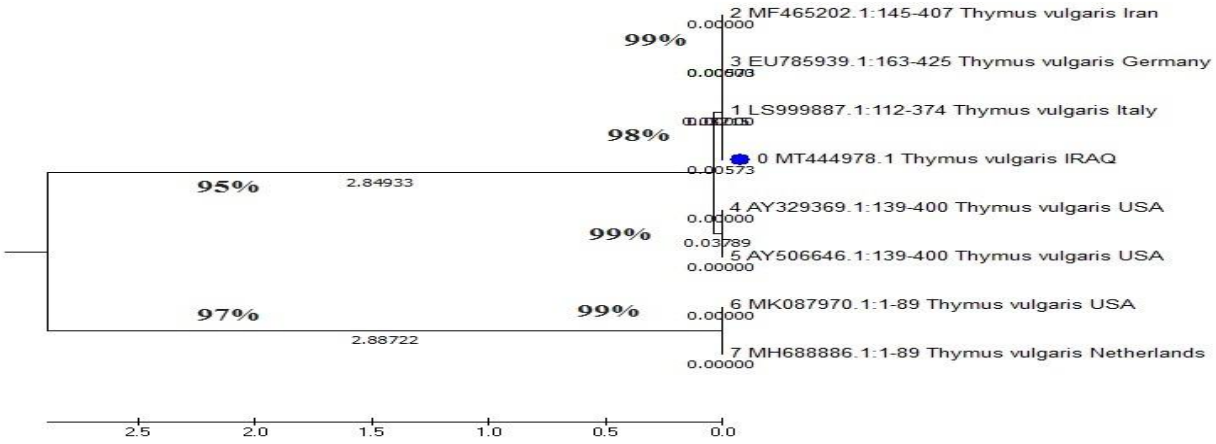

Figure (10) a phylogenetic tree of *Thymus vulgaris* with other strains. The bar indicates the genetic .distance due to the sequence difference

Figure (11) shows the analysis of the genetic tree of *Zingiber Officinale* that the sample matches the Indian sample by 99% and with the Indian and Thai sample by 98%.

Pure Sciences International Journal of Kerbala

Journal Homepage:https://journals.uokerbala.edu.iq/index.php/psijk

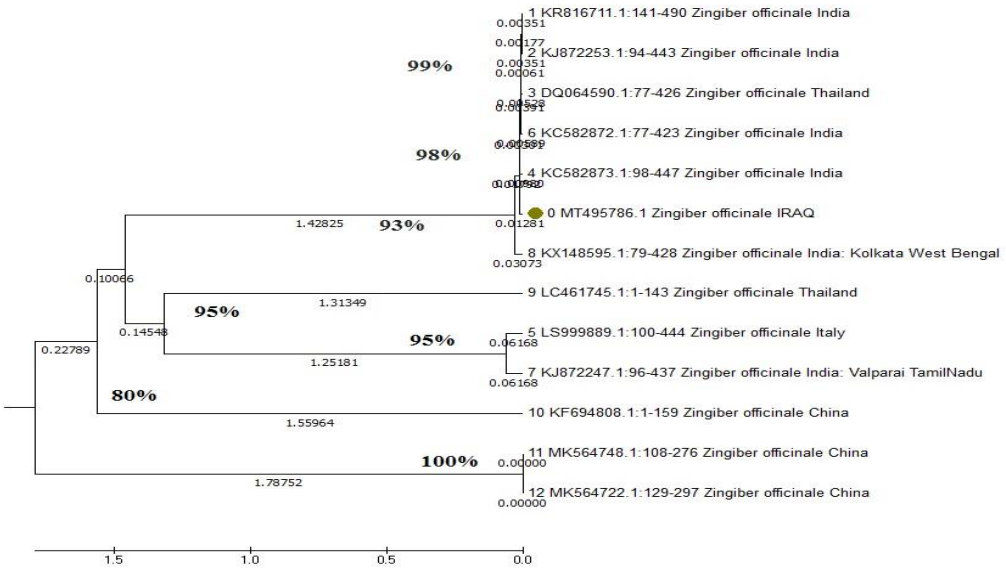

Figure (11) *Zingiber Officinale* with other strains. The bar indicates the genetic distance due to the sequence difference.

Discussion

The GC-MS analysis showed the presence of many bioactive compounds in all plants, such as phenols, flavonoids, volatile oils and terpenes, which are known to have various biological activities such as antioxidants, anti-microbial and anti-inflammatory, in addition to their protective chemical importance. The n-Hexan compound had a frequent occurrence with the highest peak area of all extracts possibly due to it being the solvent used for the dry samples. The biological activities of these compounds are indicative of the medicinal potential of these plants examined. Although some of them possess diverse pharmacological activities, and potential for synergy between compounds, the different phytochemicals discovered in different plants cannot be marginalized. Do Nascimento Santos et al. 2018, through Gcmass analysis of the alcoholic extract of Conocarpus erectus L leaves, demonstrated the presence of active compounds such as (2,3-Dimethyl-1,4-pentadiene, 2,4-Hexadiene, 2-methyl, Octane, 3). , 4,5,6-tetramethyl, Eicosane, 2-methyl, Eicosane, 7-hexyl, Olean-12-ene, Olean-12-en-3-one) possesses antioxidant and biological antifungal activity through inhibiting growth Yeasts C. albicans C. krusei C. tropicalis C. glabrata, among (Santos et al. 2018), the presence of 10 active compounds in the aqueous extract of carpes (Caffeic acid, Gallocatechin, Pauciflorol A, Myricetin,

Pure Sciences International Journal of Kerbala

Journal Homepage:https://journals.uokerbala.edu.iq/index.php/psijk

Myricetin 3-glucoronide, Quercetin, Apigenin. 7-O-glucoside, Chlorogenic acid, Fertaric acid and Discretine) and have antioxidant bilogic activity. C. erectus leaf aqueous extract contains many active compounds such as flavonoids, tannins. saponins (Nascimento et al. 2016.(

Eucalyptol is one of the compounds that appear frequently in rosemary extract and eucalyptus extract, and this is in agreement with Aprotosoaie et al (2019) where it was found that Eucalyptol (1,8-cineole) is a compound of monoterpenes and is the main compound in the volatile oil of *Eucalyptus globulus* extract and *Rosmarinus officinalis*) And extract (*Salvia officinalis*), the main active compounds found in the leaves of Eucalyptus globulus are 1,8-cineol (45-75%),, myrtenol, alpha-pinenes, beta-pinenes, pinocarvon gamma-terpenes, aliphatic aldehydes (Boland et al. 1991). Boukhatem et al (2014) studied the volatile oils in eucalyptus leaves and found that they contain 11 compounds, namely α-Pinene, Camphene, β-Pinene, 1,8-cineol, α-Campholenal, Fenchol, L-pinocarveol, Borneol, 4-Terpineol, Caren-4-ol, α-Terpineol, Myrtenol, Cis-Carveol, Globulol

The most effective compounds that are found in *Salvia rosmarinus* leaves are rosmarinic acid, Diterpenes, which contain (carnosolic acid, isorosmanol, rosmadial, rosmaridiphenol, rosmariquinone), flavonoids containing cirsimarin, diosmin, hesperidin, phegopololic, phegopolin (such as cirsimarin). ursolic acid, their 3-acetyl esters) volatile oils that contain a number of compounds such as (1,8-cineole 20-50%, alpha-pinene - 20-25%, camphor 10-25%, in addition to other compounds such as camphene, borneol). , bornyl acetate, p-cymene, limonene, linalool, myrcene, and verbenone (Haraguchi et al. 1995).

Thymus vulgaris leaves contain many active compounds, the most important of which are: volatile oils that contain many compounds (thymol 20-55%, p-cymene 14-45%, carvacrol 1-10%, gamma-terpinene 5-10%, borneol more than 8%, linalool (more than 8%), caffeic acid and its derivatives such as rosmarinic acid 1.35-0.15%, flavonoids including (luteolin, apigenin, naringenin, eriodictyol, cirsilineol, salvigenin, cirsimaritin, thymonine, including thymusine, partially as glycosides) : ursolic acid (1.9%), oleanolic acid (0.6%) (Gruenwald et al. 2007). Several studies have proven that the essential oil of thyme contains a number of active compounds such as sabinene hydrate / geraniol / geranyl acetate linalool / carvacrol / p-cymene, / -terpinyl acetate / thymol terpineol,; Thompson et al. 2003;Chizzola et al. 2008.

The main compounds found in rhizomes of *zingiber officinale* are zingiberene, beta-bisabolene, ar-curcumene, neral, geranial, D-camphor, beta-phellandrene, linalool, alpha-farnesene, zingiberol (mixture of cis- and trans-beta-). eudesmol), gingerol and

Pure Sciences International Journal of Kerbala

Journal Homepage:https://journals.uokerbala.edu.iq/index.php/psijk

shogaol (Mascolo et al. 1989). Various studies have shown that ginger oils are very complex mixtures of compounds and found many differences in chemical composition, geranial (25.9%) the main component in ginger oil (Singh et al. 2008), Zingiberene and β-sesquiterpene are the main compounds in a ratio of 10-60. % (Felipe et al. 2008). The most important active compounds that appeared in the Gcmass analysis are: geranyl acetate (18.8%), zingiberene (16.3%) and geranial (8.2%) (Sasidharan et al. 2012). The active compounds differed in their presence or absence in the extracts. This may be due to The difference in the current study with previous studies in the duration of extraction or methods of extraction, the part used for the plant or the environmental factor, the time of collecting the plant and the growing season All of these reasons are protective

Molecular Diagnosis of Medical Plants

The study included the diagnosis of five genera of medicinal plants and were registered in the Global Genebank. It was found that the use of traditional methods is insufficient in most cases due to the asymmetric phenotype and the polymorphism, as well as the different environmental conditions, it was diagnosed using the polymerase chain reaction (PCR) technique depending on Primers are intended for molecular diagnostics (Korf and Rehm 2013).

The results showed that these Iraqi plant species are considered to have the first registration in the World Genebank, according to what is shown in the registration information and the study of closeness and similarity between the recorded plants. The genetic tree was used to find out the link between the species of each sex with the species to be identified as well as the characteristics and phenotypic characteristics as a way to obtain the diagnosis. Accurate addition to the traditional diagnosis. Genotype determination is important in the classification of medicinal plants (Hao and Xiao 2015). The ITS region has been widely used in molecular classification and diagnosis due to its ease of amplification and has a wide range of variability even in highly related species (Kress, et al., 2005). The ITS rDNA region amplification was used for the purpose of determining plant species (Gao et al. 2010). The DNA sequence was first examined to confirm the nucleotide sequence and then compared with other global strains. The NCBI-BLAST-Query nucleotide-online program was used. Accurate results and their comparison with global strains ranged between 98-99%. In addition, MEGA software, an application designed for the comparative analysis of homologous gene sequences, evolutionary relationships, and the pattern of DNA and protein evolution, was used. In addition to statistical data analysis tools, MEGA also provides many facilities via serial data from

Pure Sciences International Journal of Kerbala

Journal Homepage:https://journals.uokerbala.edu.iq/index.php/psijk

internet data containers and can be displayed as phylogenetic trees (Kumar et al. 2008)

References

Srivastava, Akhileshwar Kumar. 2018. "Significance of Medicinal Plants in Human Life." Pp. 1–24 in *Synthesis of Medicinal Agents from Plants*. Elsevier.

Calixto, J. B. 2000. "Efficacy, Safety, Quality Control, Marketing and Regulatory Guidelines for Herbal Medicines (Phytotherapeutic Agents)." *Brazilian Journal of Medical and Biological Research* 33(2):179–89.

de Sousa Araújo, Thiago Antônio, Joabe Gomes de Melo, Washington Soares Ferreira Júnior, and Ulysses Paulino Albuquerque. 2016. "Medicinal Plants." in *Introduction to Ethnobiology*.

Okoye, Theophine Chinwuba, Phillip F. Uzor, Collins A. Onyeto, and Emeka K. Okereke. 2014. "Safe African Medicinal Plants for Clinical Studies." Pp. 535–55 in *Toxicological Survey of African Medicinal Plants*. Elsevier.

Azmir, J., I. S. M. Zaidul, M. M. Rahman, K. M. Sharif, A. Mohamed, F. Sahena, M. H. A. Jahurul, K. Ghafoor, N. A. N. Norulaini, and A. K. M. Omar. 2013. "Techniques for Extraction of Bioactive Compounds from Plant Materials: A Review." *Journal of Food Engineering*.

Seigler, David S. 2012. *Plant Secondary Metabolism*. Springer Science & Business Media.

Al-Surrayai, T., A. Yateem, R. Al-Kandari, T. Al-Sharrah, and A. Bin-Haji. 2009. "The Use of Conocarpus Lancifolius Trees for the Remediation of Oil-Contaminated Soils." *Soil & Sediment Contamination* 18(3):354–68.

Abdel-Hameed, El-Sayed S., Salih A. Bazaid, Mohamed M. Shohayeb, Mortada M. El-Sayed, and Eman A. El-Wakil. 2012. "Phytochemical Studies and Evaluation of Antioxidant, Anticancer and Antimicrobial Properties of Conocarpus Erectus L. Growing in Taif, Saudi Arabia." *European Journal of Medicinal Plants* 93–112.

Barnabas, C. G., and S. Nagarajan. 1988. "Antimicrobial Activity of Flavonoids of Some Medicinal Plants." *Fitoterapia* 3:508–10.

Fleming, Thomas. 2000. *PDR for Herbal Medicines*. Medical Economics.

Boland, Douglas J., J. J. Brophy, and A. P. N. House. 1991. "Eucalyptus Leaf Oils: Use, Chemistry, Distillation and

Pure Sciences International Journal of Kerbala

Journal Homepage:https://journals.uokerbala.edu.iq/index.php/psijk

Marketing."

Crozier, Alan, Mike N. Clifford, and Hiroshi Ashihara. 2008. *Plant Secondary Metabolites: Occurrence, Structure and Role in the Human Diet*. John Wiley & Sons.

Boix, Yilan Fung, Cristiane Pimentel Victório, Celso Luiz Salgueiro Lage, and Ricardo Machado Kuster. 2010. "Volatile Compounds from Rosmarinus Officinalis L. and Baccharis Dracunculifolia DC. Growing in Southeast Coast of Brazil." *Química Nova* 33(2):255–57

Houlihan, Christopher M., Chi- Tang Ho, and Stephen S. Chang. 1985. "The Structure of Rosmariquinone—A New Antioxidant Isolated FromRosmarinus Officinalis L." *Journal of the American Oil Chemists' Society* 62(1):96–98.

Madaus, Gerhard. 1979. *Lehrbuch Der Biologischen Heilmittel*. Vol. 1. Georg Olms Verlag.

Nakatani, Nobuji. 2000. "Phenolic Antioxidants from Herbs and Spices." *Biofactors* 13(1–4):141–46.

Association, British Herbal Medicine, and Scientific Committee. 1976. *British Herbal Pharmacopoeia*. British Herbal Medicine Association.

Tyler, V. E., L. R. Brady, and J. E. Robbers. 1988. "Pharmacognosy. 9th Edit." *Lea and Fabiger, Philadelphia*.

An, Kejing, Dandan Zhao, Zhengfu Wang, Jijun Wu, Yujuan Xu, and Gengsheng Xiao. 2016. "Comparison of Different Drying Methods on Chinese Ginger (Zingiber Officinale Roscoe): Changes in Volatiles, Chemical Profile, Antioxidant Properties, and Microstructure." *Food Chemistry* 197:1292–1300.

Hernández-Pérez, M., R. E. López-García, R. M. Rabanal, V. Darias, and A. Arias. 1994. "Antimicrobial Activity of Visnea Mocanera Leaf Extracts." *Journal of Ethnopharmacology* 41(1–2):115–19.

Vijisaral, E. D., R. Balamani, and S. Arumugam. 2014. "Phytochemical Analysis and GC-MS Analysis of Leaves of Macrotylomauniflorum." *European Journal of Biotechnology and Bioscience* 2(5):46–51.

Nascimento, Dayane K. D., IVONE A. SOUZA, ANTÔNIO F. M. D. E. OLIVEIRA, Mariana O. Barbosa, Marllon A. N. Santana, Daniel F.

Pure Sciences International Journal of Kerbala

Journal Homepage:https://journals.uokerbala.edu.iq/index.php/psijk

Pereira Junior, Eduardo C. Lira, and JEYMESSON R. C. VIEIRA. 2016. "Phytochemical Screening and Acute Toxicity of Aqueous Extract of Leaves of Conocarpus Erectus Linnaeus in Swiss Albino Mice." *Anais Da Academia Brasileira de Ciências* 88(3):1431–37.

Aprotosoaie, Ana Clara, Vlad Simon Luca, Adriana Trifan, and Anca Miron. 2019. "Antigenotoxic Potential of Some Dietary Non-Phenolic Phytochemicals." Pp. 223–97 in *Studies in Natural Products Chemistry*. Vol. 60. Elsevier.

Boland, Douglas J., J. J. Brophy, and A. P. N. House. 1991. "Eucalyptus Leaf Oils: Use, Chemistry, Distillation and Marketing."

Boukhatem, Mohamed Nadjib, Ferhat Mohamed Amine, Abdelkrim Kameli, Fairouz Saidi, Kerkadi Walid, and Sadok Bouziane Mohamed. 2014. "Quality Assessment of the Essential Oil from Eucalyptus Globulus Labill of Blida (Algeria) Origin." *International Letters of Chemistry, Physics and Astronomy* 17(3):303–15.

Haraguchi, Hiroyuki, Takashi Saito, Nobuyuki Okamura, and Akira Yagi. 1995. "Inhibition of Lipid Peroxidation and Superoxide Generation by Diterpenoids from Rosmarinus Officinalis." *Planta Medica* 61(04):333–36.

Thompson, John D., Jean-Claude Chalchat, André Michet, Yan B. Linhart, and Bodil Ehlers. 2003. "Qualitative and Quantitative Variation in Monoterpene Co-Occurrence and Composition in the Essential Oil of Thymus Vulgaris Chemotypes." *Journal of Chemical Ecology* 29(4):859–80.

Chizzola, Remigius, Hanneliese Michitsch, and Chlodwig Franz. 2008. "Antioxidative Properties of Thymus Vulgaris Leaves: Comparison of Different Extracts and Essential Oil Chemotypes." *Journal of Agricultural and Food Chemistry* 56(16):6897–6904.

Mascolo, N., R. Jain, S. C. Jain, and F. Capasso. 1989. "Ethnopharmacologic Investigation of Ginger (Zingiber Officinale)." *Journal of Ethnopharmacology* 27(1–2):129–40.

Singh, Gurdip, I. P. S. Kapoor, Pratibha Singh, Carola S. de Heluani, Marina P. de Lampasona, and Cesar A. N. Catalan. 2008. "Chemistry, Antioxidant and Antimicrobial Investigations on Essential Oil and Oleoresins of Zingiber Officinale." *Food and Chemical Toxicology* 46(10):3295–3302.

Felipe, Cícero Francisco Bezerra, Kamyla Sales Fonsecirc, Jose Noberto Sousa Bezerra, Marta Maria de Franccedil, and Glauce Socorro de Barros Viana. 2008. "Alterations in Behavior and

Pure Sciences International Journal of Kerbala

Journal Homepage:https://journals.uokerbala.edu.iq/index.php/psijk

Memory Induced by the Essential Oil of Zingiber Officinale Roscoe (Ginger) in Mice Are Cholinergic-Dependent." *Journal of Medicinal Plants Research* 2(7):163–70.

Sasidharan, Indu, V. V Venugopal, and A. Nirmala Menon. 2012. "Essential Oil Composition of Two Unique Ginger (Zingiber Officinale Roscoe) Cultivars from Sikkim." *Natural Product Research* 26(19):1759–64.

Korf, Bruce R., and Heidi L. Rehm. 2013. "New Approaches to Molecular Diagnosis." *Jama* 309(14):1511–21.

Hao, Da Cheng, and Pei Gen Xiao. 2015. "Genomics and Evolution in Traditional Medicinal Plants: Road to a Healthier Life." *Evolutionary Bioinformatics*.

Kress, W. John, Kenneth J. Wurdack, Elizabeth A. Zimmer, Lee A. Weigt, and Daniel H. Janzen. 2005. "Use of DNA Barcodes to Identify Flowering Plants." *Proceedings of the National Academy of Sciences of the United States of America*.

Gao, Ting, Hui Yao, Jingyuan Song, Chang Liu, Yingjie Zhu, Xinye Ma, Xiaohui Pang, Hongxi Xu, and Shilin Chen. 2010. "Identification of Medicinal Plants in the Family Fabaceae Using a Potential DNA Barcode ITS2." *Journal of Ethnopharmacology* 130(1):116–21

Kumar, Sudhir, Masatoshi Nei, Joel Dudley, and Koichiro Tamura. 2008. "MEGA: A Biologist-Centric Software for Evolutionary Analysis of DNA and Protein Sequences." *Briefings in Bioinformatics.*

First Year-First Folder-Number: 0
PSIJK 184-191

Pure Sciences International Journal of Kerbala

Journal Homepage:https://journals.uokerbala.edu.iq/index.php/psijk

Effect of the Polymer Density on Nano FiberProperties

Ahmed K. Al-Kadumi And Muhammid H. Al-Baghdadi*

Department of Physics, Collage of Education For Pure Sciences,University of Kerbala, Karbala, Iraq

P A P E R I N F O

Paper history:

Keywords:
Polymer nanofiber, polymer density, fiber radius, fiber internalpressure polymer, viscosity force.

A B S T R A C T

The present paper present a study on the influence of polymer density on fiber formation by different polymers when using the electro-hydro- dynamic (EHD) process. Parameters, such as the internal pressure, radius of fibers and the viscosity force were determined in function of the dis- tance between electrodes. The studies were done for different polymer densities (0.481, 0.529, 0.609, 0.705, 0.9249) g/cm^3. It was found that it is an important parameter influencing internal polymer pressure, diameter of produced nanofibers. The polymer density impacts also on the viscos-ity force. All these parameter: internal polymer pressure, radius of nano-fibers depend on the distance between the electrodes.

INTRODUCTION

Electrospinning is a method used for fabrication of polymer nanofibers by solidification of a polymer solution stretched by an electric field. The electric interaction force to draw charged threads of polymer solutions or polymer melts up to a fiber with diameter of up to some hundred nanometers [1-3]. In this process one observes change of the polymeric molecules on nanoscale. Figure 1 shows the shape of a polymer nanofiber with radius r. Such nanofi- bers exhibit different properties depending on polymeric molecules used [4]. The nanofiber formation is a complex process. The resulting jet (nabofiber) diameter depends on numerous factors: material used, operation design, and operating parameters. A significant part of our information on the electros- pinning process comes from empirical observations. But its complexity makes an empirical determination of parameter effects very difficult if not impossible [5-7]. One must find the radius of the jets because it is the big role that makes many application and manufactures for any nanostructure applica-tions[5, 8]. There are different physical parameters which influence the fabri- cation and the properties of obtained nanofibers. In the present work we studied the influence of the polymer density, its internal pressure and the distance between electrodes on the properties of obtained nanofibers. These are important parameters determining the quality of obtained products and possibilities of their application.

The nanofiber fabrication process can be described by mathematical models. From the charge conservation law one gets the following equation [9]:-

$$2\pi r\sigma u + k\pi r^2 E = 1 \qquad (1)$$

where σ is the surface charge density, k is the dimensionless conductivity of the fluid, E is the applied electric field, I is the electric current intensity, z is the distance between electrodes, r is the nanofiber radius and u is the drift velocity of the charges. The force balance can be obtained from the following differential equation for the drift velocity [9]:

$$\frac{d}{dz}\left[\frac{u^2}{2}\right] = \frac{1}{p}\frac{dp}{dz} + g + \frac{2\sigma E}{pr} + \frac{\partial}{\partial z}\tau \qquad (2)$$

where P is the internal pressure of the fluid, *g* is the body force, ρ is the poly-mer solution density and τ is the viscous force, s shown in Scheme 1.

By using the scaling law (power law) to represent the relation between the axis path of the polymer nanofiber of (Z) and its radius (r) by the relation[9]

$$r \propto \sim Z^b \qquad (3)$$

where b gives the strength of the dependence.

At the initial stage electric force, is affecting the jet, can be obtained fromsimplified Equation (2)

Pure Sciences International Journal of Kerbala

Journal Homepage:https://journals.uokerbala.edu.iq/index.php/psijk

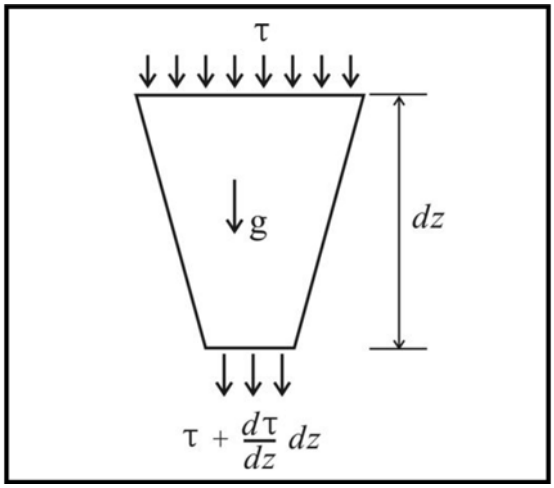

SCHEME 1
Vertical fluctuation of the viscosity force with respect to the position change.

$$\frac{d}{dz}\left[\frac{u^2}{2}\right] = -\frac{1}{p}\frac{dp}{dz} \quad (4)$$

as well as using the following approximations:

$$\frac{d}{dz}\left[\frac{u^2}{2}\right] \propto \sim r^{-2} \quad (5)$$

And

$$r \propto Z^{-1/2} \quad (6)$$

s well as making some mathematical operations one gets the following expression for the internal polymer pressure dependence on the distance between electrodes z

$$p = -p\frac{z^2}{4} \quad (7)$$

The viscosity force can be determined by using the instability stage, when thecombined electrical and viscosity forces vanishes, approximately:

$$\frac{2\sigma E}{pr} + \frac{d\tau}{dz} = \sim 0 \quad (8)$$

With some mathematical approximations, one can solve this differentialobtaining the following formula for the viscosity force τ:

$$p = -p\frac{u^2}{2} \quad (9)$$

One of the important parameter for many applications of the polymer nanofi-ber is its radius r [10]. It can be also obtained from from Equation 2:

$$\frac{d}{dz}\left[\frac{u^2}{2}\right] = \frac{2\sigma E}{pr} \quad (10)$$

and the condition $s[\sigma \propto r, E \propto r^{-2}]$, leading to

$$r = \frac{1}{2}\sqrt{\frac{p}{z}} \quad (11)$$

Equation (11) shows that the radius of nanofibers depends on the polymer density ρ and the distance z between the electrodes, as expected. It varies proportionally to the square route of their ratio ρ/z. Varying the solution den- sity one obtains nanofibers with different diameters, typically between few tens of nanometers and few tens of microns.

RESULTS AND DISCUSSION

A large number of researchers are focusing their attention on nanopolymers. Their properties are important for practical application in different devices like solar cells, biosensors, light emitting diodes (LEDs), …etc[11-14]. How- ever, as seen from Figure 1 there is a random fluctuation in the process of fibres formation and influence of experimental conditions to make the shakebetween the electrodes for a homogenous fibre formation. The study of the fluctuation-induced inhomogeneities, which are the main physical reason limiting the spatial resolution of polymeric structures obtained by nanopoly- merization, are in that sense very important.

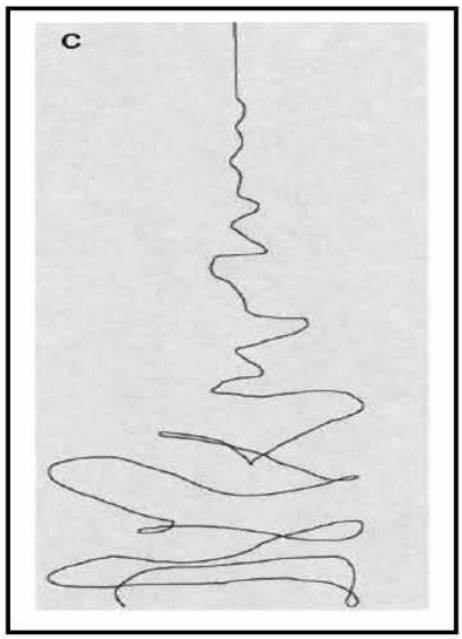

FIGURE 1
The shape of nano fiber of polymer product from electrospining [21].

The internal pressure dependence on the

Pure Sciences International Journal of Kerbala

Journal Homepage:https://journals.uokerbala.edu.iq/index.php/psijk

distance between electrodes for different density of polymers is shown in Figure 2. It is seen that for all polymer densities the internal pressure increases with increasing dis- tance between the electrodes, as expected. One can see also that at the same distance between the electrodes the internal pressure is larger in polymers with larger polymer density. These results, derived from Equation 7, are important for many applications and are subject of many related research [15-17].

The distance between the electrodes affect on the voltage of the systematicdue to the gap between the poles, and because of this the radius of the nanofiber would be decreases his can be showed in the Figure 3, then this figure shows the radius of nanofiber as a function of the distance between the elec-trodes for different density for polymer.

Figure 3 displays the variation of the radius of nanofibers with distance between electrodes. One can see the increases in the values of the radius for the same point with different density of polymer, this may be because make some difficult in explosion for the drops of the polymer between the elec- trodes, and this needs to higher value of voltage to overcome the elasticity for

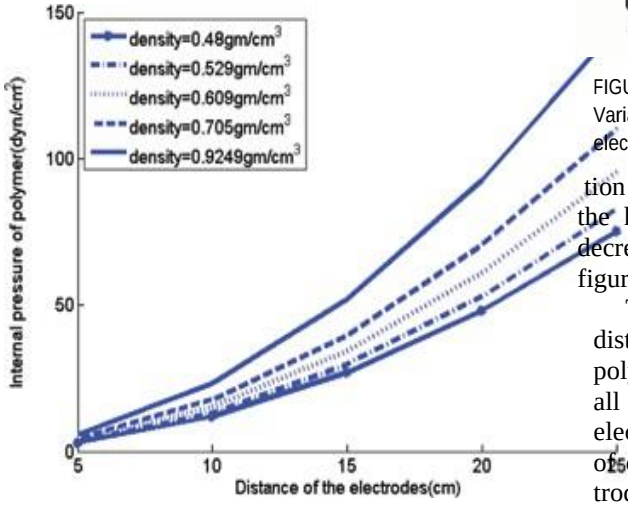

FIGURE 2.
Variation of internal polymer pressure with the distance between electrodes for different polymerdensities.

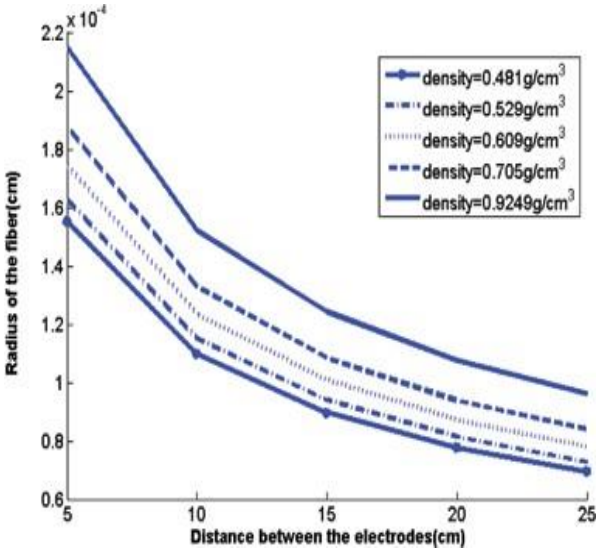

FIGURE 3
Dependence of the nanofiber radius on the distance between electrodes for different polymerdensities.

the polymer. In general, the behaviour of the sketch tends to the decreases the radius of the nanofiber with increases the distance between the electrodes because increases the explosion. The drops of the polymer due to the interac-

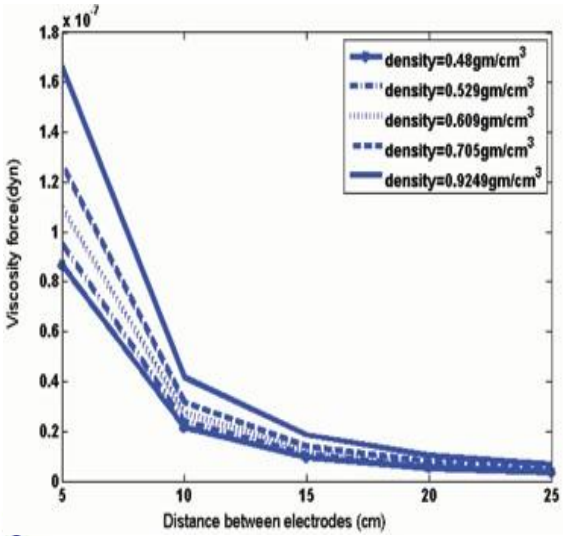

FIGURE 4
Variation of the viscosity force with the distance electrode between electrodes for different polymer densities.

tion between the charges on the surface of drop and the higher voltage of the systematic, which make decreases the radius of the nanofiber as shown in this figure.

The viscosity force dependence on the distance between the electrodes *z*, for the studied polymers, is shown in Figure 4. As expected, for all of them the force is decreasing when drifting electrodes apart. This may bedue to an exhaustion ofcharges through the distance between the electrodes when it builds up to the end. For a given distance between the electrodes the viscosity force is increasing. This can be interpreted by a large interaction between the polymer chains. This is an important point because by controlling the viscosity force may lead to obtaining new nano polymers [18-20].

4. CONCLUSIONS

We have studied influence of the polymer density and distance between the electrodes on three important for practical application parameters of nanofi- bers:

a. radius of nanofiber,
b. internal polymer pressure,
c. viscosity force.

Pure Sciences International Journal of Kerbala

Journal Homepage:https://journals.uokerbala.edu.iq/index.php/psijk

From this work one can show the effective for different polymer density on some parameter, which makes different properties of polymer nanofiber and causes variety applications. Polymer density decreases the radius of the nano-fiber polymer when its decreases, and in general the radius become very small when the nanofiber closes to the base. The internal pressure become high when the polymer density increases, and become highest near the base the viscosity force increases when the polymer density increases. All this may be come from the charge inside the polymer. The different numbers of this charge make different behaviour for this nanofiber of polymer.

REFERENCES

[1] Chronakis, I.S., (2005), Novel nanocomposites and nanoceramics based on polymer nano- fibers using electrospinning process—a review, Journal of Materials Processing Technol-ogy, 167(2-3), 283-293..

[2] Deitzel, J.M., et al., (2001), The effect of processing variables on the morphology of elec- trospun nanofibers and textiles, Polymer, 42(1), 261.

[3] Frenot, A. and I.S. Chronakis, (2003), Polymer nanofibers assembled by electrospinning, Current opinion in colloid & interface science, 8(1), 64-75.

[4] Andrea Camposeo, F.T., Maria and M.A. Moffa, (2013), yal Zussman, Dario Pisignano, Local mechanical properties of electrospun fibers correlate to their internal nanostructure,Nano Letters, 13, 5056-5062.

[5] Ahmed, F.E., B.S. Lalia, and R. Hashaikeh, (2015), A review on electrospinning for mem- brane fabrication, “challenges and applications. Desalination”, 356, 15-30.

[6] Obaid, M., et al., (2015), Effective and reusable oil/water separation membranes based on modified polysulfone electrospun nanofiber mats, Chemical engineering journal, 259, 449-456

[7] Xiong, X., et al., (2015), Flexible membranes of MoS 2/C nanofibers by electrospinning as binder-free anodes for high-performance sodium-ion batteries, Scientific reports, 5,(9254.

[8] Yoshimoto, H., et al., (2003), A biodegradable nanofiber scaffold by electrospinning and its potential for bone tissue engineering, Biomaterials, 24(12), 2077-2082.

[9] AFML, Y.W., (2007), Dynamic Modeling of the electrospinning process, Advanced mate-rials and process Engineering laboratory UBC.

[10] Thota, B.N., et al., (2018), Supramolecular Copolymerization as a Strategy to Control the Stability of Self Assembled Nanofibers, Angewandte Chemie International Edition, 57(23), 6843-6847.

[11] Bendrea, A.-D., L. Cianga, and I. Cianga, (2011), Progress in the field of conducting poly-mers for tissue engineering applications, Journal of biomaterials applications, 26(1), 3-84.

[12] Huang, J., et al., (2004), Nanostructured polyaniline sensors, Chemistry-A European Jour- nal, 10(6), 1314-1319.

[13] Liu, Y., et al., (2008), Controlling numbers and sizes of beads in electrospun nanofibers, Polymer International, 57(4), 632-636.

[14] Cremar, L., et al., (2018), Development of antimicrobial chitosan based nanofiber dress- ings for wound healing applications, Nanomedicine Journal, 5(1), 6-14.

[15] Yan, T., Z. Wang, and Z.-J. Pan, (2018), A highly sensitive strain sensor based on a carbon- ized polyacrylonitrile nanofiber woven fabric, Journal of Materials Science, 53(16),11917-11931.

[16] Sevilla, M., et al., (2018), Optimization of the Pore Structure of Biomass-Based Carbons in Relation to Their Use for CO2 Capture under Low-and High-Pressure Regimes, ACS applied materials & interfaces, 10(2), 1623-1633.

[17] Garcia, C., et al., (2018), Self-powered pressure sensor based on the triboelectric effect and its analysis using dynamic mechanical analysis, Nano Energy, 50, 401-409.

[18] Park, S.M., et al., (2018), Direct fabrication of spatially patterned or aligned electrospun nanofiber mats on dielectric polymer surfaces, Chemical Engineering Journal, 335, 712- 719.

[19] Forward, K.M. and G.C. Rutledge, (2018), Formation of core-shell fibers and particles by free surface electrospinning, Google Patents.

[20] Naeimirad, M., et al., (2018), Recent advances in core/shell bicomponent fibers and nano- fibers: A review, Journal of Applied Polymer Science, 135(21), 46265.

[21] Shin, Y. et al., Experimental characterization of electrospinning : the electrically forced jetand instabilities Polymer, 2001. 42(25)p. 09955-09967.

.

First Year-First Folder-Number: 0
PSIJK 184-191

Pure Sciences International Journal of Kerbala

Journal Homepage:https://journals.uokerbala.edu.iq/index.php/psijk

First Year-First Folder-Number: 0
PSIJK 184-191

Pure Sciences International Journal of Kerbala

Journal Homepage:https://journals.uokerbala.edu.iq/index.php/psijk

Chain Topology on Finite Sets

[1] Reyadh D. Ali , [2] Attalla T. AL-Ani

[1] Department of Mathematics, College of Education for Pure Science, University of Kerbala
[2] Department of Mathematics, College of Education for Pure Science, Ibn Al-Haithem , University of Baghdad

reyadh_delphi@uokerbala.edu.iq

Abstract:

In this work we give formulas for the numbers of T_0 chain topologies and non semi T_1 chain topologies on a set of n elements.

1 Introduction:

D. Stephen[1] gives a formula for the numbers of chain topologies on a set of n elements,N.L.Levine[2] gives the definition of semi –open sets and S. N. Maheshwari[10] gives definitions of semiT_0 and semiT_1.The aim of this paper is to find numbers of T_0 chain topologies and non semi T_1 chain topologies on a set of n elements and to study some necessary and sufficient conditions for chain topologies to satisfy certain separation properties.

Definition1.1[1]

A topology T on a set X is called a chain topology iff T is linearly ordered by inclusion $\subset$.If T is topology on$X$, and then X is called a chain space.

Definition1.2[2]

Let (X,T) be a topological space.A Subset A of X is called semi open iff for some open set O , $O \subset A \subset CLO$, Where CLO denotes the closure of O.

DefinitionS1.3[3]

A Topological space (X,T) is called semi regular iff for each closed set F in X and each $x \notin F$, there are disjoint semi open sets V_1 and V_2 in X such that$x \in V_1$ and $F \subset V_2$.

DefinitionS1.4[4]

A Topological space (X,T) is called semi connected if X cannot be written as disjoint union of two nonempty semi open sets different from X .

DefinitionS1.5[5]

A Topological space (X,T) is called R_0 iff for each open set V in X and $x \in V$,$we\ have\ \overline{\{x\}} \subset V$.

DefinitionS1.6[6]

A Finite connected topology is normal iff the intersection of all nonempty closed sets is nonempty.

DefinitionS1.7[7]

A Topological space (X,T) is called extremelly disconnected iff the closure of every open set in X is open.

DefinitionS1.8[3]

If a topological space (X,T) is extremally disconnected then $S.O.(X)$ is topology on(X) such that $S.O.(X)$ the collection of all semi open sets in X.

DefinitionS1.9[8]

Pure Sciences International Journal of Kerbala

Journal Homepage:https://journals.uokerbala.edu.iq/index.php/psijk

A Topological space (X,T) is called dense topology iff every member of T is dense in X.

Theorem 1.10

Let (X,T) be a chain space .Then

(i) Every subspace of (X,T) is a chain space.

(ii) (X,T) is hereditary normal.

(iii) $|T| \leq |X| + 1$ if X is finite.

(iv) (X,T) and $S.O(X)$ Are dense topologies on$X$.

(v) (X,T) Is R_0 iff it is indiscrete.

(vi) (X,T) Is regular iff it is indiscrete.

(vii) (X,T) Is semi regular iff it is indiscrete.

$(viii)$ (X,T) Is semi connected.

Proof

We prove $(i)-(v)$ only and others follow by the same technique.

(i) Let A be a subset of X and suppose that $(A, {}^{T}/_{A})$ is not a chain space. Then there exist two open sets B_1 and B_2 $in\ X\ such\ that$ $A \cap B_1 \not\subset A \cap B_2$ and $A \cap B_2 \not\subset A \cap B_1$ .It follow that $B_1 \not\subset B_2\ and\ B_2 \not\subset B_1$. This contradicts that (X,T) is a chain space.

(ii) Since every chain space is normal the result follows from (i).

(iii) Suppose $X = \{a_1, a_2, \dots, a_n\}$ .Then regardless of order, a maximal topology T on X should be of the form $\{\emptyset, \{a_1\}, \{a_1, a_2\}, \dots, X\}$.
So $|T| = n + 1 = |X| + 1$.

(iv) The closure of each open set in X is equal to X .so is a dense topology. It follows also that $S.O(X)$ is topology on X [10] .Obviously this topology is dense.

(v) Let $X\ be\ R_0$ and X is not indiscrete. Then there is an open set $V\ in\ X$ such that $V \neq \emptyset\ and\ V^C \neq \emptyset$ .So there is $x \in V$ consequently $\overline{\{x\}} \subset V$ .Then $\overline{\{x\}}^C$ is open in X and neither $\overline{\{x\}}^C \not\subset V\ nor\ V \not\subset \overline{\{x\}}^C$. Thus (X,T) is not a chain space .The converse is clear.

2 The Number of T_0 Chain Topologies on a Finite Set

Definition2.1 [9]

A Topological space (X,T) is called T_0if for every two distinct points x,y in X there exists an open set in X containing one of them.

Theorem2.2

If $C_0(n)$ the numbers T_0 chain topologies on a finite set X having n elements then$C_0(n) = n!$.

Proof

Regardless of order a T_0 chain topology on the set $X = \{a_1, a_2, \dots, a_n\}$ must be of the form $\{\emptyset, \{a_1\}, \{a_1, a_2\}, \{a_1, a_2, a_3\}, \dots, X\}$ obviously there are $n!$ such topologies. Thus $C_0(n) = n!$

3. The Number of Non Semi T_1 Chain Topologies on a Finite Set

Definition3.1[10]

A Topological space (X,T) is called semi T_0if for every two distinct points x,y in X there exists a semi open set in X containing one of them. It is

Pure Sciences International Journal of Kerbala

Journal Homepage:https://journals.uokerbala.edu.iq/index.php/psijk

called semiT_1 iff for every pair of distinct points x, y in X there exist semi open sets V_1 and V_2 such that V_1 contains x but not y and V_2 contains y But not x.

Remark 3.2

It is obvious that a topology T on a set X is semi T_1 if T contain a singleton $\{a\}$ such that $\overline{\{x\}} = X$ .More over if X is a chain space then the converse is also true.

Theorem3.3

If $C_S(n)$ the numbers non semi T_1 chain topologies on a finite set X having n elements then

(i) $C_S(1) = 1$, $C_S(2) = 1$

(ii)

$$C_S(n) = 1 + \sum_{i=2}^{n-1} \binom{n}{i} C_S(n)$$

Proof

(i) Obvious

(ii) Let T be a non semi T_1 chain topologies on a finite set X defined as follows

$$T = \{A_{P_i} : A_{P_i} \subset X, i = 1, \dots, k\} \cup \{\emptyset, X\}$$

such that

$$\emptyset \subset A_{P_1} \subset A_{P_2} \subset \cdots \subset A_{P_k} \subset X \quad where\ P_i > 0$$

And A_{P_i} set of P_i elements .Then A_{P_i} is not a singleton for otherwise should be semi T_1 .Consequently $T/_{A_{P_k}}$ being a chain topology on A_{P_k} , is not semi T_1 on the other hand it is obvious that every chain topology on A_{P_k} which is not semi T_1 gives a chain topology on X , by adding X only , which is not semi T_1 .The number of chain topologies on A_{P_k} which are not semi T_1 is$C_S(P_k)$ .Therefore there are $\binom{n}{P_k} C_S(P_k)$ chain topologies on X which are

3

not semi T_1 having a set of P_k elements as largest open set other than X . The indiscrete topology being non semi T_1 , we get

$$C_S(n) = 1 + \sum_{i=2}^{n-1} \binom{n}{i} C_S(n)$$

Remark 3.4

It is obvious that (X, T) is semi T_0 chain space iff (X, T) is semi T_1 chain space .

References

[1]D. Stephen, Topology on finite sets, Amer. Math. Monthly 75 (1968), 739-741.
[2]N.L. Levine, Semi-open sets and Semi-continuity in topological Space, Amer. Math. Monthly 70 (1963), 36-41.
[3]A.H. Naser, On Separation Properties, M.Sc. Dissertation ,Uni. Of Baghdad (1989) .
[4]T. Thompson, Characterizations of irreducible spaces, Kyungpook Math. J. 21(1981), 191-194.
[5]A.S. Davis, Indered systems of neighborhoods for general topological space, Amer. Math. Monthly 68 (1961), 886-893.
[6]K.H. Kim , Posets and finite Topologies, Pure and App. Math. Sc.,XIV,No.1-2(1981), 9-22.
[7]L.A. Steen and J. A. Seebach, Counter examples in topology, Holt,Rinehart Winston (1970).
[8] N.L. Levine, Dense topologies, Amer. Math. Monthly, V.75, N. 80 (1968).

Pure Sciences International Journal of Kerbala

Journal Homepage:https://journals.uokerbala.edu.iq/index.php/psijk

[9]J. L .Kelley, General Topology, D. Van. Nostrand Co., Princeton, N.J., (1955).

[10]S.N. Maheshwari, Some new separation axiom, Ann. Soc. Sci. Bruxelles89 (1975), 395-402.

First Year-First Folder-Number: 0
PSIJK 184-191

Pure Sciences International Journal of Kerbala

Journal Homepage:https://journals.uokerbala.edu.iq/index.php/psijk

SARS-COV2: Genome, animal reservoir, laboratory diagnosis and Treatment

Ayser Ashour Khalaf[1]; Alaa Shahid Jassim AL-Bdery [2];Zahraa J. Jameel[3];
[1]Department of Biology, Collage of Education for pure science, Kerbala university,Kerbala.
[2]Department of Biology, Faculty of Education for Girls, University of Kufa/Iraq.
[3]Department of Biology, College of Science Diyala University, Diyala, Iraq.

Abstract

Background: Severe acute respiratory syndrome coronavirus2 (SARS-COV2) caused Coronavirus Disease 19 (COVID-19) was identified with use of next generation sequencing in Wuhan, in the Hubei province of China (accession number MG772933.1). **Objective**: The present study highlighted on the genetic diversity of covid-19 and showed the ways for diagnosis ,the transmission and the varity of treatment that are used for covid -19. **Methods:** including Specimens collection nasopharyngeal swab (NP),Oropharyngeal swab (OP), Molecular methods RT- PCR Diagnostic, Serological Methods ELISA technique and rapid antigen tests, Chest X-ray examination **Results:** As a results showed that The orf1ab and orf1a genes located at the 5′-terminus of the genome while The 3′-terminus of the genome contains four structural proteins (S, E, M, and N) and eight accessory proteins (3a, 3b, p6, 7a, 7b, 8b, 9b, and orf14). **Conclusions** :It shows that the transmission rate of SARS-CoV-2 is higher than SRAS-CoV and the reason could be genetic recombination event at S protein in the RBD region of SARS-CoV-2 may have enhanced its transmission ability, also the molecular diagnosis is the most accuracy than other ways and there was not specific drug for treatment of covid-19.

Key words : SARS-COV2, Genom , Diagnosis , reservoir, treatment

Introduction `

The World Health Organization has classified coronary disease 19 (COVID-19) as a pandemic (1). In December 2019 in Wuhan, Hubei Province, China, acute respiratory syndrome (SARS) and respiratory syndrome (SARS-CoV -2) 2 were recognized.(2) The ability to spread is one of the most important characteristics of this virus and causes severe diseases for patients and the elderly [3,4]. In Coronaviridae, coronavirus (CoV) belongs to the genus Coronavirus All RNA CoVs are polymorphic and have a crown-shaped polymers due to the presence of spike glycoproteins on the envelope. With a size of 80-160 nm and positive polarity 27-32 kb. It should be noted that these viruses are caused by mutation and reassembly. [5] Due to the continuous development of transcription errors and RNA Polymerase (RdRP) hops, very high recombination rates for CoVs. With high mutation rate, Coronaviruses are animal pathogens found in different humans and animals[6,7] For the first time, the SARS-CoV-2 gene sequence change has been reported. Where scientists believe that genetic changes may enhance the virulence of the virus over there Two common strains, the deadly "L" strain and the less severe "S" strain [8].According to open science, SARS-CoV-2 research is the fastest moving material in human history. Within months, thousands of data and reports were published regarding the origin,

Pure Sciences International Journal of Kerbala

Journal Homepage:https://journals.uokerbala.edu.iq/index.php/psijk

genomics, genome evolution, vaccine or treatments, and molecular diagnosis of COVID-19 have been published [9,10,11,12]. SARS-CoV-2, the novel coronavirus behind COVID-19 pandemic is acquiring new mutations in its genome , Although some mutations provide benefits to the virus against human immune response, a number of them may result in their reduced pathogenicity and virulence . Although the origin of the virus continues to be a mystery, COVID-19 has displayed higher divergence in genomic sequence to its potential origins (Bat-CoV-RaTG13, or Pangolin-CoV-2019)[13](than antecedently anticipated[14] . The ordination of COVID-19 is undergoing continuous evolution. Simply months once the virus was initial reported[15,16] , there are over a hundred substitution sites known in COVID-19's macromolecule secret writing region. Most of those mutations area unit placed within the secret writing region of polyprotein 1ab (pp1ab, ORF1)[17] and structural proteins[18] The source mentioned that a previous study highlighted the evolution of the virus into two subtypes (L and S) classified by 2 complete coupled single ester polymorphisms (SNPs) at ordination locations 8792 and 28144[14] . SNP 29144 results in associate degree aminoalkanoic acid modification from LEU (L) to SER (S) in ORF8, that is meant to be associated with infective agent replication[19] . [14] found that S is quite expected that a quantity is less aggressive but more adjustable than L and in the future it will increase with frequency.5 Recent studies have indicated that one of the important mechanisms for the evolution of the virus in nature is the deletion and / or replacement of nucleotides and amino acids (AA) in the whole genome of SARS-CoV-2 (20,21,). Furthermore, high genomic diversity and rapid development of RNA viruses, receptor binding mutations (RBD), and new strains may help eliminate neutralization by antibodies targeting RBD (22). Therefore, non-RBD functional areas of diabetes S can be efficiently chosen to develop effective preventive and curative interventions against SARS-CoV-2 [23].

Genome

Several studies have analyzed genes for eighty-six whole or almost complete genomes of SARS-CoV-2 and revealed numerous mutations and deletions in cryptographic and non-coding regions. These studies provide evidence of the genetic diversity and rapid development of this new coronavirus[24]. Chan et al. have proven that the genome of the new HCoV, isolated from a cluster-patient with atypical pneumonia after visiting Wuhan,and had 89% nucleotide identity with bat SARS-like-CoVZXC21 and 82% with that of human SARS-CoV[25].

The number of open reading frames (ORFs) in the CoV genome ranges from 6-14 ,which they encoded 27 non structural proteins nsps[26]. CoV genetic material is susceptible for frequent recombination process, which can give rise to new strains with alteration in virulence[27]. The RNA genome of CoV has seven genes that are conserved in the order: ORF1a, ORF1b, S, OEF3, E, M, N in 5' to 3' direction. The two-third part of the RNA genome is covered by the ORF1a/b, which produces the two viral replicase proteins polyproteins (PP1a and PP1ab) which they encoded chymotrypsin-like protease 3CLPro ,Main protease Mpro and 1-2 papain –like protease to produce 16 nsps[28]. Because of the lack of polymerase syntax checking activity, therefore, RNA viruses has a high mutation rate. This results in RNA viruses vulnerable to developing drug resistance and escape from immune surveillance. SARS-CoV-2 has yet to have a

Pure Sciences International Journal of Kerbala

Journal Homepage:https://journals.uokerbala.edu.iq/index.php/psijk

clear mutation rate. Nevertheless, bearing in mind that the average number of differences in the even-numbered sequence was 4 (the spring range, 3--6) of the 110 sequences collected between December 24, 2019 and February 9, 2020, the mutation rate should be in the same order in SARS- CoV (0.80-2.38 x 10-3 substitution of nucleotides per site per year) [29]. The high rate of mutation results in a high level of variables within the body in RNA viruses [30]. The average total of intrahost variation in patients with COVID-19 was 4 for variants with frequency ≥ 5 % , and this incidence did not be different knowingly from that described in a study on Ebola (655 variants with frequency $\geq$ 5 % in 134 samples ; P > .05) [31].

In different SARS-CoV-2 isolates, mutations occur mainly in five genes, include S, N, ORF8, ORF3a, and ORF1ab, and there are about 42% of the differences representing non-synonymous mutation[32]. Studies have revealed an increased level of viral diversity in some patients with SARS-CoV-2, indicating that the virus has adapted to the human environment.

Genomes have begun to develop in the population[33].

Considering the close evolutionary relationships, the genome structure of CoV-2 SARS is not surprising similar to that found in other betacoronaviruses viruses, with the order of the 5 - replicase genes ORF1ab-S-envelope (E) - membrane (M) -N - 3 ′. It exceeds 21 KB the length of the ORF1ab gene for SARS-CoV-2 and contains 16 predictable non-structural proteins and a number of downstream open reading frames (ORFs), which may have a function similar to SARS-CoV. An analysis assisted in the availability of a relevant virus from Renolophos Avene (i.e. horseshoe) when sampled in in Yunnan Province , China, in 2013 is comparative genomic analysis[34]. This virus named RaTG13 is like ~96% for SARS-CoV-2 at the nucleotide sequence level[35].The spike proteins consist of two subunit S1 and S2 that had 40% amino acids similar to other SARS-COV . SARS-CoV and MERS-CoV spike proteins bind to different host receptors via different receptor-binding domains (RBDs). The angiotensin-converting enzyme 2 (ACE2) is used by SARS-CoV as one of the main receptors [36]. With CD209L acting as an alternate receptor [37], while MERS-CoV uses dipeptidyl peptidase 4 (DPP4, also known as CD26) as the primary receptor. 2019-nCoV has close evolutionary association with SARS-like coronavirus, as suggested by the Initial analysis [38].

Significantly, orf3b encodes an entirely new short protein. Moreover, the novel orf8 is likely to encode a protein secreted with alpha helix, followed by a beta sheet (s) containing six strands [39]. Another noticeable thing about COVID-19 is the ORF10 that does not contain any similar proteins in a massive NCBI depot. ORF10 is a short protein or peptide with a length of 38 residues. This exclusive protein can be used to detect the virus faster than PCR-based methods [40]. In the other hand the study of [41] indicate of that when more than 3,000 high-coverage and full sequences of the genome deposited in the GISAID database were analyzed, unique: 28881 – 28883 : GGG> AAC three-nucleotide mass mutation in the SARS-CoV-2 genome that produces two sub-strains, designated here as SARS-CoV-2g (28881-28883: the GGG genotype) and SARS-CoV-2a (28881-28883: the AAC genotype). For nations with no elaborate facilities for whole-genome sequencing, RT-PCR based testing should be recommended

Pure Sciences International Journal of Kerbala

Journal Homepage:https://journals.uokerbala.edu.iq/index.php/psijk

by targeting 28881-28883 region. This will give diagnostic information on COVID-19 together with the information on the two sub-strains: SARS-CoV-2a and SARS-CoV-2g in an infected person. This will allow gathering valuable information about the prevalence of these two strains are prevalent in those countries. Potential medications can be designed to target the 28881-28883 N protein region for modifying virus pathogenesis[41].

Animal Reservior and transmission

COVID-19 is a zoonotic disease, control of SARS-CoV-2 requires the reduction of the shedding viruses to the environment from the reservoirs (animal-person transmission) and from humans (person-person transmission). and that may assist development of SARS-CoV-2 therapeutics and vaccines [42] so what the animal reservoirs for SARS-CoV-2? From phylogenetic analyses undertaken with available full genome sequences, bats appear to be the reservoir of SARS COV2 [43] A coronavirus from an animal could possibly have been transmitted to a human, either directly or through an intermediary host such as civets, seafood or ferrets [44,42]. Andersen and his coworkers determined that the most possible origins for SARS-CoV-2 followed one of two likely states Based on viruses genomic sequencing analysis:-

1- the virus evolved to its current pathogenic state through natural selection in an animal host and then jumped to humans. While There are no documented cases of direct bat-human transmission, however, suggesting that an intermediate host was likely involved between bats and humans.

2-non-pathogenic version of the virus jumped from an animal host into humans and then evolved to its current pathogenic state within the human population.

In other research found that ferrets represent an infection and transmission animal model of COVID-19 that may facilitate development of SARS-CoV-2 therapeutics and vaccines [45].

Generally If the cell host harbors different virus of the same species, recombination gives new variants. repair mechanisms and The proofreading may support the selection of recombinant viruses strain in populations [44]. Actually, recombination between the subunits of the spike gene (in coronaviruses) has been discussed as one of the major mechanism complicated in the emergence of human SARS CoV strains from bat and civet ancestors [45]. Fig. 1 provides a schematic of animal groups that may play a role in the evolution of human coronaviruses. the contribution of each Human coronavirus may vary widely from year to year, for example 229E contributing as little as 1% to acut respiratory infections in the community in one year and up to 35% in the next. Furthermore, activity may be hetrogeneous in different geographic regions of the same country [46]

Pure Sciences International Journal of Kerbala

Journal Homepage:https://journals.uokerbala.edu.iq/index.php/psijk

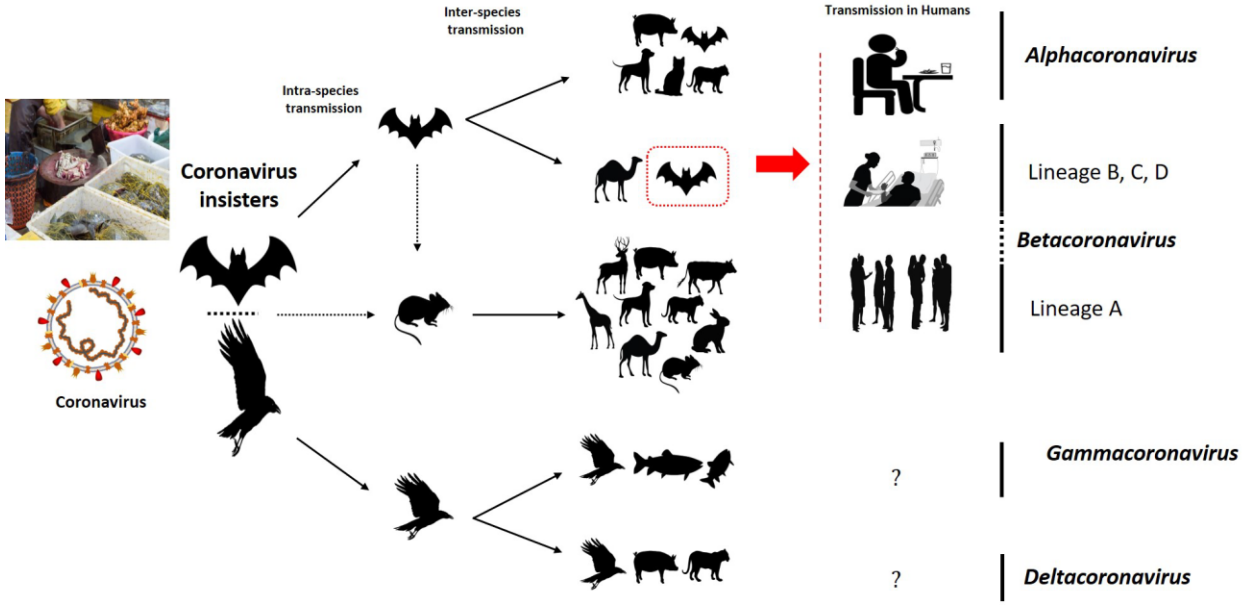

Figure 1: Summary diagram of the animal groups representing natural hosts and the putative intermediate hosts for the coronaviruses (suspected reservoirs of SARS-CoV-2 are red encircled); Dotted black arrow shows the possibility of viral transfer from bat whereas the solid black arrow represents the confirmed transfer (Adnan Shereen et al., 2020)

Human-to-human transmission of SARS-CoV-2 occurs mainly between family members, including relatives and friends who intimately contacted with patients or incubation carriers. It is reported[47] the scientists found that the SARS-CoV-2 molecular structure differed substantially from those of already known coronaviruses[48] that 31.3% of patients recent travelled to Wuhan and 72.3% of patients contacting with people from Wuhan among the patients of nonresidents of Wuhan. Transmission between healthcare workers occurred in 3.8% of COVID-19 patients, issued by the National Health Commission of China on 14 February 2020. By contrast, the transmission of SARS-CoV and MERS-CoV is reported to occur mainly through nosocomial transmission. Infections of healthcare workers in 33–42% of SARS cases and transmission between patients (62–79%) was the most common route of infection in MERS-CoV cases [49]. Direct contact with intermediate host animals or consumption of wild animals was suspected to be the main route of SARS-CoV-2 transmission. However, the source(s) and transmission routine(s) of SARS-CoV-2 remain elusive [50]

Laboratory diagnosis

When samples are collected, the biological safety conditions must be taken into consideration, depending on in terms of maintaining personal safety reported in CDC, and they are collected by health care workers or laboratory professionals [51] the isolation of samples from those infected with the virus is carried out at BSL-3 laboratories, while routine tests are performed in BSL-2 laboratories..[52,53] Specimens collection:On April 8th, CDC Organization explained the sample types and priority .the collecting size of samples is 2-3 ml:-Upper respiratory : nasopharyngeal

Pure Sciences International Journal of Kerbala

Journal Homepage:https://journals.uokerbala.edu.iq/index.php/psijk

swab (NP),Oropharyngeal swab (OP), the synthetic fiber swabs with plastic shafts are used ,the swab put in 2-3 ml of viral trasport medium.-Lower respiratory : bronchoalveolar lavage, tracheal aspirate in severe respiratory disease, sputum(rinse the mouth with water then expoctrate deep cough sputum directly into a sterile leak proof scrow cap sputum collection cup or sterile dry container. if both NP and OP collected should be combined at collection into a single vial for maximizing test sensitivity and limit testing resources. Thus, a nasopharyngeal swab is usually the collection method used to obtain a specimen for testing. Nasopharyngeal specimens may miss some infections; therefore a deeper specimen may need to be obtained by bronchoscopy. [54] SARS-CoVand MERS-CoV RNA are detected from stool, urine and blood specimens, the COVID-19 virus also can be detected in stool, blood and urine specimens but the results less reliably than from respiratory specimens [55,56]. Timing of specimen collection, when viral titres are highest, may improve the diagnostic sensitivity of rapid antigen tests for HCoVs [57] All samples should contain information such as the date of patient contact or the birth of the disease, the patient's condition if he has severe or moderate symptoms and the type of sample in addition to the date the sample was collected.[53]

Storage and Shipping:Specimens for virus detection should reach the laboratory as soon as possible after collection and Store specimen at 4-8 C° for up to 72 days after collection and storage in -70 C° for below if delay of the testing or shipping. The speciemens packaged , shipping and transporting should follow the UN Model Regulation ,and any other applicable regulations depending on the mode of transport being used. When there is likely to be a delay in specimens reaching the laboratory, the use of viral transport medium is strongly recommended. Specimens may be frozen to - 20°C or ideally -70°C and shipped on dry ice if further delays are expected. It is important to avoid repeated freezing and thawing of specimens.[58,59]

Molecular methods:The CDC 2019 –n COV Real time RT- PCR Diagnostic panel for detection and diagnosis of 2019-n COV based on amplification of viral nucleic acid. The upper and lower respiratory tract specimens collected from individuals who contact or confirmed cases with COVID-19 suitable for this technique. The results of his technique are included: Positive results are indicative active infection, while the negative results are not 2019 –n COV, the negative results could not be used as sole basis or treatment they must be combined with the history of patient if he had traveling history , clinical observation and epidemiological information.Many factors lead to the formation of negative results as: the poor quality of the sample being small in size, the delay in taking the sample or collecting it sooner than the appearance of the infection, not handling the sample correctly in terms of correct storage and charging it appropriately or due to technical reasons present in the sample itself such as viral mutations and PCR inhibition. Laboratories that test 19-covid samples, especially in countries where the virus was not previously known. The relevant WHO provides confirmatory testing For 5 positive samples and 10 negative samples collected from patients who are appropriate to determine the case by referring it to a relevant WHO laboratory that provides confirmatory testing.[60]

Serological Methods: It is difficult to diagnose the virus with serological tests and make it a routine work for diagnosis due to

Pure Sciences International Journal of Kerbala

Journal Homepage:https://journals.uokerbala.edu.iq/index.php/psijk

the difficulty in obtaining solutions and commercial materials for the purpose of diagnosis Serological tests support molecular analyzes if the samples are negative, Serum samples can be stored for these purposes and can be tested in ELISA technique For IgG and IgM detecting.[61,62]. The incorporation of colloidal gold-labeled immunoglobulin G (IgG) as the detection reagent is an approach that may increase the sensitivity of rapid antigen tests for respiratory viruses [63]Timing of specimen collection, when viral titres are highest, may improve the diagnostic sensitivity of rapid antigen tests for HCoVs [64].

Radiological Diagnosis: Chest X-ray examination in the early stage of the disease shows interstitial changes and multiple small plaque shadows. Chest CT scans play an important role in the diagnosis of acute respiratory disease syndrome (ARDS) and pneumonia as well as in the early detection of lung parenchymal abnormalities in patients at risk and provide an impression of secondary infection(65).ground-glass opacity (GGO),was the main findingin lower lung lobes; inprogressive stages(5–8days),the progression of lung disease involved three patterns of ground-glass, consolidation, and crazy paving, while in peak stages (9–13 days), dense consolidation became the prevalent feature(66).

Treatment:

When CoV-2 SARS The injury was suspected. In January 2020 the World Health Organization issued directives for the clinical management of SARS. Immediately the implementation of control and prevention with all its strategies Supportive Early Treatment and Prevention of SARS-CoV-2 Emergency Startups in this guide, described in detail [67]. Approved antivirals that did not exist yet SARS-CoV-2 infection. As a result, the virus is disabled and preventive measures stopped In order to control the spread of the disease, it is very necessary Approved antivirals that did not exist yet SARS-CoV-2 infection. This virus can be disabled by using 0.5% hydrogen Peroxide, 62-71% ethanol, 0.1% sodium hypochlorite, 0.7-1% formaldehyde, 2% glutaraldehyde, or 0.23% Povidone desires within a minute. Other antiseptics such as chlorhexidine dicluconate 0.02%, 0.55% orthophtalaldehyde, or 0.05-0.2% benzalkonium chloride is less effective [68].Although each country and region with or without outbreaks of COVID-19 Follow strict prevention or prevention measures, and reported monitoring strategies. World Health Organization , ; Food and Drug Administration (FDA), COV-2 SARS have spread worldwide ,So researchers from all over the world are working around the clock to find ways to slow the spread of the novel[69].

Clinical medicine has approved many medications for use against SARS-CoV-2 infection for clinical trials, such as: lopinavir / ritonavir[60](Lopinavir/ritonavir is a coformulation of two structurally related protease inhibitor (PI) antiretroviral agents. an essential enzyme for production of mature, infective virus. [https://link.springer.com/article/10.2165/00003495-200363080-00004),hg],

Arbidol[70] (Apart from influenza virus, arbidol was reported to inhibit a wide array of viruses by interfering with multiple steps of the virus replication cycle [71]. Interferon-alpha[60](They are secreted by various cell types, notably plasmacytoid dendritic cells, upon recognition of viral

Pure Sciences International Journal of Kerbala

Journal Homepage:https://journals.uokerbala.edu.iq/index.php/psijk

components by pattern recognition receptors (PRR), IFN-I are thus among the first cytokines produced during a viral infection.[72].Type I IFNs-a/b are broad spectrum antivirals, exhibiting both direct inhibitory effects on viral replication and supporting an immune response to clear virus infection [73].The first to suggest therapeutic efficacy in COVID-19 disease is IFN-a2b, an available antiviral intervention. "Furthermore, beyond clinical benefit to the individual patient, treatment with IFN-a2b may also benefit public health measures aimed at slowing the tide of this pandemic, in that duration of viral shedding appears shortened".[74].Favipiravir [70](Favipiravir is a pyrazine carboxamide derivative (6-fluoro-3-hy-droxy-2-pyrazinecarboxamide) and a broad-spectrum antiviral drug approved in Japan for the treatment of influenza in 2014, Favipiravir is a prodrug that is ribosylated and phosphorylated intracellularly to form the active metabolite favipiravir ibofuranosyl-5′-triphos-phate (T-705-RTP)[75].Chloroquine phosphates[70]this drug is a clinically approved drug effective against malaria, and it is known to elicit antiviral effects against several viruses, including SARS-CoV and HCoV-229E [76]. However, in vivo studies were unable to show the antiviral effectiveness of chloroquine against SARS-CoV [77]. There was another study showed the anticoronaviral properties of chloroquine by testing its in vitro and in vivo antiviral activities against the group 2 HCoV-OC43 virus. In the in vitro antiviral experiments, chloroquine showed in vitro antiviral properties against HCoV-OC43 replication in HRT-18 cells, with an EC50 of 0.306 mM [78]. Darunavir/Cobicistat[70] also drug that is a fixed-dose antiretroviral combination tablet indicated for the treatment of human immunodeficiency virus (HIV-1) infection. The drug works by selectively inhibiting the cleavage sites of HIV-1-encoded Gag-Pol polyproteins in infected cells, thereby preventing the formation of mature virus particles[https://www.clinicaltrialsarena.com/projects/prezcobix-darunavircobicistat-for-the-treatment-of-hiv-1/] . oseltamivir[70]this drug inhibits the neuraminidase enzyme, which is expressed on the viral surface,this enzyme promotes release of virus from infected cells and facilitates viral movement within the respiratory tract. In the presence of neuraminidase inhibitors, virions stay attached to the membrane of infected cells and are also entrapped in respiratory secretions [79], and methylprednisolone[70] are the classical immunosuppressive drugs, which are important to stop or delay the progress of the pneumonia, and have been proved to be effective for the treatment of acute respiratory distress syndrome (ARDS). In a recent study[80] found the administration of methylprednisolone appeared to reduce the risk of death in COVID-19 pneumonia patients with ARDS, however, of those who received methylprednisolone treatment, 23 of 50 patients died. This is a rather high mortality rate of ~50%; therefore, in terms of the indication, timing, dosage and duration, the application of methylprednisolone warrants further investigation.

Thus, other studies lead to that collective treatment of azithromycin and hydroxychloroquine has been investigated to decrease detection of viral RNA associated to the control group [81].However, concomitant cardiovascular diseases that are present in The study population, may partly explain the observation Cardiovascular toxicity and risk increased with use Chloroquine or hydroxychloroquine,

Pure Sciences International Journal of Kerbala

Journal Homepage:https://journals.uokerbala.edu.iq/index.php/psijk

especially when You use it with macrolides[82].

A study[83] stated that combining lopinavir and ritonavir SARS-CoV Clinically demonstrated benefits for patients)Less negative clinical outcomes) While [84] reported that lopinavir and ritonavir, two protease inhibitors failed totally to treatment this disease .Generally that Interferon beta-1b، Lopinavir and ritonavir are among Middle East respiratory syndrome patients Infection in the Kingdom of Saudi Arabia[85]. Preclinical evidence demonstrated of the effectiveness of remedesvier (broad spectrum antiviral nucleotide prodrug) to treat MERS-CoV and SARS-CoV infections[86].

There are many preparations (formulations) containing minerals that have antiviral activity, including cheap, safe and readily available zinc[87]. These formulations can be used as combination therapies or as adjuvant therapy aids with cyclosporine, lopinavir-ritonavir, monoclonal antibodies, ribavirin, remdesivir, interferon beta-1b, and antiviral peptides targeting 2019-nCoV[88]. a monoclonal antibody, Tocilizumab that targets the interleukin 6 receptor . It has good safety features. So that monoclonal and Polyclonal antibodies are developed for 2019-nCoV for prevention after exposure[89]. Pneumonia by COVID-19 seems to be a lung injury caused by the hyper activation immune effector cells. A great dose of vitamin C can lead to immunosuppression at the level of these effects. Hence, a high dose of vitamin C intravenously can be a useful and safe choice for treatment in the early stages of COVID-19[90].

Among recent immunotherapy treatments include the use of convalescent plasma or immunoglobulin as a last resort to improve the survival rate of SARS patients who have not benefited from other treatments.. Also, several studies have shown Shorter hospital stays and patient mortality were reduced when Treated with convalescent plasma from those who were Convalescent plasma is not treated[91]. As a treatment without severe adverse complications. However, testing is important Safety and efficacy of recovery Plasma transfer in patients With SARS - CoV – 2[92]. Several monoclonal antibodies (mAbs) targeting non-RBD regions, particularly the N-terminal domain (NTD) has recently been reported [93]. In addition to spike protein, two smaller proteins, E and M might also play important role in the viral assembly of a coronavirus, and can boost the immune response against SARS-CoV [94].

Recently there are studies that have shown the results of new X-ray crystallization results released from the major protein of SARS-CoV-2 (Mpro), computational approaches within our plans [95]. in order to contribute to an effective treatment of SARS-Cove-2 and thus, increase speed Mathematical analyzes are of these methods for the reason that they allow millions of data to be processed simultaneously [96]. A set of computational methods and algorithms included in molecular anchoring that seeks through their targets to modern relationships between targets and chemical bonds through modeling direct physical interaction with them [97].

In a study [98], it was found that preparing to evaluate some drugs that are covalent and irreversible reactions, and which may have a strong epidemiological strategy. Simulation

Pure Sciences International Journal of Kerbala

Journal Homepage:https://journals.uokerbala.edu.iq/index.php/psijk

of molecular dynamics can provide many parts of the image obtained from covalent docking.

The biological treatments as melatonin (N-acetyl-5-methoxytryptamine) is a biologically active molecule and a well-known anti-inflammatory and antioxidant molecule, with a host of health-enhancing features; use melatonin Successfully treat delirium, sleep disorder, atherosclerosis and respiratory system viral diseases and infections. Melatonin is effective in critical care patients by reducing vessel permeability and anxiety, using anesthesia, and improving sleep quality, which may also be beneficial for achieving better clinical outcomes for patients with COVID-19. It is worth noting that melatonin is very safe[99].

There is an urgent need to better understand this new virus and to develop ways to control its spread. A study [100], this study sought to obtain insights for the design of a vaccine against SARS-CoV-2 by checking for elevation Genetic similarities between SARS-CoV-2 and SARS-CoV, which caused the outbreak in 2003, and also benefit from existing SARS-CoV immunological studies. By sifting experimentally identification B cells and T cells derived from SARS-CoV in SARS-CoV immune structural proteins, This study identified a group of B-cell and T-cell-derived T cells from the spike (S) and nucleocapsid (N). Proteins that are completely identical to SARS-CoV-2.

A study has stated that viral S protein subunit vaccines produced high titres neutralizing antibody and more complete protection than live-attenuated SARS-CoV, full-length S protein, and DNA-based S protein vaccines. Protein vaccines that include the protein S unit vaccine and vaccines that specifically target the receptor binding range (RBD) of the S1 subunit of the viral S protein. Taken together, the target site is the preferred S protein / gene in the development of SARS vaccine / Middle East Respiratory Syndrome, and that the strategy can be useful in developing SARS vaccines - CoV-2[101].

Conclusions

Scientists have made progress in characterizing the new coronavirus but there are still many questions to be answered. infected person is the major factor in disease transmission. Health-care workers must also follow CDC guidelines. Any mutation occurring will be especially important. Further studies are needed to characterize how these differences affect the functionality and pathogenesis of 2019-nCoV.

References

1-Cascella M, Rajnik M, Cuomo A, Dulebohn SC, Di Napoli R. Features, Evaluation and Treatment Coronavirus (COVID-19). In: StatPearls [Internet]. Treasure Island (FL): StatPearls Publishing; 2020

2- Wang C, Horby PW, Hayden FG, Gao GF. A novel coronavirus outbreak of global health concern. *Lancet*2020.

3- Guan,W.-J.; Ni, Z.-Y.; Hu, Y.; Liang,W.-H.; Ou, C.-Q.; He, J.-X.; Liu, L.; Shan, H.; Lei, C.-L.; Hui, D.S.; et al. Clinical characteristics of coronavirus disease 2019 in China. New Engl. J. Med. 2020.

4- Guo, Y.-R.; Cao, Q.-D.; Hong, Z.-S.; Tan, Y.-Y.; Chen, S.-D.; Jin, H.; Tan, K.-S.; Wang, D.-Y.; Yan, Y. The origin, transmission and clinical therapies on

Pure Sciences International Journal of Kerbala

Journal Homepage:https://journals.uokerbala.edu.iq/index.php/psijk

coronavirus disease 2019 (COVID-19) outbreak—An update on the status. Mil. Med Res. 2020, 7, 1–10.

5- Lu, R.; Zhao, X.; Li, J.; Niu, P.; Yang, B.; Wu, H.; Wang, W.; Song, H.; Huang, B.; Zhu, N.; et al. Genomic characterisation and epidemiology of 2019 novel coronavirus: Implications for virus origins and receptor binding. Lancet 2020. 395, 565–574.

6- Woo PC, Huang Y, Lau SK, Yuen KY. Coronavirus genomics and bioinformatics analysis. Viruses 2010;2:1804–20.

7- Yin Y, Wunderink RG. MERS, SARS and other coronaviruses as causes of pneumonia. Respirology 2018;23:130–7.

8-Tang, X.; Wu, C.; Li, X.; Song, Y.; Yao, X.; Wu, X.; Duan, Y.; Zhang, H.; Wang, Y.; Qian, Z.; et al. On the origin and continuing evolution of SARS-CoV-2. Natl. Sci. Rev. 2020.

9-Islam, M. T., Croll, D., Gladieux, P., Soanes, D. M., Persoons, A., Bhattacharjee, P., Hossain, M. S., Gupta, D. R., Rahman, M. M. and Mahboob, M. G. (2016). Emergence of wheat blast in Bangladesh was caused by a South American lineage of *Magnaporthe oryzae*. BMC Biol. 14, 84. doi:10.1186/s12915-016-0309-7

10- Phan, T. Genetic diversity and evolution of SARS-CoV-2. *Infect. Genet. Evol. 2020* 81, 104260.

11- Shereen, M. A., Khan, S., Kazmi, A., Bashir, N., and Siddique, R. COVID-19 infection: origin, transmission, and characteristics of human coronaviruses. *J. Adv. Res. 2020*

12- Zhang, J., Zeng, H., Gu, J., Li, H., Zheng, L., and Zou, Q. Progress and Prospects on Vaccine Development against SARS-CoV-2. *Vaccines(2020a).* 8(2), 153.

13- Lam TT-Y, Shum MH-H, Zhu H-C, Tong Y-G, Ni X-B, Liao Y-S, Wei W, Cheung WY-M, Li W-J, Li L-F, et al. Identification of 2019-nCoV related coronaviruses in Malayan pangolins in southern China. 2020.

14- Tang X, Wu C, Li X, Song Y, Yao X, Wu X, Duan Y, Zhang H, Wang Y, Qian Z, et al. On the origin and continuing evolution of SARS-CoV-2. National Science Review. 2020.

15-Lu R, Zhao X, Li J, Niu P, Yang B, Wu H, Wang W, Song H, Huang B, Zhu N, et al.. Genomic characterisation and epidemiology of 2019 novel coronavirus: implications for virus origins and receptor binding. Lancet2020 395:565-574.

16- Ralph R, Lew J, Zeng T, Francis M, Xue B, Roux M, Toloue Ostadgavahi A, Rubino S, Dawe NJ, Al-Ahdal MN, et al. 2019-nCoV (Wuhan virus), a novel Coronavirus: human-to-human transmission, travel-related cases, and vaccine readiness. J Infect Dev Ctries 2020.14:3-17.

17- Namy O, Moran SJ, Stuart DI, Gilbert RJ, Brierley I. A mechanical explanation of RNA pseudoknot function in programmed ribosomal frameshifting. Nature 2006. 441:244-247.

18- Fehr AR, Perlman S.. Coronaviruses: an overview of their replication and pathogenesis. Methods Mol Biol 2015 1282:1-23.

19- Muth D, Corman VM, Roth H, Binger T, Dijkman R, Gottula LT, Gloza-Rausch F, Balboni A, Battilani M, Rihtaric D, et al. Attenuation of replication by a 29 nucleotide deletion in SARS-coronavirus acquired during the early stages of human-to-human transmission. Sci Rep. 2018 8:15177.

Pure Sciences International Journal of Kerbala

Journal Homepage:https://journals.uokerbala.edu.iq/index.php/psijk

20- Islam, M. T., Croll, D., Gladieux, P., Soanes, D. M., Persoons, A., Bhattacharjee, P., Hossain, M. S., Gupta, D. R., Rahman, M. M. and Mahboob, M. G). Emergence of wheat blast in Bangladesh was caused by a South American lineage of *Magnaporthe oryzae*. BMC Biol. . (2016 14, 84. doi:10.1186/s12915-016-0309-7

21- Yin, C.). Genotyping coronavirus SARS-CoV-2: methods and implications. *arXiv* preprint *arXiv (2020)*2003.10965.

22- Rahman, M. S., Hoque, M. N., Islam, M. R., Akter, S., Rubayet-Ul-Alam, A. S. M., Siddique, 829 M. A. et al.. Epitope-based chimeric peptide vaccine design against S, M and E 830 proteins of SARS-CoV-2 etiologic agent of global pandemic COVID-19: an *in silico(2020)* 831 approach. *bioRxiv* doi: https://doi.org/10.1101/2020.03.30.015164.

23- Shang, W., Yang, Y., Rao, Y., and Rao, X. The outbreak of SARS-CoV-2 pneumonia calls for viral vaccines. *npj Vaccines(2020)*. 5(1), 1-3.

24- Phan, Tung. "Genetic diversity and evolution of SARS-CoV-2." Infection, genetics and evolution 81 (2020): 104260.

25-Chan JF, Kok KH, Zhu Z, Chu H, To KK, Yuan S, Yuen KY. Genomic characterization of the 2019 novel human-pathogenic coronavirus isolated from a patient with atypical pneumonia after visiting Wuhan. Emerg Microbes Infect. 2020;9(1):221-236. [PMC free article] [PubMed] [Ref list]

26- Belouzard S, Millet JK, Licitra BN, Whittaker GR. Mechanisms of coronavirus cell entry mediated by the viral spike protein. Viruses. 2012;4:1011–33

27- Hilgenfeld R. From SARS to MERS: Crystallographic studies on coronaviral proteases enable antiviral drug design. FEBS J. 2014;281:4085–96.

28- McBride R, van Zyl M, Fielding BC. The coronavirus nucleocapsid is a multifunctional protein. Viruses. 2014;6:2991–3018.

29- Zhao Z, Li H, Wu X, et al. Moderate mutation rate in the SARS coronavirus genome and its implications. BMC Evol Biol 2004; 4:21.

30- Domingo E, Sheldon J, Perales C. Viral quasispecies evolution. Microbiol Mol Biol Rev 2012; 76:159–216.

31- Ni M, Chen C, Qian J, et al. Intra-host dynamics of Ebola virus during 2014. Nat Microbiol 2016; 1:16151.

32- Zhao, W., Song, S., Chen, M., Zou, D., Ma, L., Ma, Y., Li, R., Hao, L., Li, C., Tian, D., Tang, B., Wang, Y., Zhu, J., Chen, H., Zhang, Z., Xue, Y., Bao, Y., 2020. The 2019 novel coronavirus resource. Hereditas 42, 212–221.

33- Shen, Z., Xiao, Y., Kang, L., Ma, W., Shi, L., Zhang, L., Zhou, Z., Yang, J., Zhong, J., Yang, D., Guo, L., Zhang, G., Li, H., Xu, Y., Chen, M., Gao, Z., Wang, J., Ren, L., Li, M., 2020. Genomic diversity of SARS-CoV-2 in coronavirus disease 2019 patients. Clin. Infect. Dis.

34- Zhou, P., Yang, X.L., Wang, X.G., Hu, B., Zhang, L., Zhang, W., Si, H.R., Zhu, Y., Li, B., Huang, C.L., et al. (2020). A pneumonia outbreak associated with a new coronavirus of probable bat origin. Nature 579, 270–273.

35- Coutard, B., Valle, C., de Lamballerie, X., Canard, B., Seidah, N.G., and Decroly, E. (2020). The spike glycoprotein of the new coronavirus 2019-nCoV contains a furin-like cleavage site absent in CoV of the same clade. Antiviral Res. 176, 104742.

36- Ge X.Y. Li J.L. Yang X.L. Chmura A.A. Zhu G. Epstein J.H. Mazet J.K. Hu B. Zhang

Pure Sciences International Journal of Kerbala

Journal Homepage:https://journals.uokerbala.edu.iq/index.php/psijk

W. Peng C. et al. Isolation and characterization of a bat SARS-like coronavirus that uses the ACE2 receptor. Nature. 2013; 503: 535-538.

37- Jeffers S.A. Tusell S.M. Gillim-Ross L. Hemmila E.M. Achenbach J.E. Babcock G.J. Thomas Jr., W.D. Thackray L.B. Young M.D. Mason R.J. et al. CD209L (L-SIGN) is a receptor for severe acute respiratory syndrome coronavirus. Proc. Natl. Acad. Sci. USA. 2004; 101: 15748-15753

38- Zhou P. Yang X.-L. Wang X.-G. Hu B. Zhang L. Zhang W. Si H.-R. Zhu Y. Li B. Huang C.-L. et al. Discovery of a novel coronavirus associated with the recent pneumonia outbreak in humans and its potential bat origin.

39- Chan, Jasper Fuk-Woo, et al. "Genomic characterization of the 2019 novel human-pathogenic coronavirus isolated from a patient with atypical pneumonia after visiting Wuhan." Emerging microbes & infections 9.1 (2020): 221-236.

40- Koyama, T., D. Platt, and L. Parida. "Variant analysis of COVID-19 genomes." Bulletin of the World Health Organization (2020).

41- Laboratory biosafety guidance related to the novel coronavirus (2019-nCoV), World Health Organization; 2020 (https://www.who.int/docs/defaultsource/coronaviruse/laboratory-biosafety-novelcoronavirus-version-1-1.pdf?sfvrsn=912a9847_2).

42- Kim et al., Infection and Rapid Transmission of SARS-CoV-2 in Ferrets, Cell Host & Microbe (2020), https://doi.org/10.1016/j.chom.2020.03.023

43- Adnan Shereen, M., Khan, S., Kazmi, A., Bashir, N., and Siddique, R. (2020). COVID-19 infection: origin, transmission, and characteristics of human coronaviruses. Journal of Advanced Research S2090123220300540.

44-Kristian G. Andersen, Andrew Rambaut , W. Ian Lipkin, Edward C. Holmes and Robert F. Garry,(2020). The proximal origin of SARS-CoV-2, Nature Medicine, 26 ; 450–455

45-Ekaterina Minskaia, Tobias Hertzig, Alexander E. Gorbalenya, Vale´rie Campanacci, Christian Cambillau,Bruno Canard, and John Ziebuhr (2006). Discovery of an RNA virus 335exoribonucleasethat is critically involved in coronavirus RNA synthesis, Proceedings of the National Academy of Sciences 103(13):5108-13,10.1073/pnas.0508200103

46-Eckerle LD, Becker MM, Halpin RA, et al. Infidelity of SARS- CoVNsp14-exonuclease mutant virus replication is revealed by completegenome sequencing. PLOS Pathog. 2010;6(5):e1000896

47-Peiris, J.S.M. (2012). Coronaviruses. In Medical Microbiology, (Elsevier), pp. 587–593.

48-Guan WJ, Ni ZY, Hu Y, Liang WH, Ou CQ, He JX, et al. Clinical characteristics of coronavirus disease 2019 in China. N Engl J Med. 2020. https://doi.org/10.1056/NEJMoa2002032

49-Kang CK, Song KH, Choe PG, Park WB, Bang JH, Kim ES, et al. Clinical and epidemiologic characteristics of spreaders of middle east respiratory syndrome coronavirus during the 2015 outbreak in Korea. J Korean Med Sci. 2017;32(5):744–9

50-Guo Y, Qing-Dong Cao, Zhong-Si Hong, Tan Y, Chen S, Hong-Jun Jin, Kai-Sen Tan,

Pure Sciences International Journal of Kerbala

Journal Homepage:https://journals.uokerbala.edu.iq/index.php/psijk

De-Yun Wang and Yan Yan.(2020). The origin, transmission and clinical therapies on coronavirus disease 2019 (COVID-19) outbreak – an update on the status, Military Medical Research, 7:11

51- Laboratory biosafety guidance related to the novel coronavirus (2019-nCoV), World Health Organization; 2020 (https://www.who.int/docs/defaultsource/coronaviruse/laboratory-biosafety-novelcoronavirus-version-1-1.pdf?sfvrsn=912a9847_2).

52-Infection prevention and control during health care when novel coronavirus (nCoV) infection is suspected, interim guidance, January 2020. Geneva: World Health Organization; 2020. (https://www.who.int/publications-detail/infectionprevention-and-control-during-health-care-whennovel-coronavirus-(ncov)-infection-is- suspected20200125).

53-Global Surveillance for human infection with coronavirus disease (COVID-2019), Interim guidance, Geneva, World Health Organization, 2020. (https://www.who.int/publicationsdetail/global-surveillance-for-human-infectionwith-novel-coronavirus-(2019-ncov).

54-Michael J. Loeffelholz & Yi-Wei Tang (2020) Laboratory diagnosis of emerging human coronavirus infections – the state of the art, Emerging Microbes & Infections, 9:1, 747-756, DOI: 10.1080/22221751.2020.1745095

55-Cheng PK, Wong DA, Tong LK, et al. Viral shedding patterns of coronavirus in patients with probable severe acute respiratory syndrome. Lancet. 2004;363 (9422):1699–1700. doi:1610.1016/S0140-6736 (1604)16255-16257.

56-Poissy J, Goff ar dA ,Parmentier-Decrucq E, et al. Kinetics and pattern of viral excretion in biological specimens of two MERS-CoV cases. J Clin Virol. 2014;61(2):275– 278. doi:210.1016/j.jcv.2014.1007.1002.

57-Bruning AHL, Aatola H, Toivola H, et al. Rapid detection and monitoring of human coronavirus infections. New Microbes New Infect. 2018;24:52–55.doi:10. 1016/j.nmni.2018.1004.1007

58-Guidance to minimize risks for facilities collecting, handling or storing materials potentially infectious for polioviruses (PIM Guidance). Geneva: World Health Organization;2018. http://polioeradication.org/wpcontent/uploads/2016/07/PIM-guidance-20190122-EN.pdf.

59-Guidance on regulations for the transport of infectious substances 2019–2020. Geneva:World Health Organization; 2019. (https://www.who.int/ihr/publications/WHO-WHECPI-2019.20/en/).

60-Wei Zhang, Rong-Hui Du, Bei Li, Xiao Shuang Zheng, Xing-Lou Yang, Ben Hu, et al. Molecular and serological investigation of 2019-nCoV infected patients: implication of multiple shedding routes, Emerging Microbes & Infections 2020 9:1, 386-389 (https://www.tandfonline.com/doi/full/10.1080/222 21751.2020.1729071).

61-Li W, Liu L, Chen L, et al. Evaluation of a commercial colloidal gold assay for detection of influenza A and B virus in

Pure Sciences International Journal of Kerbala

Journal Homepage:https://journals.uokerbala.edu.iq/index.php/psijk

children's respiratory specimens. Fetal Pediatr Pathol. 2019;15:1–6.

62-Chan CM, Tse H, Wong SS, et al. Examination of seroprevalence of coronavirus HKU1 infection with S protein-based ELISA and neutralization assay against viral spike pseudotyped virus. J Clin Virol. 2009;45 (1):54–60. doi:10.1016/j.jcv.2009.1002.1011.

63-Shao X, Guo X, Esper F, et al. Seroepidemiology of group I human coronaviruses in children. J Clin Virol. 2007;40(3):207–213. doi:210.1016/j.jcv.2007. 1008.1007.

64-Bruning AHL, Aatola H, Toivola H, et al. Rapid detection and monitoring of human coronavirus infections. New Microbes New Infect. 2018;24:52–55. doi:10. 1016/j.nmni.2018.1004.1007.

65-Kim, H. Outbreak of novel coronavirus (COVID-19): What is the role of radiologists? Eur. Radiol. 2020, in press. [CrossRef] [PubMed]

66- Pan, F.; Ye, T.; Sun, P.; Gui, S.; Liang, B.; Li, L.; Zheng, D.; Wang, J.; Hesketh, R.L.; Yang, L.; et al. Time course of lung changes on chest CT during recovery from 2019 novel coronavirus (COVID-19) pneumonia. Radiology 2020, in press. [CrossRef]

67- WHO. Clinical Management of Severe Acute Respiratory Infection When Novel Coronavirus (nCoV) Infection Is Suspected. Available online: https://www.who.int/publications-detail/clinical-management-of-severeacute-respiratory-infection-when-novel-coronavirus-(ncov)-infection-is-suspected (accessed on 17 March 2020).

68- Kampf, G.; Todt, D.; Pfaender, S.; Steinmann, E. Persistence of coronaviruses on inanimate surfaces and its inactivation with biocidal agents. J. Hosp. Infect. 2020, 104, 246–251. [CrossRef]

69- Wei, Q., and Ren, Z. (2020). Disinfection measures for pneumonia foci infected by novel 926 coronavirus in 2019. *Chin. J. Disinfect.* 37, 59-62.

70- Li, H.;Wang, Y.; Xu, J.; Cao, B. Potential antiviral therapeutics for 2019 novel coronavirus. Zhonghua Jie He He Hu Xi Za Zhi 2020, 43, E002.

71- Blaising, J., Polyak, S. J. & Pecheur, E. I. Arbidol as a broad-spectrum antiviral: an update. *Antivir. Res.* 107, 84–94 (2014).

72- Liu, Y.-J., 2005. IPC: professional type 1 interferon-producing cells and plasmacytoid dendritic cell precursors. Annu. Rev. Immunol. 23, 275–306

73- Wang BX, Fish EN. Global virus outbreaks: interferons as 1st responders. Semin Immunol. (2019) 43:101300. doi: 10.1016/j.smim.2019.101300

74- Zhou, Q., Wei, X. S., Xiang, X., Wang, X., Wang, Z. H., Chen, V., ... & Fish, E. N. (2020). Interferon-a2b treatment for COVID-19. *MedRxiv*.

75- Furuta, Y., Komeno, T. & Nakamura, T. Favipiravir (T-705), a broad spectrum inhibitor of viral RNA polymerase. *Proc. Jpn. Acad. Ser. B Phys. Biol. Sci.* 93, 449–463 (2017).

Pure Sciences International Journal of Kerbala

Journal Homepage:https://journals.uokerbala.edu.iq/index.php/psijk

76- Savarino, A., L. Gennero, K. Sperber, and J. R. Boelaert. 2001. The anti- HIV-1 activity of chloroquine. J. Clin. Virol. **20:**131–135.

77- Barnard, D. L., C. W. Day, K. Bailey, M. Heiner, R. Montgomery, L. Lauridsen, P. K. Chan, and R. W. Sidwell. 2006. Evaluation of immunomodulators, interferons and known in vitro SARS-coV inhibitors for inhibition of SARS-coV replication in BALB/c mice. Antivir. Chem. Chemother. **17:**275– 284.

78- Keyaerts, E., Li, S., Vijgen, L., Rysman, E., Verbeeck, J., Van Ranst, M., & Maes, P. (2009). Antiviral activity of chloroquine against human coronavirus OC43 infection in newborn mice. *Antimicrobial agents and chemotherapy*, *53*(8), 3416-3421.

79- Gubareva LV, Kaiser L, Hayden FG. Influenza virus neuraminidase inhibitors. *Lancet*. Mar 4 2000;355(9206):827-835.

80- Wu, C. et al. Risk factors associated with acute respiratory distress syndrome and death in patients with coronavirus disease 2019 pneumonia in Wuhan, China. JAMA Intern. Med. e200994 (2020).

81- Gautret, P. et al. (2020). Hydroxychloroquine and azithromycin as a treatment of COVID-19: results of an open-label non-randomized clinical trial. *Int. J. Antimicrob. Agents* 105949.

82- Mehra MR, Desai SS, Kuy S, Henry TD, Patel AN. Cardiovascular disease, drug therapy, and mortality in COVID-19. *N Engl J Med* 2020; published online May 1. DOI:10.1056/NEJMoa2007621.

83- Chu CM. Role of lopinavir/ritonavir in the treatment of SARS: initial virological and clinical findings. *Thorax* 2004; 59: 252–56.

84- Cao, B., Wang, Y., Wen, D., Liu, W., Wang, J., Fan, G. et al. (2020). A trial of lopinavir–ritonavir in adults hospitalized with severe Covid-19. *N. Engl. J. Med.* NEJMoa2001282.

85- Arabi YM, Alothman A, Balkhy HH, et al. Treatment of Middle East respiratory syndrome with a combination of lopinavir-ritonavir and interferon- 1b (MIRACLE trial): study protocol for a randomized controlled trial. *Trials* 2018; 19: 81.

86- Sheahan TP, Sims AC, Leist SR, et al. Comparative therapeutic efficacy of remdesivir and combination lopinavir, ritonavir, and interferon beta against MERS-CoV. *Nat Commun* 2020; 11: 222.

87- Barnard DL, Wong MH, Bailey K, et al. Effect of oral gavage treatment with ZnAL42 and other metallo-ion formulations on influenza A H5N1 and H1N1 virus infections in mice. *Antivir Chem Chemother* 2007; 18: 125–32.

88- Zumla A, Azhar EI, Arabi Y, et al. Host-directed therapies for improving poor treatment outcomes associated with the Middle East respiratory syndrome coronavirus infections. *Int J Infect Dis* 2015; 40: 71–74.

89- Beigel JH, Nam HH, Adams PL, Krafft A, Ince WL, El-Kamary SS, et al. Advances in respiratory virus therapeutics - a meeting report from the 6th isirv Antiviral Group conference. Antivir Res 2019;167:45e67.

Pure Sciences International Journal of Kerbala

Journal Homepage:https://journals.uokerbala.edu.iq/index.php/psijk

90- Erol, Adnan. "High-dose intravenous vitamin C treatment for COVID-19." (2020)

91- Clark DR, Jonathan EM, JKB. Clinical evidence does not support corticosteroid treatment for 2019-nCoV lung injury. *Lancet* 2020; published online Feb 7. https://doi.org/10.1016/S0140-6736(20)30317-2.

92- Chen, L., Xiong, J., Bao, L., & Shi, Y. (2020). Convalescent plasma as a potential therapy for COVID-19. *The Lancet Infectious Diseases*, *20*(4), 398-400.

93- Wang, N. et al. (2019). Structural Definition of a Neutralization-sensitive Epitope on the MERS-CoV S1-NTD. *Cell Rep.* 28(13), 3395-405.

94- Schoeman, D., and Fielding, B. C. (2019). Coronavirus envelope protein: current knowledge. *Virol J.* 16, 69.

95- Cameron, D., Bodenreider, O., Yalamanchili, H., Danh, T., Vallabhaneni, S., Thirunarayan, K., Sheth, A. P., & Rindflesch, T. C. (2013). A graph-based recovery and decomposition of Swanson's hypothesis using semantic predications. Journal of biomedical informatics, 46(2), 238–251.

96- Gupta, M. K. (2020). In-silico approaches to detect inhibitors of the human severe acute respiratory syndrome coronavirus envelope protein ion channel. Journal of Biomolecular Structure and Dynamics, 1–11.

97- Aanouz, I. (2020). Moroccan Medicinal plants as inhibitors of COVID-19: Computational investigations. Journal of Biomolecular Structure and Dynamics, 38, 1–12.

98- Al-Khafaji, K., AL-DuhaidahawiL, D., & Taskin Tok, T. (2020). Using integrated computational approaches to identify safe and rapid treatment for SARS-CoV-2. *Journal of Biomolecular Structure and Dynamics*, (just-accepted), 1-11.

99-R.J. Reiter, Q. Ma, R. Sharma, Treatment of Ebola and other infectious diseases: melatonin “goes viral”, Melatonin Res 3 (2020) 43–57.

100-Ahmed, S. F., Quadeer, A. A., & McKay, M. R. Preliminary identification of potential vaccine targets for the COVID-19 coronavirus (SARS-CoV-2) based on SARS-CoV immunological studies. *Viruses*, (2020). *12*(3), 254.

101- Buchholz, U. J.; Bukreyev, A.; Yang, L.; Lamirande, E. W.; Murphy, B. R.; Subbarao, K.; Collins, P. L. Contributions of the structural proteins of severe acute respiratory syndrome coronavirus to protective immunity. Proc. Natl. Acad. Sci. U. S. A. 2004, 101 (26), 9804 9809.

First Year-First Folder-Number: 0
PSIJK 184-191

Pure Sciences International Journal of Kerbala

Journal Homepage:https://journals.uokerbala.edu.iq/index.php/psijk

Preparation, diagnosis and study of the inhibitory effect of copper nanoparticles before and after Erythromycin loading on *Pseudomonas aeruginosa*

K A M Hussein [1] and A A Khalaf [2]
[1,2]Biology Department , Kerbala University, Kerbala, Iraq
[1]Kiaser.a@uokerala.edu.iq
[2] Ayserashour78@gmail.com

Abstract : Pseudomonas aeruginosa is one of the opportunistic nurses, which possesses many virulence factors which makes it a high ability to resist antibiotics multidrug-resistant (MDR).leading to make Antimicrobial resistance is one of the main threats to human health because it leads to increased infection rates and mortality. The present study aimed to evaluate the mechanism of inhibitory effect of the free CuO nanocomposite and its synergistic effect with the anti-bacterial erythromycin ER after it was loaded on the CuO / ER nanoparticle on Pseudomonas aeruginosa isolated from Al-Hindiya General Hospital. The CuO nanoparticles were manufactured by using precipitation method .Diagnosis free CUO and nanoparticles after they were loaded onto nanocomposites by using the AFM atomic force microscope. the inhibition zone diameter measured by Disc Diffusion method the results was indicated the highly synergistic effect on bacteria , while the free nanoparticles are less effective, whereas the antibiotic alone gave the lowest inhibition diameter (21.25 ±0.854, 11.75 ±0.750, 8.50 ±1.040) respectively, moreover this study investigated that The release of the antibiotic ER from the CuO / ER that the second pseudo order model is more applicable to the interpretation of the behavior of ER release from CuO / ER (K = 2.60min-1 , r2 = 0.997) which indicates that the forces controlling the release of ER are flexible without dissociation and being affected by the metabolism, and the percentage of ER release was significant due to the intensity of the surface ion exchange between CuO / ER and the anion (CO3)-2 coming from CaCO, which makes the ER release rate to reach more than 98% in the medium of sodium carbonate at a concentration of 0.05 M within 250 minutes of the start time of the reaction.

Key words: Free Copper Oxide Nanoparticals , *P. aeruginosa*, Erythromycin, Synergistic effect.

Pure Sciences International Journal of Kerbala

Journal Homepage:https://journals.uokerbala.edu.iq/index.php/psijk

traditional antimicrobial agents called nanoparticles that are an effective treatment for infectious diseases and that have many Advantages compared to conventional antibiotics, including the absence of harmful , their low toxicity (6) and their ability to bacterial resistance to overcome antibiotics by interfering with multiple biological pathways, may cause mechanical disruption of the bacterial membrane.(7) . The present study aimed to evaluate the mechanism of inhibitory effect of the free CuO nanocomposite and its synergistic effect with the anti-bacterial erythromycin ER after it was loaded on the CuO / ER nanoparticle on Pseudomonas aeruginosa isolated from Al-Hindiya General Hospital. 2-

2- Materials and Methods

1.Preparation of spherical copper nanoparticle oxide: The CuO nanoparticles were manufactured by precipitation method using aqueous copper nitrate (Cu (NO3) as 2.3H2O) according to (8) follows: Prepare a 0.1 molar solution of dissolving 14 mg (Cu (NO3) 2.3H2O) in 100 ml of deionized water to form (solution No. 1).. Prepare 100 ml of solution 10. Mg NaOH)) was added to the solution in the form of drops / second drops on the walls of the vessel and the acidic function (PH) of the solution is measured until it reaches 14 the reaction is stopped. Leave the solution for two hours. after it stagnates and precipitates by centrifuging 10,000 cycles for 5 minutes, Leave the solution for 24 hours. Wash the precipitate that is black in distilled water and absolute ethanol several times until the pH

1-Introduction .Pseudomonas aeruginosa is one of the opportunistic nurses, which possesses many virulence factors, which makes it an attention to what may cause harm to human health.(1) Such as urinary tract infection, pneumonia, keratitis, external otitis and folliculitis, and it is one of the causes of acquired infection, especially for people who suffer from immune deficiency, and because of the multiple mechanisms that the bacteria as virulence factors, the bacteria have adapted to stay in environments Low nutrition and resistance to different antibiotic classes like biofilm on biotic and (2,3) . These non-biotic surfaces bacteria have a high ability to resist antibiotics multidrug-resistant (MDR).leading to make Antimicrobial resistance is one of the main threats to human health because it leads to increased infection rates and mortality. The first step in combating the development of resistance and limiting the use of antibiotics without benefit is to resort to alternative solutions, including the use of nanocomposites (4) Nanotechnology is one of the fields of science that deals with dealing with matter at the scale of 1 billion meters (i.e. 10-9 meters = 1 nanometer). Silver nanoparticles are defined as nanoparticles of silver metal whose size ranges between 1 to 100 nanometers, and are used in many fields such as medical, engineering, and magnetic fields, in energy and environmental treatment, as well as in cosmetics (5). Nanotechnology has been adopted as a way to develop new non-

Pure Sciences International Journal of Kerbala

Journal Homepage:https://journals.uokerbala.edu.iq/index.php/psijk

water removed from the ions and after completing the dissolution process, complete the volume to 50 ml with distilled water removed from the ions also, and from this concentration the concentration was prepared 0.05M .

2- Solution No. (2):
Hydrochloric acid (2M) HCl solution
Prepare this solution by mixing 4.2 ml of concentrated hydrochloric acid with a quantity of distilled water removed from the ions and then complete the volume to 50 ml with distilled water removed from the ions as well.-

2-5.Determination of Calibration Curve
The titration curve, which represents the relationship between absorption and concentration, was determined by preparing four consecutive concentrations within the range (5--20 ppm) of the antibiotic A solution used in the study. Absorption of these concentrations was measured at the maximum wavelength (max 213nm) of the antagonist. The standard between absorption and concentration was shown in Figures (3-1, 3-2). From the following straight-line equation Y = mx + b, the concentration value is found over time.

2-6. Method for estimating the inhibitory efficacy of nanocomposites and antibiotics against bacteria :
The inhibitory effect of the free CuO nanocomposite and the Erythromicin was tested by

reaches 7 and leaves 16 hours. The compound is dried at 80 ° C. 7. The product is burned in an oven temperature of 500 ° C. for 4 hours, and the result is preserved after cooling it for later use. 2-2.Diagnosis of a hybrid nanoparticle : Methods for diagnosin hybrid nanoparticles include Fourier transform infrared spectroscopy (FT-IR) and X-ray diffraction (XRD) spectrum, as well as the use of Atomic Force Microscope (AFM) and electronic scanning Election Microscope (SEM). 2-3..Diagnosis using the AFM atomic force microscope:The atomic force microscope was used to examine free and nanoparticles after they were loaded onto nanocomposites, and to measure the diameters, sizes, and assemblies of nanoparticles.The Crystallinity Index was extracted using the Crystallinity following formula Index = Dp / L.

As:
Dp = the partial volume to be measured by the AFM
L = the average crystal size, which is calculated using the Scherrer equation.

2-4. study of the release of therapeutic substance:
The method described by (9) was followed in a study that edits the therapeutic substance into a number of aqueous solutions.
:Solutions used
1-Solution No. (1): -1
Na2CO3 sodium carbonate solution
This solution was prepared by dissolving 2.65 g of sodium carbonate in a quantity of distilled

Pure Sciences International Journal of Kerbala

Journal Homepage:https://journals.uokerbala.edu.iq/index.php/psijk

agar with a diameter of 5 mm, as the distance was equal between one disk and another. Place the saturated tablets from the free nanocomposite concentrations and loaded with the antibiotic under study in the dish containing the bacterial culture, incubate for an hour in the refrigerator, and then incubated in the incubator at 37 ° C for 24 hours, and the antibiotic Erythromicin was used as a positive control . Measures of inhibition of bacterial growth (mm) were measured using a ruler after the completion of the .incubation period .

3-Result and Discussion :
Diagnosis of CuO nanoparticles by atomic force microscope images
molecular size ratios, it is 10% for molecular sizes less than 55.00 nm, and 50% was For molecular volumes less than 75.00 nm, the sizes in general were 90% less .than 100.00 nm .

measuring the inhibition zone diameter around bacterial colony by using the disc diffusion method (10) as follows: A series of decimal dilutions have been made for each bacterial isolation. 0.1 ml of appropriate dilution for each bacterial isolation was well spread on the surface of the dish by the L-Shape diffuser and the dishes were left for an hour in the refrigerator. Dilute the nanocomposites with the use of the dimethyl sulfoxide (DMSO) to obtain concentrations of macrograms / ml, as well as prepare antibiotics loaded with the nanocomposites with both concentrations. Dishes have been made saturated with free nanoparticles, antibiotic and nanocompounds with antibiotic, to be placed on the surface of the Atomic Force Microscopie (AFM) The results (3-1) of the AFM images indicate that the CuO nanoparticle has a surface roughness coefficient of 8.43 nm but with respect to the compound's

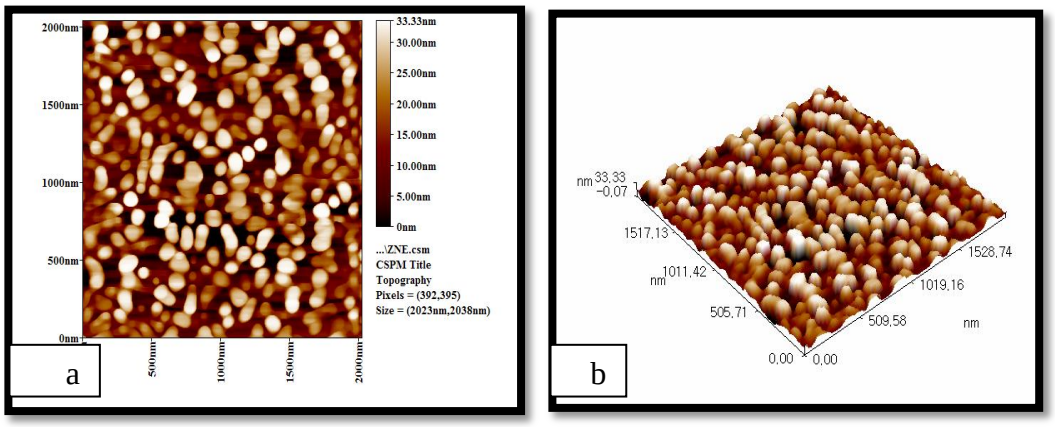

First Year-First Folder-Number: 0
PSIJK 184-191

Pure Sciences International Journal of Kerbala

Journal Homepage:https://journals.uokerbala.edu.iq/index.php/psijk

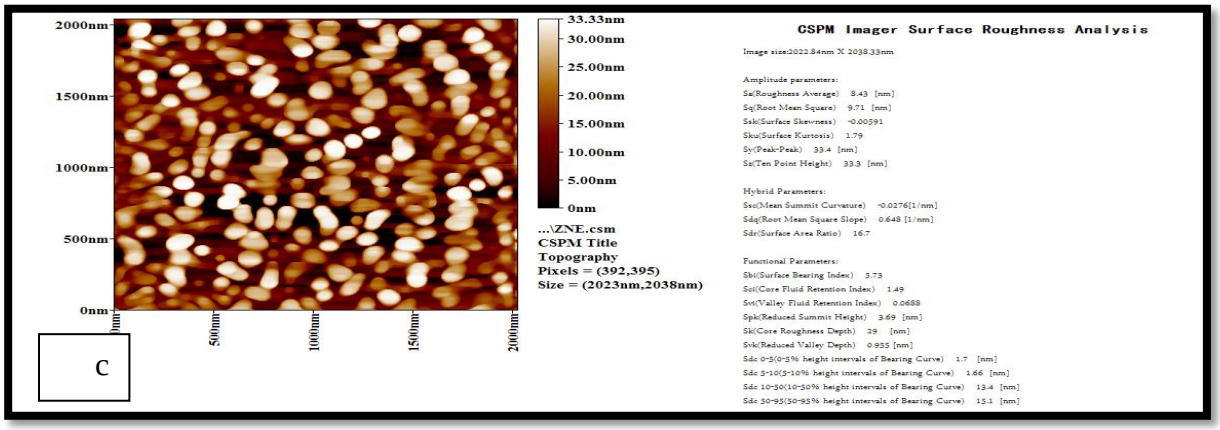

Figure (3-1) the atomic force microscope images of the free CuO nano-compound: a / three-dimensional image, b / two-dimensional image, c / two-dimensional image showing all the details of the particles.

Table (3-1) the total average particle size for free CuO nanoparticles and the different ratios for these sizes

Avg. Diameter:80.55 nm	<=10% Diameter:55.00 nm
<=50% Diameter:75.00 nm	<=90% Diameter:100.00 nm

Diameter(nm)<	Volume(%)	Cumulation(%)	Diameter(nm)<	Volume(%)	Cumulation(%)	Diameter(nm)<	Volume(%)	Cumulation(%)
55.00	1.68	1.68	80.00	10.61	50.28	105.00	7.82	93.30
60.00	10.61	12.29	85.00	8.94	59.22	110.00	4.47	97.77
65.00	8.94	21.23	90.00	10.61	69.83	115.00	2.23	100.00
70.00	8.94	30.17	95.00	8.94	78.77			
75.00	9.50	39.66	100.00	6.70	85.47			

First Year-First Folder-Number: 0
PSIJK 184-191

Pure Sciences International Journal of Kerbala

Journal Homepage:https://journals.uokerbala.edu.iq/index.php/psijk

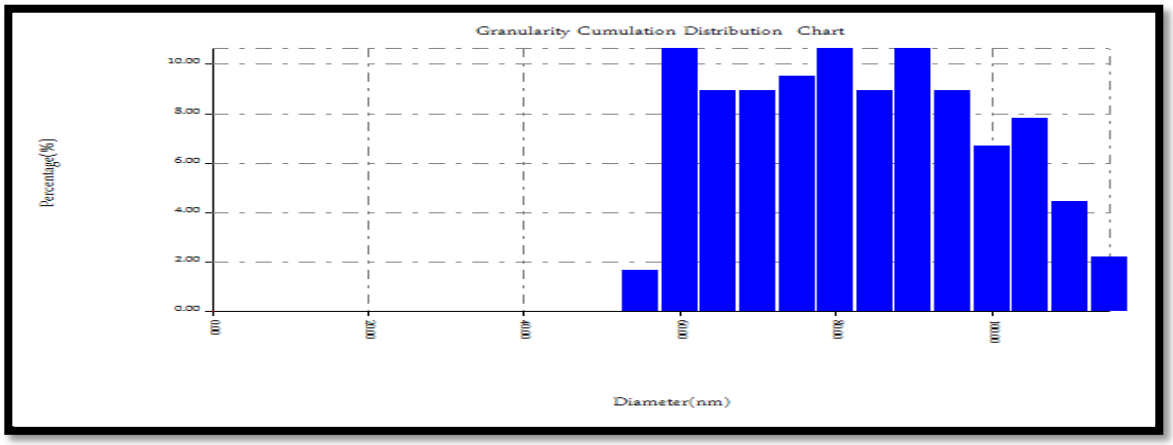

Figure (3-2) Distribution of the different ratios of free CuO particle size

:

Depending on the Zero Order equation indicated above, the values of (Ct) are plotted against the time and the correlation coefficient values are known by applying the straight-line equation

According to the zero-order equation for the anti-ER spread of the nanocomposite and CuO / ER Figures (3-3), Results indicate that there is a deviation of these values from the straight line indicating the non-compliance of the anti-liberation process ER) for the zero-rank model, as slow progressive liberalization begins until time 20 A minute, and then the acceleration begins until it reaches the highest release at a time of 150 minutes

r2 If the ER treatment is released from CuO =0.950

And constant of speed K = min^{-1} .0.0050

It is noted through the results indicated in Figure (3-3) regarding the release of anti-ER from the nanocomposition CuO / ER, that these release values are not identical to the straight line, which

The study of the kinetics of Erythromicin 3-2:antibiotic (ER) loaded with CuO Ion exchange kinetics have been studied by applying the false-zero and first-order and second-order equations to the kinematics of each of the studied nanocomposites after loading it with the ER counterpart as the zero-order was founded according to the following equation:

Ct = kot …… .. ... (zero) order

To find the first false rank, we apply the following equation

Log (1-ct / ct) = k1t1 ---------- (first order)

the following equation to find the value of second false rank

t / ct = k2Ct² + t /)

(Ct… (Second order

Pure Sciences International Journal of Kerbala

Journal Homepage:https://journals.uokerbala.edu.iq/index.php/psijk

And constant and speed K = min-1 0.0079

while, when applying the second false rank model for anti-ER release of CuO / ER nanocomposites, Figure (3-4) indicate that this model is more applicable to the interpretation of ER release behavior of these nanocomposites, as we found that

r2 if the ER treatment is released from CuO = 0.997

And the constant and the speed K = min-1 2.60

indicates the non-compliance with the release process of anti-ER treatment for the first-order false model as it happened when applying Zero rank model. Therefore, the false second order equation is applied, since ER release began with a time of approximately 20 minutes to reach above at time 140 minutes .

r2 If the ER treatment is released from CuO = 91.6

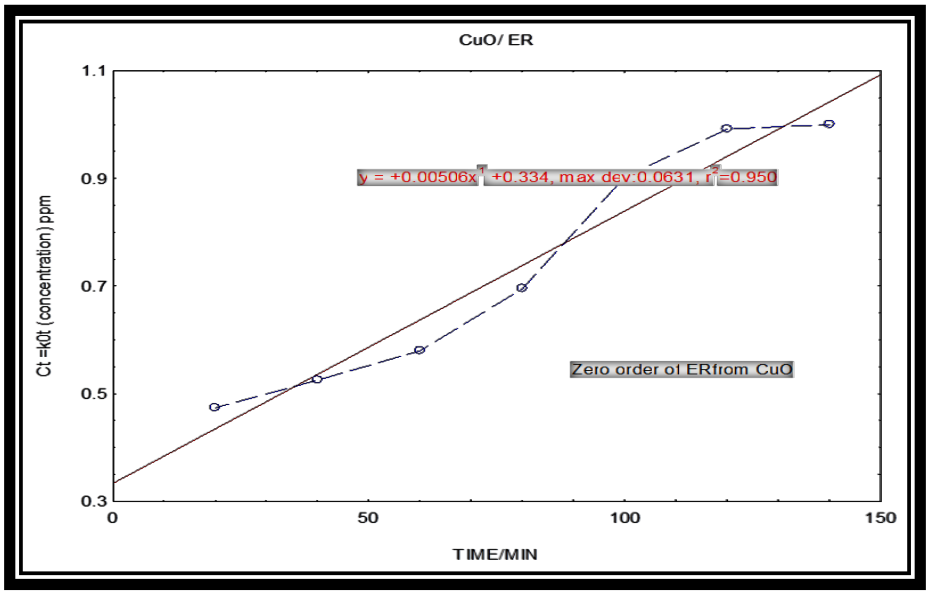

Figure (3-3) the zero rank of antibiotic releasing (ER) from CuO nanocomposite

Pure Sciences International Journal of Kerbala

Journal Homepage:https://journals.uokerbala.edu.iq/index.php/psijk

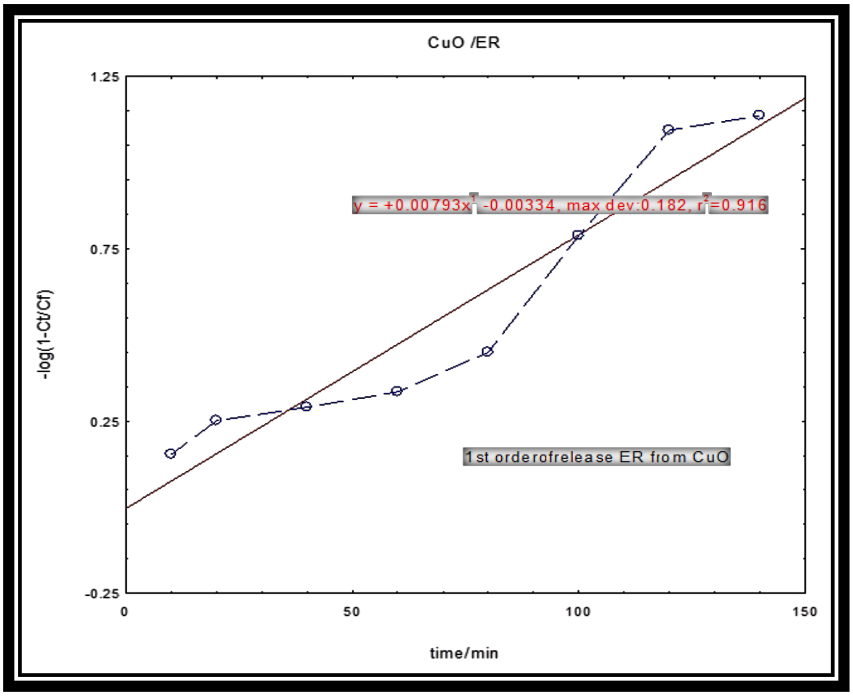

Figure (3-4) False First Rank for Antibiotic Editing (ER) of CuO Nanomode

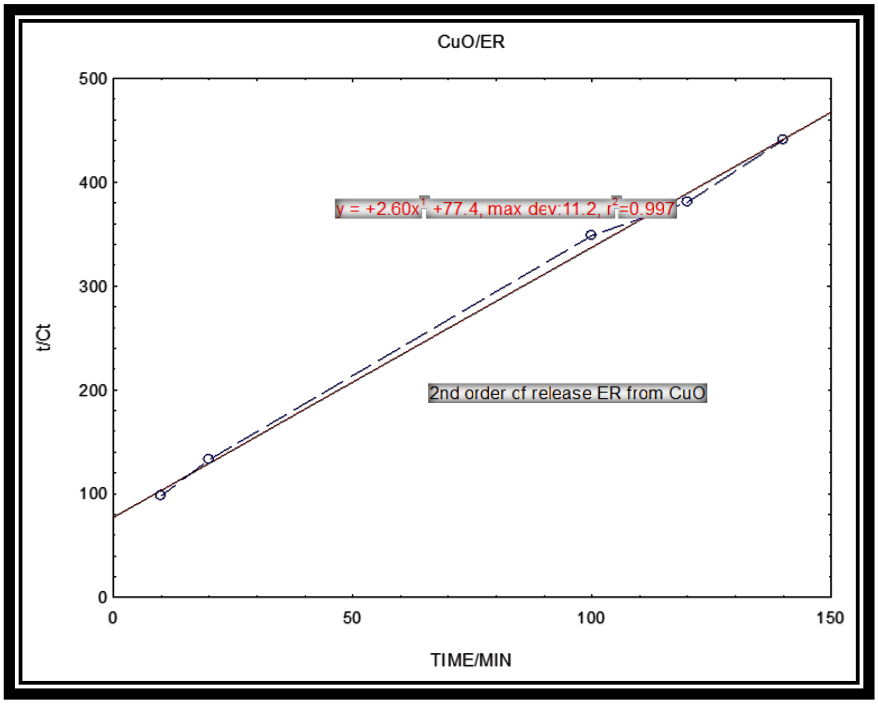

Figure (3-5) the second pseudoscopy for atibiotic releasing (ER) from CuO nanocomposite

Pure Sciences International Journal of Kerbala

Journal Homepage:https://journals.uokerbala.edu.iq/index.php/psijk

Table (3-2) Correlation coefficient and velocity constant for the zero, 1st and 2nd false ranks of the anti-ER release from CuO / ER nanocomposite

معامل الارتباط r^2 وثابت السرعة K min^{-1} للرتبة / تحرر المضاد ER	الرتبة الصفرية Zeroorder		الرتبة الكاذبة الاولى 1^{st} order		الرتبة الثانية الكاذبة 2^{nd}order	
	r^2	K min^{-1}	r^2	K min^{-1}	r^2	K min^{-1}
ER from CuO	0.950	0.0050	0.916	0.0079	0.997	2.60

the most appropriate to explain the release of Ellagic acid from the surface of zinc nanocomposite. While it does not agree with (13), they showed that the mathematical model of false first order is the most appropriate to explain the release of calcic acid from the surface of the zinc nanoparticle that approached 1 depending on the value of r2 **.**

our current study are in agreement with (11), as he showed that the paracetomol release process from the layers of the zerogel (magnesium / aluminum) compound is applied to the second-order mathematical model of the lying to explain the behavior of the release process .The results are also consistent with what. (12) found, as it showed that the second-order math model is

First Year-First Folder-Number: 0
PSIJK 184-191

Pure Sciences International Journal of Kerbala

Journal Homepage:https://journals.uokerbala.edu.iq/index.php/psijk

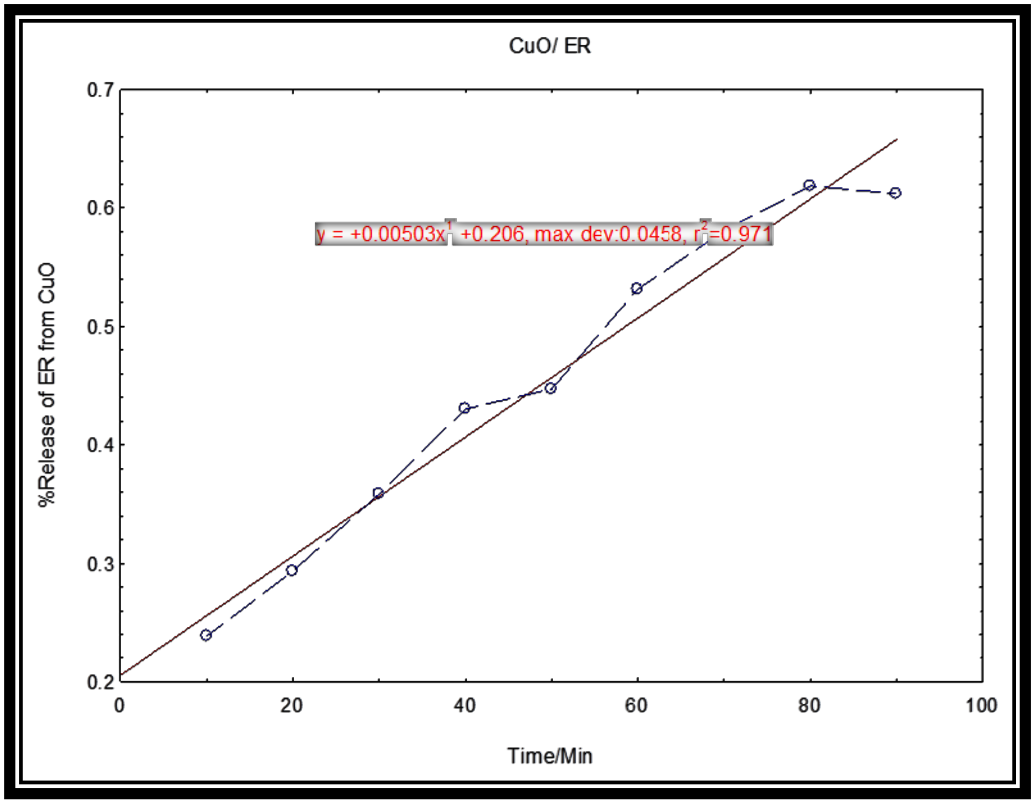

Figure (3-6): Antibiotic release percentage (ER) of CuO nanocomposite

medium of sodium carbonate is slow at the beginning of the experiment,and then it was return to be quickly. After approximately (120) minutes of the start time of the experiment are relatively constant, it can be attributed to the high concentration of carbonate ion-2 (CO3), which causes the release of increased amounts of treatment to the surrounding medium, and that the process of release is progressive, which indicates The process of ion exchange of carbonates is to be gradual, and maintains the gradual release ratio of ER and

3-3.Study of antibiotic release percentage (Cu) / ER nanocomposite

Figure (3-6) shows that the intensity of the surface ion exchange between CuO / ER and the anion-2 (CO3) coming from carbonates is large, which makes the release of ER treatment up to more than 98% in the medium of sodium carbonate with a concentration of 0.05 molar within two and a half hours of Reaction start time. Our finding of the process of launching the anti-ER from the nanocomposite CuO to the

Pure Sciences International Journal of Kerbala

Journal Homepage:https://journals.uokerbala.edu.iq/index.php/psijk

indicate that there is a clear variation in the effect of the nanocomposite and the antibiotic before and after the loading on the studied bacteria in the inhibition zone (21.25 ± 0.854) mm compared to the inhibition zone for both the free compound and the antibiotic who recorded the inhibition area (8.50 ± 1.040, 11.75 ± 0.750) mm T1 and T2 respectively . (14) suggested that silver nanoparticles work to prevent bacterial growth by their direct effect protein synthesis by correlating silver atoms with the Thiol group (SH) of bacterial enzymes thus disrupting the work of these enzymes, and the AgNP works to Changing the action of the components that make up the plasma membrane and the task in generating energy and ionic transport through this membrane by forming a S-Ag frame with the Thiol group

The nanocomposite works on the formation of the two sulfur bonds in the interaction of the oxygen and hydroxine atoms in the cell with thiol group (R-S-S-R) groups in *S.aureus, P.aeruginosa, E.coli, Helicobacterbiylori, Bacillus subtilis and .Shigella flexnri.*

the formation of a new compound with the mutual carbon ion to equal the ion released from treatment (13).

(12) observed the process of release of ellagic acid ((Ellagic acid from the surface of the zinc compound to the solution of sodium carbonate and triple sodium phosphate during a time period of 38 hours, and found that the release process is fast during the first 5 hours of the start of the experiment, as the rate of release reached (44 and 85)% to the medium of sodium carbonate And triple sodium phosphate, respectively, and then the release velocity gradually decelerates.

3-3. Inhibitory effect of CuO before and after loading Erythromicin on pseudomonas aeruginosa

The inhibitory effect of CuO nanoparticles against the bacteria P. aeruginosa was studied. the results compared with Erythromicin (ER) with its free state and after loading it into the nanocomposite and study the difference in the inhibitory effect of the free form and the synergistic form between the compound and the antibiotic. The results of Table (3-3)

Pure Sciences International Journal of Kerbala

Journal Homepage:https://journals.uokerbala.edu.iq/index.php/psijk

molecules, just as the action of ions that are soon released when they reach the invading bacterial cell cannot be ignored in the extermination of bacteria .

Antibacterial activity refers to a number of activities such as the toxicological activity of nanoparticles that are still unclear and still controversial, and antibacterial activity requires a deep explanation of the mechanisms that antibacterials use to eliminate germs.

The Agnihotri (15) study indicated that some silver nanoparticals compounds produce ROS, causing bacterial cell death. Moreover, this study suggests that there are several factors that can synergize in generating the inhibitory action of antibacterial substances more quickly by loading onto the nanocomposite. Because it has electrical properties that help in contacting bacteria, which facilitates the arrival of the antibiotic loaded on these

Table (3-3) the Inhibition Zone Diameter(IZD) for P.aeruginosa when treated with CuO :nanocomposites before and after loading Erythromicin (ER)

Treatment	**(IZD ± standard error (mm**
	pseudomonas aeruginosa
T1 (CuO)	**1.040 ± 8.50 a**
T2 (ER)	**0.750 ±11.75 a**
T3 (ER / CuO)	**0.854 ± 21.25 b**

Pure Sciences International Journal of Kerbala

Journal Homepage:https://journals.uokerbala.edu.iq/index.php/psijk

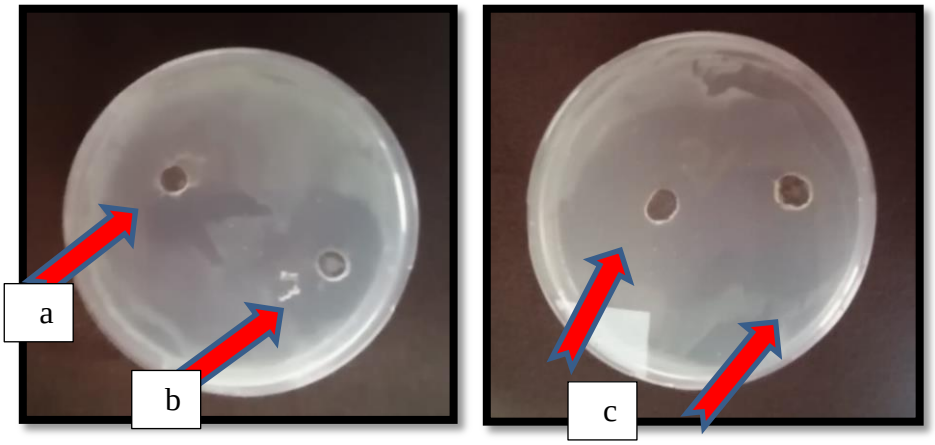

Figure(3-4) shows the inhibitory effect of CuO nanocomposite and ER antibiotic in its free and synergistic forms before and after loading. A(T1), b (T2), c (T3)

against microbial pathogens. Commun. Curr. Res. Technol. Adv., 23: 228-244.

6- **Huh** AJ, Kwon YJ. (2011)."Nanoantibiotics": a new paradigm for treating infectious diseases using nanomaterials in the antibiotics resistant era. *J Control Release*.;156(2):128-145.

7- Guzman, M.; Dille, J. and Godet, S. (2012). Synthesis and antibacterial activity of silver nanoparticles against gram-positive and gram negative bacteria. Nanomed. Nanotechnol. Biol. Med., 8: 37-45.

8-Phiwdanga, K.; Suphankija, S.; Mekprasarta, W. and Pecharapaa, W.(2013). Synthesis of CuO Nanoparticles by Precipitation Method Using Different Precursors. Energy Procedia, 34 : 740 – 745.

9- **Wang** , L . ; Liu , Y. ; Zhang , W. ; Chen , X . ; Yang , T. ; Ma , G.(2013). Microspheres and microcapsules for protein delivery: strategies of drug activity retention. *Curr. Pharm. Des.*, 19 : 6340-6352.

References

1-Deep,A.; Chaudhary, U.; and Gupta, V. (2011). Quorum sensing and Bacteria Pathogenicity: From Molecules to Disease. Journal of Laboratory Physicians, 3 (1): 4–11.

2- Moradali, M.F.; Ghods, S. and Rehm, B.H.A. (2017). *Pseudomonas aeruginosa* Lifestyle: A Paradigm for Adaptation, Survival, and Persistence. J. Front. Cell. Infect. Microbiol., 7: 39.

3- Babapour, E.; Haddadi, A.; Mirnejad, R.; Angaji, S-A. and Amirmozafari, N. (2016). Biofilm formation in clinical isolates of nosocomial *Acinetobacter baumannii* and its relationship with multidrug resistance.Asian Pac. J. Trop. Biomed., 6(6): 528–533.

4- Chaudhuri, R. G. and Paria, S. (2012). Core/shell nanoparticles: classes, properties, synthesis, mechanisms, characterization, and applications. In Chem. Rev., 112(4): 2373-2433.

5- Sahayaraj, K. and Rajesh, S. (2011). Bionanoparticles: Synthesis and antimicrobial applications.Science

Pure Sciences International Journal of Kerbala

Journal Homepage:https://journals.uokerbala.edu.iq/index.php/psijk

controlled release formulation of anticarcinogenic agent. Journal of Physics and Chemistry of Solids, 71(11):1565-1570.

14- **Gurunathan**, S. ; Han, J.W. ; Kwon, D. ; and Kim, J. (2014).Enhanced antibacterial and anti-biofilm activities of silver nanoparticles against Gram-negative and Gram-positive bacteria .*J Nanoscale Res Lett.* ; 9 (1) :373-384 .

15- **Agnihotri** ,S. ; Mukherjiabc, S. & Mukherji, S. (2014) . Size-controlled silver nanoparticles synthesized over the range 5–100 nm using the same protocol and their antibacterial efficacy . *RSC Adv*.; 4: 3974-3983.

10- **Egorove** , N.S. (1985) : Antibiotics Scientific approach . mirpublishers, Moscow.

11-Kovanda, F.; Maryskova, Z. & Kovar, P. (2011). Intercalation of paracetomol into the hydrotalcite-like host. Journal of solid state chemistry,184: 3329-3335.

12-Hussein, M. Z. ; Al Ali, S. H.; Zainal Z. & Hakim, M. N. (2011). Development of antiproliferative nanohybrid compound with controlled release property using ellagic acid as the active agent. *International Journal of Nanomedicine*, 6: 1373–1383.

13-Ghotbi,M. Y. & Hussein, M. Z. (2010). Gallate–Zn–Al-layered double hydroxide as an intercalated compound with new

First Year-First Folder-Number: 0
PSIJK 184-191

Pure Sciences International Journal of Kerbala

Journal Homepage:https://journals.uokerbala.edu.iq/index.php/psijk

Preparation and diagnosis of Xerogel nanocomposites and studying their effect on TNF-α level before and after loading Dexamethason in male white rats induced rheumatoid arthritis

Kiaser Abdulsajjad M.Hussain [1] , Ayser Ashour Khalaf [2] and Batool Abbas hussien [3]
[1, 2,3]Biology Department , Kerbala University, Kerbala, Iraq
[1]kiaser.a@uokerala.edu.iq
[2] Ayserashour78@gmail.com
[3] Batool.a@uokerbala.edu.iq

Abstract

Rheumatoid arthritis (RA) is one of the most prevalent diseases in the world, characterized by being an autoimmune disease and affecting various parts of the body joints. The current study aimed to evaluate the mechanism of reducing the effect of (RA) after it was induced in male white rat with a Complete Freund's Adjuvant (CFA) at TNF-α level by treating Xerogel Nanoparticles and dexamethasone nanocompounded (Xerogel / Dexa) . As the Xerogel nanoparticle was prepared and examined by Atomic Force Microscope (AFM), the free Xerogel nanoparticle had a surface roughness coefficient of 0.327 nm and the total percentage of volumes was 90% less than 130 nm, and the results also indicated that induced rheumatoid arthritis causes Significant increase (p <0.05) in the mean concentration of neoplastic necrosis factor (TNF-α) in the blood serum of male white rats, as they reached a concentration level (10.68 ± 461.80) Pg / ml in the positive control group (G2) for six weeks of treatment compared with the negative control group G1)), as the concentration level in it reached (69.97±0.88) Pg / ml for the same period, and there was also a significant decrease (P <0.05) in the level of concentration of TNF-α among members of the G5 group treated with the Xerogel / Dexa nanoparticle, as this concentration reached (182.98 ± 6.99) Pg / ml compared to the positive control groups (G2) treated with the free Xerogel (G3) and the group treated with free Dexa (G4) for a six-week treatment period in these groups as these concentrations reached (461.80± 10.68, 483.74± 3.59, 300.32± 4.03) Pg / ml, respectively.

Introduction

Rheumatoid arthritis (RA) is one of the most common diseases in the world, with global data reporting that it is distributed by more than 1% (Scott et al., 2005).It is characterized by the fact that it is an autoimmune disease and affects different joint parts of the body and parallel to the

Pure Sciences International Journal of Kerbala

Journal Homepage:https://journals.uokerbala.edu.iq/index.php/psijk

Synovial membrane and this stage is characterized as non-qualitative and depends on various environmental factors related to rheumatoid arthritis (RA) in the late stages of untreated cases and this type of infection in many cases ends full recovery in a short or long time or leads to chronic low-intensity inflammation responsible for the second stage of inflammation The tissue of the synovial membrane membrane and cellular oscillation with the development of inflammation and its transmission to the tissue of the meniscus Synovial cartilage is similar to chronic rheumatoid arthritis (RA) but is a non-specific inflammation. The third stage is very important, and includes stimulating immune proteins by cellular activities, and then developing and spreading the entire synovial membrane tissue inflammation and the destruction of joints.This stage causes the bone cartilage to be directly destroyed, all these manifestations represent the characteristic symptoms of RA (Denarie et al., 2017:Combe& Dougdos,2001

The current study aimed to evaluate the mechanism of reducing the effect (RA) by nanoparticles (Xerogel) after it was induced in male white rat with the material (CFA) Complete Freund's Adjuvant because of the importance of the disease in right and left sides, RA affects most often in the small joints of the hand as well as foot, knee and ankle and thus targets the synovial membrane. (Aletaha et al.,2010 ; Dopkin et al., 2008

Research evidence has confirmed there are many biological, environmental, psychological and personal factors with rheumatoid arthritis (2007 Treharne et al.)There is also no cure for arthritis yet, but it is possible to live a long and active life with rheumatoid arthritis, if appropriate rheumatoid arthritis treatment is adopted, which includes joint protection and lifestyle change, yet the treatments available at present are used to reduce the destructive inflammatory effect of the joint and prevent other complications of the disease as well as to maintain the flexibility and movement of the joint and thus reduce pain. Among the most important drugs used in the treatment of arthritis are NSAIDs and modified medicines (Majithia & Geraci, 2007).New treatments are more effective and less negative, and among these methodsUsing Nanotechnology (Vijaykumar et al., 2015)

The pathological mechanisms can be divided into three main stages, the first is the beginning stage, where some cells are migrated to the tissue of the membrane

Pure Sciences International Journal of Kerbala

Journal Homepage:https://journals.uokerbala.edu.iq/index.php/psijk

CFA (0.1) ml with right foot as positive control. group.3 G3: Arthritis induced and orally tested by Xerogel for 14 days after the induction of arthritis .4. G4: Arthritis induced and orally tested by dexamethasonefor 14 days.5.Group G5: Arthritis induced and orally tested by Xerogel/ dex for 14 days.

Preparation of Xerogel nanocomposites:

Dissolve 29.7 g of znO (NO3) hydro-hydronitrate nitrate in 167 ml of ethanol.2. Add 2 ml of ethylene claycool to the solution (Solution #1).3.4.2 g of silver nitrate (AgNO3) in 100 ml of distilled water 4.(Solution #2).5. Prepare a solution containing 26 ml of distilled water plus 0.6 ml of HNO3 (solution No. 3).6. Add the ingredients of solution #3 to solution #1 and shake the solution well (Solution #4).7. Add the components of solution 2 to solution #4.8. Add to the last solution 2g of PVP.9. Heat the resulting solution at a degree of heat up to 120 °C to vaporize two thirds of the solution above.10. The solution was recused and separated by the centrifuge and collected after which it was burned in the oven with a temperature of 400 °C.11.Save the output until use and download treatment on it (Tuncer & Seker, 2011).

Diagnosis of hybrid nanocomposite:

the society Because it is a common and widespread disease, due to the side effects and the high cost of drugs used in the treatment of this disease and reduce the damage caused by medicines, as many studies have shown that it causes disorder in some functional blood standards and liver and kidney functions and cartilage tissues in the joints.The current study is achieved through the following axes: 1.Preparation, diagnosis and study of some characteristics of the xerogel, which is made of zinc and silver.2. The development of arthritis in rats.3. The oral experimentation of animals with the nanoboat prepared Xerogel as a processing material.1.Download the treatment of Dexamethason Dexamethason Nanoboat Xerogel.2. Study the effect of xerogel nanocomposite after inducing arthritis tNF-α

Methods

Design of the experiment: The male white 5 rat was randomly distributed into 5 groups with animals per group and swallowed orally according to the weight of the rat's body for six weeks and as follows: 1.Group G1: was daily dragged by a solution of vesicle salt and promised a negative control group.2.Group G2: Induced arthritis by injecting Complete Freund's adjuvant-

Pure Sciences International Journal of Kerbala

Journal Homepage:https://journals.uokerbala.edu.iq/index.php/psijk

After starving the animals for 12 hours, they were weighed and drugged with ether, and blood samples collected 5 ml per animal directly from the heart in cardiac puncture.Blood samples are withdrawn using 5ml wine syringes in 8 weeks of the development of arthritis and after treatment the free drug, free nanocompound and nano-compound drug, as well as for the negative and positive control group.Placed in anticoagulant-free plastic tubes in order to obtain sufficient serum and later separated in centrifuge at a speed of 3000 rpm for 10 minutes, the red blood cell-free serum is separated by micropipette micropipette and the serum is distributed to clean, sterile tubes and kept in freezing at -20 m in the laboratory freezer for the purpose of measuring other functional criteria including tumor necrosis, cytokines and immune proteins.

Result and Discussion

Diagnosis of xerogel free nanocompound by Atomic Force Microscopie (AFM);

The results of the shape(3-1) of the Atomic Force Microscope (AFM) indicate that theXerogel free nanoparticles have a surface roughness coefficient of nm of 0.327, but for molecular size ratios of the compound equal to 10% of molecular sizes less than 50.00 nm, and 50% for molecular

The method used to diagnose hybrid nanovehicles included the use of Atomic Force Microscope (AFM)

The induction of arthritis by The Complete Freund Adjuvant (CFA) (CFA) (Biotechnology, Inc.).Canada Santa Cruz, according to the modus operandi used by (2014 Adeneye et al., .The development of inflammation was performed by injecting 0.1 ml of Complete Freund Adjuvant, which contains the heat-dead bacteria Mycobacterium tuberculosis in the right foot of the rat's soles after these animals were weighed and after taking a measurement The size of the foot by the measurement machine (Caplier verneir) before the start of the injection as well as the measurement of the size of the foot after 14 days of injection and after a period of six weeks of treatment. And the increase in foot thickness and stiffness.Newly developed arthritis is progressed 10-45 days from the start of the injection process (Van et al., 1988). The model for the development of arthritis by CFA has now proposed the development of this chronic infection, which is the characteristic of which is very similar to those resulting in the case of human rheumatoid arthritis (et al., 2005; Mizushima et al., 1970).

Pure Sciences International Journal of Kerbala

Journal Homepage:https://journals.uokerbala.edu.iq/index.php/psijk

.were 90% less than 130.00 nm. **sizes less than 90.00 nm, the sizes in general**

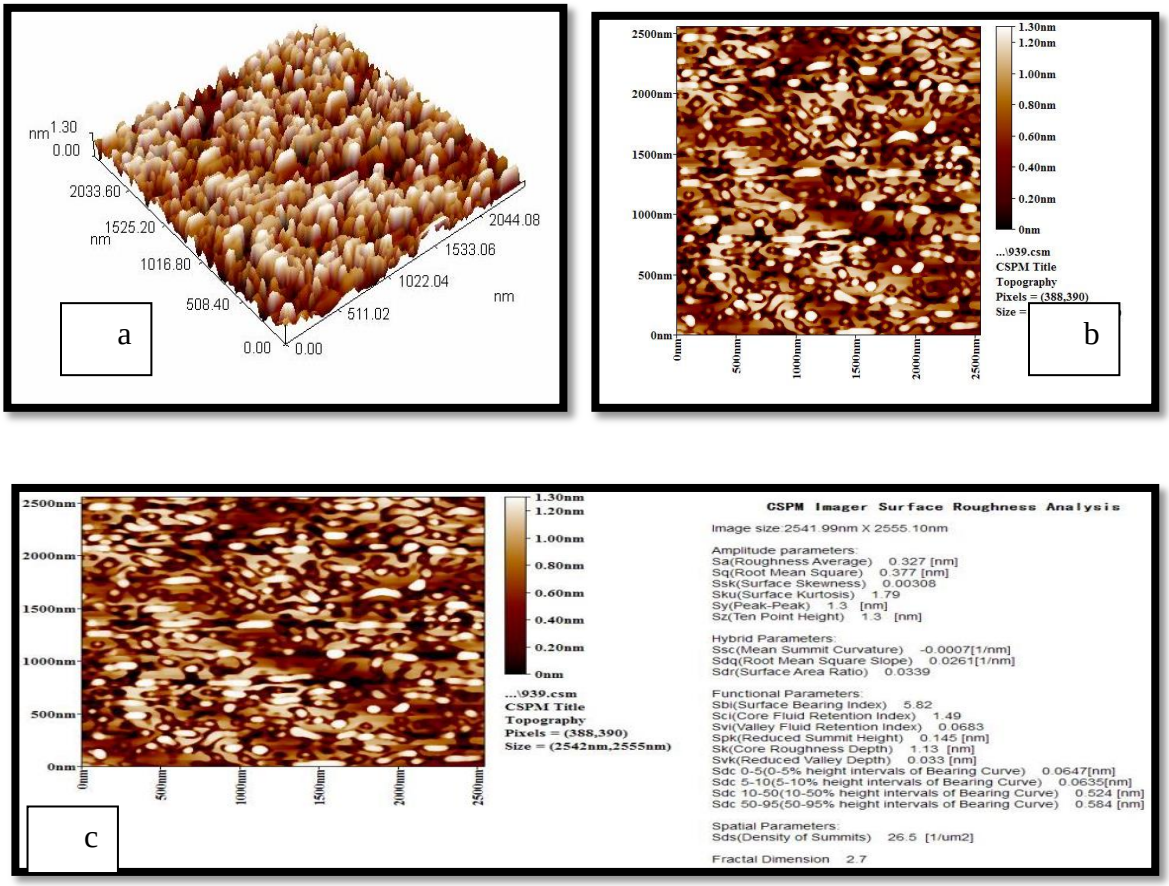

Shape (3-1) Atomic power microscope images of Xerogel free nanocomposite a/ :3D image, b/ 2D image, c/ 2D image showing all the details of the molecules

First Year-First Folder-Number: 0
PSIJK 184-191

Pure Sciences International Journal of Kerbala

Journal Homepage:https://journals.uokerbala.edu.iq/index.php/psijk

Table (3-1) Total rate of particle volumes of the Xerogel free nanocompound and the different ratios of those volumes

Avg. Diameter:94.14 nm	**<=10% Diameter:50.00 nm**
<=50% Diameter:90.00 nm	**<=90% Diameter:130.00 nm**

Diameter(nm)<	Volume(%)	Cumulation(%)	Diameter(nm)<	Volume(%)	Cumulation(%)	Diameter(nm)<	Volume(%)	Cumulation(%)
25.00	0.38	0.38	80.00	4.51	35.71	135.00	4.14	90.98
30.00	1.13	1.50	85.00	5.64	41.35	140.00	1.88	92.86
35.00	0.75	2.26	90.00	7.52	48.87	145.00	0.38	93.23
40.00	1.13	3.38	95.00	3.76	52.63	150.00	2.26	95.49
45.00	1.50	4.89	100.00	7.14	59.77	155.00	1.13	96.62
50.00	1.50	6.39	105.00	1.50	61.28	160.00	0.38	96.99
55.00	5.26	11.65	110.00	5.64	66.92	165.00	1.13	98.12
60.00	4.14	15.79	115.00	5.26	72.18	175.00	0.75	98.87
65.00	4.89	20.68	120.00	4.89	77.07	180.00	0.38	99.25
70.00	6.02	26.69	125.00	4.89	81.95	185.00	0.38	99.62
75.00	4.51	31.20	130.00	4.89	86.84	200.00	0.38	100.00

the invasion of pathogenic microorganisms and it is clear that the infiltration of single cells into the joints of mice induced by arthritis causes the secretion of tumor necrosis factor.

The same table also shows a slight increase in tNF-α concentration rates in the G3 group treated with xerogel nanocomposite for six weeks of treatment with rates of 3.59 ±483.74 pg/ml compared to a concentration rate in the Positive Control Group (G2). It was (10.68 ±461.80) pg/ml, while this increase was moral (p<0.05) compared to the negative control group (G1) at (0.88 ±69.97) Pg/ml.

The results of the current study were in agreement with the findings of Wooley 2013 (Elsabahy &) noting that nanoparticles that enter the body byThe

Effect of treatment BDexa is free and the free nanocompound charged with Dexa treatment in the concentration levels of .tNF-α tumor necrosis factor

The results of the current study table (3-2) show that the induction of reproductive arthritis by CFA causes a moral increase (p<0.05) in the concentration of tnf-α in the blood serum of white rat males as they reached a concentration level of 10.05. 68 ±461.80) Pg/ml in positive control group (G2) for six weeks of treatment compared to g1 negative control group with a concentration level (0.88 ±69.97) pg/ml for the same period, this is consistentWith the findings of a study (Namdeo and Kale, 2014) which attributed the reason for the high platelet count is due to the stimulation of the immune system against

Pure Sciences International Journal of Kerbala

Journal Homepage:https://journals.uokerbala.edu.iq/index.php/psijk

induction of TLRs, it is not known whether nanoparticles are identified by immune cells by immune cells SPECIFIC TLRs, or by other receptors.

The results of the current study in Table (3-2) indicate that animals induced by rheumatoid arthritis and dexa therapy (G4) will have lower tnf-α concentrationrates (P<0.05) with a concentration rate of 4.03 ±300.32 pg/ml compared to the positive control group (G2) and negative control (G2) for the treatment lukewarm rate of treatment, which is consistent with the rate of tetanus.With The Denarie et al., 2017) which indicated that the use of cortisone treatments including Dexamethasone has a significant role in inhibiting the production of tnf-α tumor necrosis through its effect on cyclooxygenase and cyclooxygenase enzymes. As a result, the production of TNF-α, which is mainly manufactured by pharyngeal cells during COX-1 activity, inhibits the aggregation of these cells and produces quantities of this compound as well as reduces the production of tumor necrosis through synergistic action with other treatments such as Infliximab (IFX) by reducing the composition of Antibody production of this treatment antibody towards sifx (ATI).

experimentation is subjected to complex reactions of blood cells and proteins and as soon as they enter the condensation of blood proteins on their surfaces and adsorption and proteins on the surfaces of nanoparticles equine corona (protein corona) these interactions determine the biological distribution and therapeutic effectiveness of nanoparticles and contribute to the type of immune response and here it came with the release of tumor necrosis factor TNF-α.

A similar study indicated (Aggarwal et al,.2009) that opsonization is one of the most important determinants of the arrival and distribution of nanoparticles in the body of the organism and that the stimulation of the most common protein components to surround the nanoparticles and the formation of the protein halo are proteins of the complementary, albumin, and Lipoproteins, fibrinogen, the surfaces of nanoparticles with antigen markers make them vulnerable to attack by the Mononuclear phagocytic system (MPS) blood cells are exposed to certain nanoparticles that may produce cytokines, but the exact mechanisms of cytokine production are not yet known.Unlike traditional antigens lipoproteins polysaccharides, DNA, RNA and which stimulate cytokines after

Pure Sciences International Journal of Kerbala

Journal Homepage:https://journals.uokerbala.edu.iq/index.php/psijk

direction of specific receptors of the pharyngeal cells CD46, and that the load of MTX therapy is much more effective than free treatment in inhibiting the production of tNF-α tumor necrosis factor and eliminating the progress of arthritis significantly in experimental animals.

The results of the current study coincided with the findings of Wani and others (2014), which confirmed that the effectiveness of Hydrogel nanocompounds and their consideration as smart therapeutic carriers for arthritis treatments to targeted biological sites due to their absorption capacity and high control over the release of treatment in areasInflammation which protects the joint from the action of inflammatory factors and tumor necrosis factor TNF-α due to several factors, compatibilityHigh because it contains large amounts of water help to accept it from natural tissues and this reduces the immune response trend, the ease of cracking it by the body making it vulnerable to the extrusion devices and thereby reducing its toxicity, as well as its ability to carry and maintain treatments until they reach the target tissues, and also the ability to escape from the ventricle retina and reach the target tissue and organize the liberalization of treatment in them.

The results of the table (2-3) show a moral decrease (P <0.05) in the concentration of TNF-α in members of the G5 group treated with the Xerogel/Dexa nanoboat, which amounted to 6.99 ±182.98 pg/ml compared With positive control totals (G2) and free compound therapy Xerogel (G3) and the group treated with free Dexa treatment (G4) for a six-week treatment period in these compounds as these concentrations (10.68 ±461.80), 3.59 ±483.74, 4.03 ±300.32) PG/ml respectively.

The results of the study showed an agreement with the study conducted by 2014 (Laste) which indicated that the preparation of a nanocompound of chitosan gel and non-ioncompound (niosomal) pregnant for the treatment of arthritis cortzoni /niosomal) and testing Its effectiveness on healthy volunteers in the treatment of localized psoriasis has shown a low level of tnf and no sensitization or irritation compared to the use of niosomal alone and free treatment.The results of the current study were in agreement with the findings of Roy and others 2016) which indicated that the load of MTX treatment on the nanoboat Theranostic gold (Au) half-shell NPs or Polysialic acid (PSA)-trimethyl chitosan (TMC) NPs (Xerogel) stimulates the formation of antibodies to the

Pure Sciences International Journal of Kerbala

Journal Homepage:https://journals.uokerbala.edu.iq/index.php/psijk

Table (2-3): TNF.& pg/ml cytokine concentrations before and after b treatmentDexa Free and Xerogel Free Nanoboat and Loaded With Xerogel/Dexa Treatment

Average concentration ±TNF.& Standard Line ((pg/ml	Treatment
0.88 ± 69.97 a	(G1)Nagtive control
10.68 ± 461.80 b	Positive control (G2)
3.59 ± 483.74 b	(G3) Xerogel
4.03 ± 300.32 c	Dexa (G4)
6.99 ± 182.98 d	Xerogel /Dexa (G5)

*

References

(2010). rheumatoid arthritis classification criteria. *Arthritis and Rheumatism;* 62(9), 2569-2581.

Bancroft , J.D. and Steven , A. (2008) . Theory and practice of histological technique . Seven edition .Churchill Livingstone , London . xiv- 662 .

Bresnihan, B. (1999). Pathogenesis of joint damage in rheumatoid

Alamanos, Y. & Drosos, A. ; (2005) . Epidemiology of adult rheumatoid arthritis. *Autoimmun Rev*. ; 4 : 130 - 136 .

Albrecht, M. A. ; Evan, C. W. & Raston, C. L. (2006). Green chemistry and the health implications of nanoparticles. *Green Chem.* ; 8 : 417-443.

Aletaha, D. ; Neogi, T. ; Silman, A. J. ; Funovits, J.; Felson, D. T. ; Bingham III, C. O.& Hawker, G.

Pure Sciences International Journal of Kerbala

Journal Homepage:https://journals.uokerbala.edu.iq/index.php/psijk

Infliximab . *Mediat. of Inflamma.*; 8 :1-8.

Dobkin, P. L. ; Filipski, M. ; Looper, K. ; Schieir, O. & Baron, M. (2008). Identifying target areas of treatment for depressed early inflammatory arthritis patients. *Psychother. and psychosomat.*, 77, 298 - 305.

Drury, R.A. and Wallington, E.A. (1976). Carelton's histological techniques Oxford Univ. Press, New York, Toronto.

Hansen, L. (2006). Gomori rapid one step trichrome stain; origin: Am. J. Clin. Pathol. 1950, 20:661-63.

Haroon, N. ; Aggarwal, A.; Lawrence, A.; Agarwal, V. ; Misra, R. (2007). Impact of rheumatoid arthritis on quality of life. *Mod Rheumatol*.;17:290-5.

Humason, C.L. (1979). Animal tissue techniques . Fourth edition .W. H. Freeman Co. , San Francisco . xiii – 661 .

Jawaheer , D. ; Lum, R. ; Amos, C. ; Gregersen, P. & Criswell, L. (2004) . Clustering of Disease Features Within 512 Multicase Rheumatoid Arthritis Families. arthritis. *J . Rheumatol*. 26, 717 - 9 .

Buer, J. K. (2015). A history of the term "DMARD". *Inflammopharmacology*; 23: 163-171.

Carson, F.L. and Christa, H. (2009). Histotechnology: a self-instructional text (3 ed.). Hong Kong: American Society for Clinical Pathology Press. pp. 137–139.

Cerceo, E.; Deitelzweig, S. B.; Sherman, B. M.and Amin, A. N. (2016). Multidrug-Resistant Gram-Negative Bacterial Infections in the Hospital Setting: Overview, Implications for Clinical Practice, and Emerging Treatment Options. *Microb. Drug Resist. (Larchmont, N.Y.),* **22** (5): 412–431.

Combe, B. & Dougados, M. (2001). La polyarthrite rhumatoïde est morte, vive la polyarthrite chronique évolutive. *La lettre du rhumatologue* ; 277, 3 - 4.

Denarie, D.; Rinaudo-Gaujous, M .; T Thomas, h.; Paul, S and Marotte H.(2017) . Methotrexate Reduced TNF Bioactivity in Rheumatoid Arthritis Patients Treated with

Pure Sciences International Journal of Kerbala

Journal Homepage:https://journals.uokerbala.edu.iq/index.php/psijk

Miyazaki, K. & Islam, N. (2007). Nanotechnology systems of innovation – An analysis of industry and academia research activities. *Technovation* ; 27: 661-671 .

Mohsen, I. H. & AL Dujaily, A. N.(2011). Effect of arithritis on som blood biochemical criteria in women in Najaf governorate. *Magazine of Al-Kufa University for Biology* **;** 3 (2) : 200-212.

Nair, A. B., & Jacob, S. (2016). A simple practice guide for dose conversion between animals and human. *J. of Basic and Clin. Pharm.*, *7*(2), 27–31.

Neeck, G. (2002) Fifty years of experience with cortisone therapy in the study and treatment of rheumatoidd arthritis. *Ann N Y Acad Sci*; 966:28-38.

Rasmussen, J.W. ; Martinez, E. ; Louka, P. & Wingett, D.G.(2010). Zinc oxide nanoparticles for selective destruction of tumor cells and potential for drug delivery applications. *Expert Opin. Drug Deliv* ; 7: 1063-1072.

Robert, S. ; Gicquel, T. ; Bodin, A. ; Lagente, V. & Boichot, E. (2016). Characterization of the *Arthritis Rheum*, 50 (3):736 - 741.

Khameneh, B. Diab, R. Ghazvini, K. Fazly Bazzaz, B.S. (2016). Breakthroughs in bacterial resistance mechanisms and the potential ways to combat them. *Microb Pathog*.; 95:32-42.

Klareskog , L.; Stolt, P. ; Lundberg, K. ; Kallberg, H. Bengtsson, C. & Grunewald, J.(2006). A new model for an etiology of rheumatoid arthritis: smoking may trigger HLA-DR(shared epitope)-restricted immune reactions to autoantigens modified by citrullination. *Arth. and Rheuma*..;54(1):38-46.

Maekay, A. H. & Jishnu, N. (2014). Structural Charecterization and Controlled Release Analysis of 5-Fluorocytosine-ZnO-LH Nanocomposite Against Candida Albicans. *International Journal of Scientific Engineering and Technology Research*; 3:(17) 3671 - 3679.

Majithia, V. & Geraci, S.A. (2007). Rheumatoid Arthritis: Diagnosis and Management. *American Journal of Medicine*; 120 (11), 936-939.

Pure Sciences International Journal of Kerbala

Journal Homepage:https://journals.uokerbala.edu.iq/index.php/psijk

year with rheumatoid arthritis: Coping resources as buffers of perceived stress. *British Journal of Health Psychology ;* 12 (3) : 323-345.

Vijayakumar, S. ; Vinoj, G. ; Alaikozhundan, M . B. ; Shanthi, S. & Vaseeharan, B. (2015). Plectranthus amboinicus leaf extract mediated synthesis of zinc oxide nanoparticles and its control of methicillin resistant Staphylococcus aureus biofilm and blood sucking mosquito larva. *Spectrochim. Acta Part AMol. Biomol. Spectrosc ;* 137: 886-891.

Vingsbo, C. (1996). Pristane induced arthritis in rats a new model for rheumatoid arthritis with a chronic disease course influenced by both major histocompatibility complex and nonomajor histocompatibility complex genes. Am. J. Pathol.; 149, 1675-1683 .

Yuan, Q. ; Hein, S. & Misra, R. D. K. (2010). New generation of chitosan-encapsulated ZnO quantum dots loaded with drug: Synthesis, characterization and *in vitro* drug MMP/TIMP Imbalance and Collagen Production Induced by IL-1β or TNF-α Release from Human Hepatic Stellate Cells. *PLoS ONE* ; 11(4):1-14.

Sheehan, D. and Hrapchak, B.(1980). Theory and practice of Histotechnology, 2nd Ed., pp 164-166, Battelle Press, Ohio.

Short C. L. (1974). The Antiqu ityof Rheumatoid Arthritis. *Arthritis and Rheumatism* . ;17(3):193–205.

Silman, A. J. & Pearson, J. E. (2002). Epidemiology and genetics of rheumatoid arthritis. *Arthritis Res* 4 (3): 265-272.

Skogh, T. (2005). Does a positive anti-CCP test identify a distinct arthritis entity?. *Arthritis Res Ther;* 7(6):230-232.

Storey, G. D. ; (2009). Alfred Baring Garrod (1819-1907). *Rheumatology (Oxford);* 40:1189-1191.

Tjong, S. C. & Chen, H. (2004). Nanocrystalline materials and coatings, Mater. *Sci. Eng.*, R, 45: 1- 88.

Treharne, G. J. ; Lyons, A. C. ; Booth, D. A. & Kitas, G. D. (2007). Psychological well-being across 1

Pure Sciences International Journal of Kerbala

Journal Homepage:https://journals.uokerbala.edu.iq/index.php/psijk

Elsaman, T. & Musab, M. A. (2016) . Nonsteroidal Anti-Inflammatory Drugs (NSAIDs) Derivatives with Anti-Cancer Activity. *Am. J. of Res. Com.*; 4(4): 2325-4076 .

Aggarwal, P. ; Hall, J. B. ; McLeland, C. B. ; Dobrovolskaia, M. A.& McNeil, S.E. (2009) .Nanoparticle interaction with plasma proteins as it relates to particle biodistribution, biocompatibility and therapeutic efficacy. *Adv. Drug Deliv. Rev.*; 61:428-437.

Denarie, D.; Rinaudo-Gaujous, M .; T Thomas, h.; Paul, S and Marotte H.(2017) . Methotrexate Reduced TNF Bioactivity in Rheumatoid Arthritis Patients Treated with Infliximab . *Mediat. of Inflamma.*; 8 :1-8.

Laste, G.; Cristina, I. ; Souza, C. ; Santos, V. S. ; Caumo, W. & Torres, I. L.S. (2014)**.** Histopathological Changes in Three Variations of Wistar Rat Adjuvant-Induced Arthritis Model *(IJPRS)* 3: I - 12 .

Wani, U. ; Rashid , M. ; Kumar, M. ; Chaudhary, S. ; Kumar, P.& Mishra, N.(2014).Trgeting Aspects Of Nanogel. *International Journal Of Pharmaceutical And* delivery response .*Acta Biomater*;6: 2732-2739.

Yuan, Q. ; Venkatasubramanian, R. ; Hein, S. & Misra, R. D. K. (2008). A stimulus-responsive magnetic nanoparticle drug carrier: Magnetite encapsulated by chitosan-grafted-copolymer .*Acta Biomater.*; 4: 1024-1037.

Zhoua, H . ; Yana, H. ; Senpanb, A. ; Wicklineb, S. A. ; Panb, D. G. ; Lanzab, M. ; Phama, C. T. N. ; Lanza, G. M. & Pham, C. T. N. (2012). Suppression of inflammation in a mouse model of rheumatoid arthritis using targeted lipase-labile *fumagillin prodrug nanoparticles* ; 33(33): 8632 - 8640.

Namdeo, A.G. and Kale, V.M. (2014). Antiarthitic effect of ganlangin isolated from rhizomes of alpinia officinarum in complete freund's adjuvant-induced arthritis in rats. *Intl. J. of Pharm. and Pharmaceut. Sci.*. 6(4):502-504.

Elsabahy, M.& Wooley, K. L. (2013). Cytokines as biomarkers of nanoparticle immunotoxicity . *Chem. Soc. Rev.*; 42(12): 5552-5576.

Pure Sciences International Journal of Kerbala

Journal Homepage:https://journals.uokerbala.edu.iq/index.php/psijk

2631. *Nanotechnology* ; 7(4) : 2612-